UNIVERSITY OF NOTTINGHAM

THE ROLE OF C/EBP BETA IN REGULATING UCP1 EXPRESSION IN 3T3-L1 ADIPOCYTES

QIAN LIU, BSc

Thesis submitted to the University of Nottingham

for the degree of Doctor of Philosophy

January, 2012

DECLARATION

I hereby state that the work presented in this thesis is my own, and reference to other work has been cited accordingly with full details in the references section.

No part of this thesis has been or is being concurrently submitted for any other qualification at any other university.

Qian Liu

Sign_____ Date_____

ABSTRACT

Uncoupling protein 1 (UCP1) is essential for non-shivering thermogenesis in brown adipose tissue (BAT) by dissipating proton-motive force to stimulate maximum mitochondrial respiration. cAMP-dependent protein kinase induction of UCP1, as well as the PPAR coactivator1α (PGC1α), is a typical characteristic in BAT but not in white adipose tissue (WAT). Previous work demonstrated that the overexpression of CCAAT/Enhancer Binding Protein β (C/EBPβ) could rescue the cAMP-induced PGC1α and UCP1 expression in white preadipocytes 3T3-L1 cell line, indicating a key regulatory role of C/EBPβ in brown adipogenesis. The overall aim of this study was to examine the role of C/EBPβ overexpression in regulating the transcription of UCP1 in 3T3-L1 white preadipocytes to transform them to a more brown-like cell phenotype.

Tetracycline inducible (Tet on) lentiviral, adipose-specific expression vectors for overexpressing C/EBPβ (or the control Luciferase-GFP) gene were constructed with the pLenti6 lentiviral vector backbone with TRE tight and rtTA advance regulatory elements. In the absence of doxycycline there was low basal expression from the vectors and a dose-dependent, doxycycline-induced transient, adipose-specific overexpression was observed in 3T3-L1 preadipocytes. Transduction of the pLenti6 positive control luciferase-RFP vector was successfully achieved but the C/EBPβ or LucGFP vectors constructed failed to produce highly infectious lentiviral particles, possibly due to the large size of insert which challenged the limit of the pLenti6 vector backbone. Therefore a stable inducible, adipose-specific, 3T3-L1 line overexpressing C/EBPβ was not achieved.

Transient overexpression of C/EBPβ and PRDM16 significantly increased the transcriptional activity of UCP1 promoter in the presence of forskolin in 3T3-L1 cells without stimulating PGC1α promoter activity, implying a PGC1α-independent manner of activating UCP1 transcription in 3T3-L1s. C/EBPβ overexpression alone activated the PGC1α promoter in HIB-1B and Cos7 cells but not in 3T3-L1 cells, indicating the lack of some activators in 3T3-L1 or a potential 3T3-L1 specific repressive mechanism. Co-overexpression of C/EBPβ and PPARγ in 3T3-L1 markedly stimulated the PGC1α

promoter in response to rosiglitazone and increased the UCP1 promoter activity in the presence of rosiglitazone and forskolin. This result suggests that PPARγ could make up for the lack of activator or release the 3T3-L1 repressive mechanism and mediated a PGC1α-dependent manner of activating UCP1 together with C/EBPβ in 3T3-L1 cells. Further studies demonstrated that both CRE and PPRE elements were indispensible in this PGC1α-dependent pathway of activating UCP1 promoter in 3T3-L1 cells. The results suggest that C/EBPβ and PPARγ cooperate to induce UCP1 expression in 3T3-L1 cells stimulated by PPARγ agonist and cAMP.

ACKNOWLEDGEMENTS

It would not have been possible to complete this thesis without the help and support of the kind people around me, to only some of whom it is possible to give particular mention here.

Above all, I would like to express my sincere appreciation to my supervisor Prof. Michael Lomax for his guidance and support and for offering valuable advice whenever it was needed during my research and thesis writing. I also must thank him for his patience and kindness, which has been especially important for an international student, like me. Furthermore, I thank him for that he has been always trusting me and encouraging my own ideas about the project, so that I can form the habit of independent thinking, which is invaluable for my future life. I am also grateful to Prof. Andy Salter for his advice during my research and his help in the preparation of this manuscript. His kindness greatly alleviated my anxiety on my very first day in the division and also the days afterwards.

Special thanks to Dr. Phil Hill and Tania (Division of Food Sciences), without whom it would be impossible for me to do all the lentiviral work. I thank them for their wise guidance and invaluable help on the work of vector cloning and lentivirus production, especially for their patience and kindness in the help on designing constructs, analysing results and trouble shooting. I would also like to thank Dr. Simon Lillicon (Roslin Institute) who helped a lot in the trouble shooting of my lentiviral work and kindly provided the second generation lentiviral packaging system (psPAX2). Sincere thanks also go to Prof. Francesc Villarroya for his kind gift of mutated PGC1α promoter luciferase constructs and to Dr. Georgios Karamanlidis for constructing the other luciferase reporter vectors.

A very special thanks to Dr. Angeliki Karamitri, who assisted me a lot in my first steps in this project and provided much helpful advice and technical information to my research project and thesis writing whenever I needed it, even after she's gone back to Greece. Her contribution and support played a major role in the completion of my project and her friendship has made my first years in the UK fun and pleasant. I would

also like to thank Dr. Kevin Ryan, for his patience and creative ideas in the trouble shooting of my work and his good humour which has made the lab more active. Special thanks go to my fellow PhD student Elaine Chen, for our exchanges of knowledge, skills and frustration which enriched our experience. Her accompany in the lab drove away my feeling of loneliness, especially that we could communicate in our mother tongue. I would also like to express my sincere appreciation to all the other colleagues in the Division of Nutritional Sciences and all the friends in Sutton Bonington, for their help on my research and their caring for my life, which has made me feel warm even in the coldest season in this rainy country.

Last but not least, I wish to express my deep gratitude to my beloved Mum, Dad and my boyfriend Qi, for their love, caring support, encouragement and believing in me all the time. I love them all from the bottom of my heart.

ABBREVIATIONS

18F-FDG 18F-fluorodeoxyglucose

4E-BP1 Eukaryotic initiation factor 4E binding protein 1

AAV Adeno-associated virus

ADP Adenosine Diphosphate

ANOVA Analysis of Variance

aP2 adipocyte P2

ATCC American Type Culture Collection

ATF2 Activating Transcription Factor 2

ATP Adenosine Triphosphate

BAT Brown Adipose Tissue

BMI Body Mass Index

BMP Bone Morphogenetic Protein

BP the recombination reaction to generate entry clones in Gateway Cloning

bZIP basic Leucine Zipper

C/EBP CCAAT/Enhance Binding Protein

cAMP cyclic Adenosine Monophosphate

cDNA Complementary Deoxyribonucleic Acid

ChIP Chromatin ImmunoPrecipitation

CIDEA Cell death-inducing DNA fragmentation factor α-like effector A

CMV cytomegalovirus

CNS Central Nervous System

COOH 2-(2-(4-phenoxy-2-propylphenoxy) ethyl) indole-5-acetic acid

Cox Cytochrome oxydase

CRE cAMP Regulatory Element

CREB CRE Binding protein

CtBP C-terminal-binding-protein

DEAE diethylaminoethyl

Dex Dexamethasone

DIT Diet-induced Thermogenesis

DMEM Dulbecco's modified Eagle's Media

DMSO Dimethyl sulfoxide

DNA Deoxyribonucleic Acid

Dox Doxycycline

EMSA Electrophoretic Mobility Shift Assay

ERK Extracellular siganl-related Kinase

ERR Estrogen Related Recptor

FABP4 Fatty Acid Binding Protein 4

FBS Foetal Bovine Serum

FFA Free Fatty Acid

FoxC2 Forkhead box C2

Fsk/Forsk forskolin

GSK3 Glycogen synthase kinase 3

HDAC Histone DeAcytylase

HIV human immunodeficiency virus

HMT Histone Methyltransferase

HSD hydroxysteroid dehydrogenase

IBMX isobutylmethylxanthine

IHF Intigration Host Factor

Int integrase

IRS Insulin Receptor Substrate

KRAB Krüppel-associated box

LAP Liver enriched transcriptional Activatory Protein (the active C/EBPβ isoform)

LIP Liver enriched transcriptional Inhibitory Protein (the inhibitory C/EBPβ isoform)

LR the recombination reaction to generate expression vectors in Gateway Cloning

LTR long terminal repeat

LucGFP Luciferase Green Fluorescent Protein fusion protein

LXR Liver X Receptor

MAP Mitogen-Activated Protein

MCE Mitotic Clonal Expansion

MEF Mouse Embryonic Fibroblast

MEK mitogen-activated protein kinase/ERK kinase

MLV murine leukaemia virus

MOI Multiplicity of Infection

MPTPp 1-methyl-4-phenyl-1,2,3,6-tetrahydropyridineprobenecid

mRNA messenger Ribonucleic acid

MSC Mesenchymal Stem Cell

NEAA Non-Essential Amino Acid

PBS Phosphate Buffered Saline

PCR Polymerase Chain Reaction

PEI Polyethyleneimine

PET-CT positron emission tomographic and computed tomographic

PGC PPAR Gamma Coactivator

PIC Protein Inhibitor Cocktail

PKA Protein Kinase A

PMSF phenylmethanesulfonylfluoride

polybrene 1, 5-dimethyl-1, 5-diazaundecamethylene polymethobromide

PPAR Peroxisome Proliferator-activated receptor

PPRE PPAR Response Element

pRb retinoblastoma protein

PRDM16 PRD1-BF-1-RIZ1 Homologous Domain Containing Protein 16

qRT-PCR quantitative real time PCR

RA Retinoic Acid

RARE Retinoic Acid Response Element

RFP Red Fluorescent Protein

RIP140 Receptor Interacting Protein 140

RNA Ribonucleic acid

RNAi RNA inteference

Rosi rosiglitazone

RRE Reverse Responsive Element

RT Room Temperature

rtTA reverse tetracycline-controlled transactivator

RXR retinoid X receptor

sAP2 short aP2

shRNA short hairpin RNA

SIN self-inactivating

siRNA small interfering RNA or silencing RNA

Sirt 3 Silent mating type information regulation 2, homolog 3

SNS Sympathetic Nervous System

SRC steroid receptor co-activator

SREBP sterol regulatory element binding protein

STAT signal transducers and activators of transcription

T3 triiodothyronine

Tet Tetracycline

TGF Transforming Growth Factor

TNFα Tumor Necrosis Factorα

TR Thyroid hormone Receptor

TRE (Chapter 1) Thyroid hormone Response Element

TRE (other chapters) Tetracycline Response Element

TU transduction unit

TZD thiazolidinedione

UCP1 Uncoupling Protein 1

UDP Uridine Diphosphate

VSV-G vesicular stomatitis virus G

WAT White Adipose Tissue

WHO World Health Organization

WPRE woodchuck hepatitis virus post-transcriptional regulatory element

ZF Zinc Finger

β-AR β-Adrenergic Receptor

TABLE OF CONTENTS

CHAPTER 1

1 LITERATURE REVIEW

1.1 INTRODUCTION

Obesity is an increasingly prevalent problem nowadays. According to the statistical data from World Health Organization (WHO), in 2008, more than one in ten of the world adult population was obese and in 2010 around 43 million children under five were overweight. Once considered a high-income country problem, obesity now has been on the rise in low- and middle-income countries, especially in urban settings (Flegal et al., 2005). In addition, obesity is an important risk factor in the development of metabolic syndromes such as hypertension, dyslipidaemia, cardiovascular diseases and type II diabetes. 44% of the diabetes burden, 23% of the ischaemic heart disease burden and between 7% and 41% of certain cancer burdens are contributed to overweight and obesity (Bray, 2004). Obesity is caused by imbalanced energy intake and expenditure, which leads to the accumulation of energy in adipose tissue. The strategies to prevent and treat obesity to date have had limited success although advances in understanding the control of food intake, energy expenditure and the metabolic regulation processes, have been made.

Energy is expended by obligatory and facultative thermogenesis. Obligatory thermogenesis is a necessary accompaniment of all metabolic processes involved in maintenance of the body in the living state, and occurs in all organs. It includes energy expenditure involved in ingesting, digesting, and processing food (thermic effect of food). At certain stages extra energy expenditure for growth, pregnancy, or lactation would also be obligatory. Facultative thermogenesis is superimposed on obligatory thermogenesis and can be rapidly switched on, or suppressed by the nervous system. It functions in two different manners, shivering thermogenesis which depends on the movement of muscle and non-shivering thermogenesis which occurs in brown adipose tissue (Himms-Hagen, 1989). Non-shivering thermogenic capacity can be induced either by cold exposure or high-fat diet (diet-induced thermogenesis, DIT) (Rothwell and Stock, 1979; Sellers et al., 1954), and is due to brown adipose tissue activity (Cannon and Nedergaard, 2011).

As one of the two types of adipose tissues in mammals, brown adipose tissue functions to oxidise carbohydrate and fat fuels for producing heat, while its counterpart, white adipose tissue (WAT) acts to store energy in the form of triglycerides (Farmer, 2008). The most significant characteristic of BAT at gene expression level is the unique expression of uncoupling protein 1 (UCP1), a critical gene in the non-shivering adaptive thermogenic function of BAT (Enerback S et al., 1997; Foster DO, 1978). Small mammals like rodents and human infants have large depots of BAT as to keep warm temperature (Cannon and Nedergaard, 2004), but in adult humans, the appearance of functional BAT was not confirmed until recently Yeung and colleagues identified the existence and importance of active BAT in adult humans using ^{18}F-fluorodeoxyglucose (^{18}F-FDG) positron emission tomographic and computed tomographic (PET–CT) scans (Nedergaard et al., 2007; Yeung et al., 2003). Later on, it was found that the amount of BAT is inversely correlated with body-mass index (BMI) (Cypess et al., 2009), indicating a potential role of BAT in counteracting with obesity and related diseases. Due to its function of "burning" fat, brown adipose tissue has been recognised for its potential and demonstrated anti-obesity properties. In fact, a large number of genetic studies in mice have shown that experimentally-induced increases in the amount and/or function of brown adipose tissue favour lean phenotypes, less weight gain, higher insulin sensitivity, lower levels of circulating free fatty acids and lower insulin resistance (Kopecky et al., 1995; Kopecky et al., 1996; Miner et al., 2001; Tsukiyama-Kohara et al., 2001; Xue et al., 2007).

Several nuclear factors have been associated with the formation of brown adipocytes (Gesta et al., 2007). Apart from the master regulator for adipogenesis, the transcriptional factor peroxisome proliferator-activated receptor γ (PPARγ) (Tontonoz et al., 1994c), the nuclear receptor coactivator PPARγ coactivator-1α (PGC1α) was discovered as a cold-inducible regulator of UCP1 expression, capable of inducing UCP1 expression in fibroblasts (Puigserver et al., 1998). More recently an additional PPARγ binding nuclear factor, PRD1-BF-1-RIZ1 Homologous Domain Containing Protein 16 (PRDM16), has been proposed to be the principal regulator of brown adipocyte differentiation (Kajimura et al., 2008). PRDM16 switches on the brown

adipogenic programme by forming a complex with the transcriptional factor, CCAAT Enhancer Binding Protein β (C/EBPβ) (Kajimura et al., 2009). It had been previously demonstrated that C/EBPβ could reprogramme white adipose tissue into a "brown" lineage by rescuing the cAMP inducible expression of UCP1 and PGC1α in white adipocytes (Karamanlidis et al., 2007), C/EBPβ is obviously another critical regulator in brown adipogenesis and hence a good target to investigate the white-brown transdifferentiation. Despite the importance of this gene, few studies to date have examined the regulating mechanisms of C/EBPβ on UCP1 and PGC1α transcription throughout the whole process of brown adipogenesis.

Therefore, this review will critically outline the literature on the control of adipocyte differentiation with emphasis on the molecular mechanisms regulating brown adipogenesis. The aim of the review is to bring together known regulators of brown adipocyte development to construct a model of interacting networks, especially those involving C/EBPβ. A series of studies will also be reviewed to provide an understanding of methods generating stable gene overexpression in mammalian cells and animals, which are required in investigating gene functions in adipocyte differentiation process.

1.2 ADIPOSE TISSUE

Humans, like most of the other mammals, contain essentially two types of adipose tissue: white adipose tissue (WAT) and brown adipose tissue (BAT). Adipose tissue is composed of adipocytes, stromo-vascular cells, immune cells, nerve tissue and a connective tissue matrix that all together function as an integrated unit (Kershaw and Flier, 2004). White adipose tissue is dispersed throughout the body with major intra-abdorminal depots around the omentum, intestine and perirenal areas, as well as subcutaneous depots (Gesta et al., 2007). Lipolysis in WAT releases free fatty acids (FFAs) into the circulation to provide energy for the other tissues such as liver, heart and muscle (Coppack et al., 1994). Once mainly considered as the tissue involved in insulation in a cold environment and the store for excess energy, white adipose tissue has now been acknowledged as an important organ for metabolism as it responds to signals from central nervous system (CNS) and expresses and secretes different kinds

of adipokines, which have the potential to influence various functions including food intake, metabolism and cardio-metabolic function (Trayhurn and Wood, 2005). The potential role of brown adipose tissue in promoting energy expenditure to prevent and treat obesity has resulted in this becoming a hot topic in adipose tissue research area in recent years. Brown adipose tissue, unlike WAT, is responsive for producing heat, hence a mammalian adaptation that is most obvious in rodents and human infants (Cannon and Nedergaard, 2004), since smaller animals have larger area to volume ratio so have higher risk of hypothermia. Adapted to its function, brown adipose tissue has a very unique cellular and molecular composition. Sharing basic common characteristics of adipose tissue, WAT and BAT once were considered originating from a common early precursor (adipoblast), which derives from mesenchymal stem cells (MSCs) and in turn develops into white and brown preadipocytes (Gesta et al., 2007). However, the different evolutionary and developmental features of WAT and BAT suggest that they are quite distinct tissues with separate origins (Farmer, 2008; Gesta et al., 2007). With the discovery that PRDM16-C/EBPβ complex can initiate a brown adipogenic programme from myoblasts (Kajimura et al., 2009), more and more researchers are realizing that the relation between muscle and brown fat is even closer than that between WAT and BAT. The below part of the review will summarize the basic characteristics of WAT and BAT in morphology, location, function and formation and will also collect some evidence about the origin controversies of white and brown adipose tissue.

1.2.1 Anatomy of WAT and BAT

WAT and BAT both contain white and brown adipocytes, respectively. These two types of adipocytes have distinct anatomy: white adipocytes are unilocular where the lipids are organised in a single lipid droplet for storage (Figure 1.1 A), while brown adipocytes are multilocular where lipids accumulate in many small lipid droplets (Figure 1.1 B). Brown adipocytes have numerous large mitochondria containing the uniquely expressed protein UCP1 (Figure 1.1 C and D) responsible for uncoupling of the oxidative phosphorylation to produce heat in these cells (Cinti, 2006). In white adipocytes, mitochondria are in limited number and poorly developed and most of the cytoplasm is compressed by the big lipid droplet to a thin rim containing a nucleus

and the organelles (Figure 1A)(Cinti, 2005). Apart from adipocytes, WAT and BAT are richly supplied with parenchymal nerve fibres and blood vessels but the density is considerably higher in BAT, giving it the characteristic brown colour (Cinti, 2001, 2006).

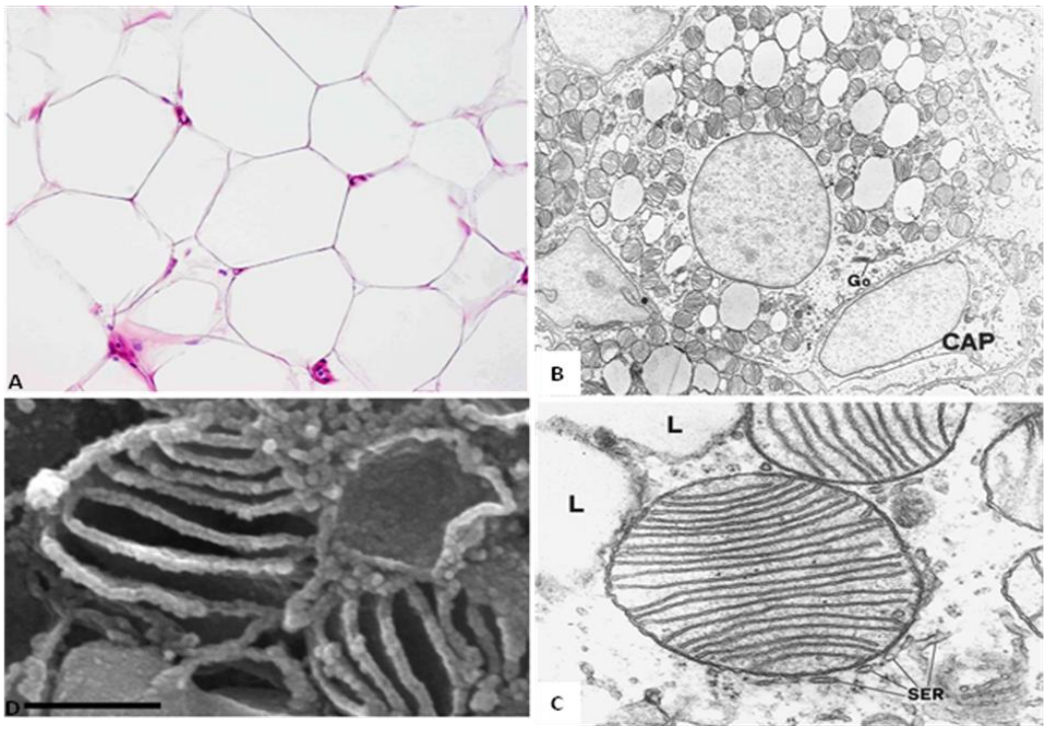

Figure 1.1 Anatomy of white adipocytes and brown adipocytes.

(A) Light microscopy of haematoxylin-eosin stained human human white adipocytes. Objective magnification 20× (Cinti, 2005). (B) Transmission electron microscopy of a neonatal rat filled with numerous small lipid droplets and typical mitochondria packed with cristae. Go, Golgi apparatus; CAP: capillary. Magnification=8700. (C) High magnification of a typical brown adipocyte mitochondrion. L, lipid droplet; SER, smooth endoplasmic reticulum. Magnification= 80000 (Cinti, 2001). (D) Scanning electron microscopy of brown adipocyte mitochondria. Scale bar: 333 nm (Cinti, 2005).

Adipose tissue consists of several depots in mammals (Figure 1.2). White adipose tissue has a prevalent distribution with major intra-abdominal depots around omentum, intestines and perirenal areas, as well as in subcutaneous depots in the buttocks, thighs and abdomen (Cinti, 2001; Gesta et al., 2007). WAT can also be found in the retro- orbital space, on the face and extremities and within the bone morrow (Gesta et al., 2007). In contrast, brown adipose tissue is not dispersed so widely. In rodents, BAT is most abundant in the neonatal period and is most concentrated in the interscapular region, and it also can be found in WAT depot, particularly after cold exposure (Figure 1.3). In humans, BAT is found in axillary, cervical, perirenal and periadrenal regions of foetuses and newborns (Cannon and Nedergaard, 2004) but decreases rapidly after birth and has been traditionally considered not significant in adults, except in patients with pheochromocytoma, where adrenergic activity is extremely high (English et al., 1973), or in outdoor workers subject to prolonged cold exposure (Huttunen et al., 1981). However, the recent morphological and scanning studies using [^{18}F]-2-fluoro-D-2-deoxy-D-glucose (FDG) positron emission tomography (PET) can successfully detect metabolically active brown fat in the cervical, supraclavicular, axillary and paravertibral regions in normal individuals (Nedergaard et al., 2007).

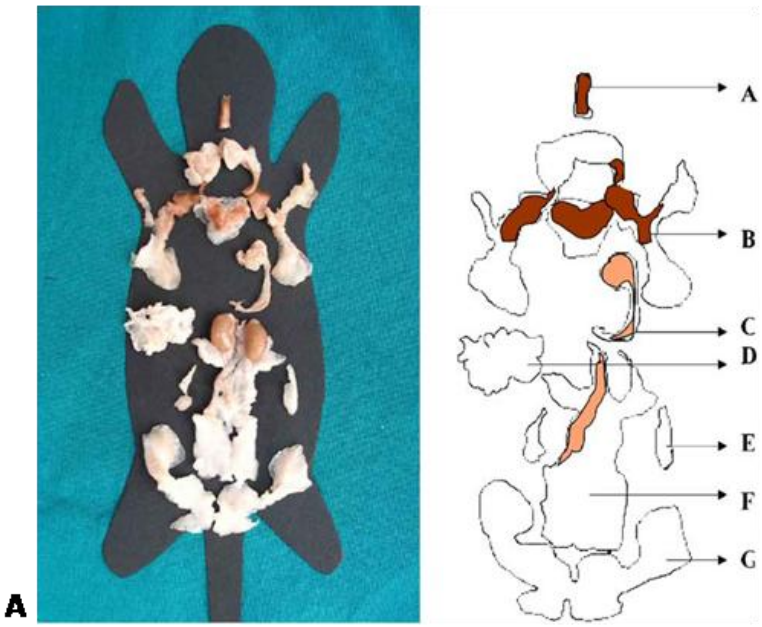

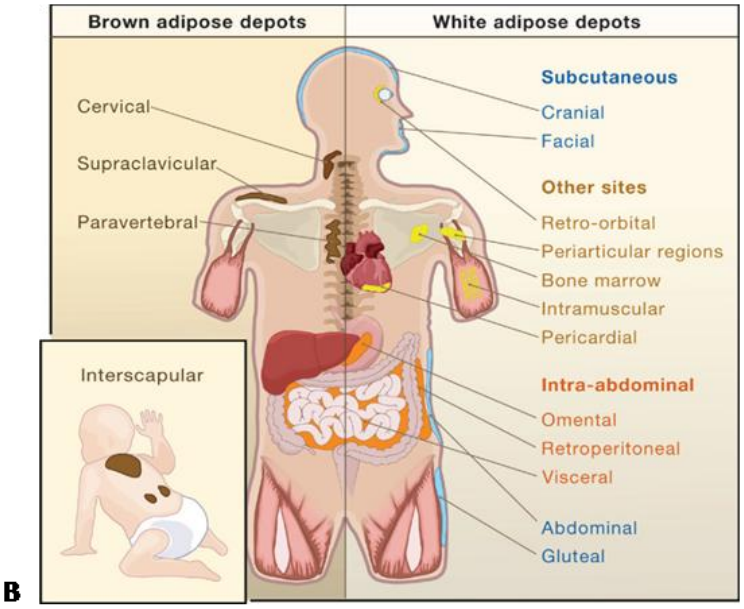

Figure 1.2 Distribution of white and brown adipose tissue in mouse and human.

(A) The adipose organ of an adult Sv129 mouse maintained at 29°C for 10 days. The organ has been dissected with the aid of a surgical microscope and each depot has been placed on the mouse profile mimicking its anatomical position. The organ is made up of two subcutaneous and several visceral depots. The most representative visceral depots are shown. Kidneys and testes were dissected together with the depots. Names of single depot: A) deep cervical; B) anterior subcutaneous (interscapular, subsapular, axillo-toracic, superficial cervical); C) visceral mediastinic; D) visceral mesenteric; E) visceral retroperitoneal; F) visceral perirenal, periovaric, parametrial and perivescical; G) posterior subcutaneous (dorso-lumbar, inguinal and gluteal). White areas made up of white adipose tissue and vrown areas composed of brown adipose tissue are indicated by the scheme (Cinti, 2005). (B) In humans, depots of white adipose tissue are found in areas all over the body, with subcutaneous and intra-abdominal depots representing the main compartments for fat storage. Brown adipose tissue is abundant at birth and still present in adulthood but to a lesser extent (Gesta et al., 2007).

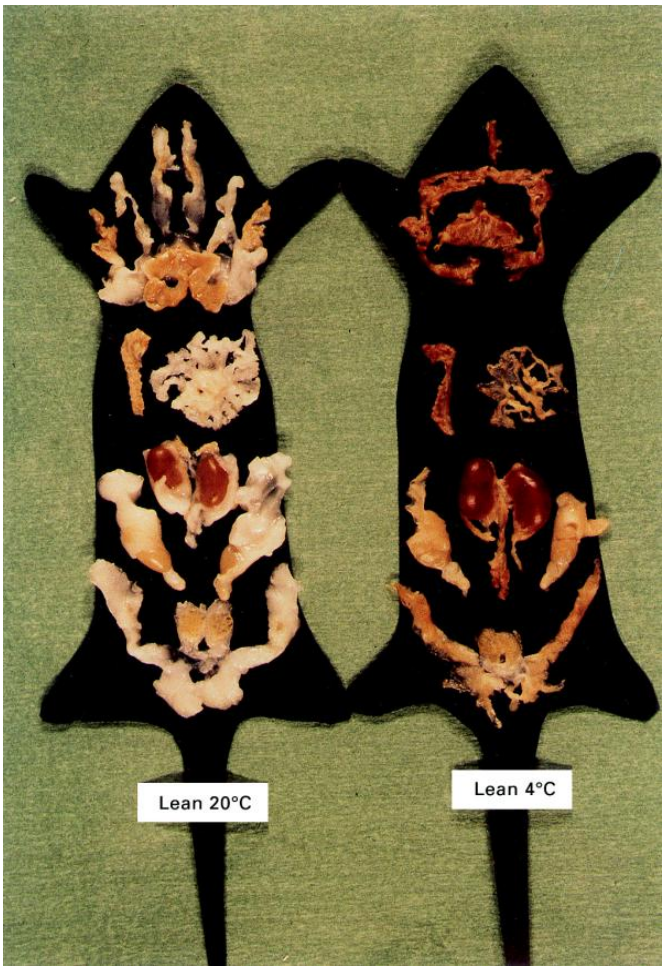

Figure 1.3 Gross anatomy of the adipose organs of adult mice kept at 20°C and 4°C.

Dissections were performed on C57BL/KS-db/+ mice aged 43 weeks. Mice were kept at 20°C or acclimated (several days) at low temperature (4°C). Most of the fat depots at 20°C have a white-yellowish colour but some areas in the upper and lower subcutaneous depots and the perirenal and mediastinic depots are brown in colour. In cold-acclimated (4°C) animals, the brown areas increase in number (Cinti, 2001).

White adipose depots in rodents and humans contain brown adipocytes which can dramatically increase in number, as well as the number of brown adipocytes in brown adipose depots, in cold-acclimated animals (Figure 1.3)(Cinti, 2001), indicating the striking plastic properties of adipose tissue.

1.2.2 Functions of adipose tissue

The most obvious function of white adipose tissue is energy storage and release besides insulation and cushioning. Excess energy is stored in WAT in the form of triglycerides, and then hydrolysed into free fatty acids and delivered to the other organs to be used as fuel (Coppack et al., 1994). In BAT the stored energy is oxidised to produce heat via uncoupling respiration (Cannon and Nedergaard, 2004). However, energy storage and release is not the only function of adipose tissue. It has been acknowledged as an important endocrine organ, secreting varieties of factors regulating the energy homeostasis in the body (Kershaw and Flier, 2004). A series of experiments about energy metabolic function of WAT and BAT will be reviewed in the following few paragraphs, emphasising on the thermogenic function of BAT, followed by studies on the endocrine role of adipose tissue.

Lipolysis refers to processes in which triglyceride is hydrolysed, via di- and monoglyceride intermediates, to fatty acids and glycerol (Renold, 1965). In WAT, where the majority of lipolysis occurs, free fatty acids are released into the circulation then absorbed and oxidized by specific tissues (e.g. liver and muscle) as fuel on demand (Coppack et al., 1994). So adipose tissue lipolysis is the major regulator of the body's supply of fatty acids for energy metabolism.

Unlike WAT, BAT has much more limited amount and locations in the body (Cannon and Nedergaard, 2004; Nedergaard et al., 2007) and the lipolysis in BAT provides FFAs for thermogenesis, as BAT mitochondria have a unique proton conductance mechanism that allows them to become reversibly uncoupled (Nicholls and Locke, 1984) and thus to oxidise both endogenous and exogenous substrates at an extremely high rate independent of the need to phosphorylate ADP (Himms-Hagen, 1984). This uncoupled respiration is controlled by the intracellular concentration of FFAs (Bukowiecki, 1984; Nicholls and Locke, 1984) and involves the specific protein uncoupling protein 1 (UCP1), which is also the unique marker of brown adipose tissue gene expression. UCP1 is located in the inner membrane of mitochondria and catalyzes a leak of protons from the intramembrane space into the mitochondrial matrix (Figure 1.4)(Klingenberg and Huang, 1999), therefore mitochondria in brown adipocytes are capable of high rates of lipid oxidation which is uncoupled from ATP

generation, so releasing the energy as heat (Cannon and Nedergaard, 2004; Scheffler, 1999). The resulting dissipation of the mitochondrial membrane potential, along with extremely high rates of mitochondrial electron transport and lipid oxidation, results in the generation of heat and the expenditure of huge amounts of chemical energy (Seale et al., 2009). BAT has been well established as a key component in non-shivering thermogenesis. Chronic cold exposure causes an increase in brown adipocytes (or recruitment) and activation of uncoupled thermogenesis in rodents and humans (Klingenspor, 2003). When an environmental temperature below the lower critical temperature is sensed by central nervous system (CNS), catecholamine is secreted from the sympathetic nerve terminals within the BAT (Cannon and Nedergaard, 2004; Klingenspor, 2003) to stimulate UCP1 expression and activate non-shivering thermogenesis. The thermogenic function of BAT is only occurs in response to adrenergic stimulation, so BAT can be activated by exposure to β-adrenergic agonists (Seale et al., 2009).

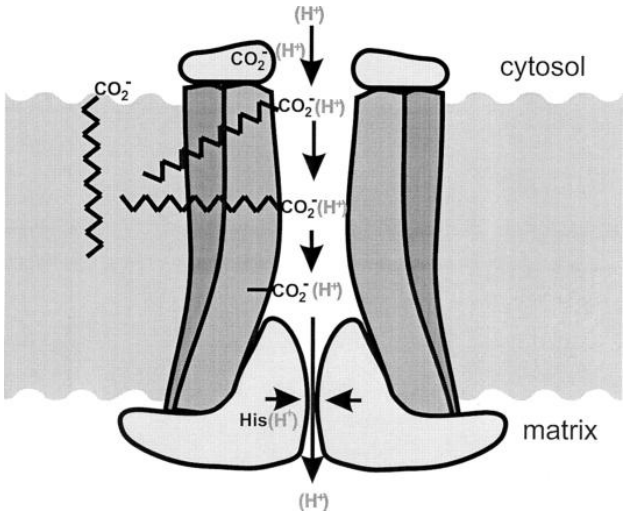

Figure 1.4 A model of the mechanism of H^+ transport by UCP1 and the role of fatty acid.

The fatty acid acts as H^+ donor/acceptor between resident carboxyl groups of UCP1. The H^+ transport path is proposed to consist of a wider aqueous pore and a narrow path lined by the loops protruding from the matrix side. The inhibition of H^+ transport occurs by closure of the narrow path under influence of nucleotide binding (Klingenberg, 1999).

Adipokines

Besides energy storage and release, adipose tissue is also an important endocrine organ, expressing and secreting varieties of bioactive peptides, known as adipokines, which act at both the local (autocrine/ paracrine) and systemic (endocrine) level (Table 1) (Kershaw and Flier, 2004). As early as 1987, adipose tissue was identified as a site for metabolism of sex steroids (Siiteri, 1987) and production of an endocrine factor adipsin, whose expression is severely impaired in obesity (Flier et al., 1987). In 1994, the identification and characterization of leptin demonstrated the role of adipose tissue as an endocrine organ (Zhang et al., 1994).

Table 1.1 Examples of adipocyte-derived proteins with endocrine functions

Cytokines and cytokine-related proteins	Leptin
	TNFα
	IL-6
Other immune-related proteins	MCP-1
Proteins involved in the fibrinolytic system	PAI-1
	Tissue factor
Complement and complement-related proteins	Adipsin (complement factor D)
	Complement factor B
	ASP
	Adiponectin
Lipids and proteins for lipid metabolism or transport	Lipoprotein lipase (LPL)
	Cholesterol ester transfer protein (CETP)
	Apolipoprotein E
	NEFAs
Enzymes involved in steroid metabolism	Cytochrome P450-dependent aromatase
	17βHSD
	11βHSD1
Proteins of the RAS	AGT
Other proteins	Resistin

(Kershaw and Flier, 2004)

Leptin (from Greek leptos, meaning thin) is a 16kD polypeptide containing 167 amino acids with structural homology to cytokines. Adipose tissue secrets leptin in direct proportion to adipose tissue mass and nutritional status, and leptin secretion from subcutaneous adipose tissue is higher than in visceral fat depots (Fain et al., 2004; Wajchenberg, 2000). The expression and secretion of leptin are also regulated by various other factors including insulin, glucocorticoids, TNFα, estrogens and CCAAT/Enhancer Binding Protein α (C/EBPα) which increase leptin level, and β3-adrenergic activity, androgen, free fatty acids and PPARγ agonist which decrease it

(Margetic et al., 2002). The primary function of leptin is to play as a metabolic signal of energy sufficiency rather than excess, thus viewed as an anti-obesity hormone (Flier, 1998).

Tumour Necrosis Factor α (TNFα) also can be expressed and secreted in adipose tissue, by both adipocytes and stromovascular cells (Fain et al., 2004). Adipocytes also express both types of TNFα receptors as membrane bound and soluble forms (Ruan and Lodish, 2003). Adipose tissue expression of TNFα is increased in obese rodents and humans and is positively correlated to adiposity and insulin resistance (Hotamisligil, 2003; Ruan and Lodish, 2003; Seckl and Walker, 2001; Stulnig and Waldhausl, 2004).

A unique adipocyte-derived hormone adiponectin was first identified (Au et al., 1999) in 1995 and it is highly and specifically expressed in differentiated adipocytes and circulates at high level in the bloodstream (Scheffler, 1999). There is a strong and consistent inverse association between adiponectin and both insulin resistance and inflammatory states (Klingenberg, 1999; Scheffler, 1999). Low adiponectin expression is asscoiated with insulin resistance in either obesity or lipodystrophy, and administration of adiponectin improves the metabolic parameters in these conditions (Echtay et al., 1999; Klingenberg, 1999). Another adipocyte-derived hormone is adipsin, which has shown positive correlation with adiposity, insulin resistance, dyslipidemia and cardiovascular disease in human studies (Klingenberg and Huang, 1999).

Around 2001, several research groups identified separately a novel gene named Resistin (resistance to insulin) that was induced during adipocyte differentiation but down-regulated by thiazolidinediones (TZDs) *in vitro* (Fukuda et al., 1987; Naquet et al., 1987; Rektor et al., 1987). *In vivo* studies in rodents confirmed the TZD mediated down-regulation and confirmed the adipose tissue-specific expression of resistin. *In vivo* treatment with recombinant resistin in rodents induces insulin resistance whereas immunoneutralization of resistin has the opposite effect (Fukuda et al., 1987). However, a clear and consistent link between resistin expression in adipose tissue or circulation resistin levels and adiposity or insulin resistance has not been

found in human epidemiological studies. Human resistin only shares 64% homology with murine resistin and is expressed at very low levels in human adipocytes (Klingenspor, 2003).

Apart from the hormones mentioned above, adipose tissue also expresses enzymes involved in the metabolism of steroid hormones, such as cytochrome P450-dependent aromatase, 3β-hydroxysteroid dehydrogenase (HSD) and UDP-glucuronosyltransferases 2B15 (Shammah-Lagnado et al., 1987; Silva et al., 1987), as well as the enzyme 11βHSD1 that primarily determines the adipose tissue-specific glucocorticoid metabolism (Seckl and Walker, 2001; Stulnig and Waldhausl, 2004).

The expression and secretion levels of the hormones and enzymes above are much higher in white adipose tissue compared with those in brown (Farmer, 2008). The studies of adipose tissue as an endocrine organ are still going on to identify and characterize more novel genes and gain further insights into the endocrine function of adipose tissue and the relationship between energy homeostasis and other physiological systems.

1.2.3 Control of adipogenesis

Adipogenesis, defined as the formation of adipocytes, results in growth of adipose tissue. During adipogenesis, precursor cells are devoid of lipid but become committed to the adipocyte lineage and are called preadipocytes. These cells may become quiescent, proliferate to increase the number of committed preadipocytes, or differentiate into mature adipocytes containing lipid droplets (Poulos et al., 2009). Preadipocytes originate from mesenchymal stem cells (MSCs); however, it is uncertain how many intermediate stages there are exactly from MSCs to mature adipocytes (Figure 1.5). Additionally, as none of the intermediate precursor cells possesses any unique morphological characteristics or gene expression markers, the differentiation process from MSCs to preadipocytes is not so well defined as the later stage that starts from preadipocytes (Farmer, 2006; Gesta et al., 2007). Therefore, the adipogenesic process reviewed here will refer to differentiation from preadipocytes to mature adipocytes, which is initiated by specific hormone signals

and involves a cascade of transcriptional events, regulated by the hormonal and nutritional environment.

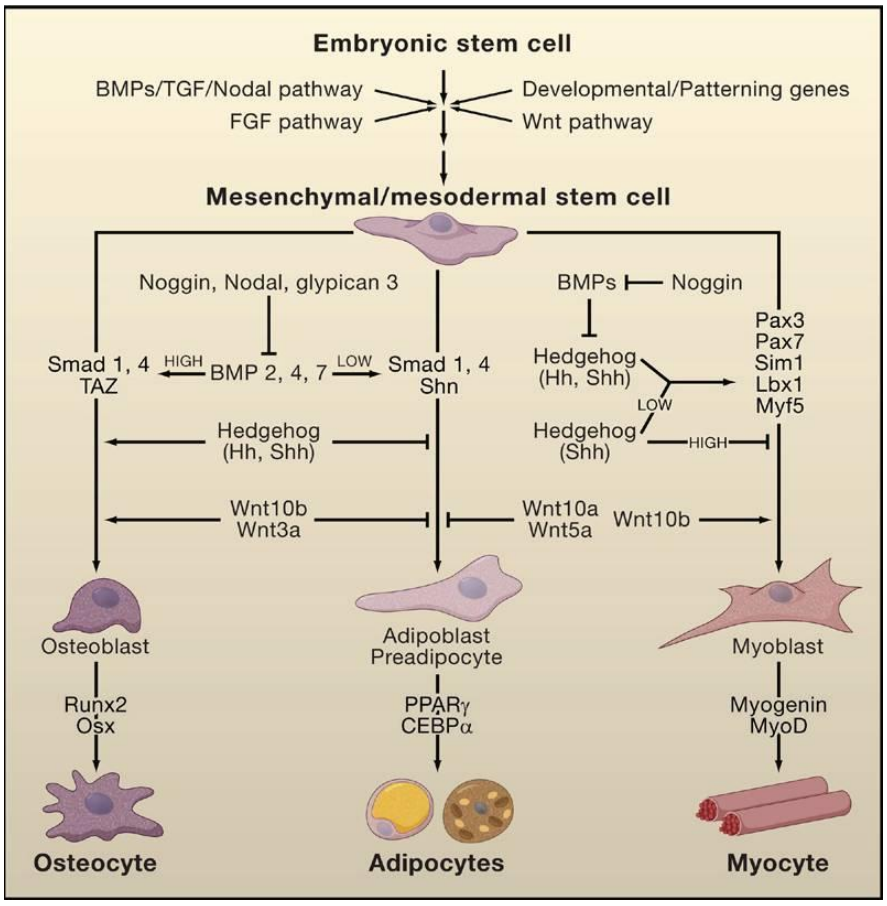

Figure 1.5 Development of mesenchymal/ mesodermal derivatives

Mesenchymal stem cells (MSCs) develop from the mesoderm and then commit into different lineages influenced by a number of factors. Once committed, MSCs give rise to undifferentiated precursors (osteoblast, adipoblast/ preadipocyte, and myoblast), which upon the expression of key transcription factors enter a differentiation programme to acquire their specific functions (Gesta et al., 2007).

The process of adipocyte differentiation has been extensively studied in mouse 3T3-L1 and 3T3-F442A white preadipocye cell lines and immortalized brown preadipocyte cell lines (Rosen and Spiegelman, 2000). Differentiation of preadipocytes can be induced by the adipogenic hormone cocktail containing isobutylmethylxanthine (IBMX), dexamethasone (Dex), insulin, triiodothyronine (T3) and foetal bovine serum (FBS) (Kajimura et al., 2008). Adipogenesis in confluent preadipocytes involves four stages: growth arrest, clonal expansion, early differentiation and terminal differentiation. These stages are controlled by a transcriptional cascade, in which PPARγ and C/EBPα are the most important factors (Farmer, 2006).

The role of PPARγ as the master regulator has been firmly proved from both *in vitro* and *in vivo* studies. The critical early evidence of the important role of PPARγ in regulating adipogenesis was found by Spiegelman and colleagues when trying to elucidate the transcriptional factors regulating expression of the adipose-specific fatty acid binding protein aP2/FABP4. This work resulted in the identification of PPARγ and its heterodimeric partner RXRα (Tontonoz et al., 1994a; Tontonoz et al., 1994b). A series of experiments in which PPARγ is ectopically expressed in nonadipogenic mouse fibroblasts have shown the capability of PPARγ to initiate the entire adipogenic program (Tontonoz et al., 1994c). PPARγ is also required to maintain the terminal differentiated state of adipocytes, and expression of a dominant-negative PPARγ in differentiated 3T3-L1 cells induces differentiation with loss of lipid accumulation and decreased expression of adipocytes markers (Gesta et al., 2007). Likewise, inducible knockout of PPARγ *in vivo* leads to death of brown and white adipocytes (Gesta et al., 2007). There are two isoforms of PPARγ (PPARγ1 and PPARγ2) generated from alternative splicing and PPARγ2 is a fat-specific marker. PPARγ2 null mice still have some white adipose tissue but are insulin resistant, indicating that PPARγ1 can partially compensate for the loss of PPARγ2 in adipogenic function but the capability of PPARγ2 in maintaining insulin sensitivity is independent of its adipogenic ability (Zhang et al., 2004a).

C/EBPα belongs to CCAAT/Enhancer Binding Protein (C/EBP) family and also plays a critical role in adipogenic programme. Like PPARγ, ectopic expression of C/EBPα can also induce adipogenesis in a variety of fibroblasts (Freytag et al., 1994). A tissue-

specific knockout of C/EBPα revealed that C/EBPα is required in the formation of WAT but not in BAT. PPARγ can induce adipogenesis in C/EBPα null mouse embryonic fibroblasts (MEFs), but C/EBPα is not able to drive the adipogenic programme in the absence of PPARγ (Rosen et al., 2002), suggesting that PPARγ and C/EBPα participate in a single pathway of adipose development in which PPARγ is the dominant factor.

Well before the discovery of PPARγ as the master regulator of adipogenesis, much endeavour had been taken to identify the molecular mechanism in adipogenesis and now it is established that a cascade of transcriptional factors eventually leads to the expression of PPARγ and C/EBPα (Farmer, 2006). Work of McKnight and associates indicated the other two members of C/EBP family, C/EBPβ and C/EBPδ, are expressed earlier than C/EBPα during differentiation in 3T3-L1 cells and responsible for regulating C/EBPα expression (Cao et al., 1991; Yeh et al., 1995). Ectopic expression of C/EBPβ in NIH 3T3 fibroblasts, alone or combined with C/EBPδ, induces the expression of PPARγ2 and, following the exposure to PPARγ ligands, facilitates the conversion of these cells into adipocytes (Wu et al., 1996; Wu et al., 1995). However, it has been shown that ectopic expression of C/EBPβ in Swiss fibroblasts is incapable of inducing C/EBPα expression to any significant extent without a potent PPARγ ligand. In support of this proposal, retroviral expression of C/EBPβ in PPARγ null MEFs also fails to stimulate the expression of C/EBPα (Zuo et al., 2006). Therefore it appears that the principal pathway of adipogenesis involves the expression of C/EBPβ and C/EBPδ, which induces PPARγ expression. PPARγ along with these C/EBPs then activate the expression of C/EBPα (Figure 1.6 A) (Farmer, 2005). Since C/EBPβ is so important in regulating the activity as well as the expression of PPARγ during the early phase of adipogenesis, Farmer and associates have done much work in identifying the signalling pathways controlling C/EBPβ activity. They have demonstrated that hormonal stimulation of confluent 3T3-L1 preadipocytes induces a rapid but transient burst of MEK/ERK signalling that coincides with the induction of C/EBPβ expression (Farmer, 2005). Point mutations at a consensus MEK/GSK3 phosphorylation site in the repressor region of C/EBPβ disabled the protein in facilitating PPARγ to activate the expression of C/EBPα and a select set of C/EBPα target genes most notably adiponectin (Figure 1.6 B) (Park et al., 2004). Studies from

Klemm and Lane suggest that cAMP regulatory element (CRE) binding protein (CREB), which is expressed in early stage of 3T3-L1 differentiation, participates in the induction of C/EBPβ expression (Zhang et al., 2004b), thus explaining the need for stimulating cAMP intracellular levels using IBMX in the adipogenic cocktail.

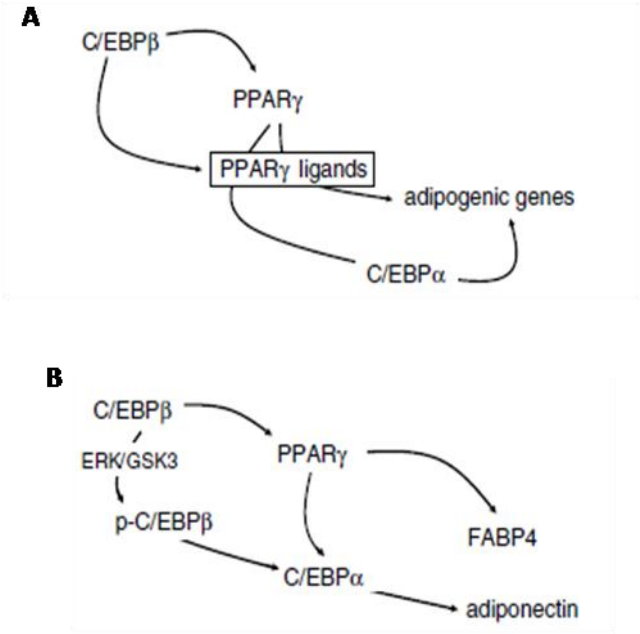

Figure 1.6 Role of C/EBPβ in regulating PPARγ expression and activity.

(A) Stimulation of C/EBPβ in response to exposure of preadipocytes to adipogenic hormones induces expression of PPARγ and leads to the production of PPARγ ligands. Activated PPARγ controls terminal adipogenesis by inducing expression of C/EBPα, which is required for the production of specific adipogenic genes (Farmer, 2005). (B) Phosphorylation of C/EBPβ at a consensus ERK/GSK site is required for the PPARγ-associated induction of C/EBPα and adiponectin expression (Farmer, 2005).

Additional factors in parallel pathways are also likely to be involved in activating PPARγ, at a stage downstream of C/EBPβ and C/EBPδ, such as the transcription factor sterol regulatory element binding protein 1c (SREBP1c). The expression of SREBP1c is significantly increased in 3T3-L1 adipocytes in response to insulin (Kim et al., 1998a). Ectopic expression of a dominant-negative SREBP1c inhibits preadipocyte differentiation, whereas the overexpression of this protein significantly enhanced the adipogenic activity of PPARγ (Kim and Spiegelman, 1996). Additional studies suggest that SREBP1c contributes to the production of PPARγ ligands, therefore facilitating the activation of PPARγ (Kim et al., 1998b). Studies on the functions of signal transducers and activators of transcription (STAT) proteins also provide support for the additional pathway regulating adipogenesis. Ectopic expression of STAT5A in non-adipogenic fibroblasts induces preadipocyte differentiation, including PPARγ activation and accumulation of lipid droplets (Floyd and Stephens, 2003).

The transcription factors responsible for adipogenesis are in turn orchestrated by the hormonal and neural environment (Gesta et al., 2007). In rodents, the sympathetic nervous system has opposing role in the recruitment and development of BAT and WAT. Differentiation of brown preadipocytes is significantly enhanced by adrenergic agents such as norepinephrine, while the proliferation and differentiation of WAT is stimulated by sympathetic denervation (Cousin et al., 1993). Adrenergic stimulators induce proliferation and differentiation of brown preadipocytes, protect mature brown adipocytes from apoptosis and increase thermogenic capacity via induction of UCP1 gene expression (Cannon and Nedergaard, 2004). Chronic cold exposure and feeding increase BAT activity via norepinephrine from sympathetic nervous system, and UCP1 expression can also be stimulated by thyroid hormone, insulin, TZD, retinoic acid (RA), cAMP and β-adrenergic agonists (Diehl and Hoek, 1999). On the contrary, glucocorticoids inhibit UCP1 expression in response to adrenergic stimulation (Soumano et al., 2000).

1.2.4 Transdifferentiaton between WAT and BAT and the origin debate

The term transdifferentiation has been used to define both a direct transformation from one cell to another with different morphology and function and to define an unusual differentiation fate from a stem cell that usually differentiates into a

different lineage (Tosh D., 2002). *In vivo* studies suggest that white adipocytes of the murine adipose organ can undergo a true reversible transdifferentiation process to brown adipocytes in physiological conditions (Himms-Hagen et al., 2000). A large amount of evidence has also been provided that chronic cold exposure induces the emergence of brown adipocytes in WAT depots in rodents (Cinti, 2001). In these conditions, the appearance of brown adipocytes in subcutaneous WAT is much more significant than that in visceral WAT (Barbatelli et al., 2010). About 17% of the adipocytes in all WAT depots of Sprague-Dawley rats become more brown like after the treatment with β3-adrenoceptor agonist CL-316, 243 for 7 days (Figure 1.2 A) (Cinti, 2009b). Chronic treatment with PPARγ agonist rosiglitazone also induces PGC1α expression and mitochondriogenesis as well as norepinephrine-augmentable UCP1 expression in epididymal WAT depots (Petrovic et al., 2009). Studies from Karamanlidis and associates indicate that overexpression of the transcription factor C/EBPβ in white preadipocyte cell line 3T3-L1 reprograms the cells towards a brown fat lineage by rescuing the cAMP-induced expression of PGC1α and UCP1 (Karamanlidis et al., 2007). Recently, PRDM16 is also shown to stimulate a select set of BAT genes when overexpressed and in association with a PGC1α/β complex in white 3T3-F442A preadipocytes (Kajimura et al., 2008). Although the hypothesis of reversible physiological transdifferentiation (Cinti, 2009a) could at least partly explain the plasticity of the appearance of brow adipocytes in WAT, without signs of apoptosis, direct evidence using lineage tracing studies are needed.

The observation of WAT-BAT conversion also implies a “common origin” hypothesis of white and brown adipocytes. Despite the distinct morphology and functions, white and brown adipocytes were originally considered differentiated from common precursor cells (adipoblasts or preadipocytes) derived from mesenchymal stem cells (Figure 1.5) (Gesta et al., 2007). However, *in vivo* fate mapping studies showed that in BAT depots, brown, but not white, fat cells arise from precursors expressing Myf5, a gene previously thought to be expressed only in the myogenic lineage (Seale et al., 2008). The striking discovery suggests that brown adipocytes have a closer relation with skeletal muscle cells other than white adipocytes. Further studies identified that the PRDM16-C/EBPβ transcriptional complex initiates the switch from myoblasts to

brown adipocytes (Kajimura et al., 2009), which enhanced the concept that brown fat and muscle share the common origin.

The debate about the transition between WAT and BAT has spurred questions about the origin and molecular characteristics of the UCP1-expressing cells observed in the classic white adipose tissue depots under certain physiological or pharmacological conditions. Petrovic and colleagues suggested that although the functional thermogenic genes are expressed, the brown-like cells appearing in WAT depots are devoid of transcripts for the novel transcription factors now associated with classic brown adipocytes (Zic1, Lhx8, Meox2 and characteristically PRDM16) or for myocyte-associated genes (myogenin and muscle-specific microRNAs) and retain white fat characteristics such as Hoxc9 expression. Co-culture experiments verified that the UCP1-expressing cells from WAT, are not proliferating classic brown adipocytes, hence constituting a subset of adipocytes called “brite” (brown-white) with a developmental origin and molecular characteristics distinguishing them as a separate class of cells (Figure 1.7) (Petrovic et al., 2009).

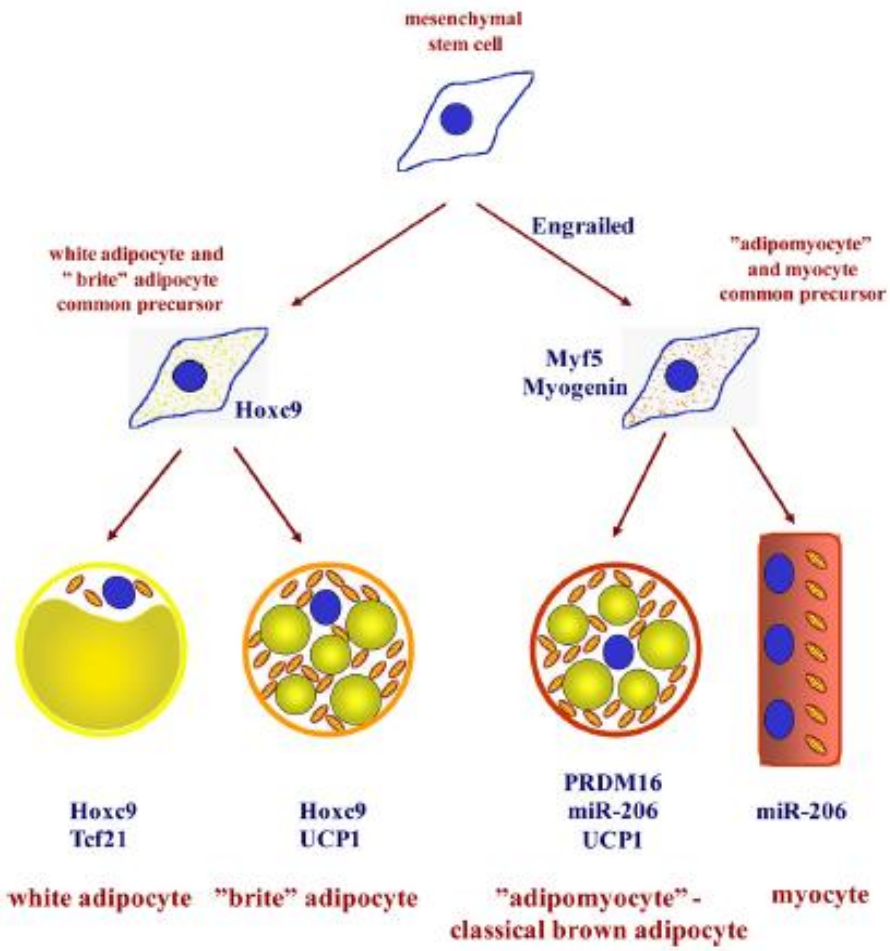

Figure 1.7 Subtypes of adipocytes and their origins

There are at least three distinguished types of adipocytes: the classic brown adipocytes (the adipomyocytes), the brite adipocytes (i.e. the brown adipocyte-like adipocytes induced in white adipocyte cultures), and the genuine white adipocytes. The adipomyocytes share their origin with myocytes, whereas brite and white adipocytes have a different origin (Petrovic et al., 2009).

1.3 TRANSCRIPTIONAL CONTROL OF UCP1 AND THE REGULATION OF THERMOGENESIS IN BAT

As mentioned above, the adaptive non-shivering thermogenesis in brown adipose tissue is mediated mainly by a brown fat marker gene UCP1. This 32kD protein was first identified in 1978 from hamster brown adipose tissue mitochondria (Nicholls et al., 1978). The regulatory promoter region of UCP1 gene has now been studied in several species, defining a conserved region as a strong enhancer responsible for tissue-specific and cAMP-dependent expression (Cassard-Doulcier et al., 1993; Kozak et al., 1994; Sears et al., 1996). This enhancer contains a canonical PPAR-responsive element (PPRE) and two putative cAMP-responsive elements (CREs), to bind with various candidate transcription factors, most notably PPARγ-RXRα heterodimer, being proposed to regulate this enhancer region (Cao et al., 2001; Sears et al., 1996).

Adaptive thermogenesis in BAT, with the most notable features of the increasing number of mitochondria (mitochondriogenesis) and the stimulated expression of UCP1, is controlled by the sympathetic nervous system (SNS) through the activation of β-adrenergic receptors (βARs). It is well established that βARs couple to G proteins and adenylyl cyclase, resulting in the elevated level of intracellular cAMP and activation of cAMP-dependent protein kinase A (PKA), which has been considered as the ultimate component activating lipolytic enzymes and expression of UCP1 and PGC1α. However, besides this classic pathway, additional signalling pathways emanate from βARs have also been reported, including the ERK and p38 mitogen-activated protein (MAP) kinase pathways (Cao et al., 2004; Kumar et al., 2007; Robidoux et al., 2006). Additionally, the synthetic TZD PPARγ agonists have also been shown to play a positive regulatory role in converting adipocytes in WAT more brown like by activating thermogenic genes like UCP1 and promoting mitochondrial biogenesis (Petrovic et al., 2009), suggesting the thermogenesis programme is regulated by multiple signalling transduction pathways.

In terms of gene expression regulation, there has been an explosion of information relating to the transcriptional control of UCP1, the hallmark gene in BAT. Several nuclear factors have been associated with the expression of UCP1. Until the recent discovery of PRDM16, the most notable was PGC1α, which also can be stimulated by

chronic cold exposure and hence is a thermoregulatory gene itself. This co-activator of PPAR greatly increases transcriptional activity of PPARγ and the thyroid hormone receptor on UCP1 promoter (Puigserver et al., 1998). Since several studies have proved that exposure of white adipocytes to potent PPARγ ligands induces a "browning" of the cells, which is likely due to a PPARγ ligand-associated induction of mitochondrial genes including UCP1 and cytochrome oxidase (Cox) (Wilson-Fritch et al., 2003; Wilson-Fritch et al., 2004), the transcription factor PPARγ is obviously playing a critical role in regulating UCP1 expression as well. PRDM16, screened from a global expression analysis of murine transcriptional components using white and brown tissue RNAs, is considered as a master regulator of brown adipogenesis and thermogenesis. C/EBPβ has been reported to reprogramme white preadipocytes into a brown-like phenotype (Karamanlidis et al., 2007) and to be involved in the muscle to brown fat cell switch (Kajimura et al., 2009), but the stimulating mechanism has not been clearly defined yet. Apart from the positive regulating nuclear factors, there are also a set of repressors which participate in the control of UCP1 transcription. CtBP-1 and CtBP-2 act as dimers with various sequence-specific DNA-binding transcriptional repressors to form complexes that recruit repressive histone modifying enzymes, which has a general inhibitory effect on the expression of the multiple genes involved in BAT adipogenesis and thermogenesis (Chinnadurai, 2007). RIP140 is another corepressor for nuclear receptors that suppresses a broad programme of metabolic genes and plays an essential role in both DNA and histone methylation of UCP1 gene (Kiskinis et al., 2007). Finally, the nuclear receptor Liver X Receptor α (LXRα) is also reported as a cAMP- and oxysterol- dependent transcriptional repressor of UCP1 (Collins et al., 2010).

1.3.1 Signalling pathways

The sympathetic nervous system controls adaptive thermogenesis in brown adipose tissue through the activation of β-adrenergic receptors. All three known βAR subtypes are expressed in adipocytes, but the main and best defined signalling pathway stimulating adaptive thermogenesis is mediated by β3-adrenergic receptor (β3AR). Studies from Cao and associates indicated that the β3AR stimulates p38 mitogen-activated protein kinase (p38 MAPK) via protein kinase A (PKA) in adipocytes and that

cAMP-dependent transcription of the mitochondrial UCP1 promoter by β3AR requires p38 MAPK. The selective β3AR agonists activate p38 MAPK in a time- and dose-dependent manner and the activation can be blocked by the specific p38 MAPK inhibitor as well as the PKA inhibitors, confirming the involvement of PKA in β3AR-dependent p38 MAPK phosphorylation (Cao et al., 2001). The activated p38 MAPK phosphorylates activating transcription factor 2 (ATF2) and PGC1α, and controls the expression of UCP1 gene through their respective interactions with a CRE and PPRE that both reside within a critical enhancer motif of the UCP1 gene. Activation of ATF2 by p38 MAPK additionally serves as the cAMP sensor that increases expression of the PGC1α gene itself in brown adipose tissue (Cao et al., 2004; Robidoux et al., 2005). Therefore, p38 MAPK plays a central role in the cAMP signalling mechanism in promoting brown fat adaptive thermogenic programme including up-regulation of UCP1 expression (Figure 1.8) (Collins et al., 2010).

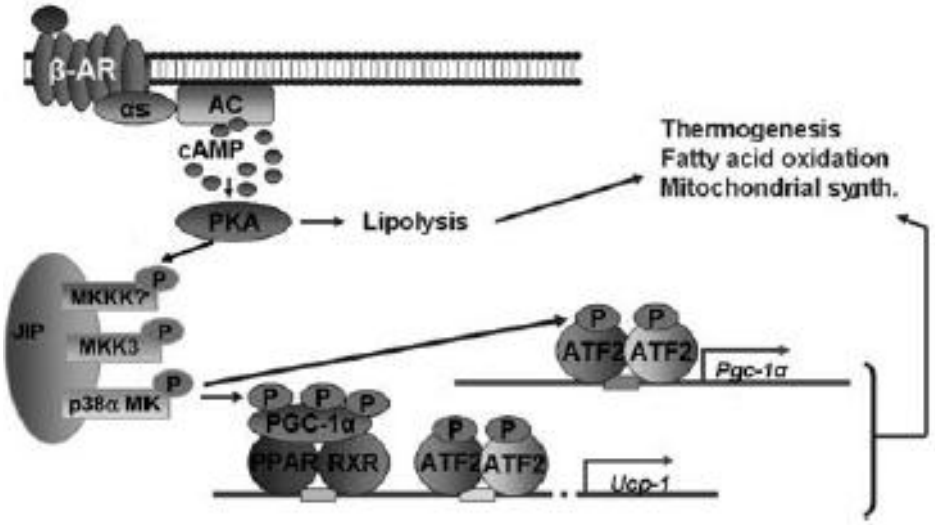

Figure 1.8 β-adrenergic receptor (βAR) activation of p38 MAP kinase in brown adipocytes activates the transcription of UCP1 and PGC1α gene for adaptive thermogenesis, mitochondrial biogenesis and fatty acid oxidation.

Direct target of p38 MAP kinase include the PGC1α coactivator and the transcription factor ATF-2. The biochemical steps (dashed arrow) between PKA and the p38 MAP kinase model are not yet defined, but current results indicate that the p38α isoform and MAP kinase-3 (MKK3) are required, together with a JIP scaffold (Collins et al., 2010).

The synthetic PPARγ ligand rosiglitazone has been shown to have the capacity of up-regulating UCP1 expression as well as the respiratory rate in brown adiocytes of rats (Teruel et al., 2005). In 2008, Petrovic and colleagues suggested a PPARγ pathway that is norepinephrine-independent but stimulates fully competent mechanism for BAT recruitment. They treated the brown preadipocytes with rosiglitazone continuously and observed an accelerated brown adipogenic process in terms of morphology and adipogenic marker aP2 expression, as well as the significantly enhanced expression of UCP1 and PGC1α even in the absence of norepinephrine. Likewise, mitochondria biogenesis is also enhanced by rosiglitazone treatment, and enables brown adipocytes to respond to the addition of norepinephrine with a large increase of oxygen consumption in a UCP1-dependent manner (Petrovic et al., 2008). Subsequently, the same group of investigators demonstrated that PPARγ activation (by rosiglitazone treatment) enables white preadipocyte cultures to acquire brown adipocyte-like characteristics at both morphological and molecular levels, although these brown-like cells were proposed to be a separate set of adipocytes ("brite" cells) different from traditionally classified brown or white adipocytes (Petrovic et al., 2009). This PPARγ mediated signalling pathway of stimulating UCP1 expression and BAT thermogenesis is not so well defined yet, but it might be the cellular explanation for the enigmatic BAT recruitment mechanism in prehibernation and prenatal states when the cAMP-dependent pathway is not functional (Petrovic et al., 2008).

It is therefore interesting to investigate the interactions between these two pathways. In fact, well before the PPARγ-dependent pathway was suggested, the effects of norepinephrine treatment on PPARγ gene expression had already been investigated. In the brown preadipocyte cell line HIB-1Bs, both a noradrenaline-induced decrease (Sears et al., 1996) and a noradrenaline-induced increase (Valmaseda et al., 1999) in PPARγ mRNA levels have been noted (4-5 hours after stimulation), perhaps reflecting variability in the characteristics and phenotypic drift in the cell line. A repressive effect of norepinephrine on PPARγ expression was also observed in primary brown (pre)adipocytes. PPARγ mRNA levels are down-regulated by noradrenaline treatment in both proliferating and differentiating primary brown (pre)adipocytes, with a lagtime of 1 hour and lasting up to 4 hours, after which expression gradually recovers.

The down-regulation is βAR induced and mediated via cAMP and PKA, but surprisingly independent of p38 MAPK, as the addition of p38 MAPK inhibitor to the noradrenaline-treated culture has no significant effect on the noradrenaline-induced repression of PPARγ expression (Lindgren et al., 2004). However, *in vivo* studies in lean and ob/ob mice demonstrated that a non-TZD PPARγ agonist 2-(2-(4-phenoxy-2-propylphenoxy)ethyl)indole-5-acetic acid (COOH)-pretreated mice have stronger responses to β3AR agonist stimulation in terms of thermogenesis, thus PPARγ agonism increases the thermogenic potential in white and brown adipose depots in both lean and obese mice under β-adrenergic stimulation (Sell et al., 2004). Also reflecting a positive correlation between the two mechanisms, the recent studies from Festuccia and colleagues indicated that the maximal UCP1 expression induced by PPARγ *in vivo* depends on the presence of basal BAT adrenergic tone. Cold exposure significantly increases UCP1 mRNA levels in innervated BAT pads of untreated rats without affecting the already high BAT UCP1 levels of rosiglitazone treated animals. A similar pattern is found in denervated pads, but with markedly lower UCP1 expression than that in the innervated pads (Festuccia et al., 2010). Although the interaction between the two pathways has not been clearly elucidated, the current studies have implied that they are not independent of each other, but have some manners of cross-talking, co-ordinately regulating the adaptive thermogenesis in brown adipose tissue.

1.3.2 Peroxisome Proliferator-Activated Receptors (PPARs)

The peroxisome proliferator-activated receptors (PPARs) are lipid-activated transcription factors involved in the regulation of lipid metabolism and adipocyte differentiation. All the three subtypes of PPARs (α, γ and δ) are expressed in brown adipocytes (Valmaseda et al., 1999). PPARs are activated in a ligand-dependent way and once activated, heterodimerize with the retinoid X receptors (RXRs) and regulate the transcription of target genes after binding to specific binding sites (PPREs). The PPAR-RXR heterodimer is responsive to both retinoic acids and PPAR activators such as fatty acids, peroxisome proliferators and TZD antidiabetic agents (Keller et al., 1993; Kliewer et al., 1992).

PPARγ has been described as the master regulator in adipogenesis, and thus has high expression levels in both white and brown adipocytes. Furthermore, studies involving the positive role of PPARγ agonist in stimulating UCP1 expression (as described above) indicate that PPARγ agonists not only promote differentiation and thus enable UCP1 gene expression but also, by themselves, can induce UCP1 to the full extent (Villarroya et al., 2007). The ability of the UCP1 gene to respond to PPARγ agonists resides in the distal complex enhance of this gene. This complex includes a PPRE which localized at -2458 to -2485 in mouse with a similar localization in rat and human UCP1 enhancers (Figure 1.9) (Cannon and Nedergaard, 2004).

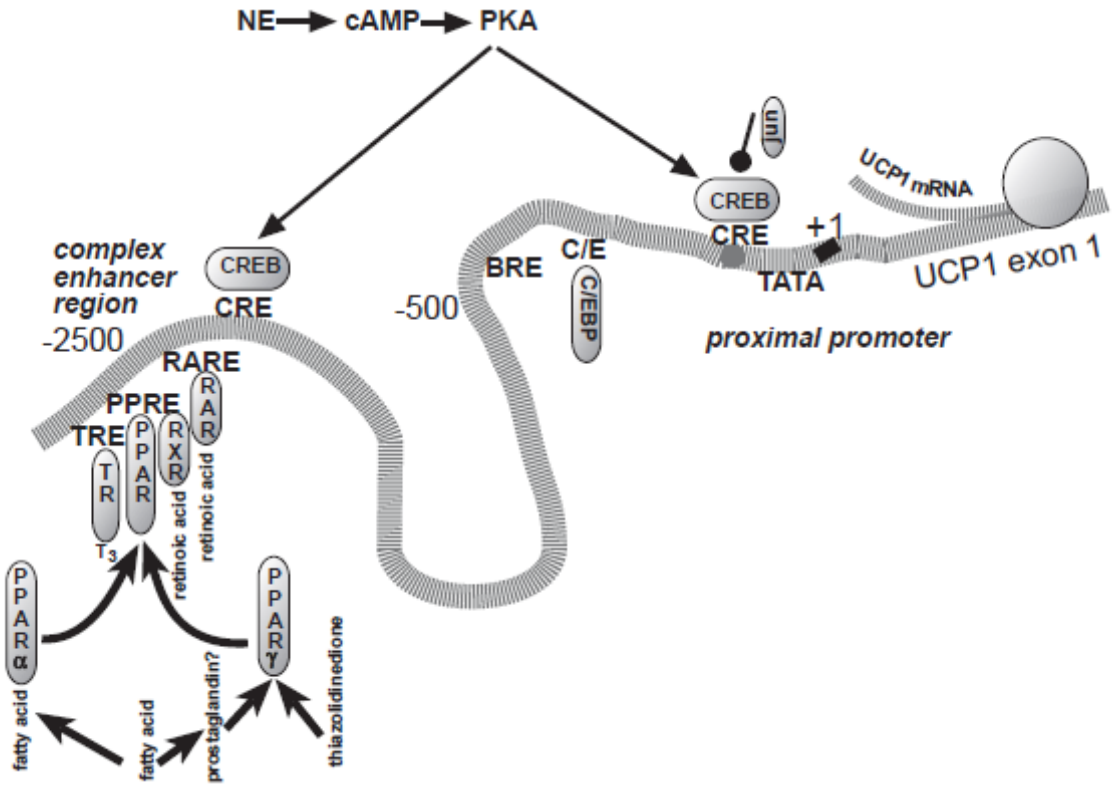

Figure 1.9 Factors controlling UCP1 gene expression.

The top part indicates the direct pathway for norepinephrine-induced UCP1 gene expression; the bottom part summarizes the presence of other transcription factors and response elements than those involved in the direct norepinephrine effect. Two regulation regions have been characterized: a proximal promoter and a distal, complex enhancer region. The proximal promoter region contains a cAMP response element (CRE) and two C/EBP sites (C/E). A complex enhancer region exists around -2500 in rodents, containing many response elements within a short sequence, some of which are even overlapping. CRE, retinoic acid response elements (RARE), PPAR response element (PPRE) and thyroid hormone response element (TRE) have all been found to locate here (Cannon and Nedergaard, 2004).

The PPRE in UCP1 promoter can bind to both PPARγ and PPARα, and also both PPARγ and PPARα agonists can induce UCP1 expression (Barbera et al., 2001). PPARα is only found in brown and not in white adipocytes (Escher et al., 2001; Gorla-Bajszczak et al., 2000), and it is first expressed when brown adipocytes are maturing (Valmaseda et al., 1999). Based on the general concept of PPARα as a transcription factor for lipid metabolism, it would be expected that PPARα was the principal PPAR isomer inducing UCP1 expression, and not PPARγ as discussed above. However, these earlier studies in the brown preadipocyte HIB-1B cells indicating PPARγ as the main regulator of UCP1 have been influenced by the fact that HIB-1B cells do not express PPARα (Nedergaard et al., 2005). Furthermore, the acute effects of injection of PPARα agonists seem larger than that of injection of PPARγ agonists in virgin mice (Pedraza et al., 2001). In support of the idea that PPARγ may not be as essential for UCP1 expression as generally considered is the observation that animals with no PPARγ expression in brown adipose tissue exhibit no decrease in UCP1 expression in differentiated brown adipocytes (He et al., 2003), suggesting at least in such a system, that PPARγ is not essential for UCP1 expression. On the contrary, there is an impaired activation of UCP1 gene expression in PPARα-null mice in several physiological situations associated with cold stress (Villarroya et al., 2007). Finally, the PPAR co-activator 1α (PGC1α, see below) can coordinate both PPARγ and PPARα in the transcriptional control of genes in adipogenesis, thermogenesis and lipid metabolism in brown fat (Villarroya et al., 2007).

1.3.3 PGC1α

Peroxisome proliferator-activated receptor (PPAR) co-activator 1α (PGC1α) was first identified as a PPARγ-interacting protein preferentially expressed in mature brown adipocyte rather than white adipocytes (Puigserver et al., 1998). PGC1α expression is highly induced and activated in brown adipocytes in response to cold exposure or β-adrenergic agonist, mediated by a cAMP-PKA signalling pathway (Cao et al., 2004; Herzig et al., 2001). Besides, PGC1α expression in adipocytes is controlled by an autoregulatory loop via PPARγ activation. Specifically, TZDs and retinoids induce PGC1α expression due to the presence of a PPRE in the distal region of PGC1α gene promoter that binds PPARγ/RXR heterodimers, and the elevated PGC1α further

coacitvates PPARγ in response to the TZDs, hence forming a positive autoregulatory loop controlling PGC1α expression (Hondares et al., 2006). PGC1α has been proposed as the dominant regulator of mitochondrial biogenesis and oxidative metabolic pathways in many cell types via its co-activation of various transcription factors, notably PPARα and PPARγ(Finck and Kelly, 2006; Handschin and Spiegelman, 2006; Lin et al., 2005; Rosen and MacDougald, 2006). Ectopic expression of PGC1α in white adipocytes induces expression of a number of mitochondrial and thermogenic genes, including UCP1 (Puigserver et al., 1998; Tiraby et al., 2003), therefore it is widely accepted that PGC1α is essential for brown adipocyte differentiation and induction of the UCP1 gene.

Several genes have been reported to influence brown fat development and function, at least in part, through regulating the expression or transcriptional activity of PGC1α. One example is the corepressor RIP140, which binds PGC1α directly and blocks its transcriptional activity on several gene promoters shared by PGC1α and RIP140, including a brown fat selective gene CIDEA (cell-death inducing DFFA-like effector A) (Hallberg et al., 2008). The steroid receptor co-activator (SRC) family members, including SRC-1, 2 and 3, have distinct and overlapping functions in controlling energy metabolism and brown fat development (Louet and O'Malley, 2007). SRC-1 reinforces the coactivation of PGC1α on PPARγ; therefore its ablation in mice caused impaired thermogenesis with reduced UCP1 expression in BAT. In contrast, SRC-2 inhibits the interaction of PPARγ with PGC1α, so its knockout in mice displays improved energy expenditure and higher adaptive thermogenesis (Picard et al., 2002). PGC1α action is reduced by acetylation and, interestingly, SRC-3 induces GCN5, the major acetyltransferase acting on PGC1α to repress its transcriptional activity (Lerin et al., 2006). Ablation of SRC-3 reduces acetylation of PGC1α, leading to an increase in mitochondria biogenesis (Coste et al., 2008; Louet et al., 2006). Retinoblastoma protein (pRb) also has been shown to repress PGC1α transcription by directly binding to its promoter (Scime et al., 2005), thus adipocytes from pRb-deficient fibroblasts or embryonic stem cells exhibit a brown fat phenotype with high mitochondrial content, and elevated expression of UCP1, PGC1α and mitochondrial genes (Hansen et al., 2004).

Taken together, these data suggested a dominant role of PGC1α in BAT development and function. In fact, both *in vivo* and *in vitro* studies have shown that genetic ablation of PGC1α greatly reduces capacity for adaptive thermogenesis in response to cold exposure or cAMP(Lin et al., 2004; Uldry et al., 2006). However, many non-cAMP-dependent brown adipocyte-selective genes are still expressed in PGC1α knockout models, and the fat differentiation programme itself is not greatly altered (Seale et al., 2009), implying that although PGC1α is crucial in regulating adaptive thermogenesis, it doesn't determine the cellular specification of brown adipocytes.

1.3.4 PRD1-BF-1-RIZ1 Homologous Domain Containing Protein 16 (PRDM16)

PRDM16 is a 140kD zinc finger protein originally identified at a chromosomal breakpoint of t(1; 3)(p36; q21)-positive human acute myeloid leukaemia cells, also named as MEL1 in humans (Mochizuki et al., 2000). PRDM16 is highly enriched in brown adipocytes compared to white adipocytes. When ectopically expressed in WAT preadipocytes or myoblasts, PRDM16 induces nearly complete brown adipogenic programme, including mitochondrial biogenesis, increased cellular respiration and expression of brown fat-selective genes, both the cAMP-inducible thermogenic genes (UCP1, PGC1α and Deiodinase-d2) and those not sensitive to cAMP such as CIDEA and Elovl3 (Seale et al., 2007). Furthermore, transgenic expression of PRDM16 in adipose tissue increases the formation of multilocular brown-like fat pockets in WAT depots in response to β-adrenergic agonist (Kajimura et al., 2010).

PRDM16 was previously shown to directly bind to a specific DNA sequence through two sets of zinc fingers (ZF1 and ZF2 domains, Figure 1.10) *in vitro* (Nishikata et al., 2003). However, abrogation of DNA binding using a point mutation did not alter the ability of PRDM16 to induce the brown fat phenotype compared to the wild-type protein, suggesting that PRDM16 was not working as a classical DNA-binding transcription factor. Further studies demonstrated that PRDM16, in addition to inducing PGC1α gene expression, directly binds to PGC1α and PGC1β to increase their transcriptional activities (Seale et al., 2007). In fact, PRDM16 interacts with a number of DNA-binding transcription factors such as PPARα, PPARγ, p53 and several members of the C/EBP family via one or more of PRDM16 zinc finger domains, resulting in

powerful coactivation of their transcriptional activities (Figure 1.11) (Kajimura et al., 2009; Seale et al., 2008).

Figure 1.10 structure of human MEL1 (PRDM16) gene

PRD indicates PR domain; DBD1, DNA-binding domain 1 (zinc finger 1, ZF1); PRD, proline rich domain; RD, repressor domain; DBD2, DNA-binding domain 2 (ZF2); AD, acidic domain (Nishikata et al., 2003).

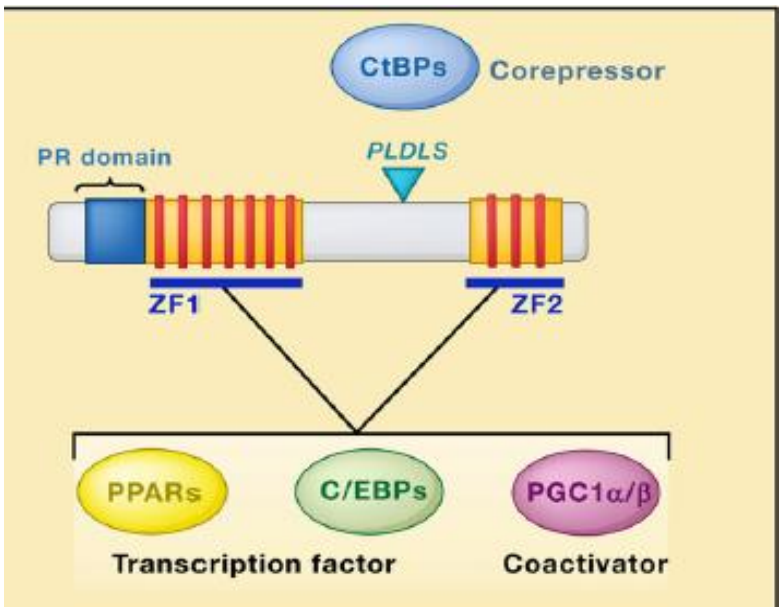

Figure 1.11 Interaction between PRDM16 and other transcriptional regulators

PRDM16 directly interacts with canonical transcription factors such as PPARγ, PPARα and C/EBP family members and transcriptional co-activators PGC1α and PGC1β through the two sets of zinc finger domains (ZF1 and ZF2). PRDM16 is also associated with the co-repressor CtBP-1/2 through its PLDLS motif (Kajimura et al., 2010).

PRDM16 represses the expression of white fat-selective genes by forming a transcriptional holocomplex with the well-known co-repressor proteins C-terminal-binding-protein-1 (CtBP-1) and CtBP-2. The repression occurs through recruiting the PRDM16/CtBP complex onto the promoters of white fat-specific genes such as resistin, and is abolished in the genetic absence of CtBP-1 and CtBP-2. PGC1α and PGC1β compete with CtBP-1/2 for binding to PRDM16 and once bound the PRDM16/PGC1α/β complex can powerfully activate brown fat genes such as PGC1α itself (Kajimura et al., 2008). Therefore, PRDM16 switches off white fat gene expression through docking with CtBP-1/2 and switches on brown fat gene expression by the activation of PGC1α/β mediated via direct protein-protein binding.

Loss of PRDM16 from brown preadipocytes not only causes nearly total loss of brown fat characteristics, but also, surprisingly, promotes skeletal myotube differentiation in culture with the features of formation of syncytia and ectopic activation of skeletal muscle-specific genes such as Myf5 and Myod. *In vivo* studies further confirmed this as BAT from PRDM16-deficient mice exhibits an abnormal morphology with reduced expression of brown fat-selective marker genes and elevated expression level of skeletal muscle-specific genes. Conversely, expression of PRDM16 in myogenic precursors drives a robust and functional programme of brown adipogenesis (Seale et al., 2008). The molecular mechanism of this brown fat/muscle switch was further investigated and evidence was provided that PRDM16 forms a transcriptional complex with the active form of C/EBPβ (also known as LAP), acting as a critical molecular unit that controls the cell fate switch from myoblastic precursors to brown adipocytes. Depletion of C/EBPβ significantly blunts the ability of PRDM16 to induce the brown adipogenesis and BAT from C/EBPβ-deficient mice displays a similar molecular signature to BAT from PRDM16-deficient mice, with reduced expression of BAT-selective genes and increased expression of skeletal muscle-specific genes (Kajimura et al., 2009). Taken together, these data indicate that a PRDM16-C/EBPβ complex controls the initiating events of the conversion from myoblastic precursors to brown adipocytes (Figure 1.12). Additionally, the combination of these two factors is sufficient to induce a fully functional brown fat programme in nonadipogenic cells such as embryonic fibroblasts and skin fibroblasts from mouse and man, with

extremely high oxygen consumption and high expression of brown fat-selective genes including UCP1 and PGC1α (Kajimura et al., 2009).

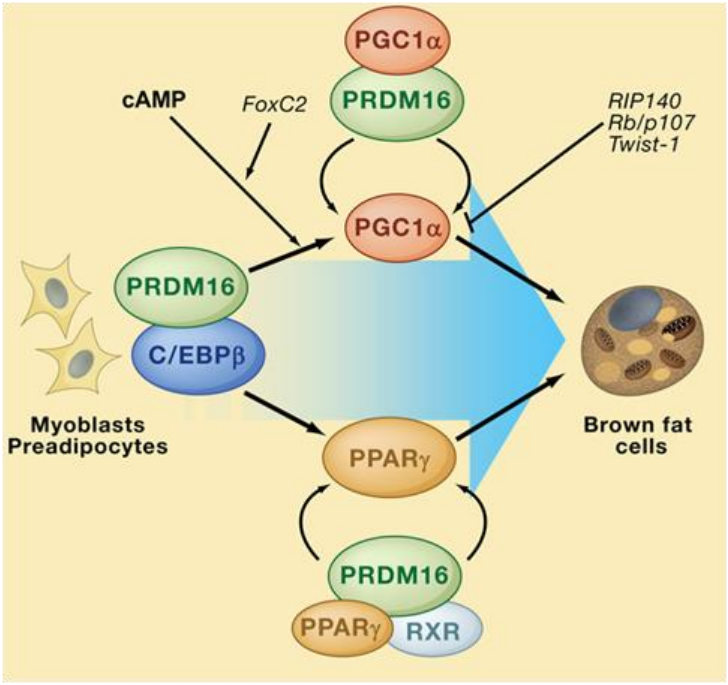

Figure 1.12 PRDM16-C/EBPβ transcriptional complex acts in Myf5-positive myoblastic precursors or preadipocytes to induce the expression of PPARγ and PGC1α.

PRDM16 coactivates PPARγ and PGC1α, which then drives a brown fat differentiation programme. The cAMP-dependent thermogenic gene programme is potentiated by FoxC2 and PRDM16. RIP140, Rb/p107 and TWIST1 antagonize the expression or transcriptional activity of PGC1α and repress brown adipogenic programme (Kajimura et al., 2010).

In conclusion, PRDM16 plays as a brown fat-specific determinant to induce the expression of genes associated with mitochondrial biogenesis, oxidative phosphorylation and oxidation of lipids, thus determining the thermogenic characteristics of brown adipocytes, although might not directly related to adipogenesis of BAT.

1.3.5 CCAAT/Enhancer Binding Protein β (C/EBPβ)

C/EBPs encompass a family of transcription factors containing basic leucine zipper (bZIP) domains that allow homo- and hetero- dimerization with bZIP transcriptional factors as well as DNA-binding elements (Lekstrom-Himes and Xanthopoulos, 1998). Several members of C/EBP family (e.g. C/EBPα, C/EBPβ and C/EBPδ) have tissue-restricted expression patterns and have been involved in the regulation of energy homeostasis (Cao et al., 1991; Roesler, 2001). C/EBPβ is most abundantly expressed in liver, BAT, WAT, reproductive tract and mammary gland (Akira et al., 1990; Descombes et al., 1990; Poli et al., 1990). There are two isoforms of C/EBPβ generated from a single exon mRNA by alternative translation, the full-length active form named LAP (liver-enriched transcriptional activatory protein, the active C/EBPβ isoforms, MW=35kD(LAP) or 38kD (LAP*)) and the truncated protein LIP (liver-enriched transcriptional inhibitory protein, the inhibitory C/EBPβ isoform, MW=21kD), which lacks the transactivation domain and acts as a dominant negative regulator of LAP (Descombes and Schibler, 1991) (Figure 1.13).

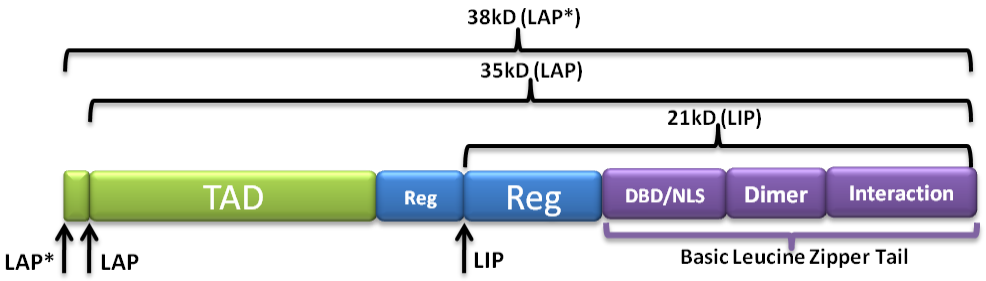

Figure 1.13 Schematic structure diagrams of C/EBPβ isoforms

The active isoforms of C/EBPβ LAP* and LAP, as well as the inhibitory isoform LIP are translated from a single exon mRNA by alternative translation. All the three isoforms share a regulatory domain (Reg) and the basic leucine zipper tail (bZIP) containing a DNA binding domain (DBD) that also serves as primary nuclear localization signal (NLS), a dimerization domain (Dimer) and an interaction domain that directly interacts with acidic DNA (negative charged). These common components constitute the inhibitory isoform LIP and both active isoforms also contain transcription activation domain (TAD) which makes them active in facilitating the transcription of some certain genes.

C/EBPβ, as reviewed above, activates PPARγ by inducing a programme leading to the synthesis of PPARγ co-activators, thus inducing a cascade of adipogenic events. The phosphorylation of C/EBPβ is essential for the expression of C/EBPα by PPARγ and a set of C/EBPα target genes (Farmer, 2005). As a crucial regulator of the two essential adipogenic regulators PPARγ and C/EBPα, C/EBPβ not only plays important roles in adipogenesis of both WAT and BAT, it also, like PPARγ, has specialized functions in brown adipocytes. C/EBPβ is enriched in brown relative to white adipocytes. Involved in the regulation of UCP1 transcription, the expression of C/EBPβ is also enhanced in BAT after cold exposure (Manchado et al., 1994) , indicating that C/EBPβ expression in BAT is regulated by βAR via the cAMP-PKA pathway. When placed in cold environment, C/EBPβ null mice cannot maintain body temperature although the expression of UCP1 and PGC1α gene is not substantially altered and the induction of gene expression by noradrenaline in BAT is preserved. The UCP1 gene promoter is repressed by LIP and since C/EBPβ null mice lack both C/EBPβ isoforms LAP and LIP, the absence of inhibitory isoform LIP may have a stronger effect than the absence of active isoform LAP upon UCP1 gene expression (Carmona et al., 2005). The cAMP-inducible PGC1α and UCP1 expression is one of the most important features of brown but not white adipocytes. Overexpression of C/EBPβ in 3T3-L1 white preadipocytes rescues the cAMP-inducible PGC1α and UCP1 expression by acting on CRE in PGC1α promoter in response to β-adrenergic agonist (Karamanlidis et al., 2007). Most notably, C/EBPβ forms a complex with PRDM16 to initiate the brown adipogenic programme from myoblastic precursor cells and even to reconstitute a brown fat programme in naïve cells when ectopically co-expressed in mouse embryonic fibroblasts (MEFs) and primary skin fibroblasts (Kajimura et al., 2009). These data consistently indicate the important role of C/EBPβ in regulating adaptive thermogenesis in BAT as well as the brown fat developmental programme, although large part of the regulation mechanism details still remains to be elucidated more clearly.

The interaction of C/EBPβ with the other (co)activators in regulating UCP1 transcription was summarized in the following hypothetical model (Figure 1.14),

consisting of the critical transcription factor PPARγ and the primary transcriptional regulators PGC1α and PRDM16.

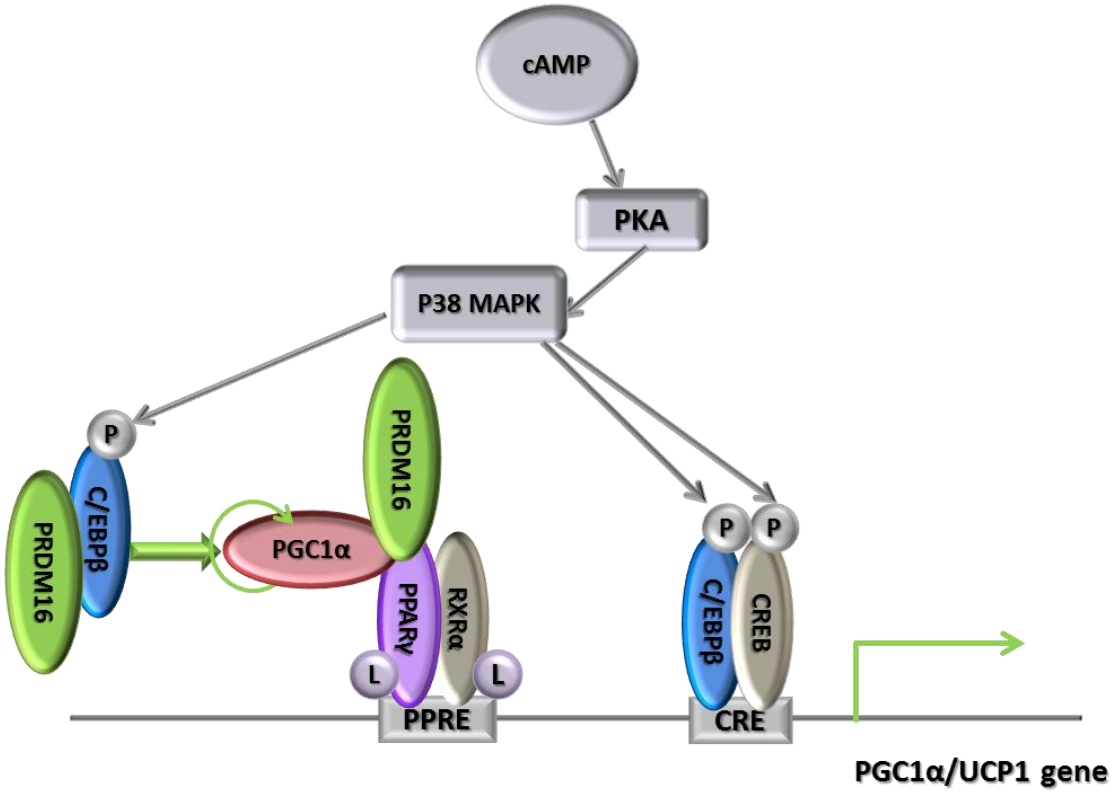

Figure 1.14 Model for C/EBPβ interacting with other (co)activators in regulating PGC1α/UCP1 transcription.

A hypothetical model for higher PGC1α/UCP1 promoter activity through higher C/EBPβ cellular concentration and phosphorylation in response to cAMP-PKA signalling pathway is proposed. C/EBPβ forms a complex with PRDM16 and stimulates PGC1α transcription, which in turn increases PGC1α expression itself and activates PPARγ in presence of PPARγ ligand. The active PPARγ together with PGC1α and PRDM16 act on the PPRE of UCP1 promoter to stimulate the transcription. Besides, C/EBPβ can also act on CRE of PGC1α/UCP1 promoter by binding CREB to activate the transcriptional activity. P: phosphate group; L: ligand.

1.3.6 Other (co)activators

Besides the main brown adipogenic and thermogenic regulators reviewed above, there are also a number of other (co)activators participating in the complicated and delicate regulating network, co-ordinately regulating the function of adaptive thermogenesis in BAT.

Forkhead box C2 (FoxC2)

FoxC2, a member of the forkhead/ winged helix transcription factor family, promotes brown fat phenotype. In particular, increased expression of FoxC2 in adipose tissue induces the expression of a set of brown fat-selective genes including UCP1, leading to a lean and insulin-sensitive phenotype in white adipose tissue. FoxC2 affects adipocyte metabolism by increasing the sensitivity of the β-adrenergic-cAMP-PKA signalling pathway through alteration of adipocyte PKA holoenzyme composition (Cederberg et al., 2001). Despite the function of promoting brown fat development, FoxC2 is not preferentially expressed in BAT relative to WAT. In fact, FoxC2 is abundantly expressed in adipose tissue, equally in WAT and BAT, at least at the mRNA level (Cederberg et al., 2001; Seale et al., 2009). It also remains to be determined whether FoxC2 is genetically required in brown adipocyte differentiation and thermogenesis by loss of function studies.

Bone morphogenetic protein 7 (BMP7)

Bone morphogenetic proteins (BMPs) are members of the transforming growth factor-β (TGF-β) superfamily and control multiple key steps of embryonic development and differentiation (Chen et al., 2004). Although some members of BMPs support white adipocyte differentiation, BMP7 promotes differentiation of the mesenchymal cell line C3H10T1/2 to the brown preadipocytes even in the absence of the normally required hormonal induction cocktail (Tseng et al., 2008). BMP7 activates a full programme of brown adipogenesis including induction of early regulators of brown adipogenesis, PRDM16 and PGC1α, increased expression of brown-fat-defining marker UCP1. BMP7 also increases adipogenic transcription factors PPARγ and C/EBPs and induces mitochondrial biogenesis, via p38 MAP kinase- and PGC1-dependent pathways. Moreover, BMP7 knockout embryos show a marked paucity of brown fat and an almost complete absence of UCP1. These data reveal a

critical role of BMP7 in promoting brown adipocyte differentiation and thermogenesis (Tseng et al., 2008).

A JmjC-containing H3K9 demethylase: Jhdm2a

JHDM2A specifically demethylates mono- and di- methyl-H3K9 through the Jmjc domain and a zinc finger. It has been reported to be important in nuclear hormone receptor mediated gene activation and male germ cell development (Yamane et al., 2006). Disruption of the Jhdm2a gene in mice results in obesity and hyperlipidemia, disrupts β-adrenergic-stimulated glycerol release and oxygen consumption in brown adipose tissue and decreases fat oxidation and glycerol release in skeletal muscles. The expression of Jhdm2a itself is induced by β-adrenergic stimulation, and it directly regulate the expression of UCP1 and PGC1α by binding to PPRE of the thermogenic genes in presence of β-adrenergic agonist, thus decreasing levels of H3K9Me2 (dimethylation of lysine 9 of histone H3) at PPRE and facilitating the recruitment of PPARγ and RXRα as well as their co-activators to the PPRE (Tateishi et al., 2009). Therefore, Jhdm2a has an essential role in regulating thermogenic gene expression in BAT by modifying the pattern of chromatin remodelling on these genes.

Insulin receptor substrate-1 (IRS-1)

IRS-1 is one of the insulin receptor substrates, involved in the signalling network of insulin promoting adipocyte differentiation. In cultured brown preadipocytes, expression of IRS-1 mRNAs and proteins is reduced gradually as the cells differentiate into mature adipocytes. IRS-1 knockout mice exhibit severe defects in brown adipogenesis and a marked decrease in the expression of the brown adipogenic marker genes including PPARγ, C/EBPα and thermogenic gene PGC1α. Reconstitution of the IRS-1 knock out cells with the IRS-1 protein rescues the adipogenic capability and restores the reduced expression of the brown adipogenic and thermogenic genes (Tseng et al., 2004). These data indicate that IRS-1 plays important role in brown adipocyte differentiation.

Silent mating type information regulation 2, homolog 3 (Sirt 3) and Estrogen-Related Receptor α (ERRα)

Sirt 3 is a member of the sirtuin family of protein deacetylases with multiple actions on metabolism and gene expression and, as a gene localized in mitochondria, its expression is associated with energy homeostasis and metabolism in brown adipocyte development (Verdin et al., 2010). The expression of Sirt 3 can be induced by PGC1α in white adipocytes and embryonic fibroblasts as part of its overall induction of a brown adipose tissue-specific pattern of gene expression. In Sirt 3 null cells, PGC1α fails to induce a complete set of brown fat-specific thermogenic gene expression. The orphan nuclear receptor ERRα is required to bind the proximal promoter of Sirt 3 for fully inducing Sirt 3 gene expression in response to PGC1α, suggested by the knockdown assays of ERRα (Giralt et al., 2011). In these studies, ERRα is acting positively in stimulating the thermogenic programme in BAT. However, studies from Luo and colleagues showed that the ERRα null mice have reduced body weight and peripheral fat deposits and are resistant to high-fat diet-induced obesity (Luo et al., 2003), implying a negative regulatory role of ERRα in the adaptive thermogenesis in BAT (Collins et al., 2010). Due to the lack of a natural ERRα ligand, determination of the physiological function of ERRα is rather limited, so more research is still required to clearly elucidate the functions of ERRα and thus to explain the controversy above.

1.3.7 Repressors

In addition to the much effort to investigate the activating or stimulatory mechanisms mentioned above, it is equally important to identify and understand the factors that repress the process of BAT adaptive thermogenesis, as potential “activators” may not work if there is active repression. Some (co)repressors have already been addressed above in the section about PGC1α (RIP140 by direct binding, SRC2 and pRb), so in the paragraphs below, some PGC1α-independent repressing mechanisms and regulators will be reviewed to further complete the whole regulating network.

Receptor-interacting protein 140 (RIP140)

RIP140 was originally identified by its ability to interact with estrogen receptors and to repress their transcriptional activity (Cavailles et al., 1995). Subsequently, RIP140 was found to bind and repress a number of other nuclear receptors including PPARs,

thyroid hormone receptors (TRα and TRβ) and estrogen-related receptors (ERRα and ERRβ), particularly important in regulating gene expression in metabolic tissues, specifically adipose tissue, muscle and liver (Francis et al., 2003). Knockout of RIP140 in mice leads to extremely lean phenotype, resistance to obesity, enhanced glucose tolerance and insulin sensitivity compared with matched wild-type littermates fed a high-fat diet. Depletion of RIP140 in white adipose tissue induces a numbers of brown fat-specific features, notably the upregulation of UCP1 (Leonardsson et al., 2004). Further studies revealed that RIP140 is essential for both DNA and histone methylation of UCP1 gene to maintain the repression. RIP140 expression promotes the assembly of DNA and histone methyltransferases (HMTs) on the UCP1 enhancer and leads to methylation of specific CpG residues and histones as judged by bisulphite genomic sequencing and chromatin immunoprecipitation (ChIP) assays, resulting in the inhibition of UCP1 gene transcription (Kiskinis et al., 2007) (Figure 1.14).

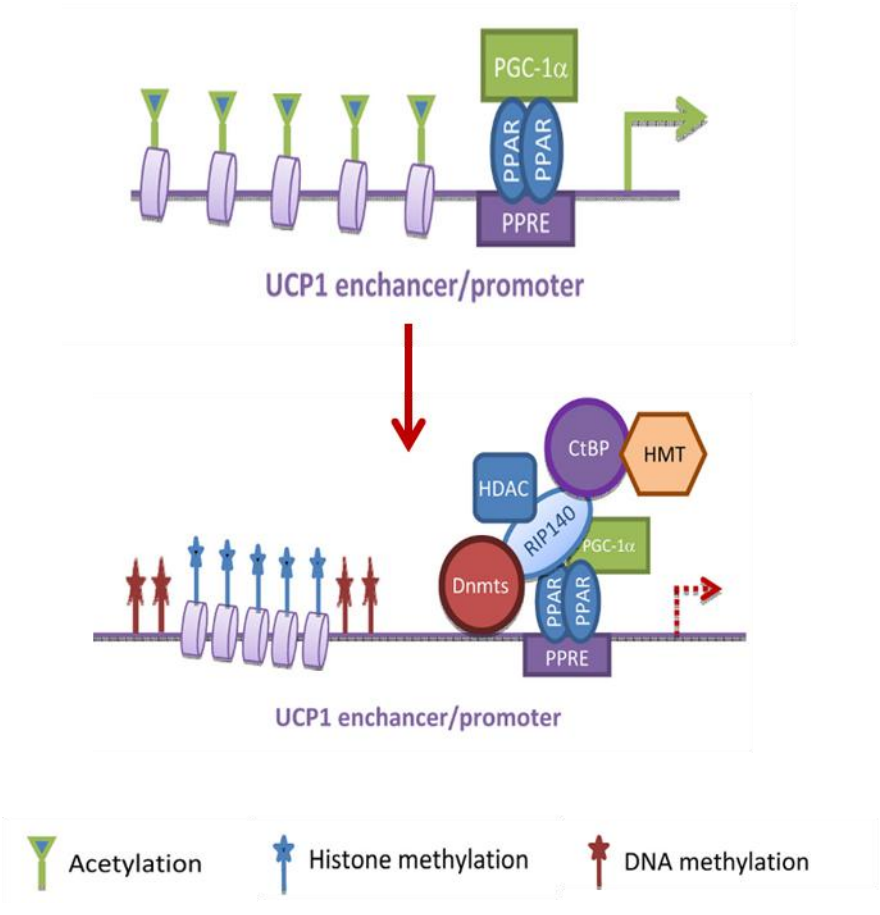

Figure 1.14 RIP140 acts as a transcriptional corepressor of UCP1 gene.

RIP140 acts as a transcriptional corepressor of PPARs, blocking UCP1 promoter activation through the recruitment of DNA methyltransferase (Dnmt), COOH-terminal binding protein (CtBP), histone methyltransferase (HMT) and histone deacytylase (HDAC) (Fritah et al., 2010).

Liver X Receptor α (LXRα)

LXRs are ligand-activated transcription factors of the nuclear receptor superfamily, characterized as key transcriptional regulators of lipid and carbohydrate metabolism (Baranowski, 2008). LXR ligand significantly blunts the response of UCP1 gene to mimicked SNS stimulation such as treatment with the βAR agonist isoprenaline or the adenylyl cyclase activator forskolin, but has no effect on cAMP-dependent PGC1α gene expression (Wang et al., 2008b). There is a direct repeat sequence (DR4), which is a potential LXR binding site, in the important enhancer region of UCP1 gene, and gel shift and ChIP assay experiments as well as the site mutation in the DR4 region firmly proved that LXRα does bind to that region to repress UCP1 gene transcription. This inhibition mechanism involves the differential recruitment of the corepressor RIP140 to an LXRα binding site that overlaps with the PPARγ/PGC1α response element, resulting in the dismissal of PPARγ (Figure 1.15) (Wang et al., 2008b). Phosphorylation of LXRα by PKA has been shown to be a necessary step involved in the repression mechanism, not required for the binding of LXRα to DR4 but indispensable for recruiting RIP140 to the site (Collins et al., 2010). The ability of LXRα to reduce energy expenditure in this way provides another mechanism of maintaining the balance between energy storage and utilization.

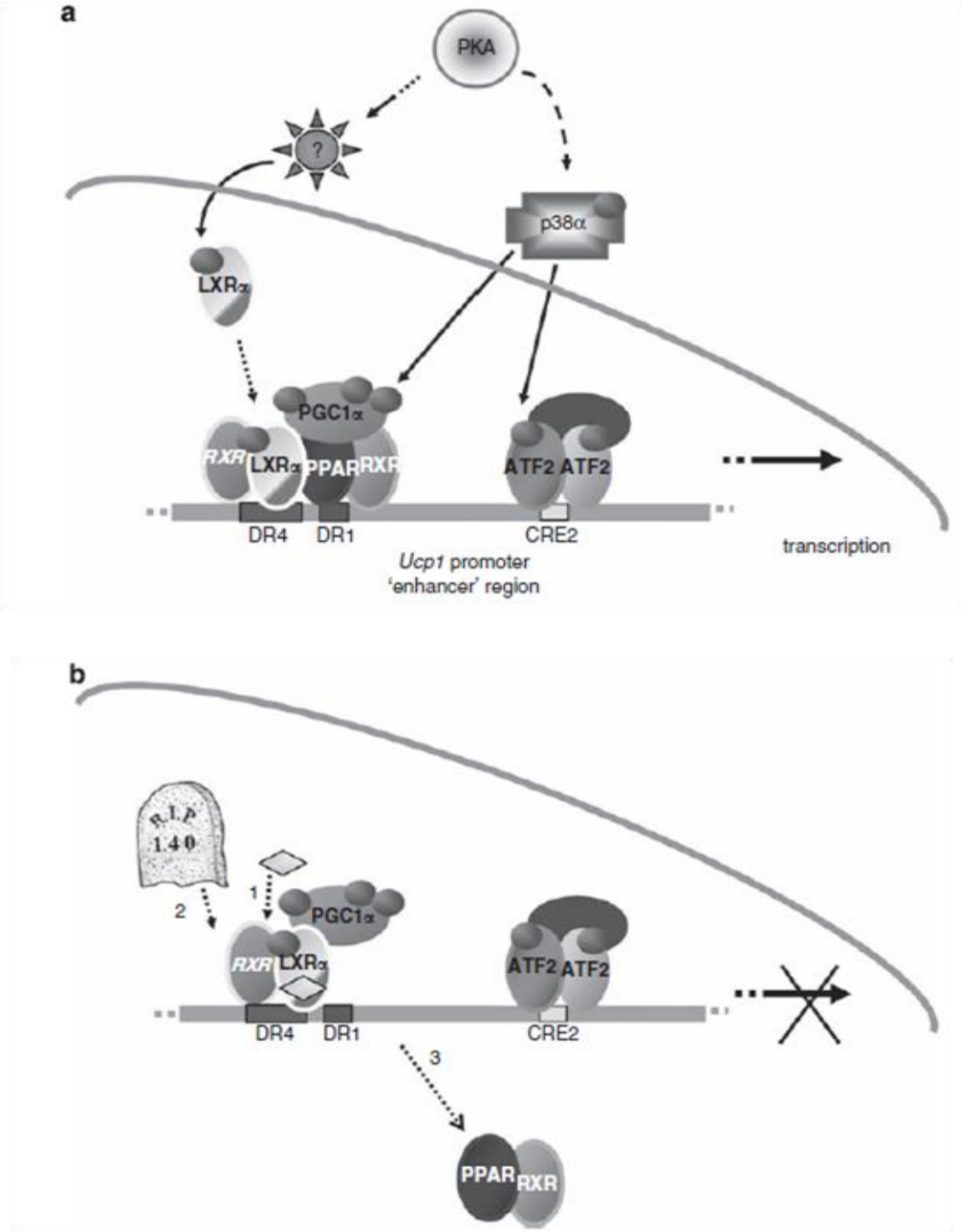

Figure 1.15 Cartoon model for LXRα regulation of UCP1 gene transcription

(a) Activation of PKA by βARs leads to p38 MAP kinase activity and phosphorylation of nuclear factors such as ATF2 and PGC1α to increase transcription of the UCP1 gene. Also in response to PKA there is phosphorylation of LXRα by an unidentified kinase. (b) When an LXR ligand is present, the nuclear corepressor RIP140 is recruited to the complex (step 2), and the critical regulator PPAR is eliminated from its DR-1 binding site (step 3), the net result of which is repression of UCP1 gene transcription (Collins et al., 2010).

Cell death-inducing DNA fragmentation factor α-like effector A (CIDEA)

Cidea is a member of the CIDE family of proteins and shares homology with the N-terminal region of the apoptotic DNA fragmentation factors Dffb and Dffa, and induces caspase-independent cell death when overexpressed (Inohara et al., 1998). Cidea is highly expressed in brown adipose tissue, thus is considered as one of the brown fat marker genes (Zhou et al., 2003). However, Cidea null mice display a lean phenotype, are resistant to diet-induced obesity and diabetes, and have a higher metabolic rate, lipolysis in BAT and core body temperature, when subjected to cold treatment (Zhou et al., 2003), implying a negative regulatory role of Cidea in thermogenic process. Unlike UCP1 that is stimulated by cold exposure, Cidea expression is down-regulated by acute cold exposure mediated by sympathetic activation of β3-adrenergic receptor, as evidenced by attenuation of the response by β-adrenergic receptor antagonists (Shimizu and Yokotani, 2009). Western blotting and immunoprecipitation studies have demonstrated that CIDEA directly binds UCP1 when the two genes are co-overexpressed in yeast cells, and that this interaction between CIDEA and UCP1 inhibits the uncoupling activity of the latter while the expression of CIDEA alone does not significantly influence the basal uncoupling activity of the cells (Zhou et al., 2003).

Although Cidea and UCP1 co-localize on the inner membrane of mitochondria and expression of both can be up-regulated by the knockdown of some common thermogenic repressors (e.g. RIP140, see above), they have opposite response to cold exposure, indicating they are regulated differently by the same signalling pathway (cAMP-PKA pathway). The inhibitory effect of Cidea on UCP1 expression may reflect a mechanism for fine tuning UCP1 activity by increasing the threshold for UCP1 activity thus rendering thermogenesis more sensitive to physiological stimuli-controlling UCP1 concentration (Zhou et al., 2003).

Eukaryotic initiation factor 4E binding protein 1 (4E-BP1)

In mammalian cells, the initiation phase of mRNA translation involves the recognition of the mRNA 5’ cap structure by the eukaryotic initiation factor 4F (dIF4F) cap-binding complex, which consists of three subunits: eIF4A, eIF4E and eIF4G(Poulin and Sonenberg, 2003). The activity of eIF4E is regulated by its interaction with a family of

three inhibitory proteins, the eIF4E binding proteins (4E-BPs). In its phosphorylated form, 4E-BP1 binds to eIF4E and prevents the formation of the eIF4F complex, thus inhibiting cap-dependent translation (Gingras et al., 1999; Haghighat et al., 1995). Therefore it was reasonable to expect the 4E-BP1 deficient cells to display a global increase in tissue protein synthesis, however, surprisingly, the 4E-BP1 knockout mice were found to contain an increased number of multilocular adipocytes in the inguinal and retro-peritoneal WAT depots and elevated PGC1α and UCP1 expression as well as increased whole body energy expenditure(Tsukiyama-Kohara et al., 2001). As a potential specific repressor of UCP1 expression, 4E-BP1 expression is decreased during cold stress and this inhibitory effect is reversed in β3-, but not β1/β2-, adrenoceptor knockout mice. The data indicated that 4E-BP1 is regulated specifically by β3-adrenergic receptor mediated pathway, in support of its role in adaptive thermogenesis (Lehr et al., 2004).

In summary of the different transcriptional regulators in controlling adaptive thermogenesis in brown adipose tissue, the features of different animal models (either knockout or transgenic models) targeting brown adipose tissue-related proteins were concluded below (Table 1.2) to provide a brief but comprehensive view on the functions of the regulators.

Table 1.2 Animal models targeting brown adipose tissue-related proteins

Reference	Model (KO/TG)	Changes in BAT	Whole body metabolic phenotype
(Cederberg et al., 2001)	TG FoxC2 in fat cells	Higher interscapular BAT and increased expression of C/EBPα, PPARγ, SREBP1 and metabolic rate in TG WAT	Lower HFD-induced weight gain and fat accumulation and improved glucose control
(Picard et al., 2002)	SRC1 KO	Higher lipid infiltration and lower expression of UCP1 and PGC1α	Higher HFD-induced weight gain, reduced metabolic rate and body temperature at 4°C
(Picard et al., 2002)	TIF2 KO	Lower lipid infiltration and higher expression of UCP1 and PGC1α	Lower HFD-induced weight gain and fat accumulation and improved glucose control. Higher metabolic rate and body

			temperature at 4°C
(Coste et al., 2008)	SRC3 KO	Lower lipid infiltration and increased mitochondrial number	Lower HFD-induced weight gain and fat accumulation and improved glucose control. Higher metabolic rate, body temperature and muscle mitochondrial content
(Scime et al., 2005)	p107 KO	White fat cells with multilocular lipid droplets and high UCP1 and PGC1α levels	Lower WAT mass and increased metabolic rate
(Tseng et al., 2008)	BMP7 KO	Lower BAT mass at birth	Mice are not viable after birth
(Tseng et al., 2008)	BMP7 TG	Increase in brown but not white fat mass	Higher metabolic rate and body temperature and lower weight gain
(Leonardsson et al., 2004)	RIP140 KO	Higher expression of UCP1 and CPT1b	Lower HFD-induced weight gain and liver fat accumulation. Higher metabolic rate
(Kang et al., 2005)	UCP1-Wnt10b TG	Lack of functional BAT with lower expression of PGC1α and UCP1	Blunted increase in body temperature after β-agonist stimulation
(Pan et al., 2009)	Adipose tissue TG twist-1	Lower expression of PGC1α and UCP1. Lower metabolic rate and mitochondrial density. Higher lipid infiltration.	Higher HFD-induced weight gain and lower body temperature at night
(Pan et al., 2009)	Twist-1 +/-	Lower lipid infiltration. Higher mitochondrial number and metabolic rate	Lower HFD-induced weight gain and higher body temperature at night
(Seale et al., 2010)	PRDM16 +/-	Lower expression of brown selective genes including UCP1, Cidea and PGC1α	Lowe metabolic rate
(Seale et al., 2010; Seale et al., 2007)	PRDM16 adipose tissue TG	Appearance of multilocular adipocytes and higher expression of BAT genes, including UCP1, Cidea and	Lower HFD-induced weight gain, less fat and more lean mass in body composition, higher metabolic rate and improved

		PGC1α, in WAT	glucose control
(Motyl et al.; Staiger et al., 2009)	C/EBPβKO	Defective lipid accumulation	Reduced peripheral fat mass, lower levels of serum insulin and leptin
(Accili et al., 1999; Kulkarni et al., 1999; Tseng et al., 2004)	IRS-1 KO	Sever defect in brown adipogenesis	Growth retarded, insulin secretory defects and reduced insulin expression
(Tsukiyama-Kohara et al., 2001)	4E-BP1 KO	Reduced WAT mass, appearance of multilocular adipocytes in WAT pad and increased UCP1 and PGC1α expression	Higher metabolic rate
(Lin et al., 2004)	PGC1α KO	Impaired cold-induced UCP1 expression	Impaired glucose homeostasis, higher O2 consumption rate, resistant to HFD-induced obesity and insulin resistance, lower body temperature at 4°C,
(Zhou et al., 2003)	CIDEA KO	Higher metabolic rate and lipolysis	Higher metabolic rate and core body temperature at 4°C, lean and resistant to HFD-induced obesity and diabetes

Abbreviations: BAT, brown adipose tissue; HFD, high-fat diet; KO, knockout mice; TG, transgenic mice; WAT, white adipose tissue.

1.4 VIRAL VECTOR-MEDIATED GENE TRANSFER TO ANIMAL CELLS

The delivery of DNA into animal cells is a fundamental and well-established procedure widely used in research, indispensable for gene cloning, the study of gene function and regulation. Most of experiments reviewed above involve gene transfer as the over-expression (gain-of-function) of a specific target gene has become the most commonly used and necessary tool in investigating the function of the gene. Additionally, most gene knockout experimental procedures (e.g. RNAi) share the identical or similar methods with that of gene transfer.

Historically, in order to deliver the DNA (or siRNA) of interest into target mammalian cells or even animals, investigators have used a number of methods, including chemical and physical transfection of naked DNA or plasmid DNA, adenoviral vector-mediated gene delivery, adeno-associated viral vector-mediated gene delivery, retroviral vector-mediated gene delivery and lentiviral vector-mediated gene delivery. Some methods only results in temporary transgene expression (transient overexpression) that won't last for long time or pass to the next generation during cell division, whereas some other methods can achieve permanent expression of the exogenous gene (stable overexpression) which can be used to construct transgenic cell lines or transgenic animals. No matter what the mediator is, the gene transfer method must obey some basic principles. First of all, the exogenous genetic material must be transported across the cell membrane. Secondly, the genetic material must be released in the cell and transported to its site of expression or activity. Finally but importantly, the exogenous genetic materials must be activated (Twyman, 2005).

Naked or plasmid DNA is usually delivered into mammalian cells with chemical or physical transfection methods. DEAE-dextran (diethylaminoethyl-dextran) was the first transfection reagent to be developed (Wall, 1999) and was very widely used to deliver plasmid DNA into mammalian cell lines until 1990s. The reagents for this method of transfection are inexpensive and the procedure is simple and efficient, although the efficiency varies among cell lines. Mostly used for transient overexpression of target genes, DEAE-dextran transfection is not particularly efficient for the production of stably transformed cell lines. Transfection using calcium phosphate is also a widely used transfection method with established cell lines, as it is

simple, reliable, applicable to many cell lines, and the reagents are inexpensive. However, not all cells are equally amenable to this transfection method, some are sensitive to the density of the precipitate, and the transfection efficiency in primary cells is very poor (Rorth et al., 1998; Twyman and Jones, 1995). The advent of lipofection reagents especially the development of cationic/neutral lipid mixtures which spontaneously associate with negatively charged DNA to form complexes, has made a breakthrough in chemical mediated-gene delivery, as it greatly increase the transfection efficiency compared to the previous methods. Cationic polymers are also used as transfection reagent, the first one of which is Polybrene (1, 5-dimethyl-1, 5-diazaundecamethylene polymethobromide) facilitating the high-efficiency transfection of certain cell lines which can be refractory to calcium phosphate transfection. Polyethyleneimines (PEIs) are another class of cationic reagents developed more recently, which contains numerous amine groups providing a large number of positive charges for interaction with DNA. Physical transfection methods include electroporation, laser poration, microinjection and transfection by particle bombardment or ultrasound, which may give high transfection efficiency in some cell lines difficult to transfect by chemicals, but require expensive devices and relatively more delicate operating skills (Twyman, 2005).

Whether chemical or physical, transfections of target DNA carried by plasmid vectors may achieve high efficiency in terms of transient over-expression, but as the efficiency for the plasmid DNA to integrate into the genome of target cell line is fairly low and the integration position in the genome is totally random, it is difficult to construct a transgenic cell line that carries the over-expressed gene and has all the physiological functions as normal as the wild type cells. As natural viruses have evolved to deliver nucleic acids safely into animal cells, mostly into the genomes actually, the viral vectors are developed, specifically for extremely high transient expression or delivery of the genes of interest into mammalian cells or animals for a stable expression. The transfer of exogenous DNA (or RNA) into animal cells as part of a recombinant viral particle is known as transduction (Twyman, 2005). The viruses that have been commonly used as the gene delivery tools include adenovirus, adeno-associated virus, retrovirus and lentivirus, which will be addressed in this review

about their molecular design, safety, application and limitation in basic research. The viral vector-mediated gene delivery (including RNAi) has been of great clinical importance as well, as it has provided a promising approach in gene medicine and gene therapy, which will also be included in the paragraphs below.

1.4.1 Adenovirus- and adeno-associated virus- mediated stable overexpression

The adenoviruses are non-enveloped DNA viruses, containing a double-stranded linear genome approximately 36 kb in length. The major advantages of adenoviral vectors are that they can be purified to extremely high titers (10^{12}-10^{13} particles per ml), which makes them highly suited for *in vivo* applications, and the efficiency of gene transfer approaches 100% if the target cells bear the appropriate receptors. Adenoviral vectors have a broad species and cellular host range including both dividing and postmitotic cells, and they are relatively easy to manipulate *in vitro*. Adenoviral vectors can take up to 7.5 kb foreign DNA. Adenoviral vectors show a low efficiency of stable transformation, so they are generally suitable for transient expression *in vitro* and *in vivo* but not useful for the production of stably transformed cell lines (Twyman, 2005).

Adeno-associated virus (AAV) is single-stranded non-enveloped DNA virus. The virus has a large host range including most dividing and post-mitotic cells. Stable integration using AAV is very efficient. Additionally, the integration of AAV into the host cell genome is more efficient in humans than other mammals, and this may reflect the specificity of the proviral insertion site. Another strong advantage is that AAV is not pathogenic in humans, which could be an advantage in gene therapy as well. However, there is one problem with AAV vectors which is the low titer of recombinant viral stocks. During the initial development of AAV as a vector, this was as low as 10^{4}-10^{5} transducing units per ml, although the careful optimization of preparation methods has increased titers to 10^{9} (Twyman, 2005).

1.4.2 Gene delivery with retroviral vectors

Retroviruses are enveloped RNA viruses, and each viral particle carries two copies of a single-stranded, positive-sense RNA genome as well as several proteins required for

infection. They are often described as either simple or complex, the former referring to the conventional oncoretroviruses such as murine leukaemia virus (MLV) and the latter to the lentiviruses (Figure 1.16) such as human immunodeficiency virus (HIV) which contain additional genes compared to the basic oncoretrovirus genome. As RNA viruses, retroviruses have unique replication strategy. After entering the cell, the virus is uncoated and the genomic RNA is transported to the nucleus where it is converted into a terminally redundant double-stranded cDNA copy by the virion protein reverse transcriptase. Then a second virion protein, integrase, inserts this cDNA copy into the host genome as well as subgenomic mRNAs encoding enzymes and structural proteins of the viral capsid. Retroviruses are advantageous vectors for numerous reasons, including the high viral titers (10^6-10^8 particles per ml), the high efficiency of stable transduction (both *in vitro* and *in vivo*) and the ability to pseudotype viral particles and thus engineer the host range of each vector. Moreover, the small viral genome is easy to manipulate in the laboratory once it has been converted into a cDNA copy, and it carries a useful promoter/ enhancer system, which can be used to drive transgene expression (Twyman, 2005).

The basic strategy to construct retroviral vectors is replacing essential viral genes with the transgene of interest and using a packaging line to supply the missing viral functions (Twyman, 2005). With high efficiency of virus production and integration, as well as relative convenient manipulation, the HIV-1 based Lentiviruses are increasingly used to realize the stable over-expression of target genes in dividing or non-dividing cell lines and *in vivo*, as well as to construct cell lines or animals with target gene knocked out. There are several commercially-available lentiviral over-expression systems, making it a commonly used tool in laboratory and preclinical research as well as clinic therapy (Invitrogen, 2010). In the next paragraphs, the molecular design and safety of using lentiviral vectors will be discussed to provide an overview of this tool, which has been used in the experimental work of this project.

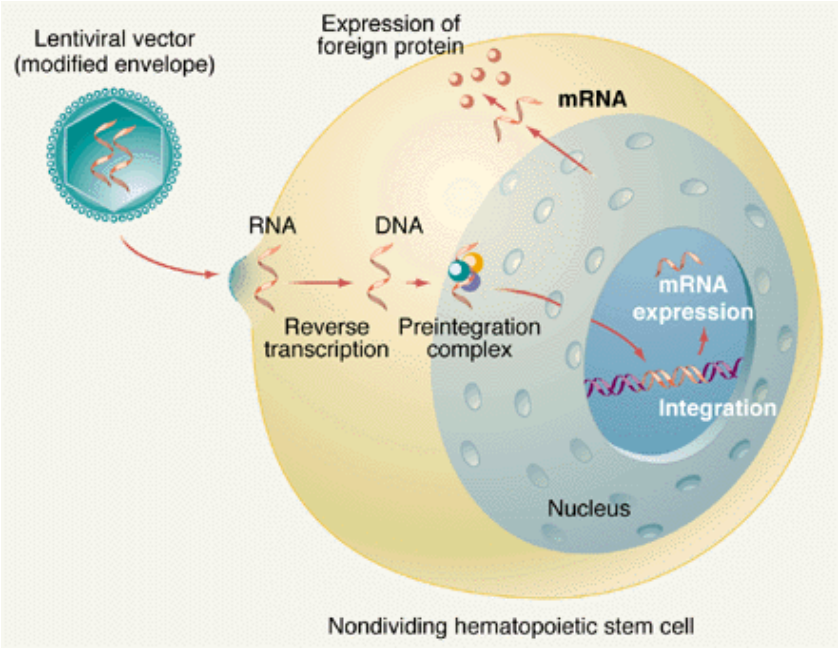

Figure 1.16 Gene transfer by a lentiviral vector

Vectors based on lentiviruses such HIV are able to infect both dividing and non-dividing cells. After the lentiviral vector has infected, for example, a nondividing (resting) hematopoietic stem cell, the vector RNA containing the exogenous gene is transcribed into DNA. The DNA forms a preintegration complex with the accessory protein Vpr, the enzyme integrase, and the protein matrix. The localization sequences of these proteins enable the preintegration complex to cross the nuclear membrane (the other viral vectors must wait for the nuclear membrane to break down during cell division before they are able to access the host DNA). Once inside the nucleus, the DNA is inserted into the host genome by integrase (Amado and Chen, 1999).

1.4.3 Lentiviral vectors: the evolving molecular design and safety

HIV-1 based lentiviral vectors were originally derived from cloned proviruses that were developed in the 1980s (Adachi et al., 1986; Ratner et al., 1987). They have undergone iterative improvement since the first description. The improvements have largely focused on the vector and helper design, which are constructed as plasmid DNAs that are transfected into HEK 293 or 293T cells to produce viral particles (Naldini et al., 1996b; Poznansky et al., 1991). The HIV-1 based lentiviral particles can be pseudotyped with heterologous envelope proteins such as vesicular stomatitis virus G envelope protein (VSV-G), to confer broad tropism for transduction of a wide variety of mammalian cell types (Naldini, 1998; Yee et al., 1994). HIV-1 based lentiviral vectors include a transducing vector and separate helper (packaging) plasmids, consisting of structural and enzymatic proteins (Gag and Pol) which are required for virion formation. From the very beginning, helper constructs have been iteratively designed to separate and remove HIV open reading frames to help ensure their safety. The accessory genes, known to be important for pathogenesis of the wild-type virus were deleted to further improve safety in case of recombination (Desrosiers et al., 1998). The native long terminal repeat (LTR) promoter was substituted with a heterologous promoter such as the cytomegalovirus (CMV) promoter (Vendel and Lumb, 2003).

To improve the efficiency of gene transfer into target cells, there have also been some modifications to match the helper constructs. Early transfer vectors were composed of a 5' LTR, major splice donor site, packaging signal encompassing the 5' part of the Gag gene, the reverse-responsive element (RRE), the envelope splice acceptor, an internal gene cassette driven by its own promoter, and the 3' LTR (Dropulic, 2011). The 3' LTR was modified to delete the U3 region, which is essential for replication of the wild-type virus. Removal of enhancers and other transcriptionally active sequences from the lentiviral 3' LTR results in a self-inactivating (SIN) LTR (Yu et al., 1986), which is considered safer than native LTR-containing vectors. The woodchuck hepatitis virus post-transcriptional regulatory element (WPRE) has been widely used to stabilize transgene mRNA levels and therefore increase transgene expression (Dupuy et al., 2005).

Basically, the lentiviral expression system in use currently consists of 4 vectors (one transgene expression vector and three helper vectors including envelope expression vector and two packaging vectors) and a packaging cell line (mostly HEK 293 or derived cells) (Figure 1.17) to produce infectious lentivirus to realize stable overexpression or knock out in target cell lines or animals.

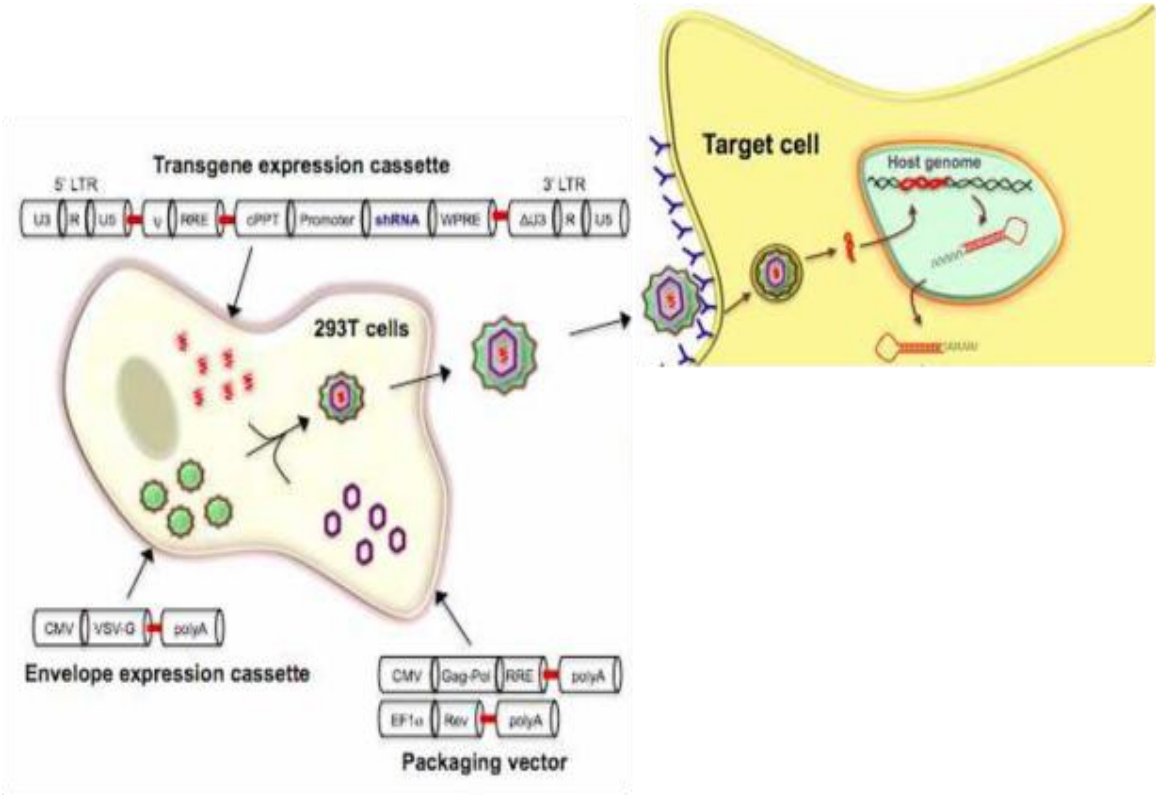

Figure 1.17 Schematic of lentiviral vector system for stable expression

Suitable host cells (such as 293T cells) are transfected with a mixture of plasmids consisting of 1) an exogenous gene expression cassette, 2) a packaging cassette and (3) a heterologous (VSV-G) viral envelope expression cassette. The generated lentivirus is then used to transduce the desired cell type for transgene expression. Because only the vector containing the transgene expression cassette (devoid of the viral structural genes) integrates into the host cell genome in the transduced cells, the gene of interest is continually expressed but infectious virus is not produced (Manjunath et al., 2009).

Other elements have been successfully incorporated into lentiviral vectors, some for specific purposes. Tetracycline (Tet) trans-activators of repressors have been used to create inducible lentiviral expression vectors (Pluta et al., 2007) and further optimization also solved the problem of high basal activity and increased transgene inducibility when combined with silencing elements such as KRAB (Krüppel-associated box) (Wiznerowicz and Trono, 2005). An alternative method for inducible gene or short hairpin RNA (shRNA) expression uses Cre-loxP recombination, but unlike the tetracycline system, this mode of transcriptional activation is generally irreversible and has particular use in transgenic animals for the study of genes that would otherwise generate embryonic lethality (Chang and Zaiss, 2003; Pluck, 1996). More recently, it has been discovered that the incorporation of cell type-specific microRNAs downstream of a transgene can restrict expression in those particular cell types (Brown et al., 2007), so the combination of positively regulating tissue-specific promoters with negatively regulating microRNAs can result in highly precise transgene expression in specific cells or tissues (Brown and Naldini, 2009). This strictly regulated expression increases the vector safety and is particularly useful in experimentation in specific cell types, especially in clinical applications.

Lentiviral vector expression system has been widely and successfully used not only in simple over-expression of individual target genes or the knock down of specific genes by shRNA, but also in functional genomics with the construct of several lentiviral vector cDNA libraries (Chilov et al., 2003; Kurita et al., 2008). It has become a powerful and indispensible molecular tool in cell engineering and animal model applications.

1.5 SUMMARY

Brown adipose tissue functions primarily to dissipate energy in the form of heat via uncoupling respiration in response to cold exposure or β-adrenergic receptor agonists (adaptive thermogenesis), therefore BAT, if controlled and regulated properly, can be a potential powerful tool to counteract obesity. The crucial gene that mediates the uncoupling respiration, also the hallmark gene of BAT, is uncoupling protein 1 (UCP1), the expression and activation of which is delicately controlled by a set of transcription factors (PPARγ, RXRα, etc.), co-activators (PGC1α, PRDM16, C/EBPβ, etc.) and co-repressors (RIP140, CIDEA, etc.) and regulated by multiple signalling pathways (cAMP-PKA pathway and PPARγ agonists mediated pathway). Preliminary studies suggested that the over-expression of C/EBPβ in white preadipocyte 3T3-L1 cell line enabled the cAMP-inducible expression of UCP1, which is an essential characteristic in brown adipocytes but lacking in white adipocytes. C/EBPβ has also been proved to be important, by forming the complex with PRDM16, in determination of the brown adipogenic lineage from myoblasts. Undoubtedly, C/EBPβ is a critical regulator in stimulating brown adipogenic differentiation programme. However, its expression during white adipocyte differentiation is greatly reduced after two days of differentiation while kept high level throughout brown adipocyte differentiation (Karamitri et al., 2009), which inspired the idea that artificially over-expressing C/EBPβ in white preadipocytes throughout the whole differentiation process might lead to a brown-like phenotype in the cells. Therefore, a series of experiments was carried out to investigate the role of C/EBPβ and its interaction with the other co-regulators such as PRDM16 in adipogenic programme in terms of chromatin remodelling. To achieve an inducible stable over-expression, the lentiviral expression system was used to select for a stable transgenic 3T3-L1 cell line.

1.6 EXPERIMENTAL OBJECTIVES

The overall hypothesis of this project is to test whether C/EBPβ, together with the other regulators like PRDM16, increases brown adipogenic differentiation programme in white preadipocytes by altering the pattern of chromatin remodelling.

The objectives of the experimental work described in this manuscript were:

1. To generate lentiviral vectors to allow tetracycline-inducible stable overexpression of C/EBPβ in white preadipocyte 3T3-L1.

2. To establish the interaction between C/EBPβ and the other transcriptional regulators.

3. To investigate if the pattern of chromatin remodelling is altered by C/EBPβ overexpression during 3T3-L1 differentiation using chromatin immunoprecipitation (ChIP).

CHAPTER 2

2 MATERIALS AND METHODS

2.1 VECTOR CONSTRUCTION

2.1.1Digest-Ligation Molecular Cloning

2.1.1.1 Polymerase chain reaction (PCR)

PCR was carried out in 200µl thin wall tubes (Star Lab™) on pre-constructed plasmid DNA using Phusion® High-Fidelity PCR Master Mix (New England Biolab), according to the manufacturer's instructions. Generally, for a 50µl reaction, 25µl master mix was used with 0.5µM of each primer and 1-10ng plasmid DNA as template (for PCR targeting C/EBPβ, 5% DMSO was added into the reaction to prevent forming secondary structure of the template). PCR was performed with the following temperature profile: an initial denaturation temperature at 98°C for 30sec, 27-30 cycles of denaturation (5-10sec at 98°C), annealing (10-30sec at optimized temperature) and extension (required time at 72°C), followed by a final extension at 72°C for 5-10min. PCR products were stored at -20°C.

2.1.1.2 Primer design

Primers were designed with Primer Express software and synthesized by MWG Biotech Ltd. (London, UK).

The criteria for the primer design are described below:

• Length of primer was between 18 and 24.

• Annealing temperature between 50°C to 60°C.

• G-C ratio was kept between 45%-55% G-C rich.

• Gs and Cs were preferred at 5' end of the primers and As and Ts were preferred at 3'end to avoid mis-priming.

• Self-annealing regions were avoided within each primer.

• Intra-primer and inter-primer homology in primer sequence was avoided.

The primer sequences to amplify the TRE (template: pL3-TRE-LucGFP-2L from Addgene Plasmid 11685) or TRE tight (template: pTRE-Tight miR-1 from Addgene Plasmid 14896) elements are listed below:

TRE_Forward: acgaagttatATCGATgaacccttcc

TRE_Reverse: ccaagcttagaACTAGTggatcggtcccggtgtcttc

TRE tight_Forward: ccccgggATCGATggccctttcgtcttcactcgag

TRE tight_Reverse: ccccgggACTAGTgcgatctgacggttcactaaac

Note: the ATCGAT is a restriction site recognized by ClaI (5') and the ACTAGT is a restriction site recognized by SpeI (3', reverse complementary sequence).

The primer sequences to amplify the template for cloning short aP2 promoter (template: pBS-aP2 <Plasmid 11424 from Addgene>)

Short aP2_Forward: cccggGCGGCCGCccaacccaaaccaaacaaagccaaac

Short aP2_Reverse: cccggGCGGCCGCggttctgactcctggcctgaacttc

Note: the GCGGCCGC is a restriction site recognized by NotI.

2.1.1.3 Restriction Endonucleases Digest

Restriction endonucleases were from either New England Biolab (NEB) or Promega. Digestions were performed according to manufacturer's instructions. Specifically, 3µg of the pLenti6/V5 backbone vector from Invitrogen was double digested by 2µl of BamHI and 2µl of XhoI with 4µl of Buffer B (Promega, 4 CORE® Buffers) in a final volume of 40µl made up with sterilized H_2O. To generate short aP2 promoter, 1µg of the short aP2 PCR product from 2.1.1.2 was digested by 1 µl of NotI with 3 µl of Buffer D (Promega) in a final volume of 30µl made up with sterilized H_2O. The vector with restriction enzymes was incubated at 37°C overnight for a complete digestion.

2.1.1.4 Gel purification of PCR products or digested DNA fragments

PCR products or digested DNA fragments were run on 1% agarose gels in 1X TAE buffer. Gel purification was performed using GenElute™ Gel Extraction Kit (Sigma) according to the manufacturer's instructions. Specifically, the digested backbone vector or target PCR product fragments were excised from agarose gel and weighed in separate colourless tubes. 3 gel volumes of the Gel Solubilization Solution was added into each gel slice and incubate at 55-60°C for 10 min until the gel slices were

completely dissolved. 1 gel volume of 100% isopropanol was added into the mixture and mixed until homogenous and then the mixture was loaded into the prepared binding columns with vacuum applied. The columns were then washed with 700µl of Wash Solution and dried before 50µl of Elution Solution was added into each column and incubated for 1 min to elute the bound DNA. The eluted DNAs were checked on 1% agarose gel again and quantified with NanoDrop® ND-1000 (NanoDrop Technologies) for the future processes or stored at -20°C.

2.1.1.5 Ligation

Ligation of insert DNA into plasmid vectors used for cloning (both digested with same endonucleases or endonucleases with compatible ends) was performed using T4 DNA ligase (Promega). For a 10µl reaction for generating pLenti TRE or pLenti TRE tight, digested plasmid DNA (100-200ng) was mixed with insert DNA at a molar ratio of 1:5 to 1:8; 1µl of 10X ligase buffer and 1.5 units of T4 DNA ligase were added into the mixed DNA. For a 10 µl reaction for generating short aP2 promoter vector pBS-sAP2, 100ng of digested and purified short aP2 PCR product was mixed with 1µl of 10X ligase buffer and 1.5 units of T4 DNA ligase. All the ligation reactions were incubated at 15°C overnight.

2.1.1.6 Transformation

The ligation products were transformed into *E.coli.* competent cells either by chemical transformation or electroporation method.

(1) Chemical Transformation

Ligated plasmid vectors were transformed in Hanahan TOP10 chemical competent cells. Competent cells were thawed on ice and 50µl of competent cells were transferred into a pre-chilled microcentrifuge tube. 2µl of ligated products were pipetted into the tube containing competent cells and the DNA/cell mixture was swirled gently to mix. Tubes were incubated on ice for 20min and heat-shocked at 42°C for 45sec. Tubes were returned to ice and after 2min 400µl of Lysogeny broth (LB) medium was added, and the samples were incubated in a shaking incubator (200rpm) at 37°C for 1 hour. The transformation mixture (100-200µl) was plated on

LB-Agar plate containing the correct antibiotics (ampicillin at 100µg/ml; kanamycin at 50µg/ml) and incubated at 37°C overnight.

(2) Electroporation

40µl of E.coli. MDS42 electroporation competent cells were taken out from -80°C and thawed out on ice for 2min. 2µl of ligated plasmid vectors were then added into the MDS42 competent cells, gently mixed and incubated on ice for 1min before being pipetted into a 0.2cm electroporation cuvette (Bio-Rad). The cuvette was then placed in the safety chamber stick of Gene Pulsar (Bio-Rad) apparatus with the settings as 25µF, 2.5kV, 200W. After one pulse (Ensure time constant>4 after pulsing!), the cuvette was removed from chamber and 1ml LB medium was added in immediately. The transformation mixture was pipetted out into a test tube and incubated at 37°C for 1 hour before spreading (10-20µl) onto LB-Agar plates containing the correct antibiotics and incubated at 37°C overnight.

Single colonies were picked from the plate (either chemically or electrically transformed) into 3ml LB medium and incubated at 37°C overnight. Plasmid minipreps (see below) were performed and the extracted plasmids were digested with specific endonucleases to identify if they were the correct clones.

2.1.1.7 Small scale isolation of plasmid DNA (Miniprep)

Zyppy™ Plasmid Miniprep Kit (Zymo Research) was used for small scale (5-15µg DNA per culture) plasmid isolation. After colonies were grown in 3ml of LB medium (12-16 hours at 37°C), an aliquot of cell suspension (500µl) was taken out to mix with 500µl autoclaved 35% glycerol and kept at -80°C for stock. Plasmid DNA was prepared according to the manufacturer's instructions. Specifically, an aliquot (~1.3ml) of the overnight bacteria culture was taken out into a 1.5ml microcentrifuge tube and centrifuged at 8000rpm for 1 min to pellet the bacteria. The bacteria pellet was then resuspended with 600 µl of sterilized water. 100 µl of 7× Lysis Buffer was added into the tube and the tube was inverted 6-8 times to mix and then incubated at room temperature for 2 min to lyse the bacteria cells. To neutralize the lysis mixture, 350 µl of 2× Neutralization Buffer was added into the tube and the tube was immediately inverted for 10 times to mix thoroughly, indicated by the appearance of yellow

precipitates. The tubes were then centrifuged at 13,500rpm for 5 min at room temperature to pellet the precipitates. The supernatant was transferred to the provided Zymo-Spin™ IIN column and incubated at room temperature for 1 min before centrifuged (top speed, room temperature, 15 sec) and discarded the flow through. 200 µl of Endo-Wash Buffer was added into each tube to wash away the endotoxin and then 400 µl of Wash-Buffer was applied onto the column for a final wash. When the column was dried out, 30 µl of Zyppy™ Elution Buffer was added directly into the centre of the column, incubated at room temperature for 1 min and then centrifuged at 13, 500 rpm for 1 min to elute the plasmid DNA. The eluted DNA was then ready for immediate use or stored at -20°C.

2.1.1.8 Large scale isolation of plasmid DNA (Maxiprep)

Zyppy™ Plasmid Maxiprep Kit was used for large scale (100-200µg DNA per culture) plasmid isolation. Colonies were grown in 200ml of LB medium for 12-16 hours at 37°C and the plasmid DNA was prepared following the manufacturer's recommendations. Briefly, 150 ml of fresh bacteria culture was centrifuged at ≥ 3,400×g for 10 min to pellet the bacteria, which was then resuspended with 15 ml of P1 Buffer. 15 ml of P2 Buffer was then added into the bacteria and the tube was inverted 4-6 times then stood at room temperature for 1 min to lyse the cells completely. 20 ml of P3 Buffer was then added into the tube to neutralize the mixture and the tube was incubated on ice for 5 min when the yellowish precipitate formed. The mixture was then added into the Zymo-Maxi Filter™/ Zymo-Spin™ VI column assembly onto a vacuum manifold to let all the liquid flow through both columns. The Zymo-Maxi Filter™ was then discarded and 10 ml of Endo-Wash Buffer was added into the Zymo-Spin™ VI column to wash away the endotoxin followed by another wash with 10 ml of Zyppy™ Wash Buffer. After drying out the residual Wash Buffer in the column by keeping the vacuum on for extra 5 min, the Zymo-Spin™ VI column was transferred into a clean 50 ml conical tube and 2-3 ml of Zyppy™ Elution Buffer was added into the column and incubated at room temperature for 1 min before centrifuged at ≥3,400×g for 1 min to elute the plasmid DNA. The eluted DNA was then ready for immediate use or stored at -20°C.

2.1.1.9 Vector sequencing

The vectors constructed were sent to MWG for sequencing and the sequencing reports are attached as Appendix E.

2.1.2 Gateway® Cloning using the MultiSite Gateway® ProKit (3-fragment cloning)

The MultiSite Gateway® Pro Kits from Invitrogen facilitate rapid and highly efficient construction of an expression clone containing the choice of two, three or four separate DNA elements. Based on the Gateway® Technology (Hartley et al., 2000; Sasaki et al., 2004; Yahata et al., 2005), the MultiSite Gateway® Technology uses site-specific recombinational cloning to allow simultaneous cloning of multiple DNA fragments in a defined order and orientation. The Gateway® Technology is a universal cloning method based on the bacteriophage lambda into the E. coli chromosome and the switch between the lytic and lysogenic pathways (Landy, 1989). In phage lambda, recombination occurs between phage and *E. coli* DNA via specific recombination sequences denoted as att sites. Recombination occurs following two pairs of strand exchanges and ligation of the DNAs in a novel form. Recombination is conservative and requires no DNA synthesis. The DNA segments flanking the recombination sites are switched, such that after recombination, the att sites are hybrid sequences comprised of sequences donated by each parental vector. Recombination reactions are catalyzed by a mixture of enzymes that bind to the att sites, bring together the target sites, cleave them, and covalently attach the DNA. The lysogenic pathway is catalyzed by phage lambda integrase (Int) and *E. coli* Intigration Host Factor (IHF) proteins (BP Clonase™ II enzyme mix) while the lytic pathway is catalyzed by the phage lambda Int and Excisionase (Xis) proteins, and the E. coli Integrateion Host Factor (IHF) protein (LR Clonase™ II Plus enzyme mix)(Invitrogen, 2006).

attB, attP, attL and attR are recombination sites that are utilized in the Gateway® Technology. attB sites always recombine with attP sites in a reaction mediated by the BP Clonase™ II enzyme mix:

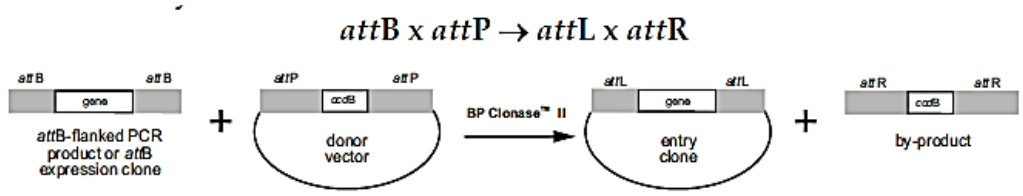

The BP reaction is the basis for the reaction between the donor vector (pDONR™) and PCR products or other clones containing attB sites. Recombination between attB and attP sites yields attL and attR sites on the resulting plasmids. The entry clone containing the PCR product is used in the LR recombination reaction (Invitrogen, 2006).

attL sites always recombine with attR in a reaction mediated by LR Clonase™ II Plus enzyme mix:

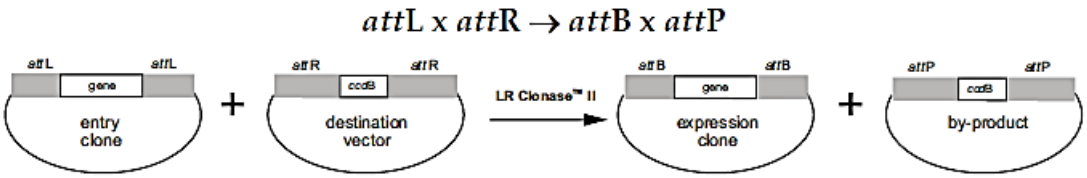

The LR reaction is the basis for the entry clone(s) × destination vector reaction. Recombination between attL and attR sites yields attB and attP sites on the resulting plasmids. The expression clone containing the PCR product is used in the expression system. The by-product plasmid contains the ccdB gene and prevents growth if taken up by the competent cells without corresponding resistance after transformation (Invitrogen, 2006).

The MultiSite Gateway® cloning system used in this project was 3-fragment cloning, i.e. to recombine the gene of interest, the reverse tetracycline-controlled transactivator (rtTA) and the promoter driving rtTA together into a pLenti6 (or modified Tet on pLenti) destination vector for conditional transient overexpression or lentivirus production. In this process, three PCR products flanked by specific attB or attBr sites and three MultiSite Gateway® Pro Donor vectors were used in separate BP recombination reactions to generate three entry clones. The three entry clones and a destination vector were used together in a MultiSite Gateway® Pro LR recombination

reaction to create the expression clone containing three DNA elements. The cloning process is illustrated as following (Invitrogen, 2006):

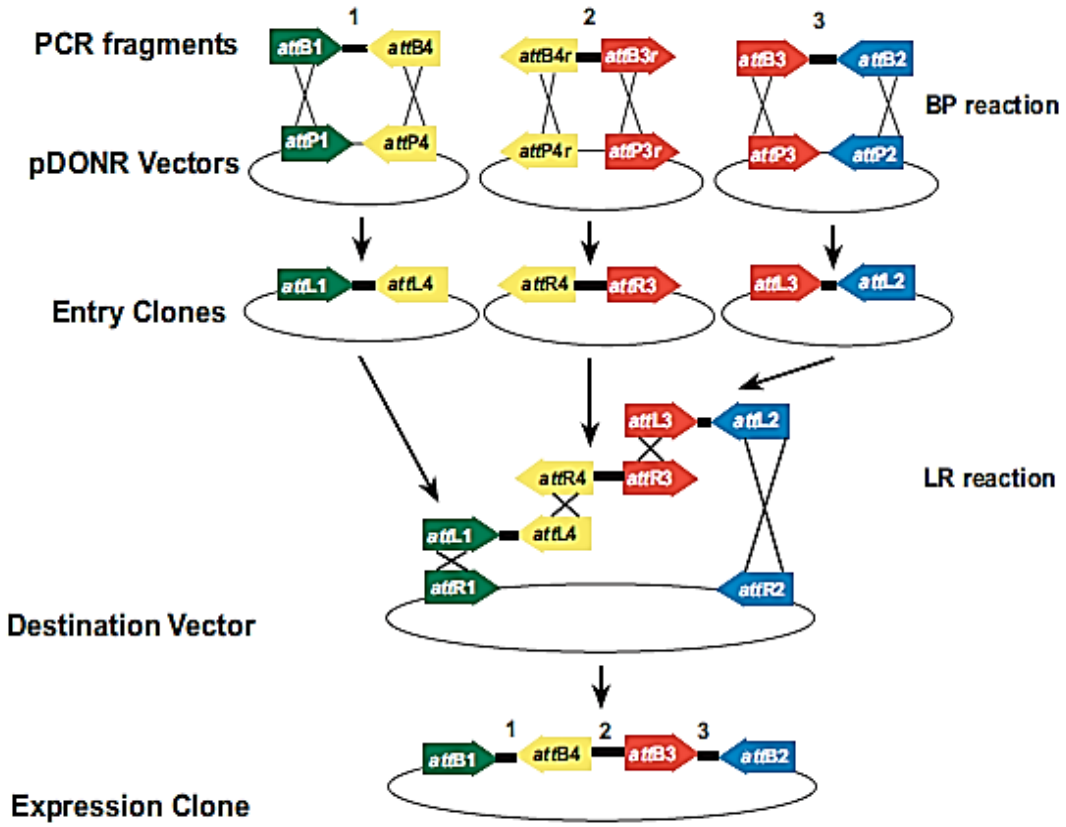

The constructed inducible lentiviral expression vectors would be able to express the gene of interest in response to the inducer doxycycline (Dox) and the mechanism of the inducible expression is explained by the diagram below:

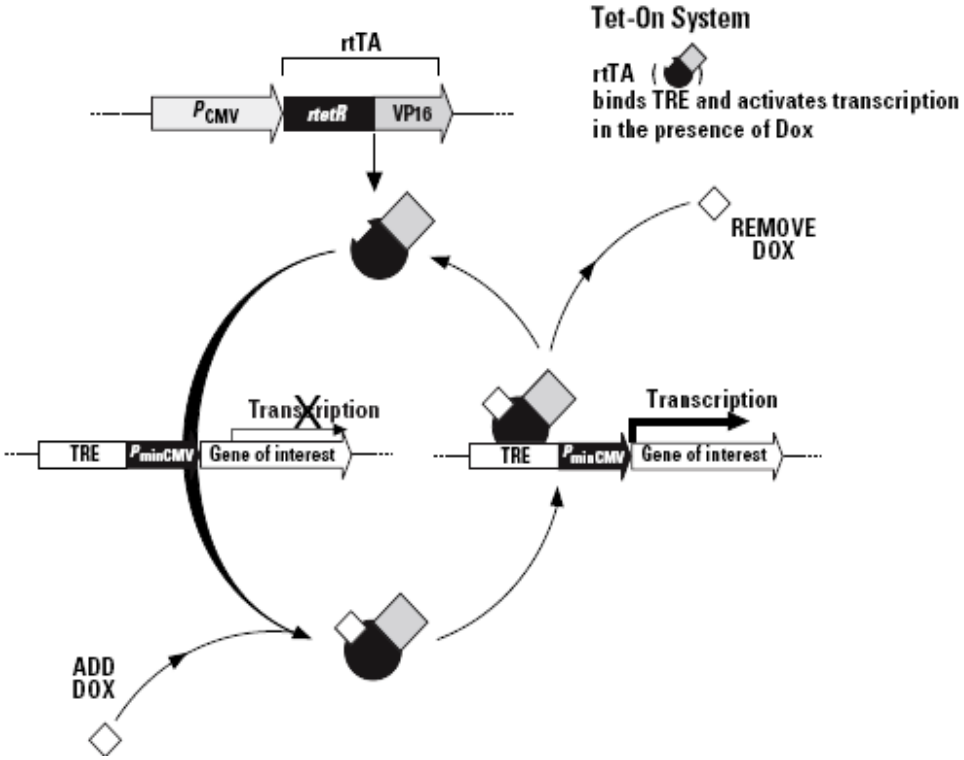

The TRE is located upstream of the minimal CMV promoter (PminiCMV) which is silent in the absence of activation. The Tet regulatory protein (rtTA) binds the TRE and activates transcription in the presence of Dox.

For an ambitious plan to realize a fat-specific inducible expression in vivo or in embryonic stem cells, a fat-specific promoter aP2 promoter and its artificial truncated form short aP2 promoter (sAP2) was to use for driving the expression of rtTA. The vector constructed with aP2 promoter would not be available for producing lentivirus due to its too big size, but for the purpose of comparing the fat specificity of the artificial sAP2 promoter with the original full length aP2 promoter, an entry clone containing full length aP2 promoter was also generated and used to generate the corresponding pLenti expression vectors in parallel with the sAP2. The plasmid pBluescript-aP2 from Addgene was used as the template for amplifying full length aP2 PCR product.

2.1.2.1 Construction of Entry Clones for 3-fragment recombination

1) Generation of the Entry Clone for the gene of interest (i.e. C/EBPβ or Luciferase/GFP (LucGFP) for control)

Appropriate PCR primers were designed against the sequence of C/EBPβ (template: pcDNA3.1-C/EBPβ plasmid from Addgene) or LucGFP (template: pL3-TRE-LucGFP-2L plasmid from Addgene), and attB1 and attB4 sites were added onto the 5' and 3' ends of the product, respectively.

C/EBPβ_attB1_Forward: *GGGG ACA AGT TTG TAC AAA AAA GCA GGC T*accatggaagtggccaacttctac

C/EBPβ_attB4_Reverse: *GGGG AC AAC TTT GTA TAG AAA AGT TGG GTG* tagcagtggcccgccgaggcc

Luc/GFP_attB1_Forward: *GGGG ACA AGT TTG TAC AAA AAA GCA GGC T*ccaccatggaagacgccaaaaac

Glob_Term_attB4_Reverse (for cloning LucGFP): *GGGG AC AAC TTT GTA TAG AAA AGT TGG G*tgagaagagggacagctatgac

Note: the italic capital letters stands for the sequence for adding in att sites.

A BP recombination reaction was performed between the attB1 and attB4-flanked PCR product and pDONOR P1-P4 to generate the entry clone for C/EBPβ or LucGFP.

2) Generation of the Entry Clone for CMV, aP2 or short aP2 (sAP2) promoter driving reverse tetracycline-controlled transactivator

Appropriate PCR primers were designed against the sequence of CMV (template: pTet on plasmid from Clontech) aP2 promoter (template: pBS-aP2 from Addgene) or sAP2 promoter (template: pBS-sAP2 constructed in 2.1.1.5), and attB4r and attB3r sites were added onto the 5' and 3' ends of the product, respectively.

CMV_attB4r_Forward: *GGGG ACA ACT TTT CTA TAC AAA GTT G*tattggctcatgtccaacattaccgcc

CMV_attB3r_Reverse: *GGGG AC AAC TTT ATT ATA CAA AGT TGT*gagctctgcttatatagacctcc

aP2_attB4r_Forward: *GGGG ACA ACT TTT CTA TAC AAA GTT G*atatcgaattcccagcaggaatcaggtagc

aP2_attB3r_Reverse: *GGGG AC AAC TTT ATT ATA CAA AGT T GT*ctgcagcacaggagggtgctatgagcc

Note: the italic capital letters stands for the sequence for adding in att sites and aP2 and sAP2 promoter entry clones share the same forward and reverse cloning primers.

A BP recombination reaction was performed between the attB4r and attB3r-flanked PCR product and pDONOR P4r-P3r to generate the entry clone for CMV, aP2 or sAP2 promoter.

3) Generation of the Entry Clone for reverse tetracycline-controlled transactivator (rtTA or rtTA advance)

Appropriate PCR primers were designed against the sequence of rtTA (template: pTet on from Clontech) or rtTAadv (PB-CA-rtTA advance from Addgene), and attB3 and attB2 sites were added onto the 5' and 3' ends of the product, respectively.

rtTA_attB3_Forward: *GGGG ACA ACT TTG TAT AAT AAA GTT G*atccagcctccgcggccccg

rtTA_polyAattB2_Reverse: *GGGG AC CAC TTT GTA CAA GAA AGC TGG GTA*gcttggtcgagctgatacttcccgtcc

rtTA adv_attB3_Forward: *GGGG ACA ACT TTG TAT AAT AAA GTT G*gcaggcttcaccatgtctagactggac

rtTA adv_glob term_attB2_Reverse: *GGGG AC CAC TTT GTA CAA GAA AGC TGG GTA*ggtcgagggatcttcataagagaagaggg

Note: the italic capital letters stands for the sequence for adding in att sites.

A BP recombination reaction was performed between the attB3 and attB2-flanked PCR product and pDONOR P3-P2 to generate the entry clone for rtTA or rtTA adv.

All the primers above were designed using the computer programme AmpliX Version 1.5.4. The forward primers must contain following structure:

1. Four guanine (G) residues at the 5'end followed by
2. the 22 or 25 bp attB or attBr site followed by
3. at least 18-25 bp of template- or gene-specific sequences

The reverse primer MUST contain the following structure:

1. Four guanine (G) residues at the 5' end followed by

2. the 22 or 25 bp attB or attBr site followed by

3. 18-25 bp of template- or gene-specific sequences

The attB-flanked PCR products were purified using GenElute™ Gel Extraction Kit (Sigma) according to the manufacturer's recommendations.

To perform the BP recombination reaction, the attB-flanked PCR product and the corresponding pDONOR vector were mixed as following

components	Sample
attB PCR products (15-150 ng)	1-7 µl
pDONR™ vector (150 ng/ µl)	1 µl
1× TE Buffer (pH 8.0)	To 8 µl

2 µl of BP Clonase™ II enzyme mix was added into each of the above sample and mixed well by vortexing briefly twice and then incubated at 25°C overnight. 1µl of Proteinase K solution was added to each reaction and Incubated at 37°C for 10min and then proceeded to transform One Shot® Mach1™ T1R Competent Cells with the method mentioned in 2.1.1.6. The correct entry clones were verified by sequencing and restriction digest as described in 2.1.1.6.

2.1.2.2 Creation of expression vectors by performing LR recombination reactions.

The 3 entry clones above and the destination vector pLenti6.2/V5 (or pLentiTRE, pLenti TRE tight) were mixed as following

components	Sample
Entry clones (10 fmoles each)	1-7 µl
Destination vector (20 fmoles)	1 µl
1× TE Buffer (pH 8.0)	To 8 µl

2 µl of LR Clonase™ Plus enzyme mix was added into each sample above and mixed well by vortexing briefly twice. The reaction was then incubated at 25°C for 16 hours. 1 µl of the Proteinase K solution was added to each reaction and incubated for 10 minutes at 37°C and then proceeded to transform One Shot® Mach1™ T1R Competent

Cells with the method described in 2.1.1.6. The correct expression vectors were verified by restriction digest as described in 2.1.1.6.

2.1.3 Luciferase reporter and expression gene plasmid constructs

The luciferase reporter constructs including pGL3-264bp or -1873bp PGC1α promoter, pGL3-CRE constructs were generated using pGL3-basic vector (Promega) by Dr. G. Karamanlidis following the manufacturer's protocol. The pGL3-3.1kb UCP1 promoter was from Dr. Kozak LP. The pGL3-2.6kb PGC1α promoter plasmid (Plasmid 8887) and pGL3-PPRE-TK plasmid (Plasmid 1015) were from Addgene. The mutated pGL3-2.6kb PGC1α promoter constructs pGL3-2.6kb PGC1α (ΔCRE) and pGL3-2.6kb PGC1α (ΔPPRE) were kindly gifts from Dr. Villarroya F.

The expression gene plasmids pcDNA3.1-C/EBPβ (Plasmid 12557), pcDNA-PRDM16 (Plasmid 15503), pcDNA-PPARγ (Plasmid 8895) and pcDNA-flag-PGC1α (Plasmid 1026) all came from Addgene.

2.2 CELL CULTURE (INCLUDING PASSAGING, FREEZING AND DIFFERENTIATING CELLS)

Handling of media and cells was carried out in an airflow cabinet (AirStream™). Prior and after use, the bench surfaces of the flow cabinet were wiped with tissue and 70% ethanol. The brown preadipocyte cell line, HIB-1B, which was isolated from brown fat tumour of a transgenic mouse (Klaus et al., 1994), was kindly provided by Prof. Bruce Spiegelman (Dana Farber Cancer Institute). The white preadipocyte 3T3-L1 cell line, which was derived from disaggregated Swiss 3T3 mouse embryos (Green and Kehinde, 1975), was bought from American Type Culture Collection (ATCC). Cell lines were obtained as frozen cultures in 90% (v/v) FBS and 10% (v/v) dimethyl sulfoxide (DMSO) and kept in liquid nitrogen until use. In order to resuscitate the cell lines, cryovials containing the cells were taken out from liquid nitrogen and transferred immediately to a water bath at 37°C. After approximately 2-3 minutes (min) cells were pipetted

out in to a 25cm^{2}flask and 5ml of pre-warmed growth medium containing Dulbecco's modified Eagle's Media (DMEM; + 4500mg/l Glucose, + L-Glutamine, - Pyruvate) supplemented with 10% (v/v) FBS, 1% (v/v) penicillin and streptomycin, and 1% sodium pyruvate and mixed by swirling. The growth media for 293FT cells contained Dulbecco's modified Eagle's Media (DMEM; + 4500mg/l Glucose, + L-Glutamine, - Pyruvate) supplemented with 10% (v/v) non heat-inactivated FBS, 1% sodium pyruvate, 0.1mM MEM Non-Essential Amino Acid (NEAA), another 2mM L-glutamine and 500µg/ml Geneticin. The flask was then incubated in a humidified environment containing 5% CO_2 at 37°C.

2.2.1 Passaging and seeding HIB-1B, 3T3-L1, Cos7, 293FT, LentiX 293T and HT1080 cells.

Sub-confluent cells were routinely passaged 1:10 to 1:20 depending on original and required cell density in T75 flasks (Corning™). Growth medium (described before) was removed; the cells were washed with pre-warmed 1x Phosphate Buffered Saline (PBS) and 2ml of trypsin/EDTA added. The cells were incubated at 37°C for about 3 min, then 8ml of pre-warmed growth medium was added and the trypsinised cells were transferred with the medium into a 25ml Universal tube and centrifuged for 5 min at 1000 rpm at room temperature (RT). The old medium was discarded and the cells re-suspended in fresh medium. As the cells start to differentiate at confluence, they were passaged at 70% confluence.

For seeding cells for experiments, cells were counted using haemocytometer, diluted according to the required cell numbers and seeded into the appropriate cell culture dishes or plates.

2.2.2 Long term storage of cells

Cells from a 70% confluent flask were detached and pelleted as above. The pellet was re-suspended in 1ml of cell freezing medium (10% DMSO and 90% FBS) and pipetted in to cryovials (usually 1ml/cryovial). They were then transferred to -80°C freezer overnight and finally to liquid nitrogen for long term storage.

2.2.3 3T3-L1 differentiation

To stimulate 3T3-L1 cells to differentiate, they were grown to confluence in growth medium in 6-well plates. Two days later, 500µM 3-isobutyl-1-methylxanthine (IBMX), 250nM dexmethasone (Dex) and 167nM insulin in 2ml/well growth medium was added. Forty eight hours later, cells were fed with fresh growth medium supplemented with 167nM insulin. This medium was replaced every other day. Lipid droplets were observed 5-6 days after the cells were induced to differentiate.

2.2.4 Oil Red O and haematoxylin counter staining

Oil red O was used to stain lipids and haematoxylin stained the nucleus. Lab coat, gloves and eye protections were required during the work. Solutions were made up in fume hood.

The 0.5% w/v stock solution of Oil Red O was made up by adding 5g Oil Red O into 1L isopropanol and heated for 2 hours at 60°C with continuous stirring then stored at room temperature in the dark. Oil Red O stock was diluted 1:1.5 in 1% dextrin (able to decrease precipitation and to intensify the stain) to make up the working solution, which was then filtered with filter paper (Whatman™) after standing at room temperature for 1 hour.

To stain the cells, growth medium was removed from the cells and they were fixed with 3.7% formaldehyde for 20min and then rinsed quickly (15 sec) with 60% isopropanol diluted in ddH_2O. Oil Red O was added into the cells and left for 20min at room temperature. Cells were then briefly washed in 60% isopropanol for 15 sec and rinsed in tap water. Haematoxylin (working solution from Sigma) was added onto the cells for 3min for counter staining and cells were then rinsed in tap water followed by brief washes (3 'dips') with Scott's tap water (1L dH_2O+ 20g sodium bicarbonate+ 3.5g magnesium sulphate). The counter-stained cells were air dried for a few minutes and covered by a layer of 50% glycerol.

2.3 TRANSIENT TRANSFECTION IN MAMMALIAN CELL LINES AND REPORTER ASSAY

2.3.1 Transient transfection in HIB-1B cells

For reporter gene assays, HIB-1B cells were seeded into 96-well plate at the density of 7000 cells/well in antibiotic free growth medium so that they could get 60-70% confluence the next day for transfection. On the day of transfection, 100ng/well reporter gene plasmid together with expression plasmids (20ng/well each) were diluted in DMEM and FugeneHD® (Roche) was added into the same mixture at a charge ratio of 3:1 to DNA. After 20 min incubation at room temperature, the transfection mixture was applied to the cells. 24 hours after transfection, the transfection medium was removed and replaced with fresh antibiotic growth medium containing appropriate treatment for the cells. For RNA extraction, cells were plated in 6-well plates and when they reached 60-70% confluence they were transiently transfected with expression plasmids (2µg DNA/well) using FugeneHD® as stated above.

2.3.2 Transient transfection in 3T3-L1 cells

Transfection protocol with Lipofectamine2000 (Invitrogen)

For reporter gene assays, 3T3-L1 cells were seeded into 24-well plates at a density of 2×10^4 cells/well in antibiotic free medium so that they could reach 90-95% confluence in two days, for transfection. On the day of transfection, the medium was removed from the cells and fresh antibiotic free media was added onto the cells about 2 hours before doing transfection. Transfection mixture was prepared in two separate tubes. One with the DNA mixture containing 400ng/well reporter gene plasmid and 50ng/well of each expression plasmid diluted in 50µl/well Optimem® and the other was Lipofectamine2000 mixture where Lipofectamine2000 was added into 50µl/well Optimem® at the charge ratio of 2:1 to DNA and incubated at room temperature for 5 min. Then the two mixtures were mixed together and incubated at room temperature for another 15-20 min before applying to the cells. Transfection medium was taken

out and fresh antibiotic medium was added onto the cells 6-8 hours post transfection. 24 hours after transfection, the transfection medium was removed and replaced with fresh antibiotic growth medium containing appropriate treatment for the cells. For RNA extraction, cells were plated in 6-well plates and when they reached 90-95% confluence they were transiently transfected with expression plasmids (2µg DNA/well) using Lipofectamine2000 as stated above.

Transfection protocol with FugeneHD® (Roche)

For reporter gene assays, 3T3-L1 cells were seeded in 24-well plates at a density of 3×10^4 cells/well in antibiotic free growth medium so that they could reach 70-80% confluence the next day for transfection. On the day of transfection, 400ng/well reporter gene plasmid together with expression plasmids (50ng/well each) were diluted in DMEM and FugeneHD® (Roche) was added into the same mixture at a charge ratio of 3:1 to DNA. After 20 min incubation at room temperature, the transfection mixture was applied to the cells. 24 hours after transfection, the transfection medium was removed and replaced with fresh antibiotic free growth medium containing appropriate treatment for the cells. For RNA extraction, cells were plated in 6-well plates and when they reached 70-80% confluence they were transiently transfected with expression plasmids (2µg DNA/well) using FugeneHD® as stated above.

As the tranfection of 3T3-L1 with FugeneHD® saved one day of time and cells were in better status because the medium was changed for fewer times compared with using Lipofectamine2000, the FugeneHD® transfection protocol was finally used for 3T3-L1 transient transfection.

2.3.3 Luciferase reporter gene assay

For measuring the firefly luciferase activity (pGL3), the multiwell plates (96 well or 24 well plates) containing the transfected cells were washed once with PBS. Then, 50 µl of phenol red-free media (DMEM; Invitrogen) and 50µl of Dual-Glo Luciferase Buffer and substrate mix were added in each well. Plates were gently rocked on an orbital shaker (Stuart Scientific) for 10 min at room temperature (RT) and then transferred into a 96-well white plate compatible with the luminometer (Turner) and the firefly luminescence was measured. To measure the renilla luciferase activity (pRL), 50µl of

Dual-Glo “Stop &Glo” buffer mixed with 0.5µl of “Stop &Glo” substrate were added into the same wells in which firefly luciferase activity had been measured. The plates were then rocked gently at RT for another 10min before the renilla luminescence was measured. Values were expressed as ratios of the luminescence from the firefly (experimental vector: pGL3) to renilla (control vector: pRL-SV40) luciferase activity.

2.4 PRODUCING LENTIVIRUS IN 293T CELLS

2.4.1 Transfection of 293FT cells to produce lentivirus

Protocol 1 (from Invitrogen “virapowerlentiviral system manual”)

5×10^6 293FT cells in 10ml antibiotic free growth medium (described before) were seeded into a 10cm dish to reach 90-95% confluence the next day for transfection. On the day of transfection, medium was removed from the cells and replaced with 5ml of growth medium without any antibiotics. In a sterile tube 9µg of the ViraPower™ Packaging Mix plasmid and 3µg of one of the plenti6 expression vectors were diluted in 1.5ml Opti-MEM® I Medium without serum and mixed gently. In a separate tube, 36µl of Lipofectamine2000 was diluted in 1.5ml Opti-MEM® I Medium without serum, gently mixed and incubated at RT for 5min. The two tubes were then combined together and incubated at RT for another 20min and then added into each plate of 293FT cells. The medium containing DNA-Lipofectamine2000 complexes was replaced with 10ml growth media without antibiotics the next day and the lentivirus could be harvested 48-72 hours posttransfection.

Protocol 2 (from Roslin Institute)

2.5×10^6 LentiX293T (293T) cells in 5ml antibiotic free growth medium (described before) were seeded into a T25 flask to reach 70-80% confluence the next day for transfection. On the day of transfection, transfection mix was prepared by adding 2µg of psPAX2 packaging plasmid, 1µg of psVSV-G plasmid, 1.5µg of one of the plenti6 expression plasmids and 17µl FugeneHD® into 145µl Opti-MEM® serum free medium. After 20min incubation at RT, the transfection mix was applied onto the cells. Medium on the cells was changed into fresh antibiotic free growth medium or serum

free medium the next morning and the lentivirus could be harvested 48 hours posttransfection.

2.4.2 Harvest and concentrate the lentivirus

Supernatant was collected from the dish or flask of transfection and centrifuged at 2000g for 5min at 4°C to pellet debris, and then filtered through a Millex-HV 0.45µm PVDF filter. Virus were then concentrated by ultracentrifuge at 52,000g for 2 hours at 4°C and resuspended in TSSM buffer (20mM Trizma base, 0.1M NaCl, 10g/L sucrose and 10g/L mannitol, pH7.4). The pellet needed to be loosened on ice on flatbed rocker for 1 hour before pippeting gently to resuspend. A spin of 2000rpm for 2min was applied to the resuspended virus to get rid of any residual debris. The concentrated virus was then aliquoted and stored at -80°C.

2.4.3 Titering the lentivirus in HT1080 cells

HT1080 cells in antibiotic free growth medium (described above) were seeded into 6-well plates at 2×10^6cells/well so they could reach 30-50% confluence the next day for transduction. On the day of transduction, each of the un-concentrated lentiviral stocks was serially diluted by the factors of 10^2, 10^3, 10^4, 10^5 and 10^6 in 1ml antibiotic free medium and then applied to the HT1080 cells with 6µg/ml polybrene. The virus-containing medium was replaced by fresh antibiotic free medium the next day and 8µg/ml blasticidin was added into the medium for selection one day later. The selection process lasted 10-12 days with medium changed every 3-4 days.

2.5 TRANSDUCTION OF STABLE CELL LINES OVEREXPRESSING C/EBP BETA (OR LUCGFP AS CONTROL) WITH LENTIVIRUS

2.5.1 Infect the 3T3-L1 preadipocytes with constitutive and inducible C/EBPβ and LucGFP control lentivirus and select with blasticidin.

3T3-L1 preadipocytes were plated in complete growth medium in 96-well plates at the density of 1.5×10^3 cells/well so the cells were 30-50% confluence the next day for transduction. On the day of transduction, the lentiviral particles containing the genes

of interest were diluted into 100µl of the growth medium so that the Multiplicity of Infection (MOI) was about 30. The diluted virus was applied to the 3T3-L1 cells with 6µg/ml polybrene. The virus-containing medium was replaced by fresh growth medium the next day and 8µg/ml blasticidin was added into the medium for selection one day later. The transduced cells were transferred into larger wells after growing confluent. The medium was changed every 3-4 days and the selection process lasted for 10-12 days so that the surviving cells reached high confluence in the wells.

2.5.2 Testing the expression of transgenes in the survived cell polyclones

The surviving 3T3-L1 cells transduced by LucGFP lentiviral particles were checked with fluorescence microscopy (Leica DFC 420C) for GFP expression according to the manufacturer's instructions. Photos were taken with 150× magnification. The LucGFP lentivirus transduced cells were also checked for the luciferase activity with luciferase assay as described in 2.3.3. The surviving cells transduced by C/EBPβ lentiviral particles were checked for C/EBPβ overexpression by measuring the relative mRNA level of C/EBPβ comparatively in mock and transduced cells using the methods that will be addressed in 2.6.

2.5.3 Select monoclones expressing the genes of interest

As the integration of viral DNAs into the cell genome is random, it is not guaranteed that every cell survives from blasticidin selection can also express the genes of interest efficiently. Therefore it is necessary to pick up single colonies of cells and to test the expression level of transgene in each colony. Two methods were used to select for the monoclone cells expressing the genes of interest.

The first one was to trypsinize the blasticidin resistant cells, count them and dilute into 5 or 2 cells/100µl growth medium into one well of 96-well plates. The growth of the cells were then monitored by microscopy day by day and the cells in the wells containing only one cell colony were picked out and transferred into bigger culture dish for further growth.

The second method was used before the selection process finished, i.e. when the cells were still at low confluence and the cell colonies could be clearly distinguished. Cloning rings (small plastic rings cut from the 200µl tips) were used to surround each

single cell colony and the cells were trypsinised within the ring and transferred into bigger culture dish.

With either method, the transferred single colonies of cells were grown until high confluence and the expression of transgenes were checked with the methods described in 2.5.2. 2-3 colonies with high level of transgene expression were stored in liquid nitrogen or kept growing for future experiments.

2.6 TEST OF GENE EXPRESSION

2.6.1 RNA Isolation (RNA extraction from cell lines, Quantification of RNA)

Total RNA from 3T3-L1 and HIB-1B cells was isolated using Trizol® reagent (Invitrogen). Cells were washed once with cold PBS and 500µl of Trizol® reagent was added into each well and pipetted in and out to break nucleoprotein complex. Reactions were incubated at room temperature for 10-15 min and then transferred to 1.5ml micro centrifuge tubes and were kept at -80°C until processing further.

To process cell lysate for RNA extraction, samples were thawed at room temperature for 10min and 100µl of chloroform was added into each sample. After 15sec vortexing, samples were incubated at room temperature for 15min and then centrifuged at 12,000g for 15min at 4°C. Supernatants were transferred to fresh 1.5ml micro centrifuge tubes and 500µl of 100% isopropanol were pipette into each sample to precipitate the RNA. Tube contents were mixed gently and incubated at room temperature for 10-20min (or -20°C overnight if necessary), followed by another centrifuge of 12,000g for 15min at 4°C. Pellet was then air-dried for 10min and resuspended in 50-100µl of nuclease-free water. RNA samples were quantified using Nanodrop according to the manufacturer's instructions and then kept at -80°C until processed further.

2.6.2 DNase treatment and cDNA synthesis

RNA used for quantitative real time PCR (qRT-PCR) was initially treated with deoxyribonuclease (DNase) to remove residual contaminating genomic DNA. 200ng of RNA were mixed with 1µl of 10× DNase buffer and 1µl of RNase-free DNase (Promega)

in a total volume of 10µl, made up with nuclease-free water and then incubated at 37°C for 20min. Reactions were stopped by adding in 1µl of DNase Stop Solution (Promega) together with 0.4µg of Random Primers (Promega). Samples were heated at 65°C for 10min to inactivate the DNase and to denature the RNA. The addition of primers before heating also allowed them to anneal better on the RNA.

For complementary DNA (cDNA) synthesis, the Omniscript® Reverse Transcriptase Kit (Qiagen) was used. The DNase treated RNA samples containing random primers were mixed with 1µl of 2'-deoxynucleoside 5'-triphosphate (dNTP) mix (5mM each dNTP), 2µl of 10× Reverse Transcripase Buffer, 1µl of Omnicript Reverse Transcriptase (4 units) and 0.25µl of Rnasin™ (RNase inhibitors from Promega) to a final volume of 20µl, made up with nuclease-free water. One control reaction was also set up containing no Omniscript but water as the replacement ("no RT" control) to test whether there was DNA contamination. Samples were centrifuged briefly and incubated at 37°C for 2 hours. cDNAs were stored at -20°C.

2.6.3 Real time PCR

The LightCycler® 480 DNA SYBR Green I Master Mix (Roche) was used in the Real Time PCR analysis. SYBR Green I binds to all double-stranded DNA molecules and on binding fluorescence at 522nm increases. All cDNA samples were diluted (1:7.5 dilution) to ensure a smaller pipetting error between reactions set up in 384-well plates. In each reaction, 7.5µl of SYBR Green I Master Mix (2X) was mixed with 5.6µl of diluted cDNA and 0.95µl of each primer (10µM). LightCycler® 480 Instrument was used to perform the PCR reactions with the following temperature profile: an initial denaturation temperature at 95°C for 15min, 35-40 cycles of denaturation (20 sec at 95°C), annealing (20 sec at optimized annealing temperature) and extension (20 sec at 72°C). The data acquisition was performed during the extension period and a melting curve was acquired between 72°C and 95°C to check for primer dimers or other non-specific amplicons. The specificity of PCR products were also checked by agarose gel electrophoresis.

The primer sequences used for measuring gene expression were provided in the following table. The primers were designed using the software Primer Express.

Name	Forward Primer (5'to 3')	Reverse Primer (5'to 3')
PGC-1α	GTGCTTCGAAAAAGAAGTCCCATA	GTTGTTGGTTTGGCTTGAGCAT
UCP1	GCCATCTGCATGGGATCAA	GGTCGTCCCTTTCCAAAGTG
PPARγ	GTGCCAGTTTCGATCCGTAGA	GGCCAGCATCGTGTAGATGA
C/EBPβ	AGCGGCTGCAGAAGAAGGT	GGCAGCTGCTTGAACAAGTTC
Resistin	CTGTCCAGTCTATCCTTGCACAC	CAGAAGGCACAGCAGTCTTGA
PRDM16	TCTTACTTCTCCGAGATCCGAAA	GATCTCAGGCCGTTTGTCCAT
RIP140	CGACTTCCAGACCCACAACA	GGCGCTCTTGGCATCGT
18S	GTAACCCGTTGAACCCCATT	CCATCCAATCGGTAGTAGCG
36B4	TCCAGGCTTTGGGCATCA	TTATCAGCTGCACATCACTCAGAAT

2.8 STATISTICAL ANALYSIS

Data in figures is presented as average ± SEM from 2 or 3 independent replicate experiments with duplicate or triplicate wells in each experiment. Effects of treatments were determined by performing Student's *t*-test or Analysis of Variance (ANOVA) as indicated in individual figure legend. Significance was accepted if $P<0.05$. All statistical analyses were performed on SPSS statistical package version 16 (SPSS Inc. Chicago, IL, USA).

CHAPTER 3

3 CONSTRUCTION OF LENTIVIRAL VECTORS ALLOWING TETRACYCLINE-INDUCIBLE STABLE OVEREXPRESSION OF C/EBP BETA IN 3T3-L1

3.1 INTRODUCTION

C/EBPβ plays an important role in adipogenesis. This has been demonstrated by promotion of 3T3-L1 differentiation and conversion of multipotent NIH3T3 fibroblasts into committed adipoblasts , by overexpression of C/EBPβ in the absence of hormone inducers (Yeh et al., 1995). Furthermore, the use of a dominant negative C/EBP (lacking functional DNA-binding and transactivation domain) that forms stable heterodimers with C/EBPβ, results in inhibition of adipogenesis and mitotic clonal expansion in 3T3-L1 preadipocytes (Zhang et al., 2004c). Moreover, C/EBPβ is also indispensible in thermogenesis for adipocytes. Its overexpression rescues the cAMP-inducible expression of PGC1α and UCP1 in white preadipocytes (Karamanlidis et al., 2007). C/EBPβ, together with PRDM16, also facilitates the switch from myoblast progenitors to brown fat cells, morphologically and functionally (Kajimura et al., 2009). However, during hormone induced differentiation of white preadipocyte 3T3-L1 cells, the expression of C/EBPβ diminishes around Day 2, whereas in brown adipocyte differentiation, C/EBPβ expression is maintained at a high level throughout the whole process (Karamitri et al., 2009; Lane et al., 1999). The different expression patterns of C/EBPβ inspired the idea that the stable overexpression of C/EBPβ in white preadipocytes 3T3-L1s throughout the differentiation process may cause more brown-like terminal differentiated adipocytes.

To construct a stable transgenic 3T3-L1 cell line overexpressing C/EBPβ, the lentiviral vector expression system was chosen, as the system is known for its high viral titer and high efficiency in delivering exogenous gene into the genome of both dividing and non-dividing mammalian cells and animals (Twyman, 2005). Moreover, to easily

control when and how much to overexpress the gene, a tetracycline controlled (Tet on) expression system was also introduced to the viral vector (Pluta et al., 2007), thus the exogenous C/EBPβ is overexpressed in the presence of the inducer doxycycline. The expression is also induced in a dose-dependent manner, so the expression level can be controlled by the concentration of doxycycline added into cells (Clontech). The Tet on expression system has two essential components, the tetracycline responsive element (TRE) and the reverse tetracycline-controlled transactivator (rtTA), both of which have evolving design and sequences. The original TRE-based promoter was developed by Gossen and colleagues (Gossen and Bujard, 1992); it can realize the inducible expression in the presence of doxycycline but has a relatively high background noise (so-called "leakiness"). The improved TRE promoter, TRE tight (developed by Clontech) demonstrates greater inducibility coupled with extremely low basal activity by closer design of the 7 tetO sequences that make up the TRE and the removal of the potential binding sites of endogenous transcription factors (Clontech). The Tet on transactivator rtTA also has been improved (rtTA advanced) by utilizing human codon preferences and removing cryptic splice sites from the mRNA sequences to improve the expression in mammalian cells. It also contains some specific mutations that both increase its sensitivity to doxycycline and significantly diminish residual binding to TREs in the absence of doxycycline (Urlinger et al., 2000). Therefore there are two versions of TREs and two versions of rtTA, thus four different combinations, to test and select for a best backbone of doxycycline inducible expression.

The aim of the experimental work described in this chapter was to construct and select for the best inducible lentiviral backbone vector using a luciferase GFP (LucGFP) reporter gene with the multi-gateway recombination cloning method, and to use this backbone to overexpress C/EBPβ in 3T3-L1 cells inducibly. More ambitiously, the fat-specific inducible lentiviral vectors were also to be constructed with either a full length or truncated fat-specific promoter (aP2 promoter) for the potential use of this vector into embryonic stem cells or pronuclear injection. Unfortunately, the full length aP2 promoter is about 5.6kb in size, which has already exceeded the maximal insert size (4-5kb in total) of pLenti6 destination vector (Invitrogen), so a 1.2kb

truncated aP2 promoter, short aP2, containing only the fat-specific enhancer and the proximal promoter of the original aP2 promoter (Graves et al., 1992), was used to generate the vectors for lentivirus production. However, to compare the fat specificity of the two versions of aP2 promoter, both were used in plasmid vector construct and the consequential test for fat specificity in a transient transfection system.

The specific objectives of the experimental work described in this chapter include

1. To integrate TRE or TRE tight into the original pLenti6/V5 destination vector to make the tetracycline inducible lentiviral backbone vectors.

2. To clone the LucGFP reporter gene with either rtTA or rtTA advance transactivator into the TRE or TRE tight modified lentiviral destination vector to make the four inducible lentiviral vectors expressing LucGFP.

3. To test the four inducible lentiviral vectors in 3T3-L1 and HIB-1B preadipocyte cell lines using transient transfection method and to use the best one to overexpress C/EBPβ.

4. To put the fat-specific promoter into the best inducible lentiviral backbone(s) to make the fat-specific inducible lentiviral vectors expressing LucGFP.

5. To investigate the adipogenic conditions in the transient system to test the fat specificity of the fat-specific inducible lentiviral vectors in preadipocyte cell lines and to select for the best one to overexpress C/EBPβ.

3.2 EXPERIMENTAL DESIGN

3.2.1 Construction of tetracycline inducible lentiviral vector backbone with ligation-mediated cloning

The tetracycline response element (TRE) was amplified from a plasmid named pL3-TRE-LucGFP-2L (Addgene) by PCR, and ClaI and SpeI restriction sites were added onto the 5’ and 3’ ends of the PCR product respectively. An improved version of TRE, TRE tight was amplified from the plasmid pTRE-Tight miR-1 (Addgene) by PCR and the

same restriction sites ClaI and SpeI were added onto the 5' and 3' ends of PCR product as well. Each PCR product was then cloned into the original pLenti6/V5 destination vector as described in 2.1.1. The modified destination vectors, named pLenti TRE and pLenti TRE tight, were then identified by restriction digest and DNA sequencing.

3.2.2 Construction of entry clones of CMV promoter, aP2 promoter, short aP2 promoter, C/EBPβ, Luciferase/GFP (LucGFP), and rtTA or rtTA advance with BP reaction (Gateway cloning) and the generation of constitutive and inducible (non-tissue specific) lentiviral expression vectors of LucGFP with LR reaction (Gateway cloning)

The lentiviral expression vectors were designed to integrate three components into the backbone, the gene of interest (LucGFP or C/EBPβ), the promoter (CMV, aP2 or short aP2) driving the expression of the transactivator, and the transactivator (rtTA or rtTA advance). Therefore all the genes of interest, promoters and transactivators were cloned into corresponsive entry clone backbones as described in 2.1.2.1. The entry clones were checked by restriction digest and DNA sequencing. The constitutive lentiviral expression vector of LucGFP was generated from the recombination of the entry clones of LucGFP, CMV and rtTA integrated into pLenti6/V5 destination vector by LR recombination reaction as described in 2.1.2.2. The non-tissue specific inducible lentiviral expression vectors of LucGFP were generated in the same way but with an inducible lentiviral destination backbone vector, thus contained four combinations between two different inducible backbones (TRE and TRE tight) and two different transactivators (rtTA and rtTA advance). All the lentiviral expression vectors generated above were checked by restriction digest.

3.2.3 Selection for the best inducible backbone and to use the backbone for C/EBPβ overexpression.

The four non-tissue specific inducible lentiviral expression vectors of LucGFP were introduced into 3T3-L1 and HIB-1B preadipocytes by plasmid DNA transfection method to transiently overexpress the luciferase and GFP genes in the presence of doxycycline (Dox). Cells were seeded in 24-well plates and transfected with the

inducible expression vectors by FugeneHD® as described in 2.3.2 and Dox was added to the cells 24 hours post transfection. Luciferase activity was measured 24 hours after adding Dox as described in 2.3.3. The vector(s) displaying low basal expression level (low "leakiness") and good inducibility were used to generate C/EBPβ expression vector(s) by LR reaction.

3.2.4 Generation of fat-specific inducible expression vectors of LucGFP with the aP2 and short aP2 entry clones and the best inducible backbone.

The best non-tissue specific inducible lentiviral expression backbone(s) selected above were used to generate the fat-specific inducible lentiviral expression vectors of LucGFP together with entry clones of LucGFP and aP2 or short aP2 by LR recombination reaction. The generated vectors were checked by restriction digest.

3.2.5 Investigation on transient adipogenic conditions to test the fat-specific lentiviral expression vectors in a transient overexpression system.

Two methods were used to stimulate the adipogenic programme transiently in HIB-1B and 3T3-L1 preadipocytes. The first was to treat the confluent HIB-1B and 3T3-L1 preadipocytes in 6-well plates with 10μM rosiglitazone for 24 hours and in the latter 3 hours 10μM forskolin was added in before extracting RNA from the cells as described in 2.6.1. The second was to transiently transfect the preadipocytes with overexpression plasmids of C/EBPβ and PPARγ and to treat the cells with 10μM rosiglitazone 24 hours post-transfection and RNA was extracted from the cells 24 hours after adding rosiglitazone. The extracted RNAs were used to synthesize complimentary DNA (cDNA) as described in 2.6.2 and to perform real time PCR (described in 2.6.3) to detect if the expression of adipogenic marker gene aP2 was elevated compared with control groups. The effective adipogenic condition(s) were used to check the fat specificity of the fat-specific inducible lentiviral expression vectors of LucGFP. These vectors were introduced into HIB-1B and 3T3-L1 preadipocytes by plasmid transfection method (see 2.3.1 and 2.3.2) and treated with the transient adipogenic conditions as described above. Dox was given to the cells 24 hours before the luciferase activity was measured to check the fat-specificity and inducibility of each vector.

3.3 RESULTS

3.3.1 Identification of tetracycline inducible backbone pLenti-TRE and pLenti-TRE tight

The inducible lentiviral backbone vectors pLentiTRE and pLentiTRE tight derived from the original lentiviral vector pLenti6/V5 were digested with BamHI and XhoI separately at 37˚C for 4 hours before running a 1% agarose gel to check the sizes of digested fragments (Figure 3.1). The putative sizes of the fragments in each digest were obtained from the Vector NTI software from Invitrogen, and indicated in the text below the figure. Seen from the gel image, all the three vectors, pLenti6/V5, pLentiTRE and pLentiTRE tight, gave correct fragments in both BamHI and XhoI digests, indicating the proper identity of the modified inducible lentiviral destination vectors.

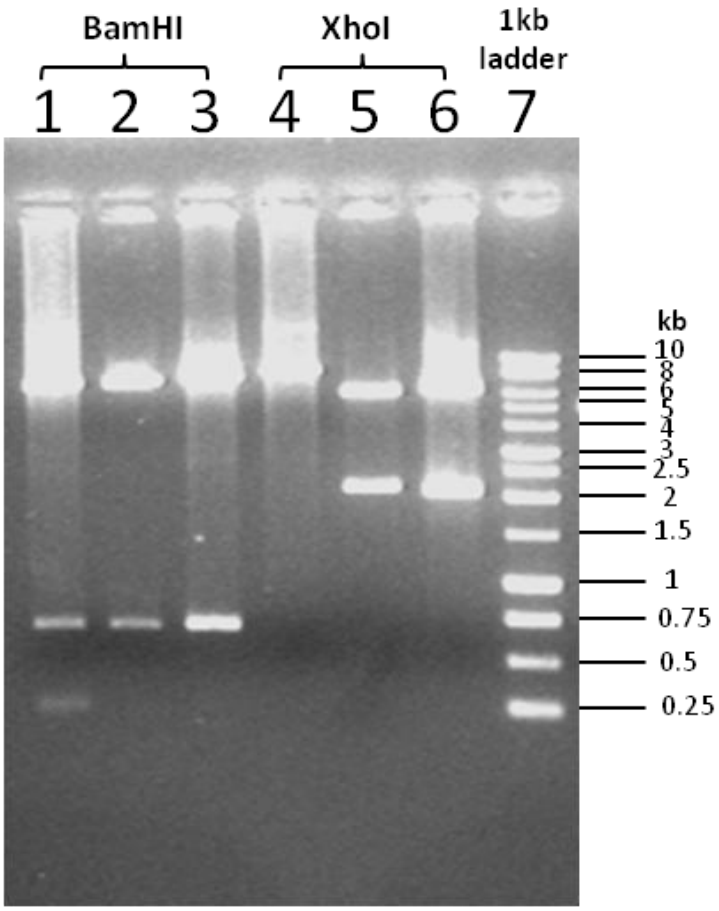

Figure3.1 Restriction digest of pLenti6/V5, pLenti TRE and pLenti TRE tight destination vectors

pLenti6/V5 (Lane 1 &4), pLenti TRE (Lane 2&5) and pLenti TRE tight (Lane 3&6) were digested by either BamHI or XhoI as indicated. 1kb ladder was loaded in Lane 7 and the size of each band has been labeled on the right. The putative sizes of digested fragments (in bp) were Lane1 (7749+ 703+ 236), Lane 2 (7874+ 703), Lane 3 (7733+ 703), Lane 4 (8688), Lane 5 (6329+ 2198) and Lane 6 (6344+ 2092).

3.3.2 Restriction digests of entry clones of CMV promoter, aP2 promoter, short aP2 promoter, LucGFP, rtTA and rtTA advance

Entry clones of CMV promoter, aP2 and short aP2 promoter, LucGFP, rtTA and rtTA advance derived from BP reactions were examined by double digests (Figure 3.2) with the restriction enzymes indicated in the text below the figure. The putative sizes of the fragments were obtained from Vector NTI (Invitrogen) and indicated below the figure as well. All the digested entry clones demonstrated correct sizes of the fragments in the agrose gel electrophoresis, indicating the correct identity of the entry clones.

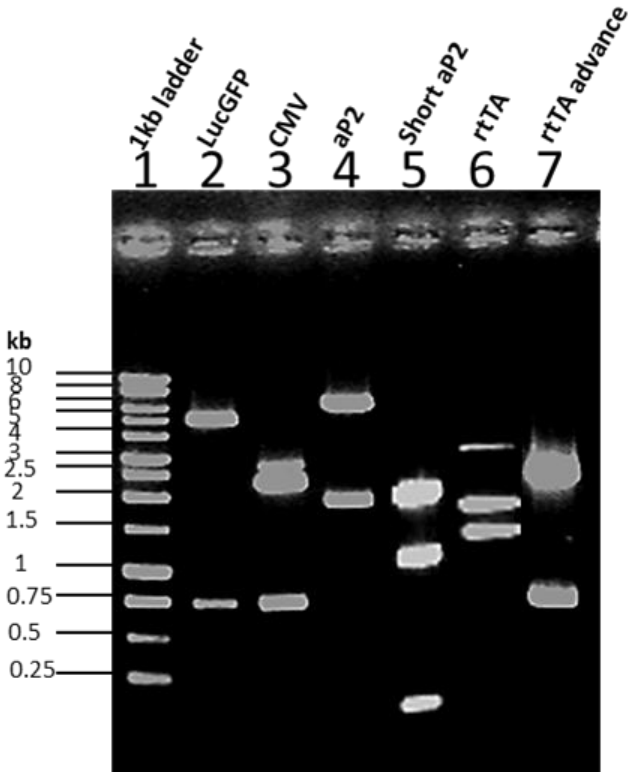

Figure 3.2 Restriction digest of entry clones

Entry clones of LucGFP, CMV promoter, aP2 promoter, short aP2 promoter, rtTA and rtTA advance were digested with specific restriction enzymes. 1kb ladder was loaded in Lane 1 and the size of each band has been labelled on the left. The putative sizes of digested fragments were Lane 2 (BamHI+ HindIII, 5081+ 754), Lane 3 (SpeI +PstI, 2247+ 733), Lane 4 (SpeI+ PvuI, 6054+ 1863), Lane 5 (EcoRI+ PstI, 2206+ 1179+ 164), Lane 6 (EcoRI+ PstI, 2159+ 1598) and Lane 7 (XbaI+ XmaI, 2304+ 735).

3.3.3 Restriction digests of the 4 inducible expression vectors of LucGFP (TRE rtTA, TRE tight rtTA, TRE rtTA adv and TRE tight rtTA advance)

The constitutive lentiviral expression vector of LucGFP pLenti6/v5-LucGFP and the four non-tissue specific inducible lentiviral expression vectors of LucGFP, pLentiTRE LucGFP rtTA, pLentiTRE tight LucGFP rtTA, pLentiTRE LucGFP rtTA advance and pLentiTRE tight rtTA advance were checked by double digests (Figure 3. 3) with the enzymes indicated in the text below the figure. The putative sizes of digested fragments were obtained from the analysis of Vector NTI (Invitrogen) and also indicated below the figure. The agarose gel image demonstrated that all the expression vectors examined gave correct fragment sizes in the digest, indicating the correct identity.

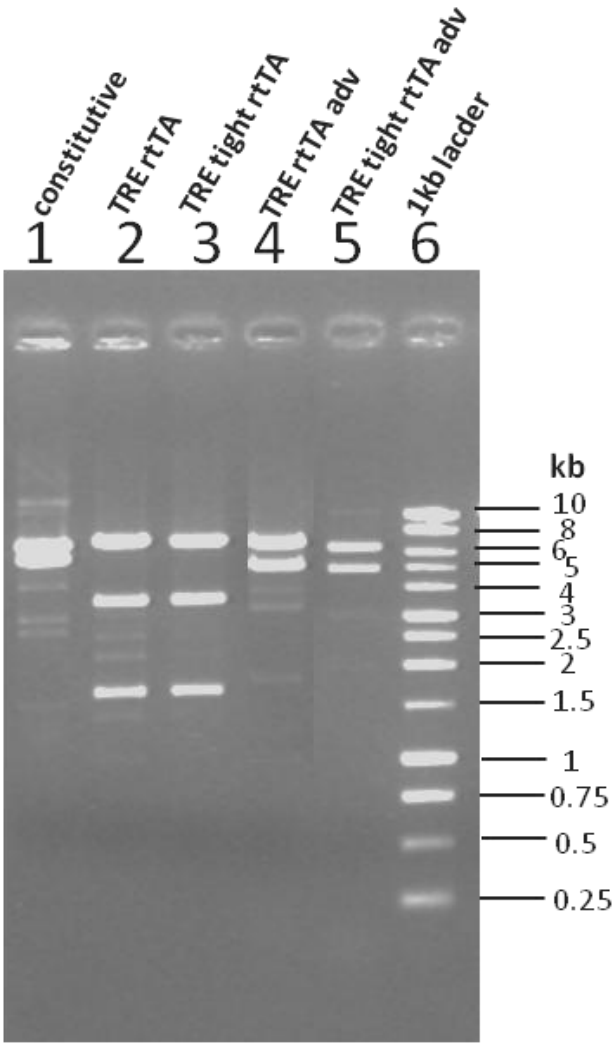

Figure 3.3 Restriction digest of non-tissue sepcific lentiviral expression vectors of LucGFP

Constitutive and the four inducible (non-tissue specific) lentiviral expression vectors of LucGFP were digested with specific restriction enzymes. The putative sizes of digested fragments were Lane 1 (PstI+ XhoI, 6951+ 5838), Lane 2 (PstI+ BamHI, 7300+ 3638+ 1690), Lane 3 (PstI+ BamHI, 7209+ 3638+ 1690), Lane 4 (PstI+ SacII, 6771+5139), Lane 5 (PstI+ SacII, 6680+5113). 1kb ladder was loaded in Lane 6 and the size of each band has been labelled on the right.

3.3.4 Comparison of the 4 inducible LucGFP lentivral expression vectors in 3T3-L1 and HIB-1B preadipocytes

The four non-tissue specific inducible lentiviral expression vectors of LucGFP were introduced separately into 3T3-L1 and HIB-1B preadipocytes by transient transfection. 1μM doxycycline (Dox) was given to the cells 24 post-transfection and treated for 24 hours before luciferase assay (Figure 3.4). Results demonstrated that the pLentiTRE LucGFP rtTA advance and pLentiTRE tight LucGFP rtTA advance had low basal activity in the absence of Dox and the induced activity (5.5 and 6 fold induced, respectively, $P<0.05$) of both were comparable with the constitutive vector in 3T3-L1 cells (Figure 3.4A). In HIB-1B cells (Figure 3.4B), the pLentiTRE LucGFP rtTA advance had even lower basal activity and a better induciblity (7.7 fold induced, $P<0.05$) although the absolute value of induced luciferase activity was only half of the constitutive value. Similar to the result in 3T3-L1, pLentiTRE tight LucGFP rtTA advance in HIB-1B cells also had relative low leakiness and good inducibility (6.2 fold induced, $P<0.05$), and the induced luciferase activity was comparable to that of the constitutive value.

Figure 3.4 Comparison of different Tet on LucGFP vectors (CMV driven) by luciferase assay in 3T3-L1 (A) and HIB-1B (B) preadipocytes.

HIB-1B and 3T3-L1 preadipocytes were transiently transfected with different Tet on LucGFP vectors (CMV driven), the empty vector pLenti TRE (negative control) or the constitutive vector pLenti 6 CMV LucGFP (positive control). Cells were given 1μg/ml doxycycline (Dox) 24 hours post-transfection and treated for 24 hours. Luciferase activity was relative to the value from the cells transfected with TRE tight LucGFP CMV rtTA adv vector without doxycycline induction. Results represent mean ± S.E.M from 2 independent replicate experiments performed in triplicate wells. Student's *t*-test was used to analyse the data. *$P<0.05$ caused by gene overexpressions with respect to "TRE rtTA (-Dox)" group; #$P<0.05$ caused by Dox with respect to the group overexpressing the same vector without Dox treatment.

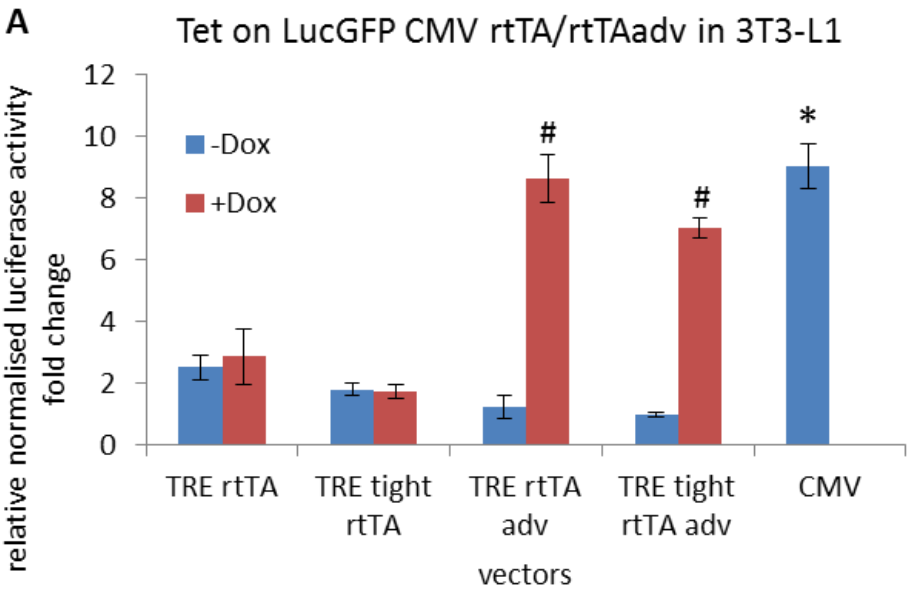
A
Tet on LucGFP CMV rtTA/rtTAadv in 3T3-L1
relative normalised luciferase activity
fold change
12
10
8
6
4
2
0
-Dox
+Dox
#
#
*
TRE rtTA
TRE tight rtTA
TRE rtTA adv
TRE tight rtTA adv
CMV
vectors

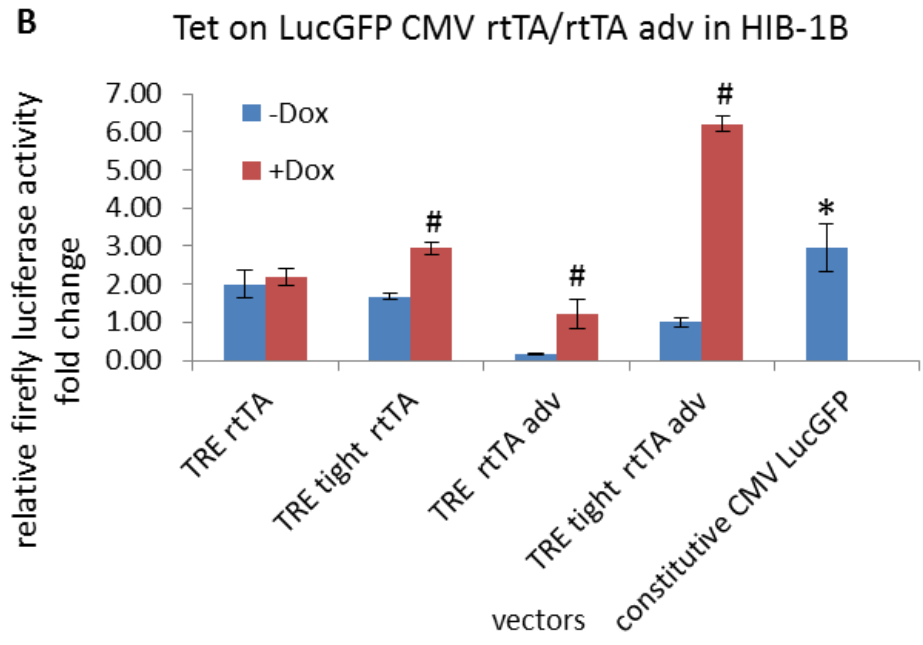
B
Tet on LucGFP CMV rtTA/rtTA adv in HIB-1B
relative firefly luciferase activity
fold change
7.00
6.00
5.00
4.00
3.00
2.00
1.00
0.00
-Dox
+Dox
#
#
#
*
TRE rtTA
TRE tight rtTA
TRE rtTA adv
TRE tight rtTA adv
constitutive CMV LucGFP
vectors

The results demonstrated clearly that the improved version of transactivator rtTA advance could significantly decrease the basal expression of the vectors in the absence of Dox, compared with the original transactivator rtTA. In terms of the absolute expression level in presence of Dox, the combination of TRE with rtTA advance performed slightly higher than the combination of TRE tight with rtTA advance in 3T3-L1 cells, but in HIB-1B cells, the results were quite opposite that the expression level of TRE+ rtTA advance was much lower than that of TRE tight+ rtTA advance, which might reflect the various sensitivity of different cell lines to the elements. It was also known that the expression of the Tet on vectors could be induced by Dox in a dose-dependent manner (Tang et al., 2009), so the dose response experiment of both vectors (TRE rtTA advance and TRE tight rtTA advance) were performed in 3T3-L1 cell line (Figure 3. 5). The results demonstrated that the TRE LucGFP rtTA advance vector (blue line) was more sensitive to doxycycline than TRE tight LucGFP rtTA advance vector (red line), as the luciferase activity of the former was upregulated 8 fold by low concentration (0.5μg/ml) of Dox while the fold change of the latter was 4 at the same concentration of Dox. The fold change at 1μg/ml Dox, the concentration used in the previous induction experiments, was 12 and 5 for the two vectors respectively, which were different from the previous experiment in Figure 3.4A (5.5 and 6 fold respectively), might reflect the normal variety between experiments because of the slight different situations of the cells. The activity of TRE LucGFP rtTA advance vector increased when doxycycline concentration increased from 0.5 μg/ml to 1 μg/ml (from 8 fold to 12 fold relative to the basal activity) but did not significantly vary from 1 μg/ml to 3 μg/ml doxycycline treatments (12, 10, 11, 13 fold at 1, 1.5, 2 and 3 μg/ml). The activity achieved the peak at 5 μg/ml to 17.8 fold relative to basal activity and started to decrease to 13 fold at 8 μg/ml. The activity of TRE tight LucGFP rtTA advance vector did not significantly vary from 0.5 μg/ml to 1.5 μg/ml (all about 4 fold relative to basal activity) but increased to 7 and 7.6 fold at 2 μg/ml and 3 μg/ml respectively, decreased to 6 fold at 5 μg/ml and further reduced to 3 fold at 8 μg/ml. The different properties of the dose responding curves might imply some intrinsic differences derived from the structures of these two vectors or the different interactions between the vectors and the host cells. Although the TRE LucGFP rtTA advance vector displayed higher sensitivity and inducibility than TRE

tight LucGFP rtTA advance vector, the inducibility of both vectors were acceptable. Therefore either of the two backbones could be chosen to produce the corresponding non-tissue specific inducible lentiviral expression vectors of C/EBPβ and to generate the fat-specific inducible vectors of LucGFP.

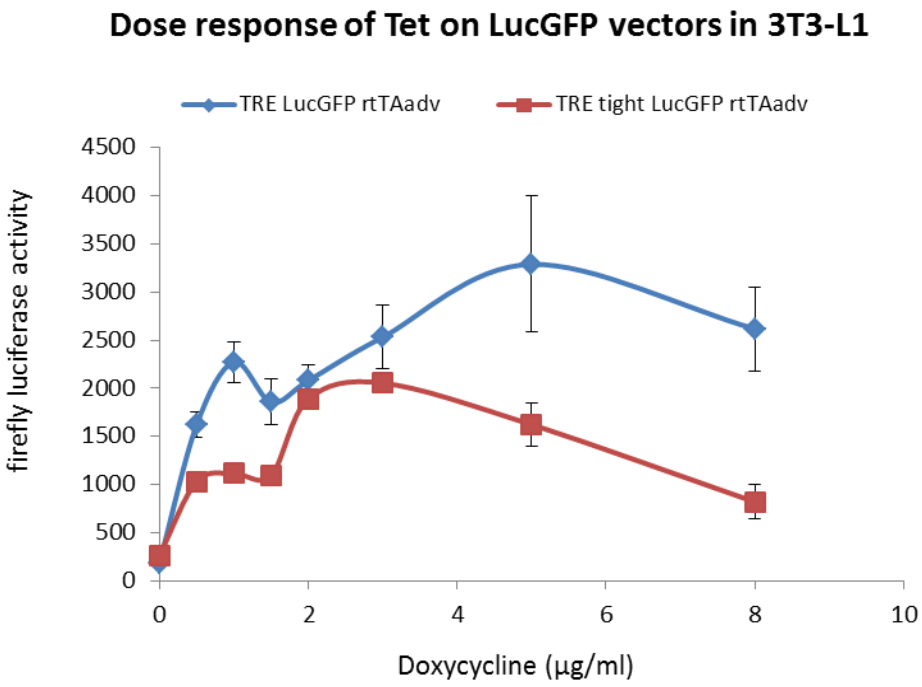

Figure 3.5 The Tet on LucGFP vectors responded to doxycycline in a dose-dependent manner

3T3-L1 preadipocytes were transfected with either TRE LucGFP rtTA advance or TRE tight LucGFP rtTA advance vector. Doxycycline was added into the cells 24 hours post transfection at the concentration indicated in the graph. Firefly luciferase activity was measured 24 hours after the addition of doxycycline. The error bars represent S.E.M from 2 independent replicate experiments performed in triplicate wells.

3.3.5 The inducible overexpression of C/EBPβ with the selected Tet on pLentiviral vector backbone in 3T3-L1

Since both pLenti TRE tight rtTA advance and pLenti TRE rtTA advance backbones were showed to be equally efficient for inducible expression of LucGFP in 3T3-L1 cells, and the former was even more efficient than the latter in terms of expression level in HIB-1B cells, the pLenti TRE tight rtTA advance backbone was chosen to express the C/EBPβ gene. The C/EBPβ entry clone was constructed as described in 2.1.2.1 and checked by restriction digest (Figure 3.6A) and DNA sequencing. The constitutive and non-tissue specific Tet on lentiviral vectors for expressing C/EBPβ, pLenti6-C/EBPβ and pLenti TRE tight-C/EBPβ CMV rtTA advance, were constructed by LR reactions as described in 2.1.2.2 and checked by restriction digest (Figure 3.6A). To check the expression level and inducibility of the vectors, the empty pLenti-TRE vector, pLenti6-C/EBPβ and pLenti TRE tight-C/EBPβ CMV rtTA advance vectors were transfected into 3T3-L1 preadipocytes by Fugene HD mediated transient transfection and 1μg/ml doxycycline (Dox) or vehicle was added to cells transfected with the Tet on C/EBPβ vector for 24-hour treatment before the cells were lysed for RNA extraction. Gene expression level of C/EBPβ was analysed by quantitative real-time PCR and normalised to 18S expression (Figure 3.6B) and results showed that doxycycline induced ($P<0.001$) the expression of C/EBPβ 4 fold in the cells transfected with the Tet on C/EBPβ vector, but the induced expression level was still significantly lower ($P<0.001$) than that in the cells transfected with constitutive pLenti6-C/EBPβ vector. It seemed that although with the same plentiviral vector backbone pLenti TRE tight CMV rtTA advance, the inducibility of the Tet on C/EBPβ vector was not as good as that of the Tet on LucGFP vector (6 fold induced in Figure 3.4A), implying the inducible expression cassette might have different sensitivity to doxycycline depending on specific target genes. Although not as high as the constitutive expression, the doxycycline induced C/EBPβ expression level was still 10 fold higher ($P<0.05$) than the endogenous C/EBPβ expression measured from the cells transfected with empty vector pLenti TRE; given that even in HIB-1B brown preadipocytes where C/EBPβ is sensitive to cAMP stimulation in differentiation, the cAMP stimulus forskolin only induces C/EBPβ expression by, at most, 6 fold during the

differentiation process (Karamitri et al., 2009), the 10 fold higher C/EBPβ overexpression induced by doxycycline in 3T3-L1 cells should be sufficient.

Figure 3.6 Constitutive and inducible overexpression of C/EBPβ in 3T3-L1 preadipocytes by plentiviral expression vectors

(A) Entry clone of C/EBPβ (Lane 1), constitutive expression vector pLenti-C/EBPβ (Lane 2) and Tet on expression vector pLenti TRE tight-C/EBPβ rtTA adv (Lane 3) were digested with specific restriction enzymes. The putative sizes of digested fragments were: Lane 1 (EcoR I, 2815+1514), Lane 2 (XhoI, 8958) and Lane 3 (XhoI, 6344+3989). 1kb ladder was loaded in Lane 6 and the size of each band has been labelled on the right. (B) 3T3-L1 preadipocytes were grown to 70% confluence in 6-well plates and then transiently transfected with the empty pLenti TRE vector, the constitutive pLenti6-C/EBPβ or the inducible pLenti TRE tight-C/EBPβ CMV rtTA advance vectors by Fugene HD. 1µg/ml doxycycline (Dox) or vehicle was added to the cells transfected with the inducible C/EBPβ vector and treated for 24 hours. RNAs were extracted from the cells 48 hours post transfection and the mRNA level of C/EBPβ was quantified by real-time PCR and normalised against 18S expression. Results represent mean ±S.E.M from two independent replicate experiments performed in duplicate wells. Student's t-test was used to analyse the data. *P<0.05 caused by overexpressions with respect to control; #P<0.05 caused by Dox with respect to the group overexpressing the same vector without Dox treatment.

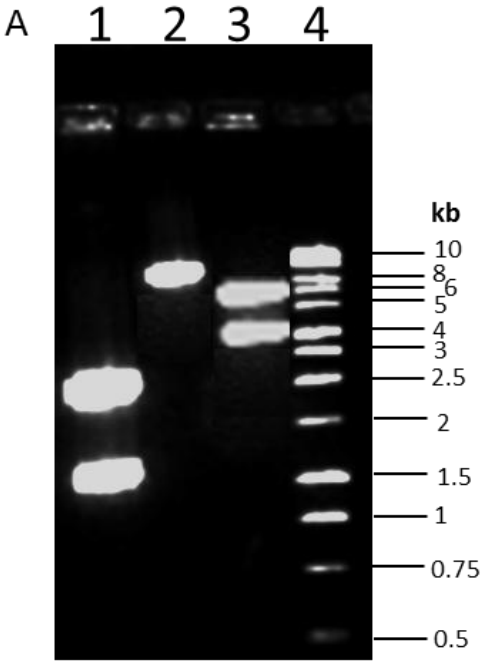
A
1
2
3
4
kb
10
8
6
5
4
3
2.5
2
1.5
1
0.75
0.5

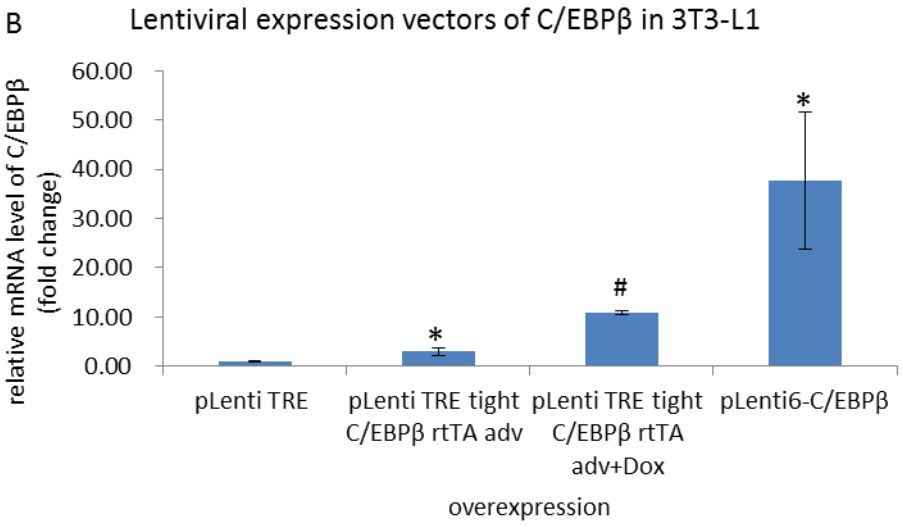
B
Lentiviral expression vectors of C/EBPβ in 3T3-L1
relative mRNA level of C/EBPβ (fold change)
60.00
50.00
40.00
30.00
20.00
10.00
0.00
*
*
#
pLenti TRE
pLenti TRE tight C/EBPβ rtTA adv
pLenti TRE tight C/EBPβ rtTA adv+Dox
pLenti6-C/EBPβ
overexpression

3.3.6 Restriction digests of the 4 fat-specific inducible expression vectors of LucGFP

Entry clones of LucGFP, rtTA advance and aP2 or short aP2 were integrated into either pLentiTRE or pLentiTRE tight destination vector by LR recombination reactions to generate the fat-specific inducible lentiviral expression vectors of LucGFP. The constructed vectors were identified by restriction digest (Figure 3.7) with the enzymes indicated in the text below the figure. The putative sizes of digested fragments were calculated by VectorNTI (Invitrogen) and indicated in the figure legend. All the digested vectors demonstrated correct sizes of the fragments in the agarose gel electrophoresis.

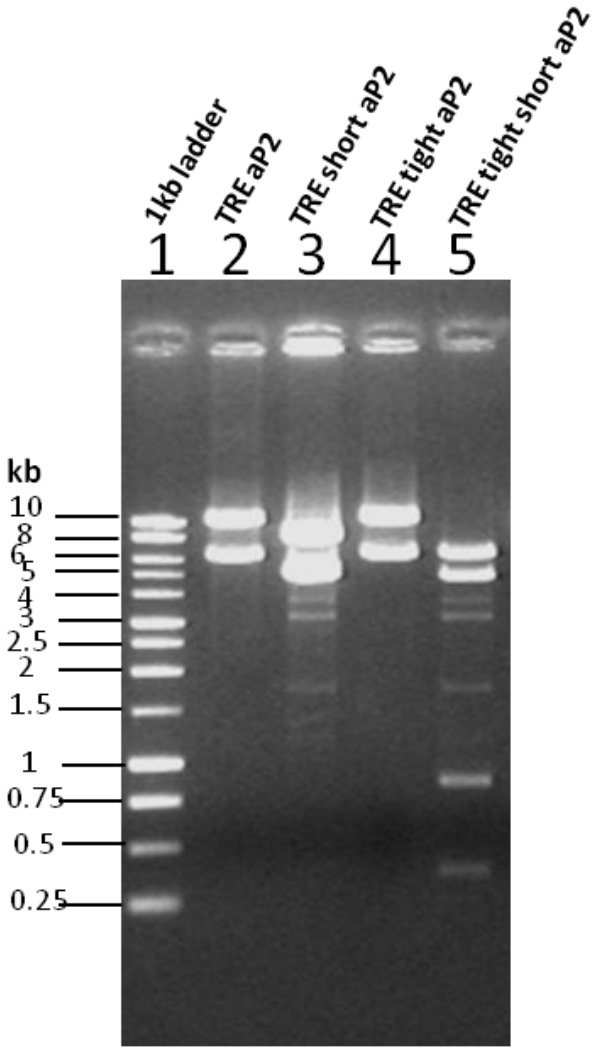

Figure 3.7 Restriction digest of fat-specific inducible sepcific lentiviral expression vectors of LucGFP

Fat-specific inducible lentiviral expression vectors of LucGFP with either full length aP2 or truncated aP2 (short aP2) promoter were digested by specific restriction enzymes. 1kb ladder was loaded in Lane 1 and the size of each band has been labelled on the left. The putative sizes of digested fragments were Lane 2 (XhoI, 10518+ 6329), Lane 3 (PstI, 7650+4829), Lane 4 (XhoI, 10412+ 6344) and Lane 5 (PstI, 7559+ 4829).

3.3.7 Investigation of adipogenic conditions for transient transfection in 3T3-L1 and HIB-1B

The transiently overexpressed luciferase or GFP signals were only detectable 48-60 hours post transfection, and then the signals diminished as the expression was not stable. In order to test the fat-specificity and inducibility of the four fat-specific inducible lentiviral expression vectors of LucGFP (TRE LucGFP aP2 rtTA advance, TRE tight LucGFP aP2 rtTA advance, TRE LucGFP short aP2 rtTA advance and TRE tight short aP2 rtTA advance), an adipocyte culture differentiation induction system in which aP2 was expressed within 24h of induction had to be found to test the constructs in a transient overexpression system. Rosiglitazone has been described to stimulate adipocyte differentiation by activating the master regulator of adipogenesis PPARγ (Lehrke and Lazar, 2005). Forskolin, as an agonist of β-adrenergic receptor, also favours adipogenesis through activating the cAMP-PKA pathway (Yarwood et al., 1995). Therefore the first adipogenic recipe chosen was to treat confluent preadipocytes with both 10μM rosiglitazone and 10μM forskolin acutely, and then to measure the mRNA level of aP2 (Figure 3.8). aP2 expression in treated HIB-1B cells was increased by over a hundred fold ($P<0.001$) compared with the control HIB1B cells (Figure 3.8B), which implied a good adipogenic effect of this recipe in this cell line. However, aP2 expression level was only increased by around 4 fold ($P<0.05$) in the 3T3-L1 cells (Figure 3.8A), indicating this induction system was not good enough for 3T3-L1 to stimulate quick adipogenesis, probably because rosiglitazone and forskolin both favour brown adipogenesis more than white and the activation of some “brown” genes might have a somewhat suppressive effect on “white” gene expression or white adipogenesis.

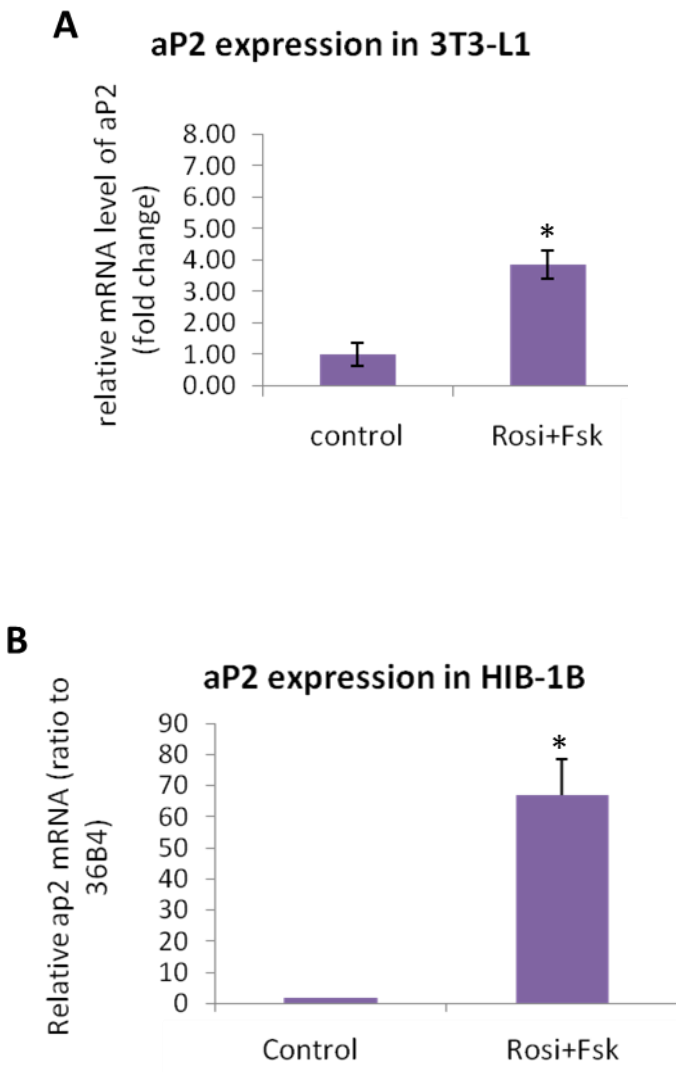

Figure 3.8 Stimulation of adipogenesis by acute treatment of rosiglitazone and forskolin in 3T3-L1 and HIB-1B cells

10 µM rosiglitazone (Rosi) were added into confluence 3T3-L1 and HIB-1B cells and 10µM forskolin (Fsk) was added into the culture 12 hours later. RNAs were extracted from the cells 12 hours after adding forskolin and the mRNA level of aP2 gene in treated 3T3-L1 (A) and HIB-1B (B) cells was determined by quantitative real time PCR and normalised against 36B4 housekeeping gene expression. Each bar represents the mean ± S.E.M from 2 independent replicate experiments performed in duplicate wells. *P<0.05 by Student's *t*-test with respect to controls.

Based on the knowledge that C/EBPβ and PPARγ expression both play critical roles in the early adipogenic programme, the second approach was to mimic their increase in expression after adipogenic induction by transiently overexpressing C/EBPβ and PPARγ into 3T3-L1 cells and then activating PPARγ by adding 10μM rosiglitazone. aP2 gene expression was then measured to check if the adipogenesis was stimulated by the treatment. To determine the best treatment time for rosiglitazone (Rosi) to activate PPARγ, three different time points, 14 hours, 24 hours and 48 hours were used (Figure 3.9A). The results showed that 24 hours treatment with rosiglitazone gave the best activating effect on PPARγ to stimulate adipogenesis, but the highest aP2 expression stimulated by co-overexpression of C/EBPβ and PPARγ activated by rosiglitazone was still only increased ($P<0.05$) 3-4 fold compared with the control cells transfected with pcDNA, which was similar to the level stimulated by rosiglitazone and forskolin co-treatment without overexpression of the transcription factors, as described above (Figure 3.8A). Moreover, when taking into account the expression level of aP2 in mature differentiated 3T3-L1 adipocytes, which was more than a hundred fold compared with the 24 hour control cells transfected with pcDNA (Figure 3.9B), the 3-4 fold increase by the co-overexpression and rosiglitazone treatment indicated that the treated cells were still at a very early stage of differentiation.

A

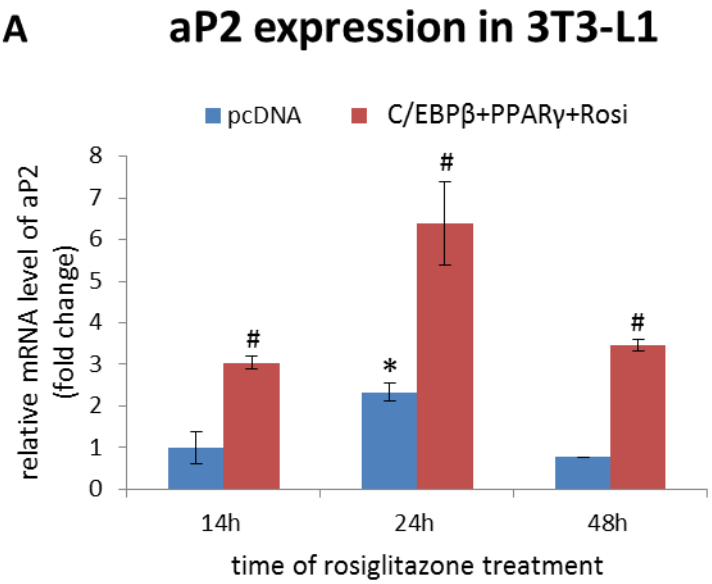
aP2 expression in 3T3-L1
pcDNA
C/EBPβ+PPARγ+Rosi
relative mRNA level of aP2 (fold change)
8
7
6
5
4
3
2
1
0
#
*
#
#
14h
24h
48h
time of rosiglitazone treatment

B

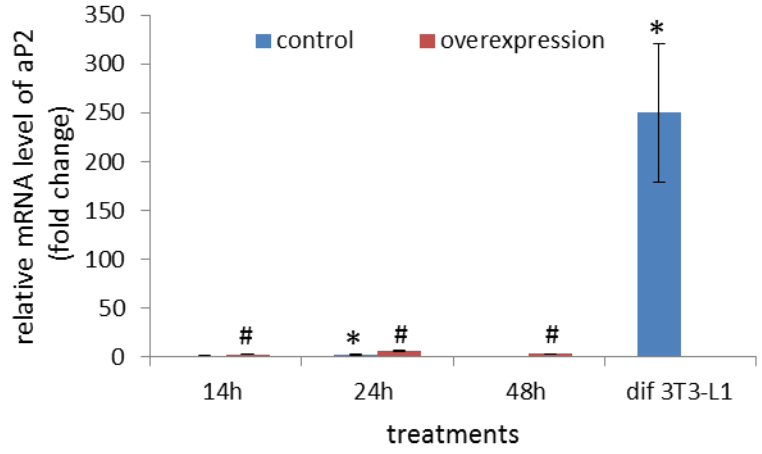
aP2 expression in 3T3-L1
control
overexpression
relative mRNA level of aP2 (fold change)
350
300
250
200
150
100
50
0
#
*
#
#
*
14h
24h
48h
dif 3T3-L1
treatments

Figure 3.9 Stimulation of adipogenesis by overexpression of C/EBPβ and PPARγ in 3T3-L1 cells

(A) 3T3-L1 preadipocytes were transfected with C/EBPβ and PPARγ by FugeneHD. 10 μM rosiglitazone (Rosi) were added into the cells 24 hours post-transfection and RNA was extracted from the cells 24 hours after adding rosiglitazone. (B) The differentiated 3T3-L1 cells (dif 3T3-L1) were derived from a standard differentiated protocol. The mRNA level of aP2 gene in treated cells was determined by quantitative real time PCR and normalised against 18s housekeeping gene expression, relative to the value from the 14 hours pcDNA transfected cells. Each bar represents the mean ± S.E.M from 2 independent replicate experiments performed in duplicate wells. Student's *t*-test was used to analyse the data. *P<0.05 caused by time of Rosi treatment or differentiation with respect to the control at 14h; #P<0.05 caused by overexpression with respect to the control at the same time point.

Although the two systems induced aP2 expression levels well below those observed in fully differentiated cells, there was induction of early adipogenesis so the two protocols were thought to be sufficient to test the fat-specific expression vectors.

3.3.8 Comparison of 4 fat-specific inducible lentiviral LucGFP expression vectors in 3T3-L1 and HIB-1B

The four fat-specific inducible lentiviral LucGFP expression vectors were first transiently overexpressed in 3T3-L1 preadipocytes, co-overexpressed with C/EBPβ and PPARγ and treated with rosiglitazone for 24 hours before detecting the luciferase activity from the cells (Figure 3.10). Data was analysed by two-way ANOVA with each adipogenesis inducible lentiviral vector. Results showed that the vector with full length aP2 promoter and TRE-rtTA advance combination demonstrated relatively good doxycycline and adipogenic inducibility, i.e. the co-overexpression of C/EBPβ and PPARγ and rosiglitazone treatment induced a higher (P<0.001) luciferase activity (~ 2 fold) compared to the control group, and the addition of doxycycline further stimulated (P<0.001) the luciferase expression to about 9 fold compared to the control value (Figure 3.10A, left). However, the vector with aP2 promoter and TRE

tight-rtTA advance combination didn't show any adipogenic inducibility as there was no significant difference between the groups with or without the co-overexpression and rosiglitazone treatment, either in absence or presence of doxycycline, although Dox significantly induced the promoter activity (P<0.001) (Figure 3.10A, right).

In the vectors constructed with short aP2 promoter (sAP2), neither with TRE-rtTA advance nor TRE tight-rtTA advance combination was able to demonstrate good adipogenic or doxycycline inducibility (Figure 3.10B). As neither of the TRE tight-rtTA advance vectors could give adipogenic inducibility in the above test, only the two vectors with TRE-rtTA advance were used in the further investigations.

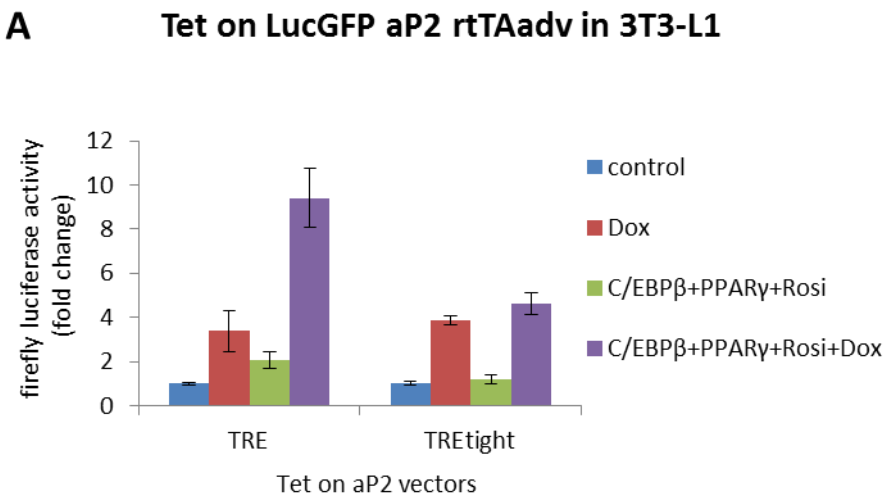

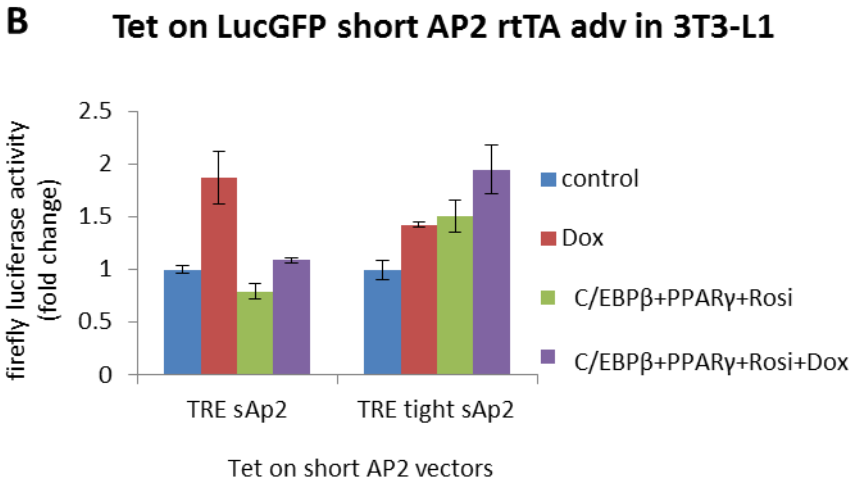

Figure 3.10 Test of fat specific inducible lentiviral expression vectors of LucGFP in 3T3-L1.

The inducible LucGFP lentiviral vectors with full length aP2 promoter (Tet on aP2 vectors, A) or with truncated aP2 promoter (Tet on short aP2 vectors, B) were co-overexpressed with C/EBPβ and PPARγ into 3T3-L1 preadipocytes. 10μM rosiglitazone (Rosi) and 1μM doxycycline (Dox) were added to the cells 24 hours post-transfection as indicated and treated for 24 hours before luciferase assay. Firefly luciferase activity was interpreted relative to the control value (no co-overexpression, no drug treatments) of each group. Each bar represents the mean ± S.E.M from 2 independent replicate experiments performed in triplicate wells. Data was analysed by two-way ANOVA with each lentiviral vector. (A) TRE aP2 (left): Dox ($P<0.001$) and adipogenic condition ($P<0.001$) both significantly increased aP2 promoter activity and there was no interaction ($P=0.18$) between the two treatments; TRE tight aP2 (right): Dox ($P<0.001$) significantly increased aP2 promoter activity while adipogenic condition not ($P=0.31$) and there was no interaction ($P=0.091$). (B) Neither Dox nor adipogenic condition treatment had significant effect on short aP2 promoter activity ($P>0.05$).

The selected two fat-specific vectors, pLenti TRE LucGFP aP2 rtTA advance and pLenti TRE LucGFP short aP2 advance were then tested in the other transient adipogenic condition, i.e. treatment of rosiglitazone and forskolin, in both 3T3-L1 and HIB-1B preadipocytes (Figure3.11). Data was analysed by two-way ANOVA. In 3T3-L1 cells, the vector with full length aP2 promoter (Figure 3.11A, left) had a higher ($P<0.001$) luciferase activity when treated with rosiglitazone and forskolin compared to the untreated cells (~1.7 fold), and the addition of doxycycline induced ($P<0.001$) further expression to about 4 fold over the basal value of untreated cells, but the stimulatory effect was not so significant as that in the other condition of C/EBPβ and PPARγ co-overexpression (3 and 9 fold before and after Dox induction, respectively; Figure 3.10A, left). The vector with short aP2 promoter (Figure 3.11A, right) also showed adipogenic inducibility ($P=0.008$) in 3T3-L1 cells, but the magnitude increased (25%) was not as high as with full length aP2 promoter vector (56%). In HIB-1B cells, Dox ($P<0.001$) and Fsk+Rosi ($P<0.001$) treatments independently increased the luciferase activity of both full length and short aP2 promoter driven vectors and the fold increased by Fsk+Rosi treatment was higher than that in 3T3-L1 cells with or without Dox.

The results from HIB-1B experiments indicated that the adipogenic inducible expression vectors with either full length or truncated aP2 promoter were able to express the reporter genes in fat cells with good inducibility in response to doxycyline. However, experiments in 3T3-L1 cells didn't show consistent results (as shown in Figure 3.8 and 3.9) since neither of the transient adipogenic conditions was ideal for 3T3-L1 preadipocytes in terms of the expression level of adipogenic marker gene aP2, explaining why the fat specific vectors showed very low or even no adipogenic inducibilityin this cell line as they were not stimulated properly.

A

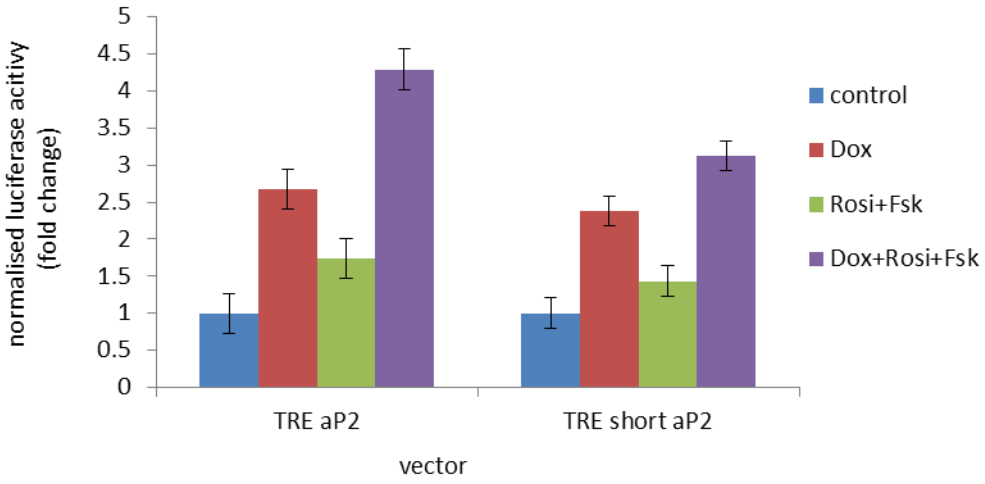
Fat-specific TRE LucGFP in 3T3-L1
normalised luciferase acitivy (fold change)
5
4.5
4
3.5
3
2.5
2
1.5
1
0.5
0
TRE aP2
TRE short aP2
vector
control
Dox
Rosi+Fsk
Dox+Rosi+Fsk

B

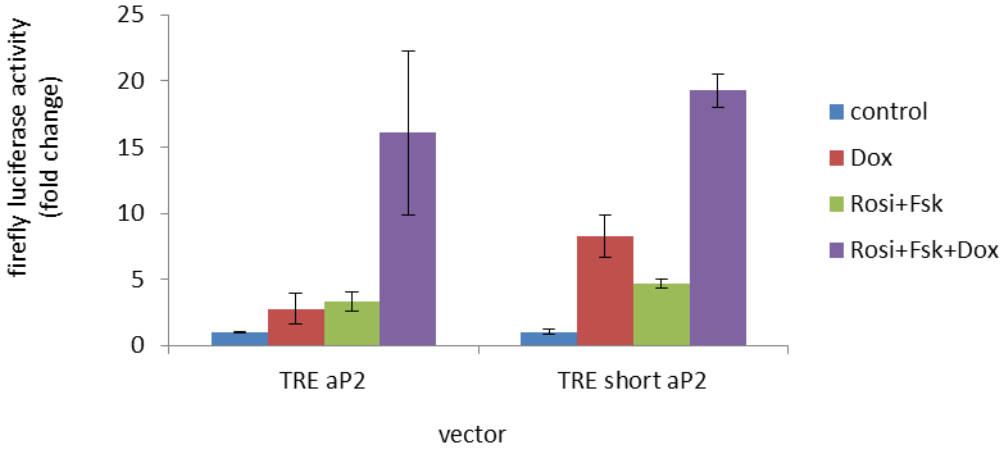
Fat specific TRE LucGFP in HIB-1B
firefly luciferase activity (fold change)
25
20
15
10
5
0
TRE aP2
TRE short aP2
vector
control
Dox
Rosi+Fsk
Rosi+Fsk+Dox

Figure 3.11 Test of fat specific inducible lentiviral expression vectors of LucGFP in 3T3-L1 and HIB-1B preadipocytes.

The two fat specific expression vectors, pLenti TRE LucGFP aP2 rtTA advance and pLenti TRE LucGFP short aP2 rtTA advance were transiently expressed into 3T3-L1 (A) or HIB-1B (B) preadipocytes. 10µM Rosiglitazone (Rosi) and 10µM forskolin (Fsk), as indicated, were added to the cells 24 and 36 hours post-transfection respectively. 1µM doxycycline (Dox) was added to the cells 24 hours post-transfection to induce the expression of the Tet on vectors. Luciferase assay was carried out 48 hours after transfection and firefly luciferase activity was interpreted relative to the control value (no Rosi, no Fsk, and no Dox) of each group. Each bar represents the mean ± S.E.M from 2 independent replicate experiments performed in triplicate wells. Data was analysed by two-way ANOVA with each lentiviral vector. (A) left: no interaction between Dox and Fsk+Rosi treatments ($P=0.111$) but Dox ($P<0.001$) and Fsk+Rosi ($P<0.001$) both independently increased aP2 promoter activity; right: no interaction between Dox and Fsk+Rosi treatments ($P=0.459$) while Dox ($P<0.001$) and Fsk+Rosi ($P=0.008$) both independently increased short aP2 promoter activity. (B) No interaction between Dox and Fsk+Rosi treatments ($P>0.05$) and Dox and fsk+Rosi independently increased both full length and short aP2 promoter activity ($P<0.001$).

3.4 DISCUSSION

The tetracycline inducible expression vectors constructed in the above experimental work showed different levels of basal activity and inducibility as a result of different combinations of tetracycline response elements (TRE or TRE tight) with reverse tetracycline-controlled transactivators (rtTA or rtTA advance). The first combination used in the project was pLentiTRE LucGFP rtTA, but the basal activity of the vector was high and it nearly had no sensitivity to doxycycline (Figure 3.4). The inducibility was slightly improved (~2 fold, $P<0.05$) when the vector was linearized (data not shown) but still not good enough for the requirement of inducible expression. There were two potential reasons responsible for the leakiness, 1) the residual binding of rtTA to tetO sequence of TRE in the absence of inducer ligand doxycline (Baron and Bujard, 2000) and 2) the basal transcriptional activity of the tetracycline responsive promoter even without binding to rtTA. Replacing the TRE with TRE tight (the latter was supposed to be a more tightly controlled tetracycline response element), did not improve the inducibility but the basal activity was slightly reduced (Figure 3.4), indicating that the residual binding of rtTA to tetO sequence should be the primary reason contributing to the leakiness and poor inducibility of the vectors.

Replacing the original rtTA with rtTA advance, which contains specific mutations that both increase its sensitivity to doxycycline and significantly diminish residual bindings to tetO sequence in the absence of inducer ligand (Urlinger et al., 2000), greatly improved the inducibility of the Tet on vectors with lower basal activity (50% decreased) and much higher induced expression (7-8 fold)(Figure 3.4). However, even the low basal activity could cause problems if the target cell lines or animals were very sensitive to the overexpressed gene, as even the basal expression of the gene was enough to stimulate some certain physiological changes in such ultra-sensitive cells and the tetracycline-dependent regulation of the gene expression might make no sense or even cause harm to the cells. Fortunately, the endogenous expression level of the gene of interest in this project, C/EBPβ, was not that low (Figure 5.1C) in 3T3-L1 (pre)adipocytes, so the cell line should probably be able to tolerate the influence of the basal expression of C/EBPβ from the inducible overexpression system. Additionally, as the expression of C/EBPβ is increased by 2-3 fold in BAT during cold

exposure (Karamitri et al., 2009), our aim to induce C/EBPβ expression by around 10 fold was at physiological level.

The inducible vectors with either TRE or TRE tight and rtTA advance displayed similar inducibility and expression levels in 3T3-L1 cells (Figure 3.4A), but in HIB-1B cells, the TRE rtTA advance vector showed low expression level of LucGFP although the inducibility was even better than the vector with TRE tight rtTA advance (Figure 3.4B). The difference might reflect the natural variance of different cell lines in response to different regulatory sequences. So if the vector backbones were used to overexpress other genes in HIB-1B cells, the TRE rtTA advance vector would be suitable for the genes that HIB-1Bs were ultra-sensitive to because of its very low basal activity and the TRE tight rtTA advance vector would be suitable for the genes which had high endogenous expression in the cells.

When the fat specific promoters were introduced into the inducible expression vectors, the difference between the two inducible backbones was even more obvious. In 3T3-L1 cells, the full length aP2 promoter driving TRE rtTA advance vector, in the presence of doxycycline the adipogenic induction, displayed stimulated luciferase activity of about 3 fold over the unstimulated value, whereas the luciferase activity of aP2 promoter driving TRE tight rtTA advance vector was not increased at all by the adipogenic conditions (Figure 3.10A). The difference seemed to show that some specific regulatory sequences in the TRE tight element might influence the fat specificity of the aP2 promoter, but this could not be confirmed as the same experiments were not done in any other cell line.

The adipogenic induction conditions used for 3T3-L1 increased aP2 expression by 3 fold, not comparable to the aP2 expression levels in the routinely differentiated 3T3-L1 cells (Figure 3.8A and Figure 3.9), whereas the rosiglitazone and forskolin treatment was able to successfully induce adipogenesis in HIB-1B cells within 48 hours, in terms of aP2 expression (Figure 3.8B). It is well known that differentiation of 3T3-L1 cells requires a critical early phase of mitotic clonal expansion (MCE), when the confluent growth arrested cells re-enter cell cycle and prepare for the differentiation for 48 hours (Tang et al., 2003b). It has been demonstrated that the

MCE is a prerequisite for differentiation of 3T3-L1 preadipocytes to adipocytes, but the differentiation of HIB-1B preadipocytes does not require this phase. This difference could possibly explain why the same adipogenic induction conditions worked well in HIB-1B but had poor effect in 3T3-L1 preadipocytes since the MCE was omitted as it would not have allowed measurement of the reporter expression from the transiently transfected vectors.

Even without perfect adipogenic conditions, the full length aP2 promoter driving TRE rtTA advance vector still showed the adipogenic inducibility in 3T3-L1 cells, whereas the vector with the same backbone but short aP2 promoter did not display clear adipogenic inducibility under the same conditions (Figure 3.11A). This observation suggested that other regions of aP2 promoter, besides the enhancer and proximal promoter, might contribute to aP2 expression in response to adipogenic signals. This was shown not to be the case as the short aP2 promoter driving vector showed adipogenic inducibility in HIB-1B cells, and it is therefore reasonable to conclude that when the short aP2 driving vector is integrated into the genome of 3T3-L1 preadipocytes and experiences MCE and the routine differentiation induction protocol, the gene of interest should be able to express in a fat specific manner in the presence of doxycycline.

CHAPTER 4

4 PRODUCTION OF LENTIVIRUS PARTICLES AND TRANSGENIC CELL LINES OVEREXPRESSING C/EBP BETA

4.1 INTRODUCTION

The ViraPower™ Lentiviral Expression System (Invitrogen) was used to produce lentiviral particles containing constitutively active vectors expressing the target C/EBPβ or the control LucGFP gene. This system allows creation of replication-incompetent, HIV-1-based lentiviral particles that are used to deliver and express the gene of interest in either dividing or non-dividing mammalian cells. The major components of the system include 1) an expression plasmid containing the gene of interest (C/EBPβ or LucGFP as control in this project) under the control of chosen promoters (TRE-CMV in this work), and elements that allow packaging of the construct into virions (contained in the pLenti6/V5 destination vector backbone); 2) an optimized mix of the three packaging plasmids (pLP1 (gag/pol), pLP2 (rev), and envelope plasmid pLP/VSVG, Appendix F) that supply the structural and replication proteins *in trans* that are required to produce the lentivirus; and 3) the 293FT cell line, which allows production of lentivirus following cotransfection of the expression plasmid and the plasmids in the packaging mix (Invitrogen, 2010). This system has been reported to have several advantages as following: 1) the HIV-1-based lentivirus generated from the system effectively transduces both dividing and non-dividing mammalian cells, thus broadening the potential application beyond those of traditional Moloney Leukaemia Virus (MoMLV)-based retroviral system (Naldini, 1998); 2) it efficiently delivers the gene of interest to mammalian cells in culture or *in vivo* (Dull et al., 1998); 3) it provides stable, long-term expression of a target gene beyond that offered by traditional adenoviral-based systems (Dull et al., 1998; Naldini et al., 1996a); 4) it produces a pseudotyped virus with a broadened host range (Yee et al., 1994); and 5) it includes multiple features designed to enhance the biosafety of the system.

Besides producing lentivirus with the pLP 3-plasmid packaging system, a second generation of packaging plasmid for producing virus, psPAX2, together with the envelope plasmid pCMV-VSVG, was also used in experiments to try to increase the production efficiency. psPAX2 contains a robust CAG promoter for efficient expression of packaging proteins: gag, pol and rev (Appendix F). The second generation system has been reported to produce a higher titer lentivirus, compared with the lentivirus packaged by the first generation packaging plasmids (Addgene). The second generation packaging system has a higher transfection efficiency when transfected into 293FT cell line, as only 2 plasmids are transfected compared to 3 plasmids which decreases the virus production efficiency (see Discussion for details).

The aim of this part of the work was to produce lentiviral particles that could generate stable inducible expression of C/EBPβ (or LucGFP) in the target cell line 3T3-L1 preadipocytes. The lentiviral vectors pLenti TRE tight C/EBPβ (or LucGFP) rtTA advance were used for virus production. However, as the virus production system needed to be optimized first, a constitutively-expressed control pLenti6-LucGFP vector was used for optimizing the virus production system. Another positive control vector pLenti6-LucRFP (kind gift from Dr. Phil Hill, see schematic diagram of structure in Figure 4.5 A) was also used for comparison with the lentiviral vectors generated in our system, to establish virus production and transduction efficiency.

The specific objectives of the experimental work described in this chapter were

1. To produce lentiviral particles containing constitutive LucGFP in 293FT packaging cell line.

2. To optimize the viral titer to at least 10^5 TU/ml.

3. To optimize the transduction conditions in 3T3-L1 preadipocytes and to select monoclones from the transduced cells.

4. To apply the optimized conditions with the inducible pLenti TRE tight C/EBPβ (or LucGFP) rtTA advance vectors to produce transgenic cell lines that stably overexpress the target gene.

4.2 EXPERIMENTAL DESIGN

4.2.1 Transfection of packaging cell line 293FT with the constitutive lentiviral expression vector of LucGFP to produce lentiviruses

Two different protocols were used to produce lentivirus in 293FT cell line, as described in 2.4.1, the first from the ViraPower™ Lentiviral Expression System Manual (Invitrogen) and the other kindly provided by Mr Simon Lillico, Roslin Institute. The basic principles of the two protocols were the same, i.e. to transiently transfect 293FT cell line with the lentiviral expression vector and packaging plasmid mix for packaging the lentiviral particles containing the gene of interest and to harvest the lentivirus by collecting the culture supernatant after the packaged viral particles have been released from the 293FT cells. Besides the different packaging plasmids, the two protocol also employed different transfection reagents when transfecting 293FT cells: lipofectamine 2000® (Invitrogen) with the ViraPower ™ system and Fugene HD® (Roche) with the Roslin protocol. Lentivirus production was performed with these two protocols in parallel to determine which one gave higher viral titer. The need for high viral titer in this project was due to the difficulty in transducing 3T3-L1 cells, as it requires a multiplicity of infection (MOI) to be 30 compared to the easily transduced HT1080 cell line which only needs MOI to be 1 (Invitrogen).

4.2.2 Ultracentrifugation of the produced lentivirus to increase the titer

To further increase the lentiviral titer, the viral particles harvested from the supernatant of transfected 293FT cells were concentrated by ultracentrifugation as described in 2.4.2. The lentiviruses before and after ultracentrifugation were titered in HT1080 cell line as described in 2.4.3 to determine the viral titer and the effect of ultracentrifugation.

4.2.3 Transduction of the target 3T3-L1 cell line with the LucGFP lentivirus vector to determine transduction efficiency and to select for a monoclonal cell line overexpressing the LucGFP gene

3T3-L1 preadipocytes were transduced with the concentrated and purified lentiviral particles containing the constitutively expressing LucGFP vector as described in 2.5.1. The transduced 3T3-L1 cells were screened for GFP expression using fluorescence microscopy and selected for single cell colonies that overexpress LucGFP efficiently as

described in 2.5.1. As the lentivirus integrates into the cell genome randomly, it is necessary to pick several single colonies and to quantitatively measure the expression level of the transgene by luciferase assay. This step was also necessary to estimate how many colonies to pick from the blasticidin resistant cell colonies to guarantee there was at least one colony that could efficiently overexpress the gene of interest. This then provided guidance when selecting cell colonies overexpressing C/EBPβ gene.

4.2.4 Production of inducible LucGFP and C/EBPβ lentivirus, transduction of 3T3-L1 cells and selection for the corresponding monoclonal transgenic cell lines

The pLenti TRE tight C/EBPβ (or LucGFP) rtTA advance lentiviral vector was transfected into 293FT cell line with optimized packaging protocol to produce the lentiviral particles containing the inducible C/EBPβ (or LucGFP). The viral particles were then used to transduce 3T3-L1 preadipocytes and select for the stable cell lines overexpressing C/EBPβ (or LucGFP) in the presence of doxycycline, using the protocol optimized with constitutive LucGFP virus. The selected cell lines were then tested for the expression level of C/EBPβ (or LucGFP) mRNA (as described in 2.3.3) with different doxycycline concentrations to establish a dose response relationship.

4.3 RESULTS

4.3.1 Comparison of Lipofectamine 2000® or Fugene HD® transfection reagents with ViraPower™ packaging plasmid mix for transfecting constitutively active LucGFP lentiviral vector in 293FT cells.

The ViraPower™ Lentiviral Expression System Manual (Invitrogen) suggests that 293FT cells should be transfected by the lipofectamine 2000® transfection reagent for packaging lentiviral particles. However, transfection efficiency using lipofectamine was lower compared with Fugene HD® in routine transient transfection in our laboratory, using both 3T3-L1 and HIB-1B cells (data not shown). Given that transfection efficiency was especially important for the multi-plasmid transfection system, it was necessary to compare the transfection efficiency of these two reagents in 293FT cells when mediating the 4-plasmid transfection (3-plasmid packaging mix

and one expression vector). As described in 2.4.1, 5×10^6 293FT cells in 10ml medium were transfected with 9µg of the ViraPower ™ Packaging Mix plasmid and 3µg of the constitutive LucGFP lentiviral expression vector (pLenti6-LucGFP) by either 36µl of lipofactamine 2000® or 36µl of Fugene HD®. 60 hours post transfection, photos of the transfected cells were taken using the fluorescence microscope (Figure 4.1). Results showed clearly that more cells were transfected by Fugene HD® when fluorescence was compared with that of the lipofectamine 2000® transfected cells, and that the fluorescence in the former was more intense than the latter. These data indicated that Fugene HD® was much more efficient in mediating a 4-plasmid transfection in 293FT cells than lipofectamine 2000®; therefore the Fugene HD® was used in all of the following transfections in 293FT cells.

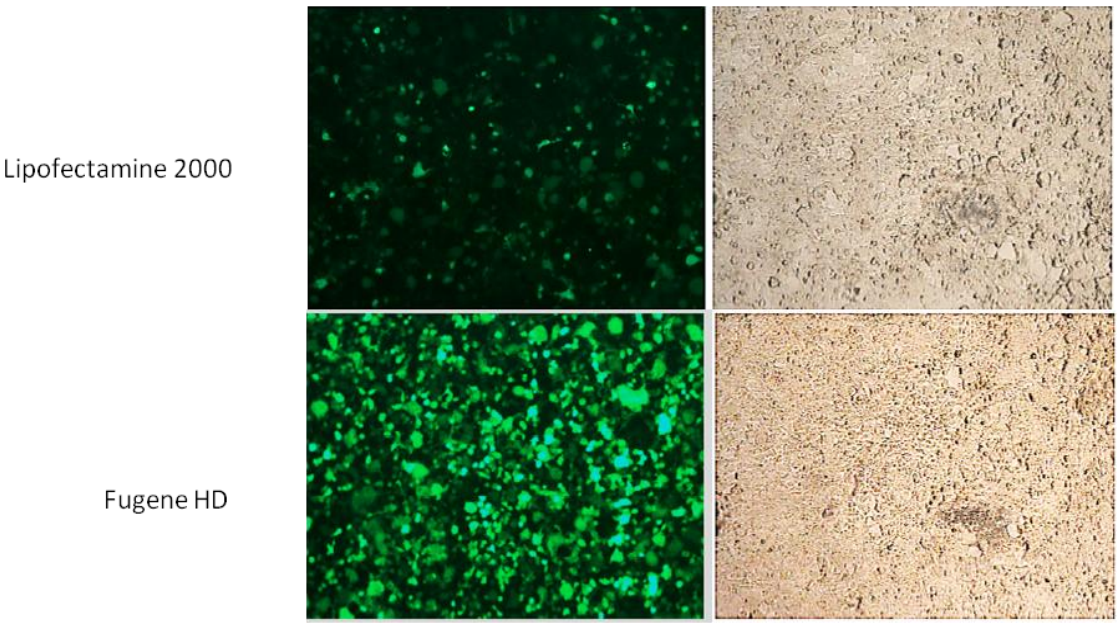

Figure 4.1 Fugene HD® transfection reagent increased transfection efficiency in 293FT cell line compared to lipofectamine 2000®.

293FT cells were grown to 90%, (for Lipofectamine 2000® transfection) or 80% (for Fugene HD® transfection) confluence, and were then tranfected with pLenti6-LucGFP and ViraPower™ packaging plasmids using Lipofectamine 2000® and Fugene HD®, respectively. Photos were taken under fluorescence microscope 60 hours post transfection (magnification=100). The exposure time for both fluorescent photos was 2.0 seconds at the magnification of 100.

4.3.2 Comparison of the titers of lentivirus produced from ViraPower ™ packaging system and psPAX2 packaging protocols

The improved protocol of ViraPower™ packaging system with Fugene HD® transfection reagent was used in parallel with the psPAX2 packaging protocol to produce lentiviral particles containing the constitutive LucGFP gene, for comparing the virus producing efficiency of these two packaging systems. As described in 2.4.1, the pLenti6-LuGFP expression vector was co-transfected with either packaging plasmid mix into 293FT cells using the corresponding protocol. Photos of the transfected cells were taken 60 hours post transfection (Figure 4.2), and show that both methods gave similar percentage (50-60%) of fluorescent cells out of total cell numbers. However, the morphology of the 293FT cells transfected with different packaging mix was markedly different. The ViraPower™ packaging mix transfected cells looked much healthier than the cells transfected with psPAX2 packaging mix. As expression of VSV-G glycoprotein causes 293FT cells to fuse, resulting in the appearance of syncytia (large, multinucleated cells) (Invitrogen, 2010), it was logical to infer that the psPAX2 packaging mix was able to express more VSV-G glycoprotein thus probably to package more lentiviral particles than the ViraPower™ packaging mix.

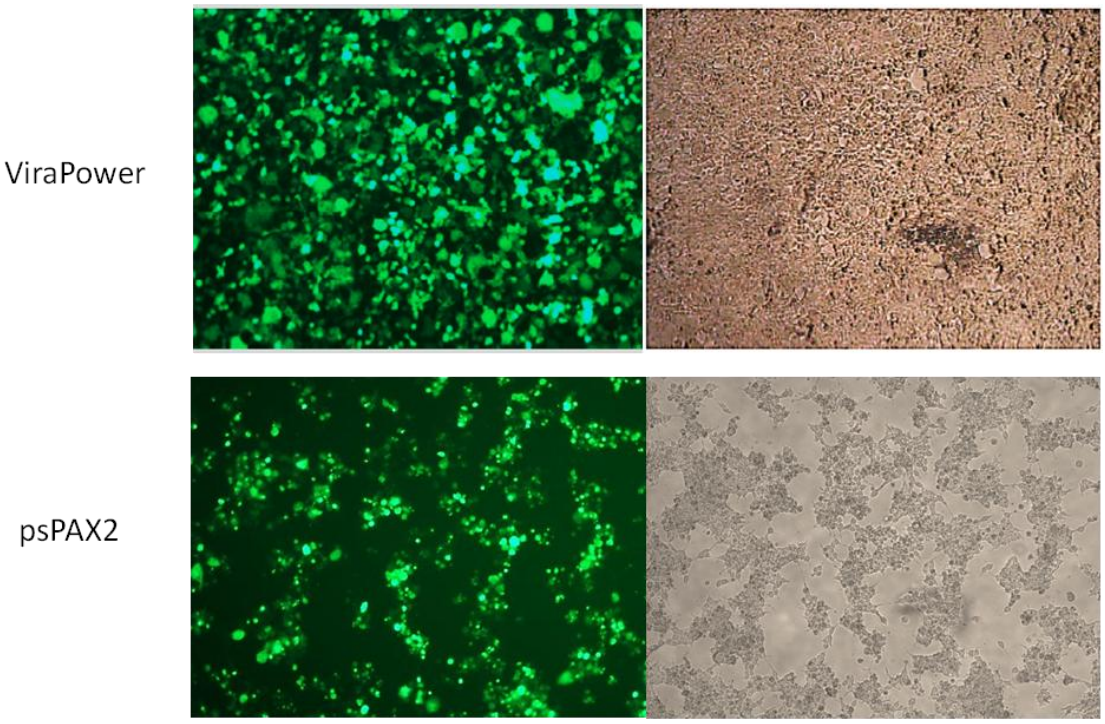

Figure 4.2 psPAX2 packaging plasmid mix caused more syncytia formation in the cells than ViraPower™ packaging plasmids when transfected into 293FT cell line.

293FT cells were transfected with either ViraPower™ (upper panel) or psPAX2 (lower panel) packaging mix together with pLenti6-LucGFP expression vector using Fugene HD®. Photos were taken under fluorescence microscope 60 hours post transfection (x100 magnification). The exposure time for both fluorescent photos were 2.0 seconds.

The lentiviral particles produced from the two protocols were diluted by 10^{-6}, 10^{-5},10^{-4}, 10^{-3} and 10^{-2} and applied to the HT1080 cells for titering (Figure 4.3). Calculated from the figure, the viral titers of ViraPower™ and psPAX2 packaged lentivirus were 3×10^{2} TU/ml and $(20\times10^{2}+2\times10^{3})/2= 2\times10^{3}$ TU/ml respectively before ultracentrifugation. The psPAX2 packaged lentiviral particles were concentrated by ultracentrifugation as described in 2.4.2 and then diluted by 10^{-5}, 10^{-4}, 10^{-3} and 10^{-2} before performing the titering experiment. The viral titer of the psPAX2 packaged particles was $(15\times10^{4}+2\times10^{5})/2= 1.75\times10^{5}$ TU/ml after ultracentrifugation, nearly 90 fold higher than the titer before concentration. The results suggested that psPAX2 packaging mix could produce the lentivirus with about 7 fold higher titer than that of the virus produced by the ViraPower™ packaging mix and ultracentrifugation could markedly increase viral titer by about 10^{3} fold. But even with ultracentrifugation, the protocols just barely achieved the required threshold of viral titer 10^{5} TU/ml with the pLenti6-LucGFP expression vector, indicating that the virus production process was not that efficient.

Figure 4.3 Titers of the lentiviral particles from ViraPower™ and psPAX2 packaging system.

Lentiviral particles produced with pLenti6-LucGFP vector from either ViraPower™ (top) of psPAX2 (middle) packaging system were diluted by 10^{-6}, 10^{-5}, 10^{-4}, 10^{-3} and 10^{-2} then applied to HT1080 cells for titering. 6 μg/ml of polybrene was used to facilitate transduction. The titers of the lentivirus were 3×10^{2} TU/ml (top) and 2×10^{3} TU/ml (middle) respectively. The lentivirus produced from psPAX2 system (middle) were concentrated by ultracentrifugation (52,000g, 2 hours, 4°C) and diluted by 10^{-2}, 10^{-3}, 10^{-4} and 10^{-5} then titered in HT1080 cells (bottom). The label "Pre 10^{-1}" indicates the cells were transduced by the pre-concentrated lentivirus diluted by 10^{-1}. The titer of the concentrated virus was 1.75×10^{5} TU/ml.

Mock 10^{-6} 10^{-5}

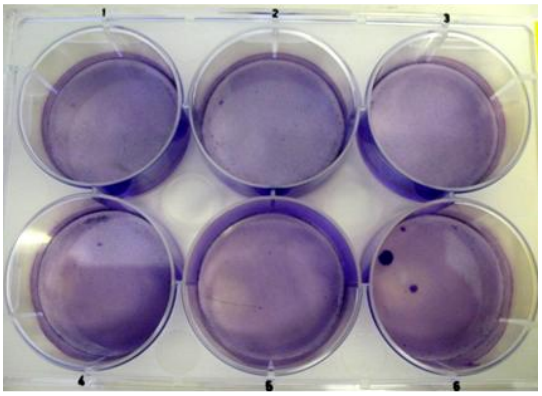

10^{-4} 10^{-3} 10^{-2}

Mock 10^{-6} 10^{-5}

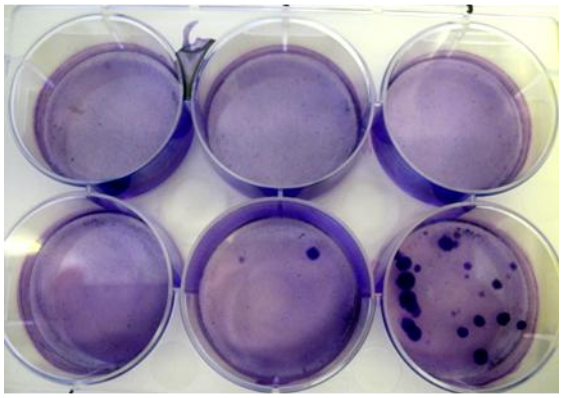

10^{-4} 10^{-3} 10^{-2}

Mock Pre 10^{-1} 10^{-5}

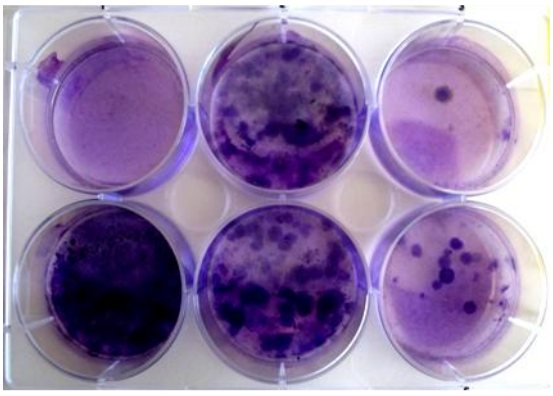

10^{-2} 10^{-3} 10^{-4}

4.3.3 Infection of 3T3-L1 preadipocytes with concentrated constitutive LucGFP lentivirus

Although the concentrated lentiviral particles containing constitutive LucGFP did not achieve a titer higher than 10^5 TU/ml suggested as being necessary for efficient transduction (ViraPower™ Manual, Invitrogen), an attempt was made to transduce 3T3-L1 preadipocytes with the lentivirus by reducing the cell numbers to increase the multiplicity of infection (MOI). The transduction was performed in 96-well format with 1500 cells seeded in each well and 100µl of the concentrated constitutive LucGFP lentivirus (titer= 1.75×10^5 TU/ml) was diluted 1: 2 and applied to the cells at MOI=30, as described in 2.5.1. Photos were taken of the transduced 3T3-L1 cells 24 hours post infection (Figure 4.4), showing some fluorescent particles which seemed to be located outside the cells instead of glowing from inside the cell itself. During the following blasticidin selection process, the green fluorescence diminished gradually, and the luciferase assay performed on these blasticidin resistant 3T3-L1 cells, failed to give any luciferase activity above the background value (data not shown). These data indicated a failure in transducing 3T3-L1 cells with the constitutive LucGFP lentivirus. Possible reasons for this are that the lentivirus was not so efficiently infectious (low titer or poor purity) that some parts of the pLenti6-LucGFP expression vector did harm to the virus packaging process, or that the 3T3-L1 preadipocytes were even more difficult to transduce than expected.

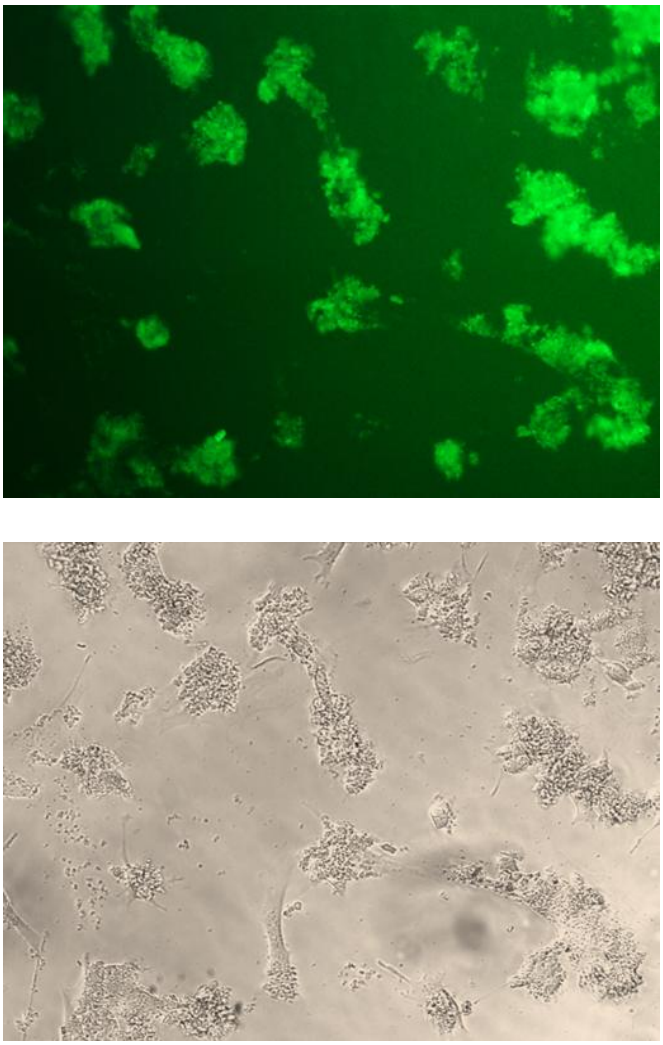

Figure 4.4 Transduction of 3T3-L1 cells with the concentrated LucGFP lentivirus

3T3-L1 preadipocytes were seeded in 96-well plate and transduced the next day with lentivirus produced from pLenti6-LucGFP at MOI=30. 6 µg/ml of polybrene was used to facilitate transduction. Photos were taken under Leica DFC 420C fluorescence microscope 24 hours post transduction with the magnification=100 and 2.0 seconds of exposure time (fluorescent image).

To further investigate the cause of the unsuccessful transduction, a positive control vector pLenti6-LucRFP which had successfully been employed in transduction experiments (kind gift from Dr. Phil Hill) was used to produce lentivirus and then to infect 3T3-L1 cells in parallel with the pLenti6-LucGFP vector. The positive control pLenti6-LucRFP vector shared the same backbone of pLenti6/V5 with pLenti6-LucGFP, but the luciferase gene in this vector was fused with a red fluorescent protein (RFP) instead of GFP, and didn't contain the CMV-rtTA element which, although not performing any role in the constitutive pLenti6-LucGFP vector expression, was included in the construct for the convenience of cloning.

4.3.4 Comparison of lentiviral production from pLenti6-LucGFP and pLenti6-LucRFP

To compare the pLenti6-LucGFP and pLenti6-LucRFP vectors directly in producing lentivirus, parallel experiments were performed to prepare lentiviral particles using either of the two expression vectors with the psPAX2 packaging plasmid mix, in 293FT cell line (Figure 4.5B). The harvested lentiviral particles without ultracentrifugation were applied to HT1080 cells for titering (Figure 4.6). Figure 4.5 showed transfection of a lower percentage of green fluorescent cells (~50%) compared to that of red fluorescent cells (70-80%) out of total cell numbers, demonstrating that different lentiviral expression vector did have different packaging efficiencies, at least in 293FT cells. The viral titers of LucGFP and LucRFP lentiviruses calculated from Figure 4.6 were 2×10^3 and 3.6×10^5 respectively, indicating that the pLenti6-LucRFP vector was more efficient than pLenti6-LucGFP vector in producing infectious lentivirus.

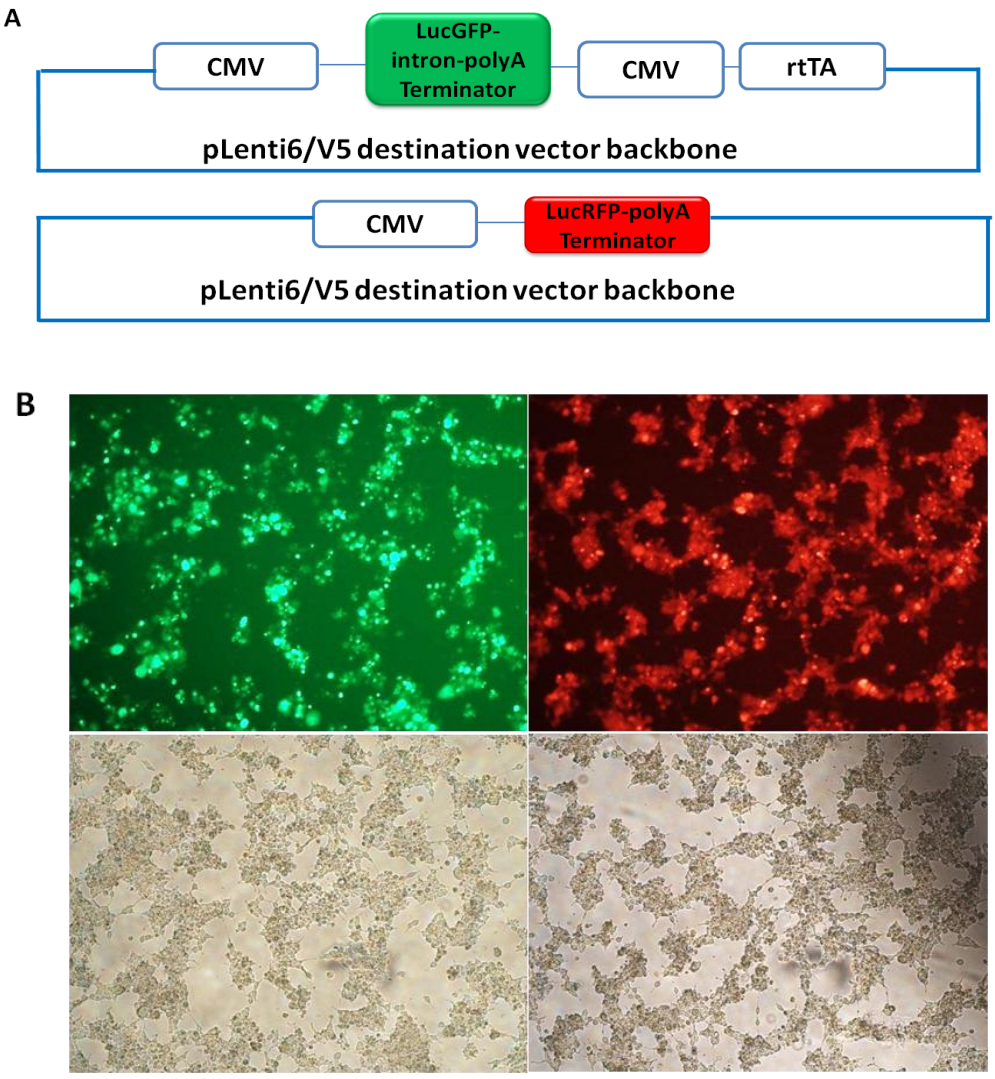

Figure 4.5 Transfection of 293FT cells to produce LucGFP or LucRFP lentivirus

(A) Schematic diagram of the structures of pLenti6-LucGFP (upper) and pLenti6-LucRFP (lower) vectors. pLenti6-LucGFP contained the Tet on regulatory element rtTA and the CMV promoter to drive rtTA while pLenti6-LucRFP did not have these components. The gene LucGFP contained rabbit βglobin intron and polyA terminator to facilitate the expression in mammalian cells, while the pLenti6-LucRFP gene only possessed a polyA terminator but no intron. (B) 293FT cells were transfected with psPAX2 packaging plasmid mix together with either pLenti6-LucGFP (left) or the control pLenti6-LucRFP (right) vector by Fugene HD. Photos were taken under fluorescence microscope 60 hours post transduction before harvesting the lentiviruses. The magnification was 100 fold and exposure time for fluorescent images was 2.0 seconds.

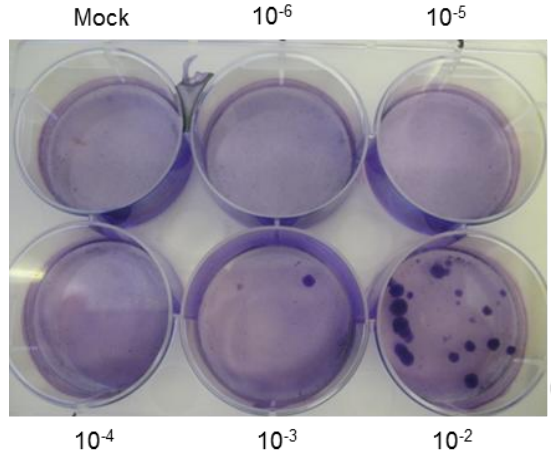

LucGFP
$(20X10^2+ 2X10^3)/2= 2X10^3$ TU/ml

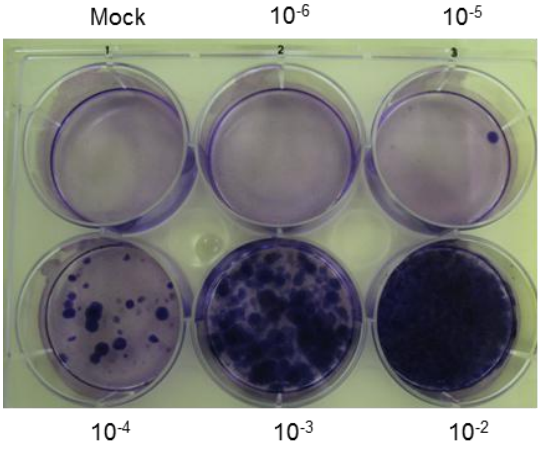

LucRFP
$(42X10^4+3X10^5)/2=3.6X10^5$ TU/ml

Figure 4.6 Titers of the lentiviral particles produced from either pLenti6-LucGFP or pLenti6-LucRFP vector

Unconcentrated Lentiviral particles produced with either pLenti6-LucGFP (upper) or pLenti6-LucRFP (lower) vector from psPAX2 packaging system were diluted by 10^{-6}, 10^{-5}, 10^{-4}, 10^{-3} and 10^{-2} then applied to HT1080 cells for titering. 6 µg/ml of polybrene was used to facilitate transduction and 8µg/ml of blasticidin was added into the culture 48 hours post transduction for 12-day selection. The titer of the LucGFP lentivirus was 2×10^3 TU/ml (upper) while the LucRFP lentivirus had the titer of 3.6×10^5 TU/ml (lower).

To check the importance of target cell type, LucGFP and LucRFP lentiviral particles were concentrated by ultracentrifugation as described in 2.4.2 and then the easily-transducible cell line HT1080 was infected with each concentrated virus as described in 2.5.1 at MOI=1. Fluorescence from the transduced cells was checked by Leica Fluorescence microscope 3 days post-transduction (Figure 4.7). The transduced cells were at full confluence 3 days after transduction, but very few LucGFP transduced cells had green fluorescence and the fluorescence was quite weak as shown in the photo (Figure 4.7, left), whereas 70-80% of the LucRFP transduced cells showed clear red fluorescence (Figure 4.7, right). These data confirmed that the LucRFP lentiviral particles were more infectious than LucGFP virus, consistent with the result from the titering experiment (Figure 4.6).

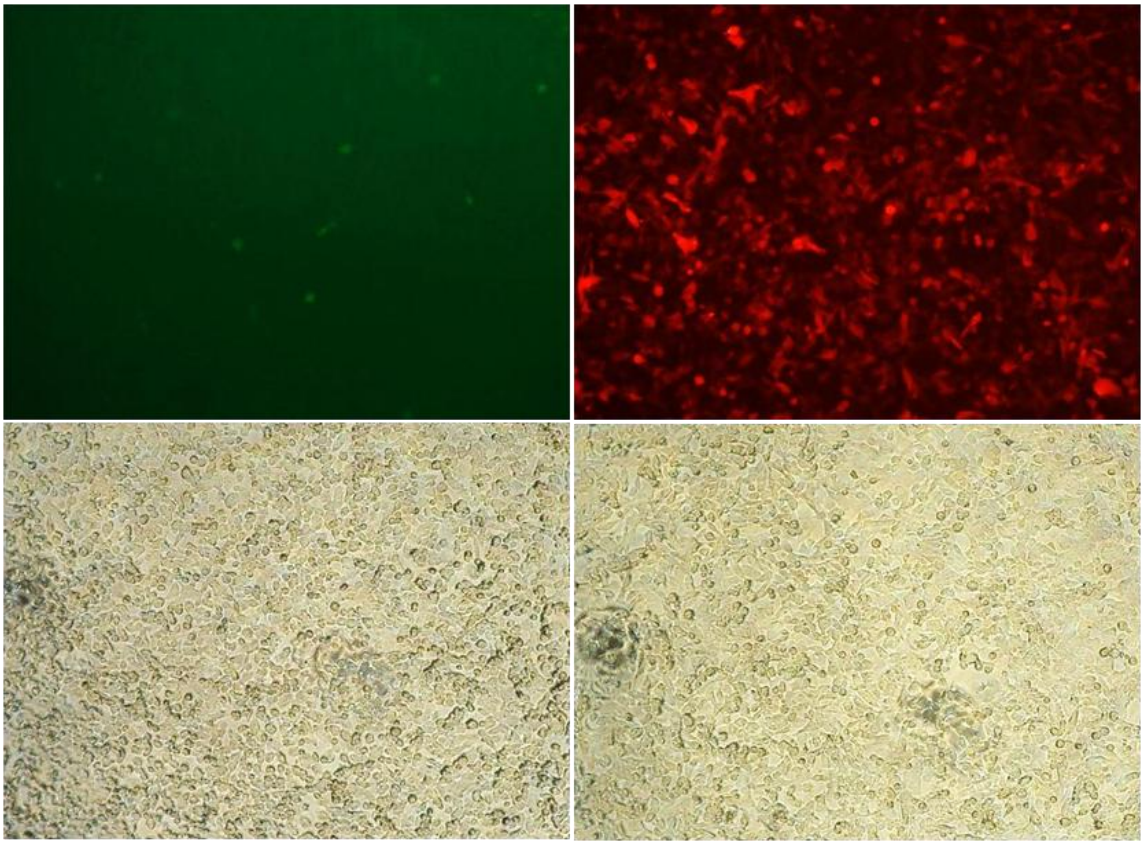

Figure 4.7 Transduction of HT1080 cells with lentiviral particles produced from either pLent6-LucGFP or pLenti6-LucRFP vector

HT1080 cells were seeded in 96-well plate and transduced the next day with concentrated lentiviruses produced from pLenti6-LucGFP (left) or pLenti6-LucRFP (right) at MOI=1. 6 µg/ml of polybrene was used to facilitate transduction and 8µg/ml of blasticidin was added into the culture 48 hours post transduction for selection. Photos were taken under a fluorescence microscope 3 days post transduction with the x100 magnification. The exposure time of the green fluorescent image (left) was 4.0 seconds while the red fluorescent image used 1.5 seconds for exposure.

4.3.5 Transduction efficiency varies in different cell lines

To address the question whether the unsuccessful transduction in 3T3-L1 cells with LucGFP lentivirus (Figure 4.4) was also partly due to the specific difficulty to transduce 3T3-L1 cell line, the positive control LucRFP lentiviruses were used to infect HT1080, 293FT and 3T3-L1 cell lines in parallel as described in 2.5.1 at MOI=1, 5 and 30 respectively. The red fluorescence from the three cell lines was checked by microscopy 4 days post transduction (Figure 4.8). Results showed that 70-80% of the transduced HT1080 cells were glowing bright red fluorescence (Figure 4.8, top), 30-40% of the transduced 293FT cells were glowing red although the fluorescence was not as bright as seen in HT1080s (Figure 4.8, middle), while less than 10% of the transduced 3T3-L1 cells were glowing red and the fluorescence was quite weak (Figure 4.8, bottom). The data indicated clearly that 3T3-L1 cell line was more difficult to transduce compared with the other two, which also could be a reason for the unsuccessful transduction shown in Figure 4.4, besides that the LucGFP lentivirus was not efficiently infectious.

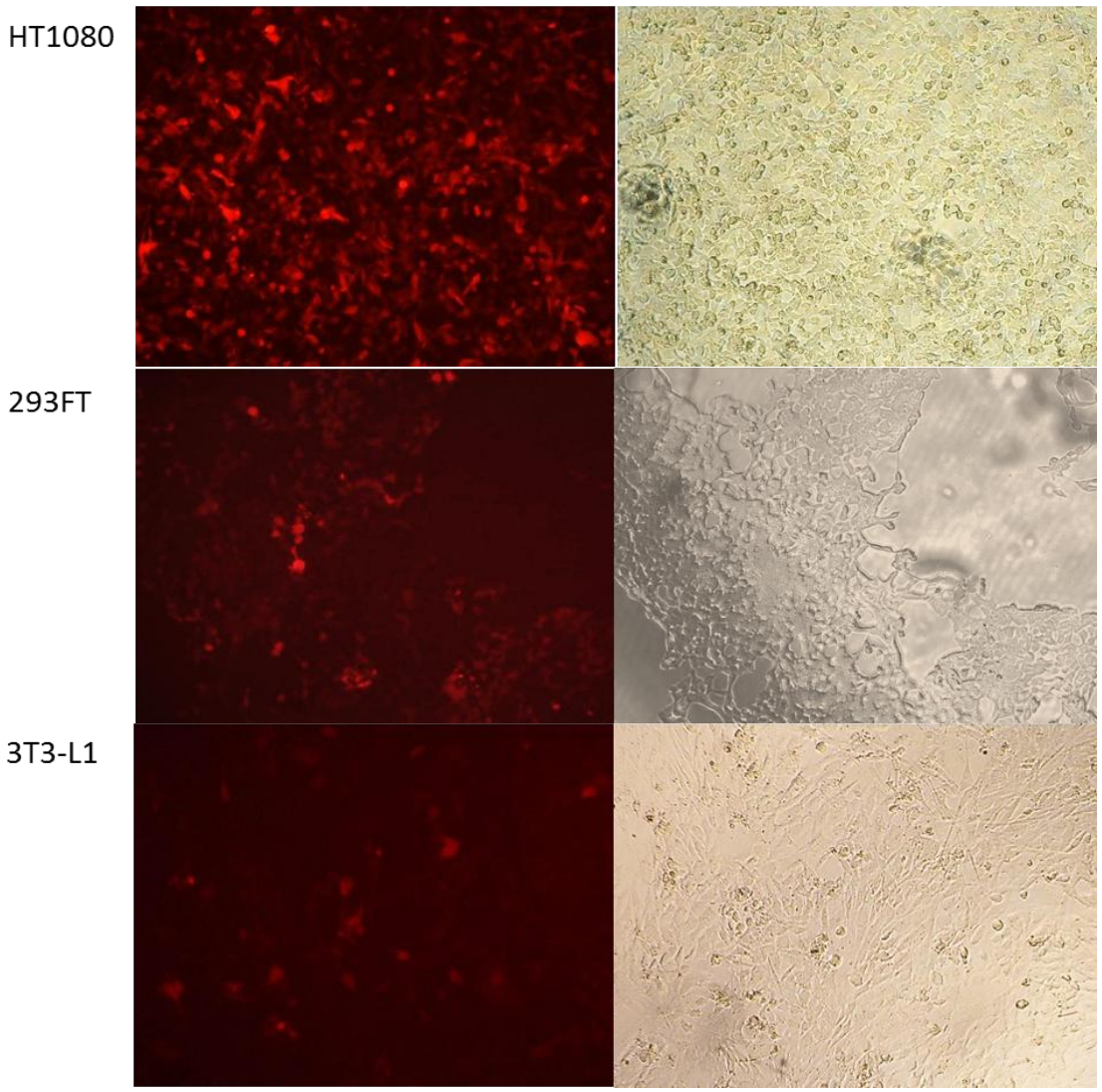

Figure 4.8 3T3-L1 cells were more difficult to transduce compared with HT1080 or 293FT cells

HT1080 (top), 293FT (middle) and 3T3-L1 (bottom) cells were seeded in 96-well plate and transduced by the lentivirus produced from pLenti6-LucRFP vector at the MOI=1, 5 and 30 respectively. 6 µg/ml of polybrene was used to facilitate transduction and 8µg/ml of blasticidin was added into the culture 48 hours post transduction for selection. Photos were taken under a fluorescence microscope 4 days post transduction with the magnification=100. The exposure time of the fluorescent images were 1.5 seconds.

4.3.6 Monoclonal selection of transduced 3T3-L1 cells overexpressing LucRFP control gene

Although the 3T3-L1 cell line proved difficult to transduce, even with the LucRFP lentivirus, monoclonal selection could be used to achieve the stable integration of a vector, despite poor transduction efficiency. Therefore following the LucRFP transduction experiments in 3T3-L1 cells, described in 4.3.4, cells were grown in a 96-well plate until 80% confluence then divided into two groups, 1) to be trypsinised, counted then seeded at 2 or 5 cells per well into a 96-well plate and selected for wells containing single cell colony under microscope; 2) all the cells to be transferred into 6-well plates for a larger growing space so that single colonies could be obtained by the "cloning ring" method, as described in 2.5.3. Twelve single colonies of cells were picked from both methods and seeded into 24-well plates and allowed to reach confluence at which point a luciferase assay was performed as described in 2.3.3, to determine which colonies expressed the LucRFP transgene efficiently (Figure 4.9). The data demonstrated that 4 (Clone 2, 8, 9 and 10) out of 12 single colonies had higher ($P<0.001$) luciferase activity compared with the polyclone cells (blasticidin resistant cells without monoclonal selection), and the highest expression (Clone 8) achieved 5.5 fold over the level of polyclone cells. The 1 in 3 rate (4 out of 12 colonies) indicated that to get one monoclone with high expression of transgene, about three single colonies should be picked and grown from the transduced and blasticidin-selected cells. It was also clear in the graph that 7 single colonies (Clone 1, 3, 4, 5, 6, 7 and 12) had nearly no expression of luciferase and the luciferase activity in the other colony (Clone 11) was also much lower ($P<0.01$) than that in the polyclone cells, firmly demonstrating that the transgene expression in transduced cells varied very much depending on where it integrated into the cell genome.

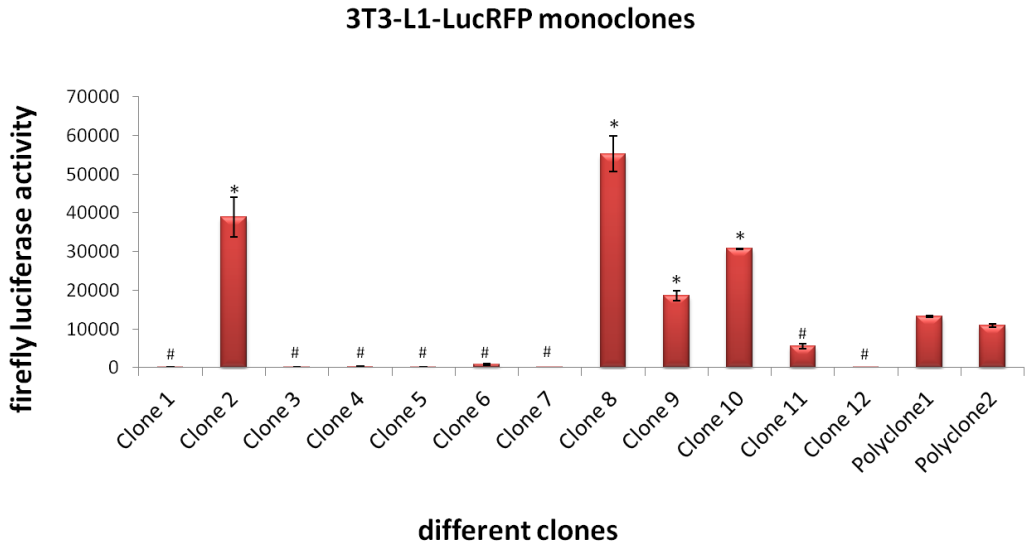

Figure 4.9 Different expression levels of luciferase activity in monoclones of 3T3-L1 stably expressing LucRFP

3T3-L1 preadipocytes transduced by LucRFP lentivirus were selected using 8μg/ml blasticidin and monoclones separated as described in 2.5.3. The separated single colonies were re-seeded into 24-well plates and grown to full confluence. Luciferase assay was then performed on these colonies. Polyclone 1 and 2 stands for two multi-colonies of the transduced and selected 3T3-L1 cells which did not undergo the monoclone separation process. Results are means ± S.E.M from a single experiment performed in triplicate wells. Student's *t*-test was used to analyse the data. *: significant increases ($P<0.05$) with respect to Polyclone 1; #: significant decreases ($P<0.05$) with respect to Polyclone 1.

At the same time, the LucGFP lentivirus transduced 3T3-L1 cells were also selected for monoclones, using identical methods with the LucRFP lentivirus transduced cells. There were some cells surviving from the chronic blasticidin selection, but displayed no green fluorescence under the microscope and no luciferase activity (data not shown).

4.4 DISCUSSION

When optimizing the protocol for lentivirus production, the transfection efficiency in 293FT packaging cell line was considered as a primary factor. Figure 4.1 showed that the efficiency of Fugene HD® mediated transfection was about 50-60% while the lipofectamine 2000® mediated transfection had an efficiency of less than 10%, judged from the ratio of green fluorescent stained cells to total cell numbers in the field. In the lentivirus packaging system, only the cells which have been transfected with the lentiviral expression vector and all the packaging vectors would be able to package viral particles successfully. Assuming the 293FT cells did not discriminate different plasmids of similar sizes in terms of transfection efficiency, then the efficiency of transfection of the lentiviral expression vector, estimated from the number of green fluorescent cells, should be similar to that of any other plasmid and every transfection event should be random and independent of each other. Therefore in the ViraPower™ packaging system containing 3 packaging plasmids and the lentiviral expression vector, if the transfection efficiency was 60%, the chance for a single cell to be able to produce viral particles would be $(60\%)^4$= 13%. But if the transfection efficiency dropped to 10%, the chance would decrease to $(10\%)^4$= 0.01%, which was nearly impossible to produce viral particles. In 4.3.2, the capability of two different lentivirus packaging systems was compared. Although there was no significant difference in transfection efficiency (50-60%, Figure 4.2), the 2-plasmid packaging system psPAX2 had an advantage as a 60% transfection efficiency here could result in the chance of $(60\%)^3$=21.6% to successfully package viral particles, which was 1.7 fold of that with ViraPower™ packaging system. Furthermore, the 293FT cells transfected with the psPAX2 packaging plasmids looked unhealthier, corresponding to syncytia formation, resulting in areas devoid of cells (Figure 4.2). Given that the expression of the VSV-G, glycoprotein of vesicular stomatitis virus, which is responsible for enabling viral entry, has the function of fusing cells and forming syncytia (Norkin, 2010), it would be predicted that the high expression of VSV-G would cause morphological changes to the cells and expect the formation of syncytia to indicate increased expression levels of the packaging plasmids. Therefore it could be inferred from Figure 4.2 that the psPAX2 packaging mix had a higher packaging efficiency than the

ViraPower™ packaging system, which was later confirmed in the titering experiments (Figure 4.3).

It was planned to produce lentiviral particles mediating the inducible expression of C/EBPβ (or LucGFP) in the target cell line and to select for monoclones with stable expression of the transgene from transduced 3T3-L1 cells. However, the pilot experiments with the constitutive LucGFP lentiviral expression vector, pLenti6-LucGFP, did not succeed, which indicated some essential problems with the virus production and transduction system or the structure of the designed lentiviral expression vectors. Therefore the work with the inducible LucGFP and C/EBPβ lentiviral expression vectors could not be carried out without first optimising the transduction system.

Using a positive control pLenti6-LucRFP vector, it was demonstrated that the protocols were capable of producing efficiently infectious lentiviral particles (Figure 4.6) and mediating high level stable expression of the insert gene in the target cell line 3T3-L1 (Figure 4.8 and 4.9). However, the identical process didn't work well with pLenti6-LucGFP vector that was constructed in 3.3.3, implying that the problem must be due to the structural difference between the positive control pLenti6-LucRFP and the LucGFP vectors. As mentioned in 4.3.3, the pLenti6-LucGFP vector differed from the pLenti6-LucRFP vector in two ways. Firstly the pLenti6-LucGFP vector contained an additional Tet on regulatory antigen element (rtTA) coupled to a CMV promoter used to drive rtTA expression. And secondly, the LucGFP construct contained a Rabbit βGlobin Intron between the coding region of the gene and the polyA terminator whereas the LucRFP construct contained no introns before or after the polyA terminator. All the extra elements made the pLenti6-LucGFP vector ~1.8kb bigger in size than the pLenti6-LucRFP vector resulting in the total insert size of the former being around 5kb which was nearly the maximum allowed by the lentiviral vector expression system (Invitrogen, 2010). It is indicated in the protocol that the virus titer drops approximately 2-fold for each kb over 4kb of insert size and that the insert should not exceed 5.6kb. The larger size of the vector could therefore be the explanation for the low titer of the LucGFP lentivirus. Ultracentrifugation was therefore employed to concentrate and obtain a suitable virus titer (Invitrogen, 2010), resulting in an increased titer for the LucGFP virus by 10^2 fold (Figure 4.3). However,

when the concentrated lentivirus were applied to the 3T3-L1 cells, the cells were still not transduced efficiently as there were lots of green fluorescent particles outside the cells but no fluorescence were observed inside the cells (Figure 4.4). A possibility that was considered was that the ultracentrifuged LucGFP viral particles were not resuspended properly thus formed clumps which prevented the viral particles from efficiently infecting the cells. To avoid this, the ultracentrifuged lentivirus was briefly sonicated (Danovaro et al., 2001; Yen et al., 2009) to resuspend more efficiently and then used to transduce the 3T3-L1 cells but no improvements were observed (data not shown), indicating it was not the improper resuspension that had caused the problem. However, when the concentrated LucGFP lentivirus was titered in HT1080 cells, no obvious cell clumping was observed. Given that the growth medium for HT1080 cells contained the non-heat inactivated FBS while 3T3-L1 medium consisted of heat inactivated FBS, it could be some remaining active components in the former medium that helped preventing the clumping in HT1080 cells. As the growth of 3T3-L1 cells was interfered by the non-heat inactivated FBS (data not shown), the hypothesis could be tested, though not done yet, by using the heat inactivated FBS for maintaining HT1080 after transduction with concentrated LucGFP lentivirus. If the transduced HT1080 cells were still not clumped with the heat inactivated FBS, it would be more probable that the clumping was a feature of some poorly transduced cells such as 3T3-L1 when the virus could not enter the cells; however, no such phenomena has been reported in literature.

As for the optimal MOI of infecting 3T3-L1, although it was 30 as recommended from Invitrogen User Manual, there were different suggestions from different research groups. The Life Science Group from Bio-Rad company successfully transduced 3T3-L1 preadipoctes using virus-containing supernatant at a concentration of 40-120ng p24 per 10^5 cells which is equivalent to MOI of 1-3 (Schmidt and Al-Hasani, 2007), while another group used 200-400ng p24 per 10^5 cells which equivalent to MOI of 5-10 to realize an effective transduction in 3T3-L1 (Carlotti et al., 2004). Although the insert of our LucGFP virus was challenging the size limit of the system, the higher MOI used (around 30) to transduce the 3T3-L1 cells should be able to overcome the disadvantage from the size; yet the transductions were still not successful.

Since concentrating the virus and using a higher MOI failed to sort out the problem of the low infectious LucGFP lentivirus, it is possible that the size of the pLenti6-LucGFP vector needed modifying to generate vectors with the same functions but more suitable for lentivirus production. As the final target was to realize inducible expression of target genes, the Tet on regulatory element rtTA and its CMV promoter cannot be removed. It has been suggested by Twyman that the intron in the insert gene of the lentiviral vector might have a negative effect on virus production, i.e. to decrease the viral titers (Twyman, 2005). Therefore, one practical solution would be to remove the Rabbit βGlobin Intron, which will reduce the insert size by about 0.6kb. This decrease in size might still be insufficient to produce virus efficiently according to ViraPower™ protocol. Stuke and colleagues once got tetracycline-regulated highly inducible expression of human prion protein in murine 3T3 cells by transfecting the TRE-CMV driving prion vector into the 3T3-L1 cell line which had already been stably integrated with the Tet-off vector (Stuke and Strom, 2005). Pan et al also described the work to co-transduce murine macrophage cells derived from a mouse strain expressing rtTA with two lentiviruses: one was to constitutively express a selectable surface marker and the other to express "the gene of interest" driven by a doxycycline-inducible promoter (Pan et al., 2008). These data implied another approach which might be able to sort out the size problem of our lentiviral vectors: to divide a single Tet on lentiviral vector into two vectors, one containing the TRE modified promoter that drives the expression of the C/EBPβ (or LucGFP), the other containing the rtTA and its promoter. In this way, both vectors can be smaller in size but the target cell line has to be double transduced to have both C/EBPβ (or LucGFP) and rtTA gene expression cassettes integrated into a single genome.

To summarize, the experimental work in this chapter compared the first and second generation of lentivirus production system ViraPower™ and psPAX2 packaging plasmid mix, and the latter 2-plasmid system had higher efficiency than the former 3-plasmid system in packaging lentiviral particles in 293FT cell line. However, the first try of producing constitutive LucGFP lentiviral particles failed to achieve high titer and to effectively transduce the target cell line, 3T3-L1, even after the viral titer was increased to 10^5 TU/ml by ultracentrifugation and the MOI was as high as 30.

Meanwhile the positive LucRFP lentivirus was 3×10^2 fold higher in viral titer than the LucGFP virus and successfully transduced 3T3-L1, although at a higher MOI (30) compared with the MOI used in HT1080 (MOI=1) and 293FT (MOI=5) cells. Monoclonal 3T3-L1 cells stably expressing LucRFP were successfully separated through the processes described in 2.5.3, but the processes failed to result in LucGFP transduced monoclonal 3T3-L1 cells although blasticidin-resistant cell colonies were obtained.

In conclusion, the whole procedure of producing lentiviral particles with second generation packaging plasmid mix psPAX2, transducing target cell line 3T3-L1 and selecting for monoclonal transduced cells was successful, demonstrated by the data with positive LucRFP vector. The data also showed that the 3T3-L1 cell line was more difficult to transduce compared to HT1080 and 293FT cell lines. However, the lentivirus produced from constructed constitutive LucGFP vector was low infectious even after being concentrated to higher titer (10^5 TU/ml), probably due to the size of the designed vector challenging the limit of the lentivirus production system (5kb) and the problem could only be solved by re-designing the vectors.

Therefore in the absence of a successful lentiviral vector for overexpressing genes, in the following parts of the project transient overexpression was used to investigate the interaction between C/EBPβ and other factors in regulating the expression of UCP1 gene in 3T3-L1 cell line.

CHAPTER 5

5 INTERACTION BETWEEN C/EBP BETA, PGC1 ALPHA, PRDM16 AND PPAR GAMMA IN REGULATING UCP1 EXPRESSION DURING 3T3-L1 DIFFERENTIATION

5.1 INTRODUCTION

The transcription factor C/EBPβ has been found to play a critical role in adipogenesis and thermogenesis, specifically stimulating the expression of the adipogenic master regulator PPARγ and the hallmark gene of brown adipose tissue UCP1 respectively (see 1.3.5). The cAMP-PKA signalling pathway modulates both C/EBPβ and PPARγ expression, interacting with the PPAR ligand mediated signalling pathway and the activation of co-activators PGC1α and PRDM16, etc. Stimulation of the cAMP-PKA and PPAR signalling pathways with forskolin and rosiglitazone, respectively, has been shown to increase the thermogenic activity of brown fat (Cao et al., 2004; Robidoux et al., 2005; Teruel et al., 2005) but the exact mechanisms responsible for the interplay between the two pathways has not been elucidated. A hypothetical model of the mechanism by which C/EBPβ stimulates UCP1 expression was proposed in the Introduction (Figure 1.14) involving interaction with the (co)activators PGC1α and PRDM16 and the (co)repressors RIP140 and CIDEA, in response to the specific signalling pathways.

Previous work in our lab demonstrated that C/EBPβ binds to cAMP Response Element (CRE) on the proximal promoter of PGC1α to activate transcription (Karamanlidis et al., 2007). It was proposed that C/EBPβ was able to stimulate UCP1 expression in the 3T3-L1 white preadipocytes cell line, by increasing PGC1α expression (Karamanlidis et al., 2007). It has been illustrated in Figure 1.9 that the UCP1 promoter also contains CREs and a PPAR response element (PPRE) which facilitates its transcription in response to cAMP-PKA or PPAR ligand mediated signalling pathways respectively. The

aim of this chapter was to investigate the mechanism by which C/EBPβ acts on the UCP1 promoter. Two luciferase reporter vectors with artificial promoters were used, one with 3 repeated DR1 of PPRE as an enhancer in a TK promoter driving luciferase expression (pGL3-PPRE-TK) and the other with 6 repeated CREs as the promoter (pGL3-CRE).

Ideally, the role of C/EBPβ in 3T3-L1 differentiation should be tested using a stable overexpression system (as described in Chapter 3), in which C/EBPβ is stably overexpressed and switched on/off by the presence or absence of doxycycline throughout the whole differentiation process of 3T3-L1. However, as the previous work failed to produce highly infectious lentivirus to realize the stable overexpression of C/EBPβ in 3T3-L1, the transient transfection method (as described in 1.4) was used to test the model described in Figure 1.14, and investigate the interaction between C/EBPβ and PPARγ, PGC1α and PRDM16, in the regulation of UCP1 expression in 3T3-L1 cells. The main limitation of the transient transfection method is that the overexpression vector can only be transfected at high efficiency, before the cells are fully confluent so the effect of the overexpression must be tested, at latest, one day post confluence, to avoid loss of vector overexpression. Therefore, the experiments performed in this way can only demonstrate the effect of C/EBPβ overexpression on UCP1 expression in 3T3-L1 at confluence. The data gained from these experiments only reveals mechanisms directing the development of the brown adipogenic programme during the very early stages of differentiation. The transient transfection system is also very useful for the investigation of the interaction between regulatory molecules in modulating the acute regulation of the transcriptional activity of the UCP1 promoter and UCP1 mRNA expression, triggered by the cAMP-PKA signalling pathway.

The specific objectives of the experimental work described in this chapter were:

1. To investigate how the gene expression pattern of C/EBPβ, PGC1α, PPARγ, PRDM16 and UCP1 changes in response to chronic rosiglitazone or acute forskolin treatment during 3T3-L1 differentiation.

2. To investigate the effect of C/EBPβ, co-overexpressed with PRDM16 or PPARγ, on UCP1 transcription in confluent 3T3-L1 preadipocytes.

3. To locate where C/EBPβ acts on the promoter of UCP1, i.e. whether C/EBPβ binds to PPRE or CRE on UCP1 promoter.

5.2 EXPERIMENTAL DESIGN

5.2.1 Analysis of gene expression profiles in 3T3-L1 differentiation and the effects of rosiglitazone/forskolin on gene expression

3T3-L1 cells were grown to confluence on 6-well plates in 2ml/well growth medium and two days later (DAY 1), the induction medium containing 10% FBS, 500μM IBMX, 250nM dexamethasone and 167nM insulin was applied to the cells and treated for 48 hours. The medium was then changed to maintenance medium containing 10% FBS and 167μM insulin for another 6 days (DAY 8) as described in 2.2.3. 1μM rosiglitazone was added to the differentiation medium from DAY 1. On DAY 8 of differentiation, 10μM forskolin was added to the cells and treated for 3 hours before cells were lysed for RNA extraction as described in 2.6.1. cDNAs were synthesised (as described in 2.6.2) from the extracted RNA and quantitative real time PCR (described in 2.6.3) was used to measure the expression of UCP1, C/EBPβ, PPARγ, PGC1α and PRDM16.

To investigate the time course of rosiglitazone effect on gene expression pattern in 3T3-L1 cells during differentiation, 1μM rosiglitazone was added to the differentiation medium of 3T3-L1 cells from DAY1 of differentiation. Cells were lysed for RNA extraction on DAY 0, 1, 2, 3, 4, 5, 6, 7, 9, 11 and gene expression of UCP1, C/EBPβ, PPARγ and aP2 was measured by quantitative real time PCR as described in 2.6.3.

5.2.2 Effects of C/EBPβ and PRDM16 co-overexpression on transcriptional activity of UCP1 and PGC1α promoters.

To investigate whether C/EBPβ could increase transcription from the UCP1 promoter, and the interaction with PRDM16, 3T3-L1 preadiocytes were seeded into 24-well plates. At 80% confluence, a 3.1kb UCP1 promoter luciferase reporter vector (3.1UCP1 pGL3-Luc) or 2.6kb PGC1α promoter reporter vector (2.6PGC1α pGL3-Luc) were separately co-transfected with C/EBPβ and/or PRDM16 expression vectors into 3T3-L1 cells as described in 2.3.2. 36 hours later, 10μM forskolin was added to the

transfected cells and 12 hours later, firefly luciferase activity was measured as described in 2.3.3 to quantify the transcriptional activity of either promoter with the overexpression of C/EBPβ and/or PRDM16.

To further confirm the results from the reporter assay experiments described above, mRNA level of UCP1 was also measured in 3T3-L1 transfected with C/EBPβ and/or PRDM16. Cells were seeded in 6-well plates and transfected with 1μg of C/EBPβ and/or 1μg of PRDM16 vector as described in 2.3.2. 10μM forskolin was added into the culture about 40 hours post transfection and treated for 3 hours before the cells were lysed for RNA extraction as described in 2.6.1. The mRNA level of C/EBPβ, PRDM16, UCP1 and PGC1α was quantified by real time PCR to check if the overexpression was successful and the effect of the overexpression on the endogenous expression of UCP1 and PGC1α.

5.2.3 Effects of C/EBPβ and PPARγ co-overexpression on transcriptional activity of UCP1 and PGC1α promoter.

To investigate whether C/EBPβ could increase the transcriptional activity of UCP1 promoter when co-overexpressed with PPARγ, 3T3-L1 preadiocytes were separately transfected with either the 3.1 UCP1 pGL3-Luc vector or 2.6 PGC1α pGL3-Luc vector, together with C/EBPβ and/or PPARγ expression vectors as described in 2.3.2. 10μM PPARγ ligand rosiglitazone was added to the cultures 24 hours post transfection with 10μM forskolin added to the transfected cells 12 hours after rosiglitazone. Firefly luciferase activity was measured 48 hours post transfection as described in 2.3.3 to quantify the transcriptional activity of either promoter with the overexpression of C/EBPβ and/or PPARγ.

To further confirm the results from the reporter assay experiments described above, the mRNA level of UCP1 was also measured in 3T3-L1 transfected with C/EBPβ and/or PPARγ. Cells were seeded in 6-well plates and transfected with 1μg of C/EBPβ and/or 1μg of PPARγ vector as described in 2.3.2. 10μM rosiglitazone was added to the cells 24 hours after transfection and treated for 24 hours. 10μM forskolin was added to the culture about 40 hours post transfection and treated for 3 hours before the cells were lysed for RNA extraction as described in 2.6.1. The mRNA level of C/EBPβ, PPARγ,

UCP1 and PGC1α was quantified by real time PCR to check if the overexpression was successful and the effect of the overexpression on the expression of UCP1 and PGC1α.

5.2.4 Effects of C/EBPβ on PPRE and CRE in 3T3-L1.

To locate where C/EBPβ acts on the UCP1 and PGC1α promoters, the artificial reporter vectors containing either PPRE or CRE driven luciferase reporter plasmids (pGL3-PPRE-TK or pGL3-CRE) were co-transfected with C/EBPβ into the 3T3-L1 preadipocytes in 24-well plates as described in 2.3.2. 24 hours post transfection, 10μM rosiglitazone was added to the cells transfected with pGL3-PPRE-TK and treated for 24 hours, while 10μM forskolin was added to the cells transfected with pGL3-CRE 36 hours post transfection and treated for 12 hours. Luciferase assay was performed 48 hours after transfection to check if the overexpression of C/EBPβ increased the luciferase expression activated by PPRE or CRE.

Data in figures is presented as average ± SEM from 2 or 3 independent replicate experiments with duplicate or triplicate wells in each experiment. Effects of treatments were determined by performing Student's *t*-test or Analysis of Variance (ANOVA) as indicated in individual figure legend. Significance was accepted if $P<0.05$.

5.3 RESULTS

5.3.1 The effect of rosiglitazone (chronic) and forskolin (acute) on the expression of C/EBPβ, PPARγ, PGC1α, PRDM16 and UCP1 in 3T3-L1 before and after differentiation.

The synthetic PPARγ agonist triglitazone has been reported to stimulate brown adipogenesis in 3T3-L1 preadipocytes or fibroblasts over-expressing PPARγ (Vernochet et al., 2009). Acute treatment of norepinepharine is also said to favour brown fat differentiation (Petrovic et al., 2009). These findings have confirmed the important role of both signalling pathways in brown adipogenesis and inspired the idea to test the effect of another PPARγ agonist rosiglitazone and the cAMP inducer forskolin, on differentiation of the white preadipocyte 3T3-L1 cell line. We tested the hypothesis that chronic treatment with rosiglitazone and acute treatment with forskolin could stimulate brown adipogenic gene expression phenotypes during the

3T3-L1 differentiation process. The 3T3-L1 preadipocytes were differentiated as described in 2.3.3.

Figure 5.1 Forskolin and Rosiglitazone effects on gene expressions in differentiated 3T3-L1.

3T3-L1 preadipocytes were grown to 100% confluence in DMEM containing 10% FBS. 2 days post confluence, cells were induced to differentiate by DMEM containing 10% FBS, 0.5mM IBMX, 167nM Insulin and 250nM dexamethasone with or without rosiglitazone (Rosi, 1μM) for 2 days. After induction, cells were maintained in DMEM containing 10% FBS and 167nM Insulin with or without Rosi for another 6 days before RNA extraction. Forskolin (Forsk) was added to the cells 3 hours before RNA extraction as indicated. Gene expression levels of UCP1 (A), PGC1α (B), C/EBPβ (C), PPARγ2 (D), RIP140 (E) and Resistin (F) was analyzed by quantitative real-time PCR and normalized against 18S expression. 3T3-L1 pre stands for the data from 3T3-L1 preadipocytes (Day 0); DIF 3T3-L1 stands for the data from differentiated 3T3-L1 adipocytes (Day 8). Results represent mean ± S.E.M from 2 independent replicate experiments performed in triplicate wells. *P<0.05 by Student's *t*-test due to differentiation with respect to 3T3-L1 pre samples; data of differentiated cells was analysed by two-way ANOVA.

A UCP1 expression in differentiated 3T3-L1

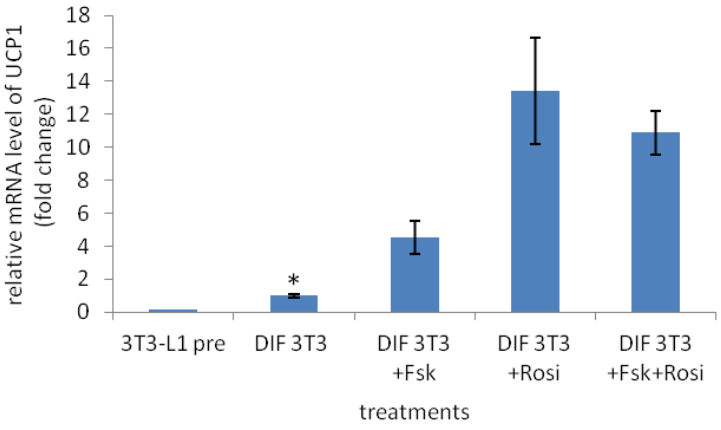

2-way ANOVA:	P-value
Fsk	<0.001
Rosi	<0.001
Fsk×Rosi	0.072

B PGC1α expression in differentiated 3T3-L1

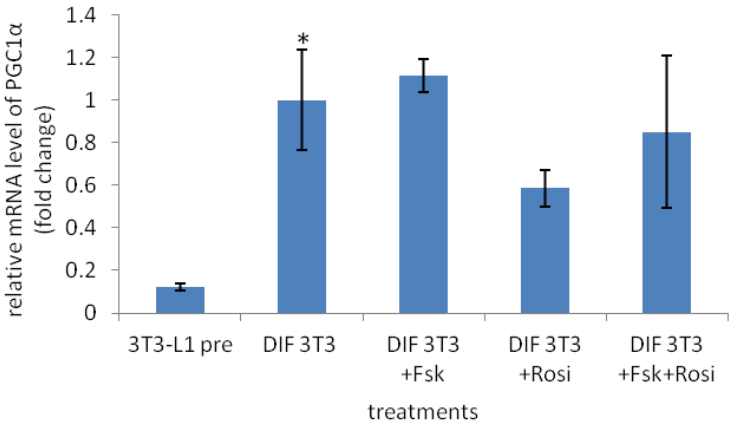

2-way ANOVA:	P-value
Fsk	0.47
Rosi	0.048
Fsk×Rosi	0.27

C C/EBPβ expression in differentiated 3T3-L1

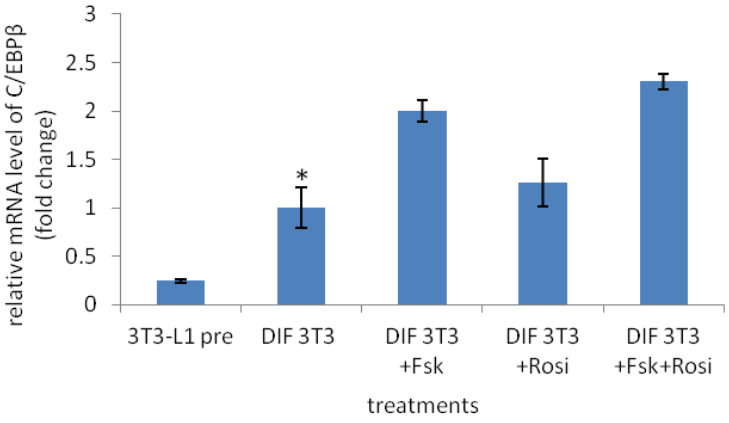

2-way ANOVA:	P-value
Fsk	0.032
Rosi	0.56
Fsk×Rosi	0.18

D

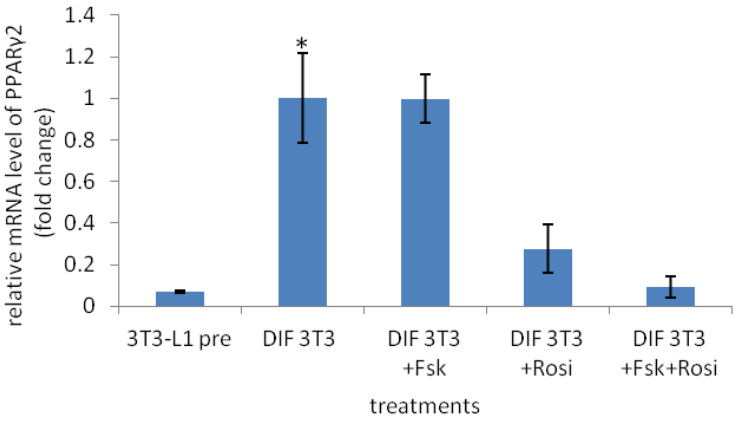

2-way ANOVA:	P-value
Fsk	0.67
Rosi	0.006
Fsk×Rosi	0.075

E

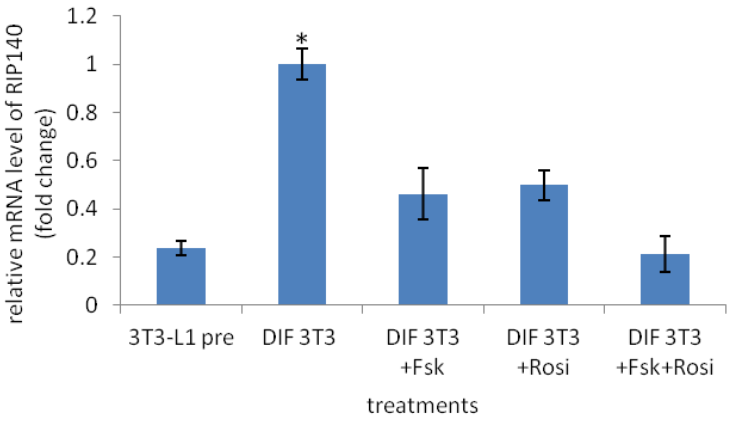

2-way ANOVA:	P-value
Fsk	0.009
Rosi	0.008
Fsk×Rosi	0.047

F

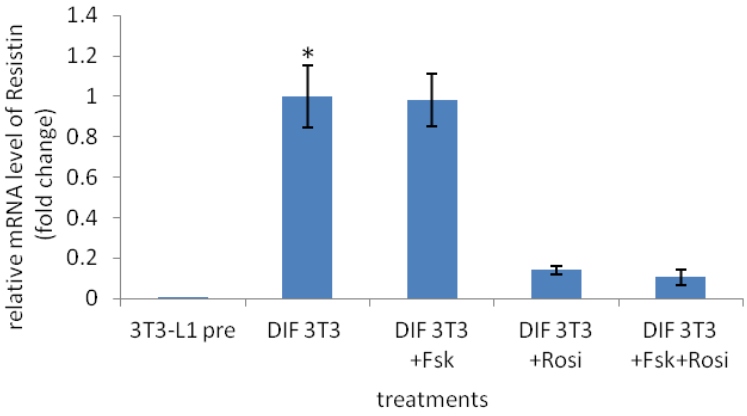

2-way ANOVA:	P-value
Fsk	0.79
Rosi	0.004
Fsk×Rosi	0.28

As shown in Figure 5.1A, the expression of UCP1 was increased ($P<0.01$) 7 fold by differentiation and in differentiated 3T3-L1 adipocytes, UCP1 expression was significantly increased ($P<0.01$) 4.5 fold by the treatment of forskolin or 13.4 fold by rosiglitazone, but there was no additive effect when treating cells with both drugs. The expression of PGC1α was increased ($P<0.01$) 8 fold in differentiated cells compared to preadipocytes (Figure 5.1B), but forskolin treatment did not further increase the expression and rosiglitazone treatment slightly reduced PGC1α expression ($P=0.048$). C/EBPβ expression was increased ($P<0.01$) 4 fold by differentiation and in mature 3T3-L1 adipocytes, the acute treatment of forskolin increased ($P<0.05$) C/EBPβ expression 2 fold but rosiglitazone treatment had no significant effect on C/EBPβ expression in fully differentiated 3T3-L1 cells (Figure 5.1C). RIP140 has been reported as a co-repressor of UCP1 transcription and thermogenesis in brown adipose tissue (Kiskinis et al., 2007); its expression was significantly stimulated ($P<0.01$) by the 3T3-L1 differentiation process but this stimulation was reduced ($P<0.01$) by about 50% by the treatment with either forskolin or rosiglitazone, but there was no significant interaction between the two drug treatments (Figure 5.1E). The pattern of RIP140 expression responses to treatments during differentiation was opposite to the pattern for UCP1 expression (Figure 5.1A). As the marker gene of adipogenesis, PPARγ2 expression was markedly increased ($P<0.001$) 14 fold after differentiation compared to the expression level in preadipocytes, but forskolin treatment had no significant effect on PPARγ2 expression in mature adipocytes (Figure 5.1D). Surprisingly, treatment with PPARγ ligand rosiglitazone significantly reduced ($P<0.01$) the expression of PPARγ2 by 72% in differentiated 3T3-L1 cells. As one of the genes induced during adipogenesis (Kershaw and Flier, 2004), resistin displayed the identical expression pattern with that of PPARγ, greatly increased ($P<0.001$) by differentiation process (1200 fold) but significantly decreased ($P<0.01$) by 86% by the treatment of rosiglitazone (Figure 5.1F), consistent with data in literature (Steppan et al., 2001). The down-regulation of PPARγ and resistin by rosiglitazone treatment indicated an impaired white adipogenesis, at least in terms of lipid accumulation. To further validate this conclusion, another set of 3T3-L1 cells were differentiated with or without 1μM rosiglitazone for 12 days, and then counter-stained by haematoxylin and Oil Red O as described in 2.2.4 to check the lipid

accumulation as a reference of white adipogenesis. It was clear in Figure 5.2 that there were lots of big lipid droplets (stained red) in the adipocytes without rosiglitazone treatment (Figure 5.2, upper) while the adipocytes differentiated with rosiglitazone had much fewer and smaller lipid droplets (Figure 5.2, lower), confirming that rosiglitazone did impaired lipid accumulation in white adipogenesis.

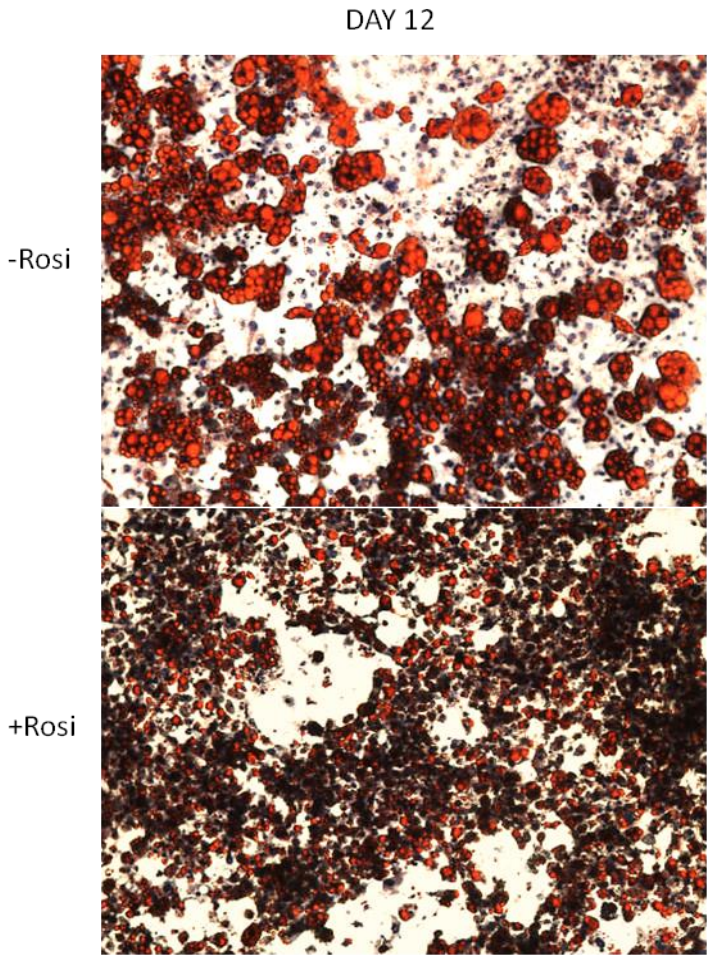

Figure 5.2 Haematoxylin-Oil Red O counter staining of 3T3-L1 adipocytes differentiated with or without rosiglitazone treatment.

3T3-L1 preadipocytes were differentiated as described in 2.3.3, with or without 1µM rosiglitazone in the induction and maintenance medium from DAY 0 of differentiation. At DAY 12, medium was removed from the cells and the differentiated cells were then stained by Oil Red O and Haematoxylin as described in 2.2.4. Photos were taken using Leica DFC 420C microscope (bright field) with the magnification of 100.

5.3.2 Time course of lipid droplet accumulation and the expression of C/EBPβ, PPARγ, aP2 and UCP1 in 3T3-L1 differentiation in response to chronic treatment of rosiglitazone.

An experiment was first conducted to examine the effect of rosiglitazone treatment on the time course of lipid droplet accumulation during 8 days of differentiating 3T3-L1 cells. It was observed that the 3T3-L1 cells treated with rosiglitazone seemed to differentiate at a faster pace compared with the ones without rosiglitazone treatment, especially on DAY 3 when the cells treated with rosiglitazone started to accumulate lipid droplets while there were no lipid droplets appearing in the cells without rosiglitazone (Figure 5.3A). On DAY 5, there were more lipid droplets accumulating in the rosiglitazone treated cells than the untreated ones, but the difference gradually disappeared and the two sets of cells looked similar in terms of lipid droplet accumulation on DAY 6 (Figure 5.3A). By DAY 7 and DAY 8, there seemed to be more lipid droplets in the cells without rosiglitazone treatment than in the treated cells, although the difference was slight (Figure 5.3B). Given that there were more lipid droplets accumulated in the fully differentiated 3T3-L1 adipocytes without rosiglitazone treatment than the treated cells (Figure 5.2), it was reasonable to infer that in the late stage of differentiation (DAY 8 to DAY 12), rosiglitazone inhibited the formation of lipid droplets.

Figure 5.3 Daily progress of 3T3-L1 differentiation with or without rosiglitazone.

3T3-L1 preadipocytes were grown to 100% confluence and differentiated as described in 2.3.3, with or without 1μM rosiglitazone (Rosi) in the induction and maintenance medium from DAY 0 of differentiation. Photos in bright field were taken daily from DAY 0 to DAY 8 using Leica DFC 420C microscope. (A) Photos from DAY 0 to DAY 3 were taken at the magnification of 100. (B) Photos from DAY 4 to DAY 8 were taken at the magnification of 400.

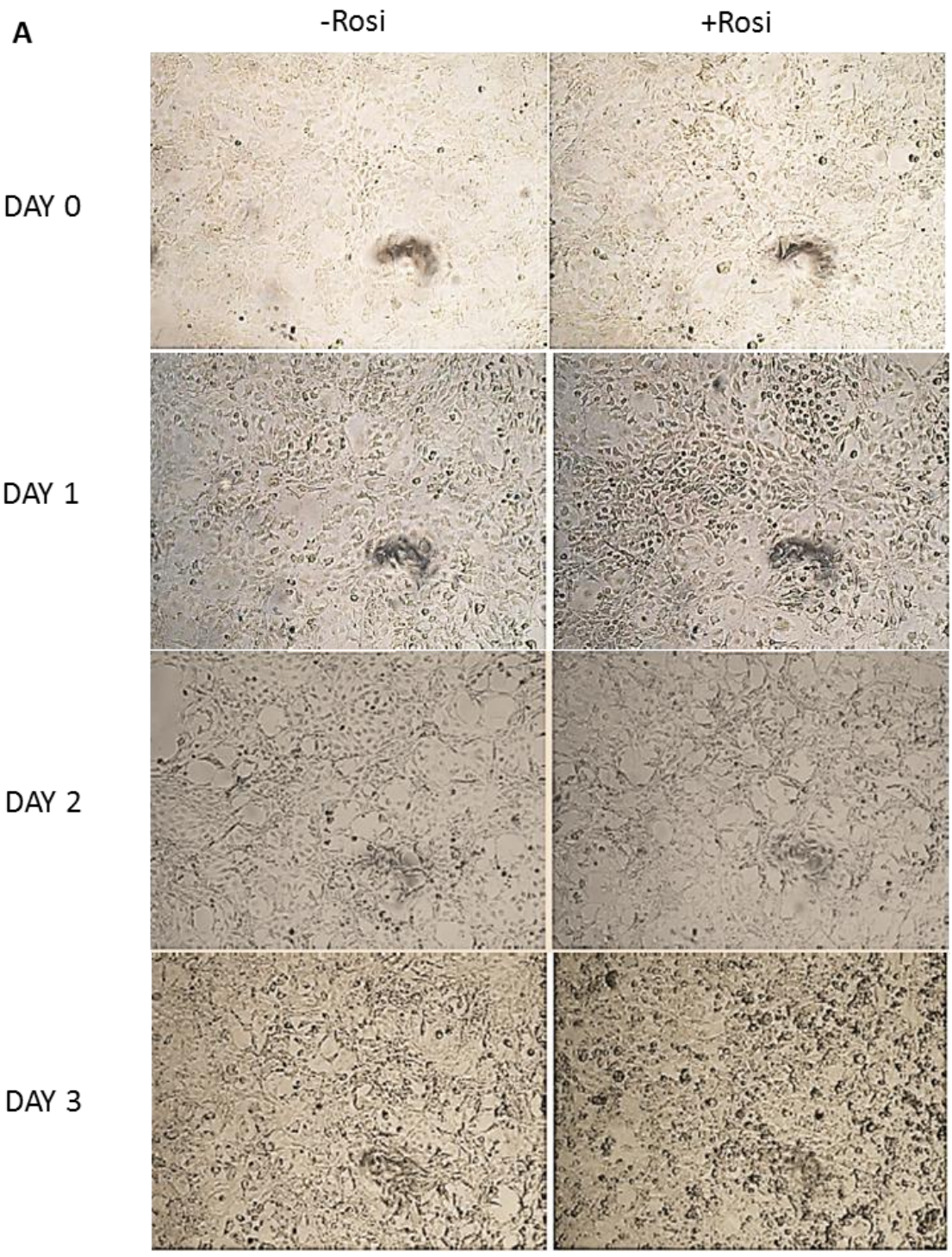
A
-Rosi
+Rosi
DAY 0
DAY 1
DAY 2
DAY 3

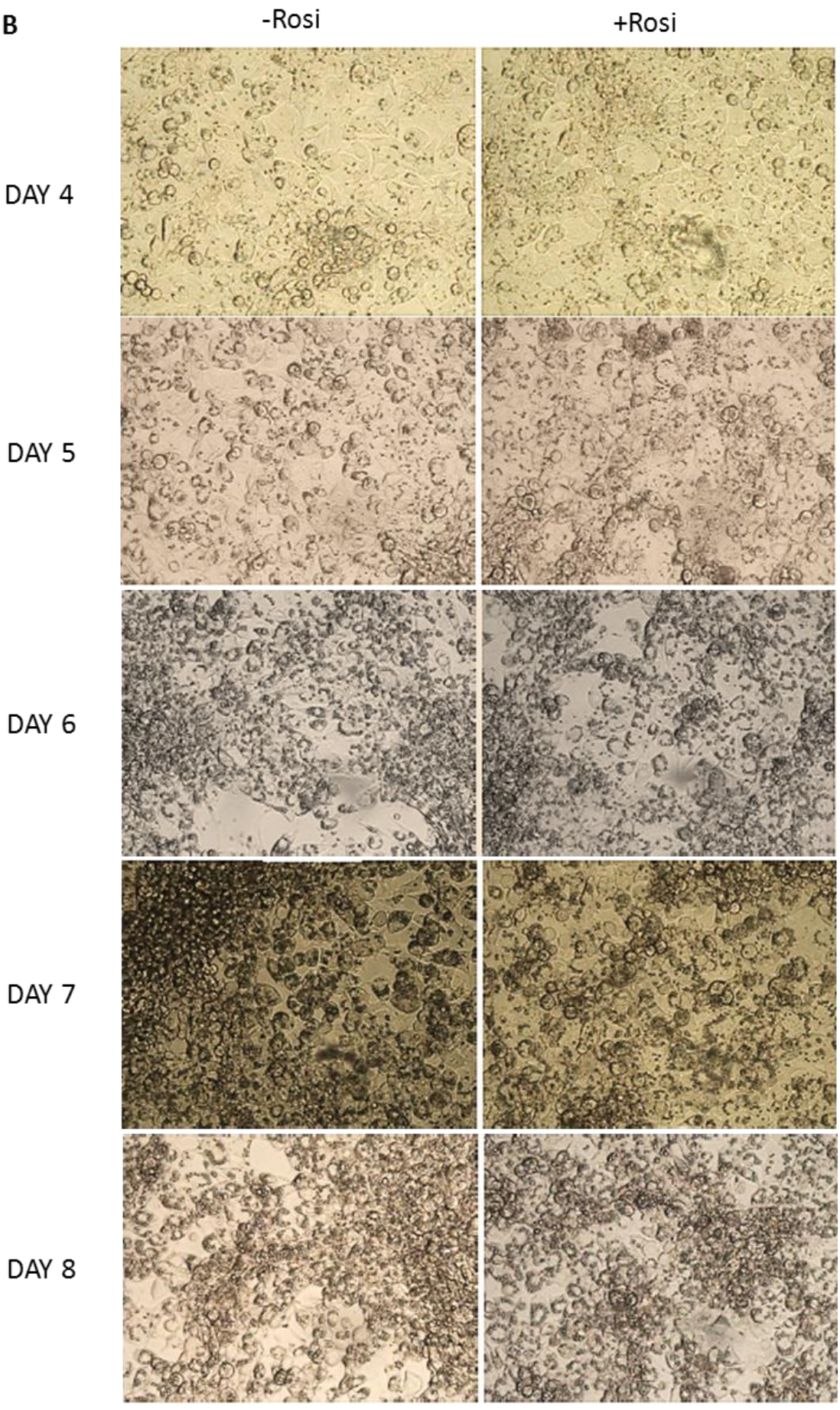
B
-Rosi
+Rosi
DAY 4
DAY 5
DAY 6
DAY 7
DAY 8

To investigate how the expression pattern of critical adipogenic and thermogenic genes was influenced by rosiglitazone treatment during different stages of 3T3-L1 differentiation, a time course experiment was performed in differentiating 3T3-L1 cells using the same protocol and over the same period as described in 5.3.1. 3T3-L1 preadipocytes were grown to confluence and, 2 days later as described in 2.3.3, induced to differentiate with or without 1µM rosiglitazone. Cells were lysed for RNA extraction on DAY 0, 1, 2, 3, 4, 5, 6, 7, 9, 11 as described in 2.6.1 and quantitative real-time PCR was used to measure the expression level of C/EBPβ and the adipogenic marker gene PPARγ as well as aP2 and UCP1 genes (Figure 5.4).

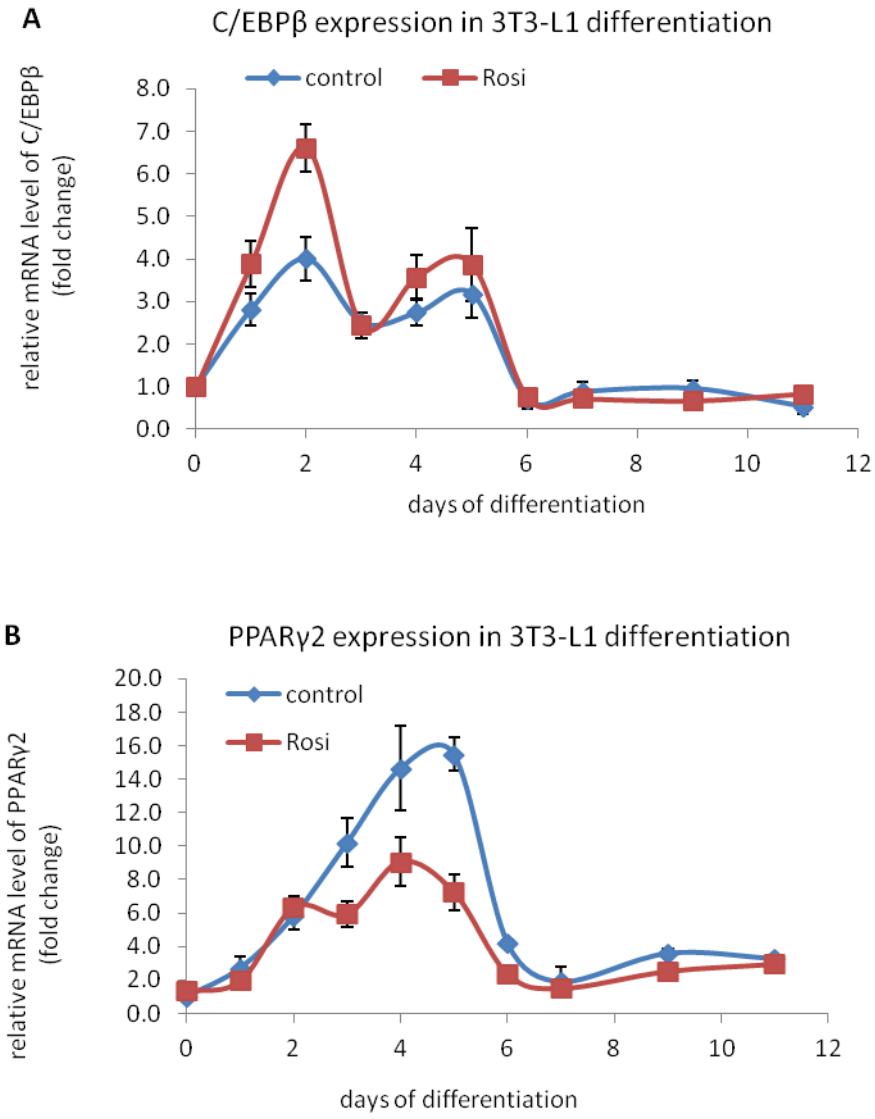

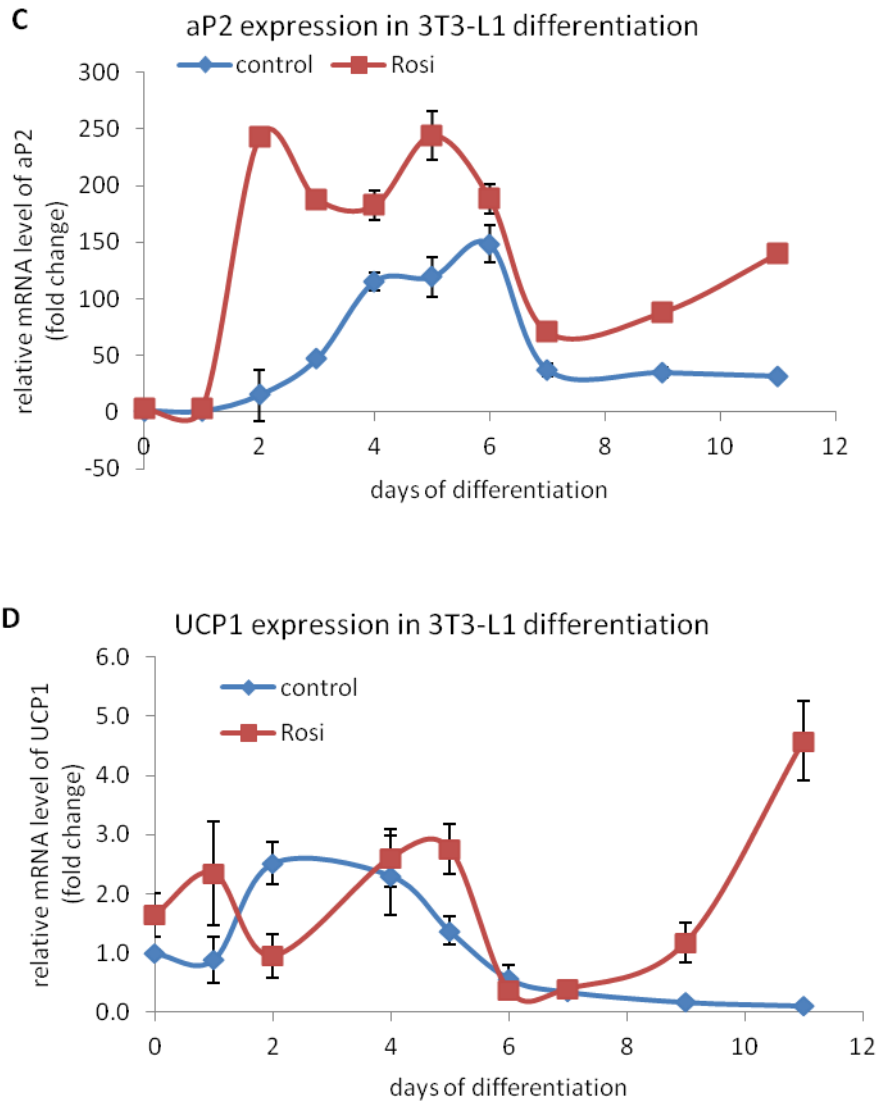

Figure 5.4 Time course of PPARγ, C/EBPβ, aP2 and UCP1 expression during 3T3-L1 differentiation progress.

3T3-L1 preadipocytes were differentiated as described in 2.3.3, with or without 1μM rosiglitazone (Rosi) from DAY 0. Cells were lysed for RNA extraction on DAY 0, 1, 2, 3, 4, 5, 7, 9 and 11 as described in 2.6.1 and gene expression of C/EBPβ (A), PPARγ (B), aP2 (C) and UCP1 (D) was analysed by quantitative real-time PCR and normalized against 18S expression. Results represent mean ± S.E.M from 2 independent replicate experiments performed in duplicate wells. Data was analysed by two-way ANOVA and $P<0.001$ for time×Rosi for all the four genes.

Two-way ANOVA analysis indicated that the effect of rosiglitazone significantly differed ($P<0.001$) depending on differentaition time for all the four genes tested. Expression of C/EBPβ (Figure 5.4A) increased 4 fold in the first 2 days of differentiation and rosiglitazone up-regulated its expression to 6.7 fold. However, the expression level decreased afterwards and there was no response to rosiglitazone. Expression of PPARγ (Figure 5.4B) reached the peak, which was about 14 fold higher compared with the preadipocytes, on DAY 4-5, but decreased afterwards. Rosiglitazone down-regulated the peak expression of PPARγ by 40-50% but had no significant effect before or after it. The expression of aP2 increased after DAY 3 and peaked between DAY 4-6, returning to just above basal by DAY 7 of differentiation. Rosiglitazone treatment up-regulated the early response in aP2 expression, producing a pronounced 15 fold higher rise at DAY2 which was sustained until DAY 6 and then fell by DAY 7, but still remaining higher than the control cells (Figure 5.4C). UCP1 expression was significantly up-regulated 2 fold between 2-4 days of differentiation, falling back to baseline afterwards. Rosiglitazone treatment suppressed UCP1 expression only at DAY 2 but stimulated expression from DAY 9 (Figure 5.4D).

5.3.3 Different responses of UCP1 and PGC1α promoter to co-overexpression of C/EBPβ and PRDM16 in 3T3-L1 cells.

It has been reported that C/EBPβ is able to form a complex with PRDM16 to initiate a brown adipogenic lineage from Myf5 positive progenitors by increasing expression of PGC1α (Kajimura et al., 2009). To investigate whether the combination of C/EBPβ and PRDM16 could stimulate the expression of the brown adipogenic genes such as UCP1 and PGC1α in white 3T3-L1 preadipocytes, C/EBPβ and PRDM16 expression vectors were co-transfected with either 3.1UCP1 pGL3-Luc or 2.6PGC1α pGL3-Luc reporter vectors, into 3T3-L1 cell line as described in 2.3.2. 10μM forskolin was added into the cell culture 36 hours post transfection and 12 hours later the cells were assayed for luciferase luminescence as described in 2.3.3, to measure the transcriptional activity of both promoters (Figure 5.5). Data was analysed by three-way ANOVA. Figure 5.5A showed that C/EBPβ and PRDM16 had a significant interaction ($P=0.026$), indicating a synergistic effect on increasing transcriptional activity of 3.1kb UCP1 promoter in 3T3-L1. Forskolin addition to increase cAMP further induced ($P<0.001$) the C/EBPβ and/or PRDM16 stimulated transcriptional activity of the UCP1 promoter. In contrast,

overexpression of C/EBPβ or PRDM16 alone failed to activate the 2.6kb PGC1α promoter (Figure 5.5B). But there was significant interaction (P=0.006) between C/EBPβ and PRDM16 when co-overexpressed. Forskolin treatment had marginal significant effect (P=0.051).

Figure 5.5 Co-overexpression of C/EBPβ and PRDM16 activated the transcription of UCP1 but not PGC1α in 3T3-L1.

3T3-L1 preadipocytes were grown to 70-80% confluence and then transfected with pGL3-3.1kb UCP1 promoter (A) or pGL3-2.6kb PGC1α promoter (B) in the presence of C/EBPβ and/or PRDM16 overexpression as indicated in the graphs. Forskolin (10μM) was added to the cells 36 hours post transfection, and luciferase assay was carried out 48 hours post transfection. Firefly luciferase activity was relative to the values from the cells transfected only with the promoter vector and treated with DMSO. Results are mean ± S.E.M from 3 independent replicate experiments performed in triplicate wells. The data was analysed by three-way ANOVA. As neither C/EBPβ nor PRDM16 had significant interaction (P>0.05) with forskolin, the P values of the vector-drug interactions are not indicated in the figures.

A

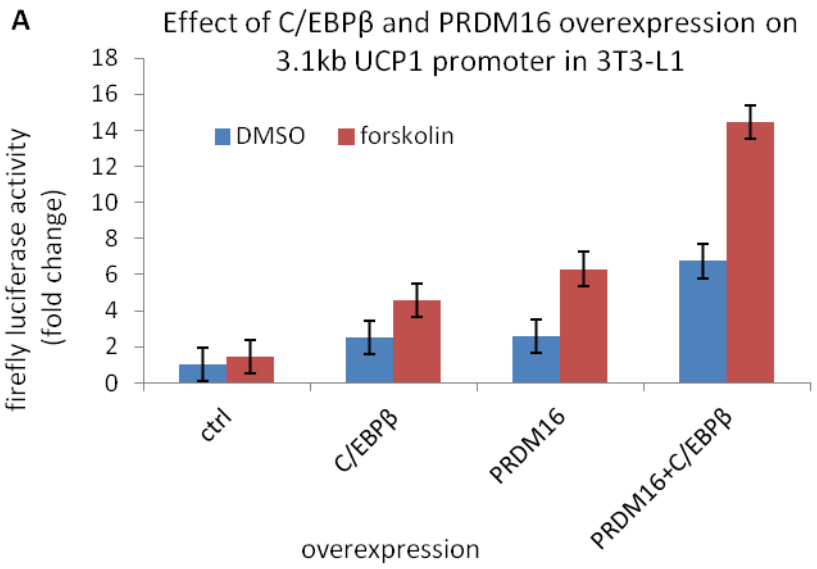

3-way ANOVA:	P-value
C/EBPβ	<0.001
PRDM16	0.001
forskolin	<0.001
C/EBPβ×PRDM16	0.029

B

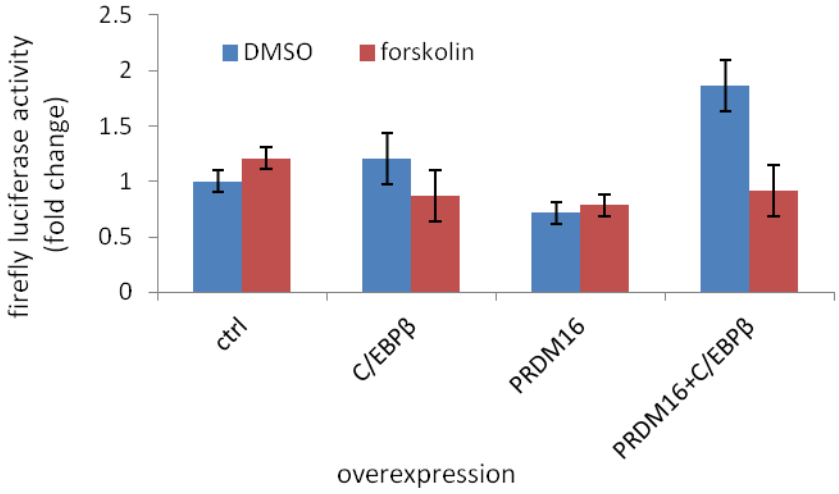

3-way ANOVA:	P-value
C/EBPβ	0.056
PRDM16	0.99
forskolin	0.051
C/EBPβ×PRDM16	0.006

To further confirm the results from reporter assays above, 3T3-L1 preadipocytes were transfected with C/EBPβ or/and PRDM16 overexpression vectors as described in 2.3.2, and 36 hours post transfection, cells treated with 10μM forskolin for 3 hours before the cells were lysed for RNA extraction. The mRNA level of UCP1 and PGC1α was determined by quantitative real-time PCR (Figure 5.6). Data was analysed by three-way ANOVA. Despite successful overexpression of C/EBPβ and PRDM16, as demonstrated by increased mRNA levels (Figure 5.6A&B), the expression of UCP1 or PGC1α was not significantly altered, even after forskolin treatment (Figure 5.6C&D, $P>0.05$). When checking the PCR products of the UCP1 and PGC1α RT-PCR on 2% agarose gel, the bands at expected size (75bp) for UCP1 or PGC1α looked faint for the control samples (Lane 1&2) (Figure 5.6E), probably because the expression of both genes were too low in the template to pick up by PCR and the PCR signals were possibly primer dimers or other non-specific amplification. Interestingly, there was a significant C/EBPβ×PRDM16×forskolin interaction ($P=0.004$) in Figure 5.6A: the mRNA level of C/EBPβ was higher in the cells co-transfected with C/EBPβ and PRDM16 than those only transfected with C/EBPβ although the C/EBPβ mRNA in the cells transfected with only PRDM16 remained at the same level with that in the mock transfected cells; moreover, the co-overexpression of PRDM16 abolished the forskolin-induced increase of C/EBPβ in the cells overexpressing C/EBPβ only. This suggested a synergistic positive feedback effect of C/EBPβ-PRDM16 co-overexpression on expression of C/EBPβ from the overexpression plasmid. But the same effect was not shown on PRDM16 expression, as the expression did not significantly differ in the cells transfected with only PRDM16 and the ones co-transfected with both vectors (Figure 5.6B). However, as both the overexpression vectors were driven by constitutive promoter CMV, it was less likely that one of the overexpressed genes could be regulated by the other, so the observation above might just result from different levels of mRNA turnover, and this also suggested that Western Blotting should be a more reliable method to detect gene expression as it directly reflects the difference at protein level. Alternatively, as the exogenous C/EBPβ and PRDM16 were both driven by the CMV promoter in the overexpression vectors, there might be some competition for transcription factors when overexpressing the two genes in the transfected 3T3-L1 cells.

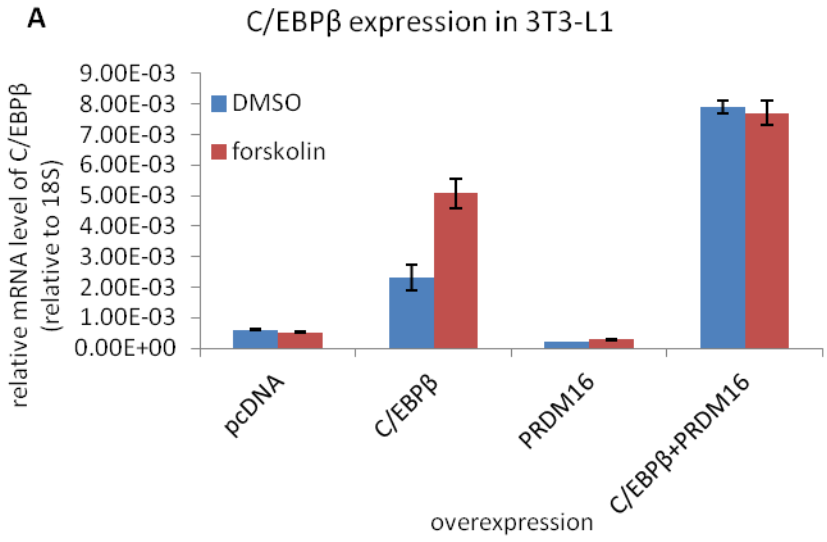
A
C/EBPβ expression in 3T3-L1
relative mRNA level of C/EBPβ (relative to 18S)
9.00E-03
8.00E-03
7.00E-03
6.00E-03
5.00E-03
4.00E-03
3.00E-03
2.00E-03
1.00E-03
0.00E+00
DMSO
forskolin
pcDNA
C/EBPβ
PRDM16
C/EBPβ+PRDM16
overexpression

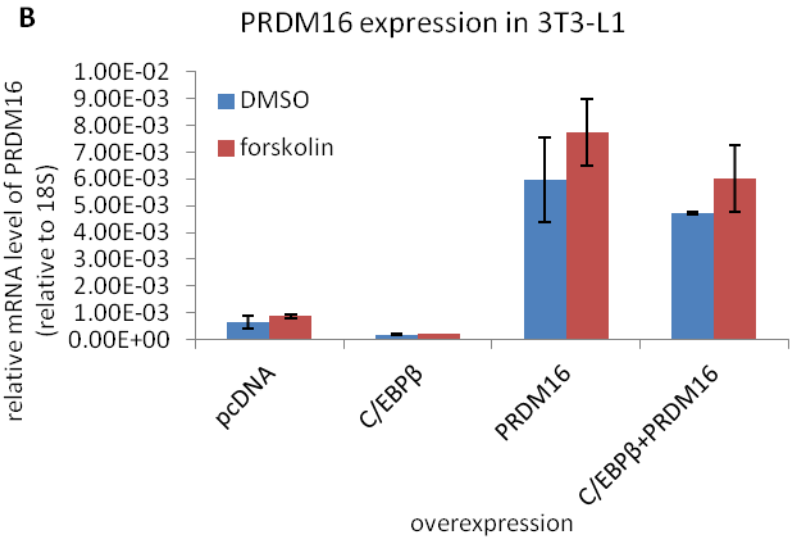
B
PRDM16 expression in 3T3-L1
relative mRNA level of PRDM16 (relative to 18S)
1.00E-02
9.00E-03
8.00E-03
7.00E-03
6.00E-03
5.00E-03
4.00E-03
3.00E-03
2.00E-03
1.00E-03
0.00E+00
DMSO
forskolin
pcDNA
C/EBPβ
PRDM16
C/EBPβ+PRDM16
overexpression

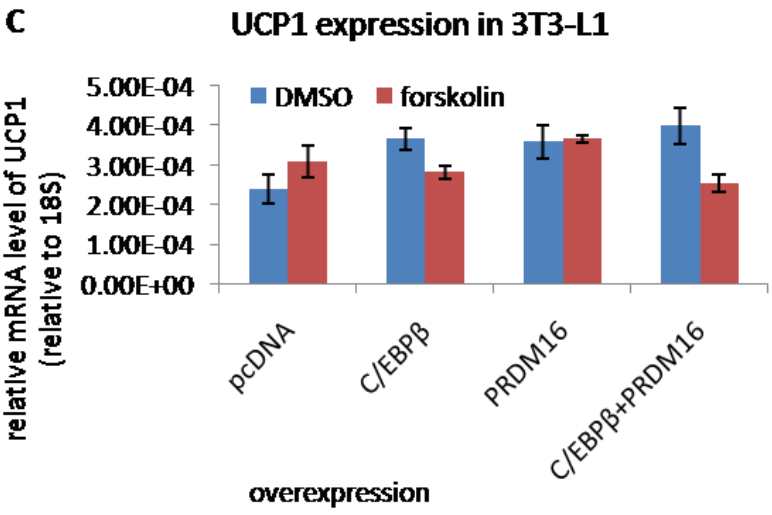
C
UCP1 expression in 3T3-L1
relative mRNA level of UCP1 (relative to 18S)
5.00E-04
4.00E-04
3.00E-04
2.00E-04
1.00E-04
0.00E+00
DMSO
forskolin
pcDNA
C/EBPβ
PRDM16
C/EBPβ+PRDM16
overexpression

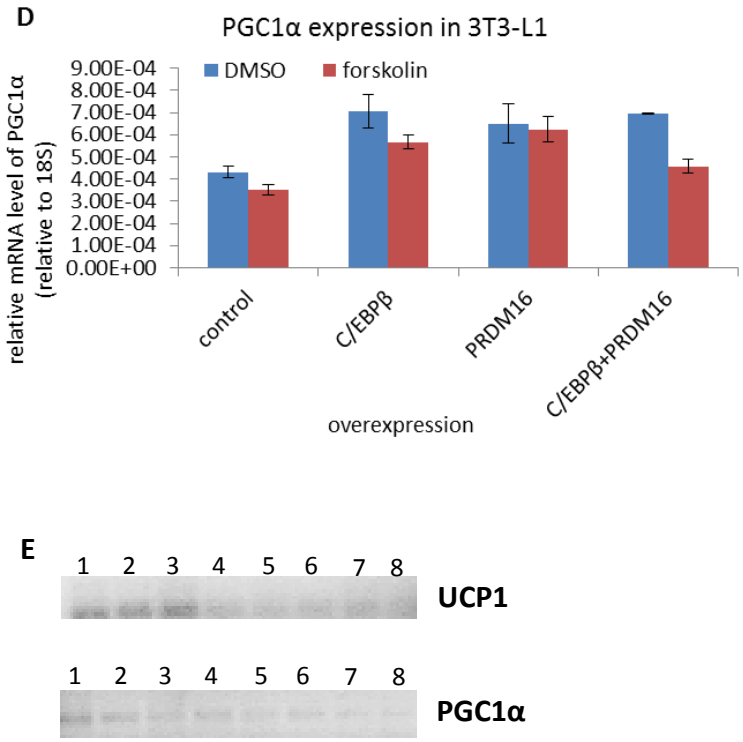

Figure 5.6 The expression level of UCP1 and PGC1α was not changed by overexpression of C/EBPβ or/and PRDM16 in 3T3-L1 preadipocytes.

3T3-L1 preadipocytes were grown to 70-80% confluence in 6-well plates and then transfected with over expression vectors for C/EBPβ or/and PRDM16 (or just pcDNA as mock) by Fugene HD as described in 2.3.2. 36 hours post transfection, 10μM forskolin was added to the cell culture and treated for 3 hours before the cells were lysed for RNA extraction. The mRNA level of C/EBPβ (A), PRDM16 (B), UCP1 (C) and PGC1α (D) was determined by quantitative real-time PCR and normalised against 18S expression. Results represent mean ± SD from one of the duplicate experiments performed in triplicate wells. Data was analysed by three-way ANOVA: (A) $P=0.004$ for C/EBPβ×PRDM16×forskolin; (B) $P<0.001$ for PRDM16; (C) $P>0.05$; (D) $P>0.05$. (E) The PCR products of UCP1 (upper) and PGC1α (lower) were checked by electrophoresis on a 2% agarose gel. Template list: Lane 1- pcDNA transfected cells, Lane 2- pcDNA transfected cells treated with forskolin, Lane 3- C/EBPβ transfected cells, Lane 4- C/EBPβ transfected cells treated with forskolin, Lane 5- PRDM16 transfected cells, Lane 6- PRDM16 transfected cells treated with forskolin, Lane 7- C/EBPβ and PRDM16 cotransfected cells, Lane 8- C/EBPβ and PRDM16 cotransfected cells treated with forskolin.

5.3.4 Effect of C/EBPβ and PPARγ co-overexpression on PGC1α promoter and UCP1 promoter in 3T3-L1.

It is widely accepted that PGC1α is essential for brown adipocyte differentiation and induction of the UCP1 gene, as the ectopic expression of PGC1α in white adipocytes induces expression of a number of mitochondrial and thermogenic genes including UCP1 (Puigserver et al., 1998; Tiraby et al., 2003). However, the above data suggests that C/EBPβ increased UCP1 promoter activity independent of activating PGC1α transcription (Figure 5.6) despite the results of previous literature (Kajimura et al., 2009; Karamanlidis et al., 2007). A possible model for explaining these inconsistent results is that C/EBPβ indirectly regulates PGC1α expression to increase UCP1 expression, through interaction with other regulators that were not optimised. Since PPARγ is a critical transcription factor necessary to activate both the PGC1α and UCP1 promoters (Hondares et al., 2006), it was the first candidate to examine the effect of co-overexpression with C/EBPβ, on the transcriptional activity of 3.1kb UCP1 promoter and 2.6kb PGC1α promoter. Although the overexpression of C/EBPβ on its own increased ($P<0.001$) transcription activity of 3.1kb UCP1 promoter in the absence and presence of forskolin (Figure 5.6A), the addition of rosiglitazone did not further stimulate the transcription activity (Figure 5.7A). In contrast, PPARγ overexpression alone failed to activate the 3.1kb UCP1 promoter even with forskolin and rosiglitazone. When C/EBPβ and PPARγ were co-transfected together, there was a significant ($P<0.05$) stimulation of the 3.1kb UCP1 promoter activity in the presence of both forskolin and rosiglitazone (Figure 5.7A), even though there was no further response, compared with C/EBPβ overexpression alone, in the absence or presence of forskolin only. When the transcriptional activity of the 2.6kb PGC1α promoter in response to the same treatments was assessed, there was no effect of overexpression of either C/EBPβ or PPARγ alone, or with rosiglitazone treatment but co-overexpression of the two genes significantly stimulated ($P<0.05$) the 2.6kb PGC1α promoter activity and the treatment of rosiglitazone further enhanced ($P<0.01$) this stimulating effect (Figure 5.7B). There was significant interaction between C/EBPβ and PPARγ ($P=0.001$).

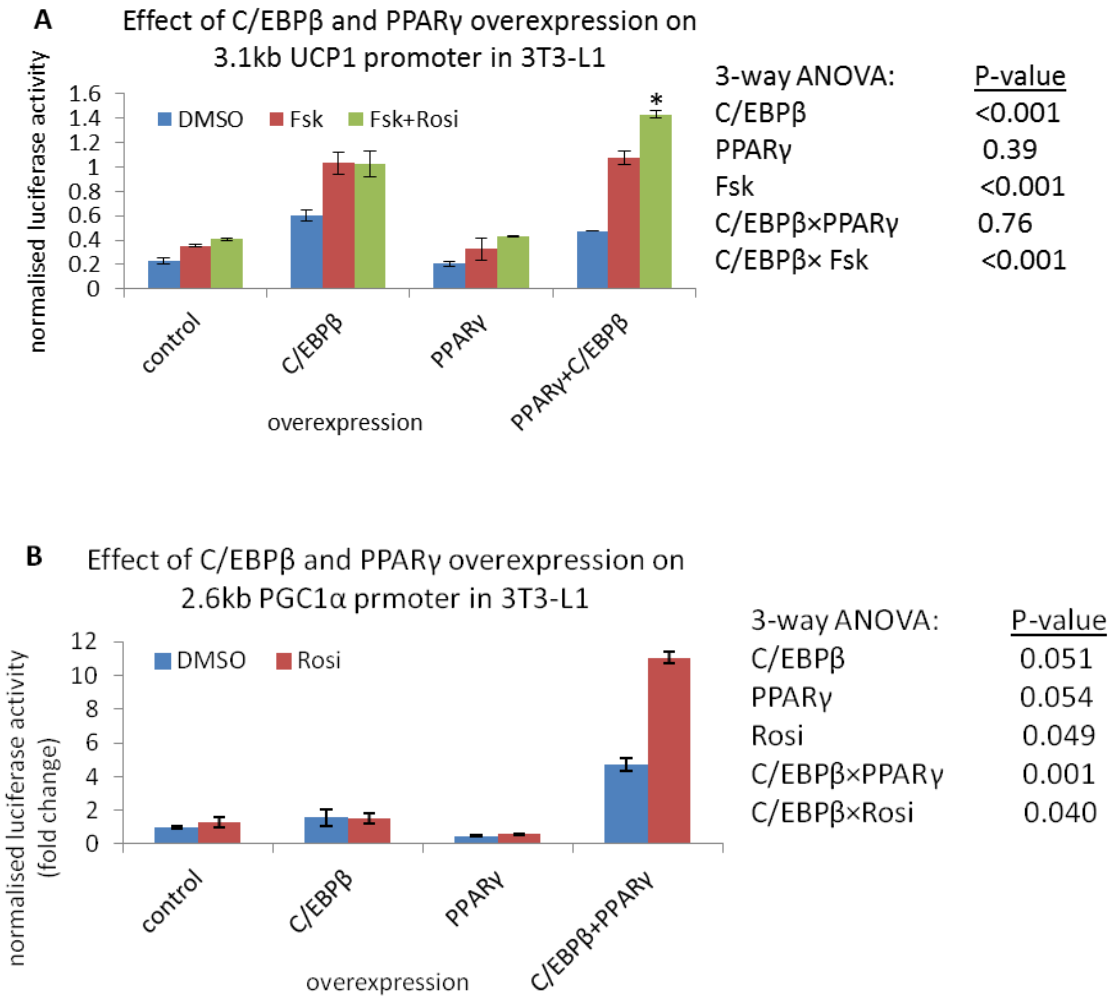

Figure 5.7 Effect of overexpression of C/EBPβ and PPARγ on 3.1kb UCP1 promoter and 2.6kb PGC1α promoter activity in 3T3-L1

3T3-L1 preadipocytes were grown to 70-80% confluence and then transfected with 3.1UCP1 pGL3-Luc (A) or 2.6PGC1α pGL3-Luc (B) in the presence of C/EBPβ and/or PPARγ overexpression as indicated in the graphs. 10μM rosiglitazone (Rosi) was given to the cells 24 hours post transfection while 10μM Forskolin (Fsk) was added into the cells 36 hours post transfection as indicated. Luciferase assay was carried out 48 hours post transfection. Firefly luciferase activity was normalised to renilla luciferase activity. Results are mean ± S.E.M. of 2 or 3 independent replicate experiments performed in triplicate wells. Data was analysed by three-way ANOVA. P values of vector-drug interactions are not indicated if not significant. (A) *P<0.05 by Student's *t*-test compared to the cells overexpressing the same vector(s) but treated with Fsk only.

To confirm the results from reporter assay above, 3T3-L1 preadipocytes were transfected with C/EBPβ or/and PPARγ expression vector as described in 2.3.2, and the mRNA level of UCP1 and PGC1α was determined by quantitative real-time PCR (Figure 5.8). Data was analysed by three-way ANOVA. The overexpression of C/EBPβ and PPARγ was successful, demonstrated by increased mRNA levels (Figure 5.7A&B). Interestingly, significant C/EBPβ×PPARγ×FskRosi interaction was observed when checking either C/EBPβ (P=0.026) or PPARγ (P=0.002) expression. However, the expression of UCP1 or PGC1α was not significantly increased, even after Fsk+Rosi treatment (Figure 5.7C&D), although significant C/EBPβ×PPARγ interaction (P<0.001) was observed when checking PGC1α expression. The PCR products of UCP1 and PGC1α were run on a 2% agarose gel, there were no clear bands at the expected size, similar to Figure 5.6E (data not shown), indicating the expression of UCP1 and PGC1α was still too low to pick up, so the real time PCR data in Figure 5.8 C&D was not reliable.

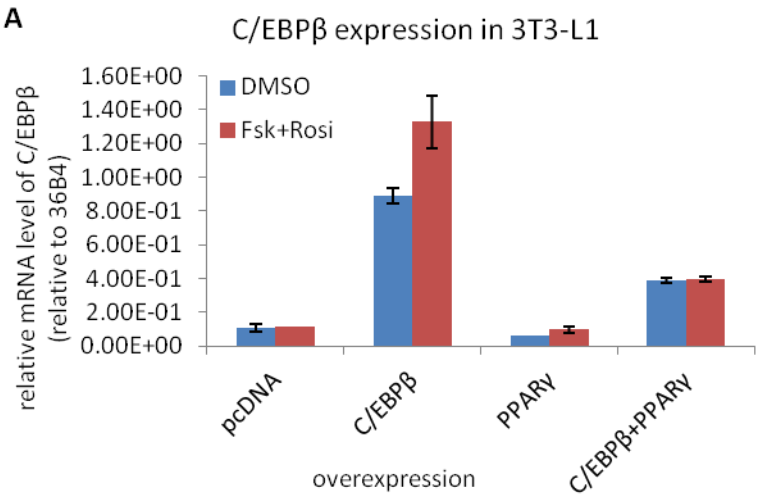

B

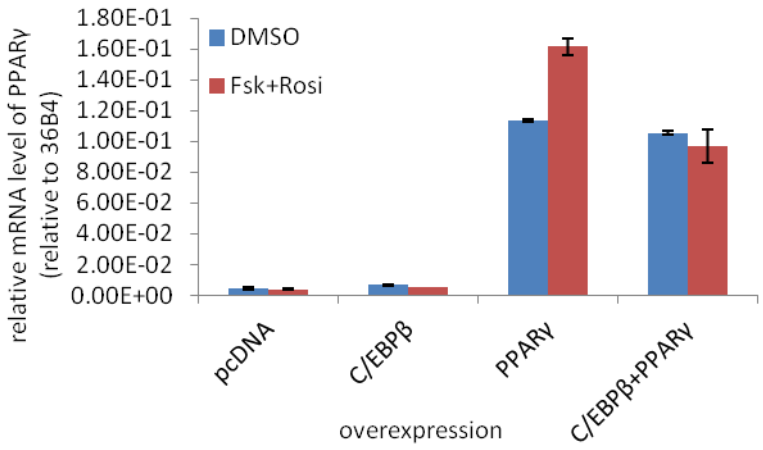
PPARγ expression in 3T3-L1
relative mRNA level of PPARγ (relative to 36B4)
1.80E-01
1.60E-01
1.40E-01
1.20E-01
1.00E-01
8.00E-02
6.00E-02
4.00E-02
2.00E-02
0.00E+00
DMSO
Fsk+Rosi
pcDNA
C/EBPβ
PPARγ
C/EBPβ+PPARγ
overexpression

C

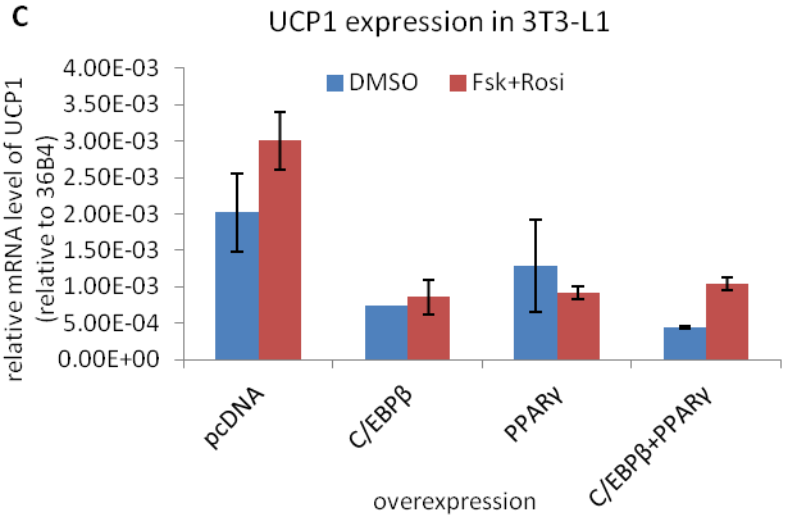
UCP1 expression in 3T3-L1
relative mRNA level of UCP1 (relative to 36B4)
4.00E-03
3.50E-03
3.00E-03
2.50E-03
2.00E-03
1.50E-03
1.00E-03
5.00E-04
0.00E+00
DMSO
Fsk+Rosi
pcDNA
C/EBPβ
PPARγ
C/EBPβ+PPARγ
overexpression

D

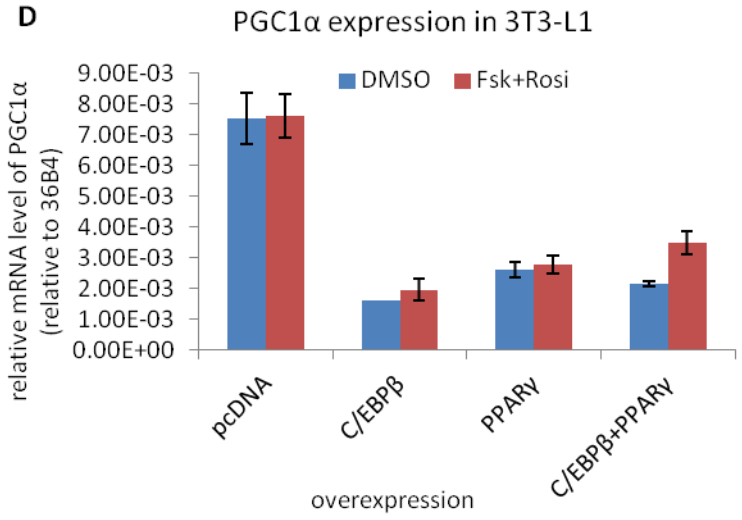
PGC1α expression in 3T3-L1
relative mRNA level of PGC1α (relative to 36B4)
9.00E-03
8.00E-03
7.00E-03
6.00E-03
5.00E-03
4.00E-03
3.00E-03
2.00E-03
1.00E-03
0.00E+00
DMSO
Fsk+Rosi
pcDNA
C/EBPβ
PPARγ
C/EBPβ+PPARγ
overexpression

Figure 5.8 The expression level of UCP1 and PGC1α was not changed by overexpression of C/EBPβ or/and PPARγ in 3T3-L1 preadipocytes.

3T3-L1 preadipocytes were grown to 70-80% confluence in 6-well plates and then transfected with expression vector of C/EBPβ or/and PRDM16 (or just pcDNA as mock) by Fugene HD as described in 2.3.2. 24 hours post transfection, 10μM rosiglitazone (Rosi) was added into the cells and treated for 24 hours and 10μM forskolin (Fsk) was also added into the cell culture as indicated and 3 hours before the cells were lysed for RNA extraction. The mRNA level of C/EBPβ (A), PPARγ (B), UCP1 (C) and PGC1α (D) was determined by quantitative real-time PCR and normalised against 36B4 house-keeping gene expression. Results represent mean ± SD from one of the duplicate experiments performed in triplicate wells. Data was analysed by three-way ANOVA: (A) P=0.026 for C/EBPβ×PPARγ×FskRosi; (B) P=0.002 for C/EBPβ×PPARγ×FskRosi; (C) P>0.05 for all variables and interactions; (D) P<0.001 for C/EBPβ×PPARγ.

5.3.5 Different responses of C/EBPβ and PPARγ co-overexpression on PGC1α promoter in different cell lines (3T3-L1, HIB-1B, Cos7).

The present study (Figures 5.5B and 5.7B) failed to confirm a previous study which demonstrated that C/EBPβ overexpression in 3T3-L1 preadipocytes increases the transcription activity of the proximal promoter of PGC1α in response to cAMP (Karamanlidis et al., 2007). However, the previous study used a proximal 264bp PGC1α reporter construct, compared to the full length 2.6kb PGC1α promoter employed in the present study. A previous study (Kajimura et al., 2009) suggested that C/EBPβ and PRDM16 could form an activating complex to stimulate PGC1α transcription in brown preadipocytes but co-overexpression with C/EBPβ and PRDM16 also failed stimulate PGC1α transcription in 3T3-L1 cells in present work (Figure 5.5B). Surprisingly, the co-overexpression of C/EBPβ and PPARγ in 3T3-L1 cells significantly increased the transcriptional activity of 2.6kb PGC1α promoter in the absence or presence of rosiglitazone (Figure 5.7B). These results suggest that 3T3-L1 may lack PPARγ, or contain repressive factors which inhibit C/EBPβ from activating PGC1α transcription, which is removed by co-overexpression with PPARγ. To test these hypotheses, C/EBPβ was overexpressed with or without PPARγ into two

different cell lines, HIB-1B and Cos7. The transfected cells were also treated with 10μM rosiglitazone for 24 hours before they were used for luciferase assay and the luciferase activity data was compared with that obtained from 3T3-L1 cells (Figure 5.9). Four-way ANOVA on the data suggested that all the three cell types responded to rosiglitazone ($P<0.001$), especially when C/EBPβ was overexpressed. There is a cell type× C/EBPβ× PPARγ interaction ($P=0.002$), but all three cell types showed similar responses to C/EBPβ and/ or PPARγ overexpression and rosiglitazone treatment, although the magnitude varied. Hence C/EBPβ and PPARγ were synergistic in increasing 2.6kb PGC1α promoter activity in all the three cell types and this stimulatory effect was enhanced by the addition of rosiglitazone. However, the various magnitude of the stimulatory effect of C/EBPβ overexpression alone might reflect different PPARγ expression backgrounds in different cell types.

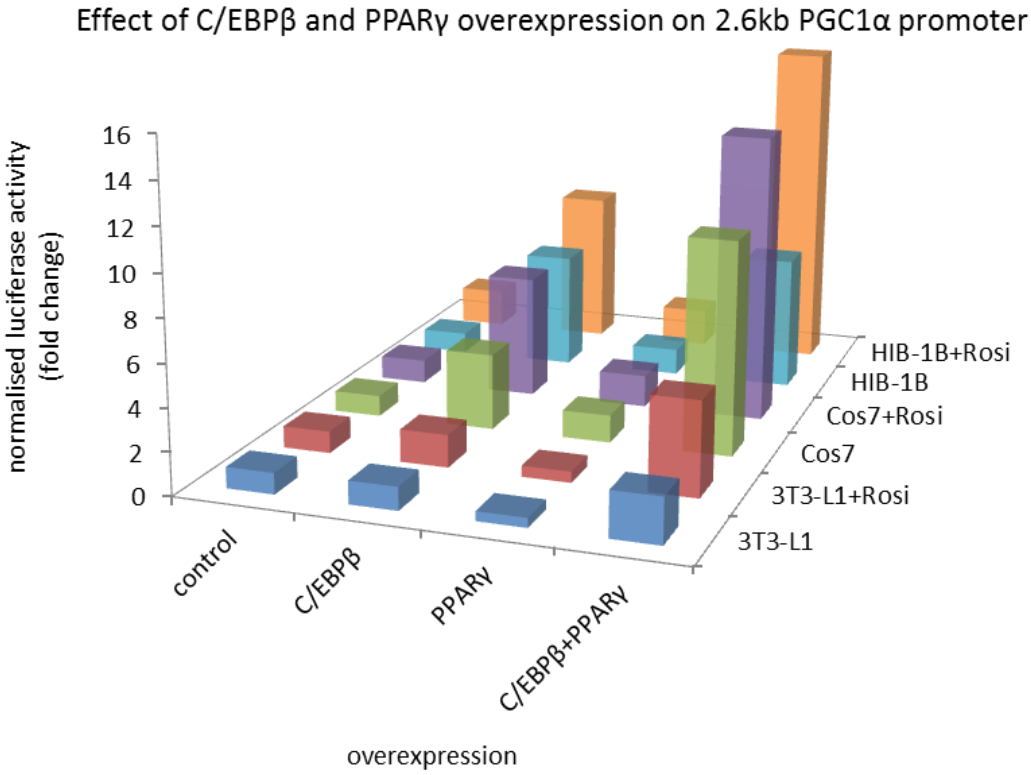

4-way ANOVA			
	P value		P value
Cell Type	<0.001		
C/EBPβ	<0.001	Cell Type×C/EBPβ	<0.001
PPARγ	<0.001	Cell Type×PPARγ	<0.001
Rosi	<0.001	Cell Type×Rosi	0.15
C/EBPβ×PPARγ	<0.001	Cell Type×C/EBPβ×PPARγ	0.002
C/EBPβ×Rosi	<0.001	Cell Type×C/EBPβ×Rosi	0.519

Figure 5.9 Effect of C/EBPβ and PPARγ overexpression on 2.6kb PGC1α promoter.

3T3-L1 preadipocytes, Cos7 kidney fibroblasts and HIB-1B preadipocytes were grown to 70-80% confluence and then transfected with 2.6PGC1α pGL3-Luc vector in the presence of C/EBPβ and/or PPARγ overexpression as indicated in the graphs. 10μM rosiglitazone (Rosi) was given to the cells 24 hours post transfection and treated for 24 hours before luciferase assay was carried out. Firefly luciferase activity was normalised to renilla luciferase activity and relative to the values from control cells without rosiglitazone treatment. Results are average values of 2 or 3 independent replicate experiments performed in triplicate wells. Data was analysed by 4-way ANOVA. The interactions that are not listed in figure were insignificant ($P>0.05$).

5.3.6 Effects of C/EBPβ co-overexpressed with PRDM16 or PPARγ on pGL3-PPRE-TK and pGL3-CRE reporter vectors in 3T3-L1 in response to rosiglitazone and forskolin, respectively.

It is well described that full length UCP1 and PGC1α promoter both contain PPRE and several CRE response elements, which allow them to bind different transcription factors such as PPARγ and C/EBPβ (Cannon and Nedergaard, 2004; Karamanlidis et al., 2007). The results described above demonstrated that C/EBPβ increased transcription activity of 3.1kb UCP1 promoter with or without co-overexpression of PRDM16 in response to forskolin and that C/EBPβ up-regulated 2.6kb PGC1α promoter activity when co-overexpressed with PPARγ. To investigate whether the stimulating effects of C/EBPβ were due to the interactions between C/EBPβ and the corresponding *cis* elements (PPRE or CRE) on the UCP1 and PGC1α promoters, artificial luciferase reporter vectors driven either by repeated CRE (pGL3-CRE) or PPRE-TK (pGL3-PPRE-TK) was co-transfected with C/EBPβ, PRDM16 or/and PPARγ into 3T3-L1 cells and treated with 10μM forskolin or/and 10μM Rosiglitazone. Data was analysed by three-way ANOVA. Results from the luciferase assays (Figure 5.10) demonstrate that the pGL3-CRE reporter vector was highly induced by forskolin ($P<0.001$), but that overexpression with C/EBPβ, PRDM16, PPARγ or the combined overexpression were

unable to further alter the cAMP sensitivity of pGL3-CRE reporter vector. Rosiglitazone also elicited no further stimulating effect on CRE when combined with forskolin (Figure 5.10A). Three-way ANOVA indicated that there were significant interactions (P≤0.001) between overexpression (vector) and drug treatments (Rosi or Fsk+Rosi) in stimulating pGL3-PPRE-TK reporter vector (Figure 5.10B). This reporter vector had no response to addition of rosiglitazone but combined addition of rosiglitazone and forskolin stimulated transcription. Overexpression with C/EBPβ or PPARγ, but not PRDM16, also increased transcription from the pGL3-PPRE-TK reporter, with these effects being increased by addition of rosiglitazone and further increased by combined addition of rosiglitazone and forskolin. The greatest response of the pGL3-PPRE-TK vector was observed in response to the combined overexpression with C/EBPβ and PPARγ in the presence of rosiglitazone and forskolin (Figure 5.10B). These results were consistent with the findings from cells transfected with 2.6PGC1α pGL3-Luc vector and C/EBPβ or/and PPARγ (Figure 5.7B) except that in the presence of rosiglitazone, C/EBPβ and PPARγ overexpression on their own were able to up-regulate the pGL3-PPRE-TK activity and an additive effect was observed when both genes co-overexpressed (Figure 5.10B).

The results from the pGL3-PPRE-TK luciferase reporter experiments suggest that the stimulatory effect of C/EBPβ and PPARγ overexpression on transcription from the 2.6kb PGC1α promoter might be due to the interaction with the PPRE located in the promoter. However, the results in Figure 5.10A seemed not to support the hypothesis that C/EBPβ and PRDM16 stimulated UCP1 promoter activity through interaction with CRE, since pGL3-CRE had no response to C/EBPβ or/and PRDM16 overexpression.

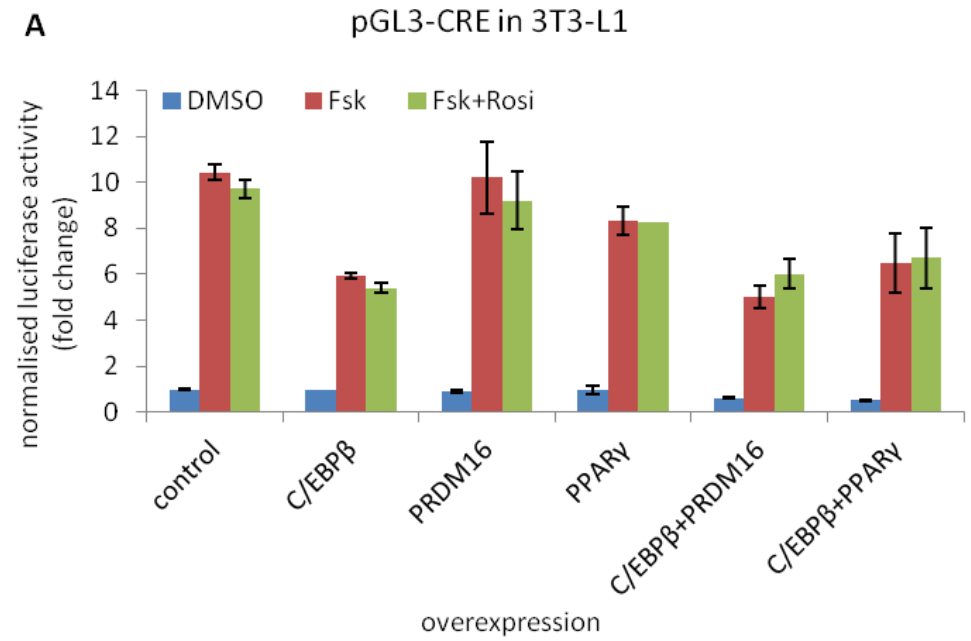
A
pGL3-CRE in 3T3-L1
DMSO
Fsk
Fsk+Rosi
normalised luciferase activity (fold change)
14
12
10
8
6
4
2
0
control
C/EBPβ
PRDM16
PPARγ
C/EBPβ+PRDM16
C/EBPβ+PPARγ
overexpression

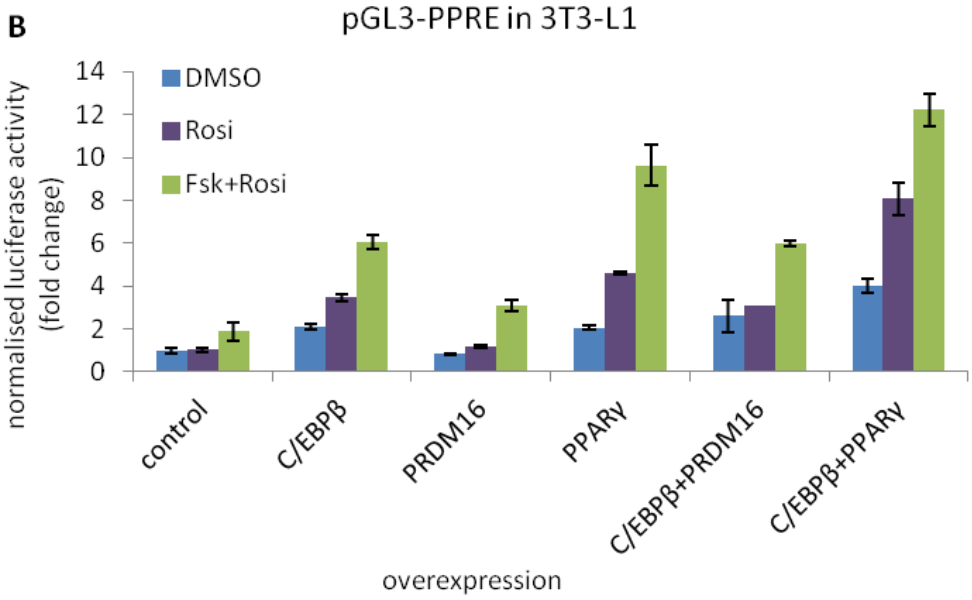
B
pGL3-PPRE in 3T3-L1
DMSO
Rosi
Fsk+Rosi
normalised luciferase activity (fold change)
14
12
10
8
6
4
2
0
control
C/EBPβ
PRDM16
PPARγ
C/EBPβ+PRDM16
C/EBPβ+PPARγ
overexpression

Figure 5.10 The effect of C/EBPβ overexpression on CRE and PPRE elements in 3T3-L1 preadipocytes.

(A) 3T3-L1 preaidpocytes were grown to 70-80% confluence when transfected with pGL3-CRE vector in the presence of overexpression of C/EBPβ, PRDM16 or/and PPARγ. Cells were treated with 10μM forskolin (Fsk) for 12 hours or the combination of 10μM rosiglitazone (Rosi) and 10μM Fsk as indicated before luciferase assay was carried out 48 hours post transfection. (B) 3T3-L1 preadipocytes were transfected with pGL3-PPRE-TK reporter vector together with the overexpression of C/EBPβ, PRDM16 or/and PPARγ. Cells were treated with 10μM Rosi or the combination of 10μM Rosi and 10μM Fsk before measuring the luciferase activity 48 hours post transfection. Firefly luciferase activity was normalised to the renilla luciferase activity and relative to the values from cells transfected with only reporter vector and treated with DMSO. Results represent mean ± S.E.M. of independent duplicate experiments performed in triplicate wells. Data was analysed by three-way ANOVA: (A) $P>0.05$ for vector×Fsk and vector×FskRosi, $P= 0.062$ for vector, $P<0.001$ for Fsk and FskRosi; (B) $P\leq0.001$ for vector×Rosi and vector×FskRosi.

To further investigate whether the stimulatory effect of C/EBPβ-PPARγ co-overexpression on 2.6kb PGC1α promoter was through the CRE or PPRE *cis* elements on the promoter, the mutated 2.6PGC1α pGL3-Luc reporter vectors (ΔCRE or ΔPPRE, Figure 5.11A) were transfected into 3T3-L1 preadipocytes with co-overexpression of C/EBPβ and PPARγ as described in 2.3.2. 10μM rosiglitazone was added to the cells and treated for 24 hours respectively before the cells were collected for luciferase assay (Figure 5.11B). Three-way ANOVA indicated that the synergistic stimulatory effect of PPARγ co-overexpression and Rosi treatment on the 2.6kb PGC1α promoter was significantly affected ($P=0.040$) when the CRE or PPRE was mutated in the promoter. Consistent with the data shown in Figure 5.7B, co-overexpression of C/EBPβ and PPARγ significantly increased the 2.6kb PGC1α promoter (blue bars) activity in 3T3-L1 cells compared with that in the cells overexpressing C/EBPβ alone and rosiglitazone treatment further increased this stimulating effect. The mutation in

CRE (red bars) markedly attenuated the stimulating effect of C/EBPβ-PPARγ co-overexpression on the 2.6kb PGC1α promoter and rosiglitazone treatment could not rescue the attenuation. The mutation in PPRE (green bars) also reduced the stimulating effect of the co-overexpression even further and completely blocked the response to rosiglitazone, resulting in a remarkable decrease in luciferase activity compared to that in the cells overexpressing both C/EBPβ and PPARγ and treated with rosiglitazone. These data suggested that both CRE and PPRE were indispensable for C/EBPβ and PPARγ co-overexpression to maximally stimulate 2.6kb PGC1α promoter activity in response to rosiglitazone in 3T3-L1 preadipocytes.

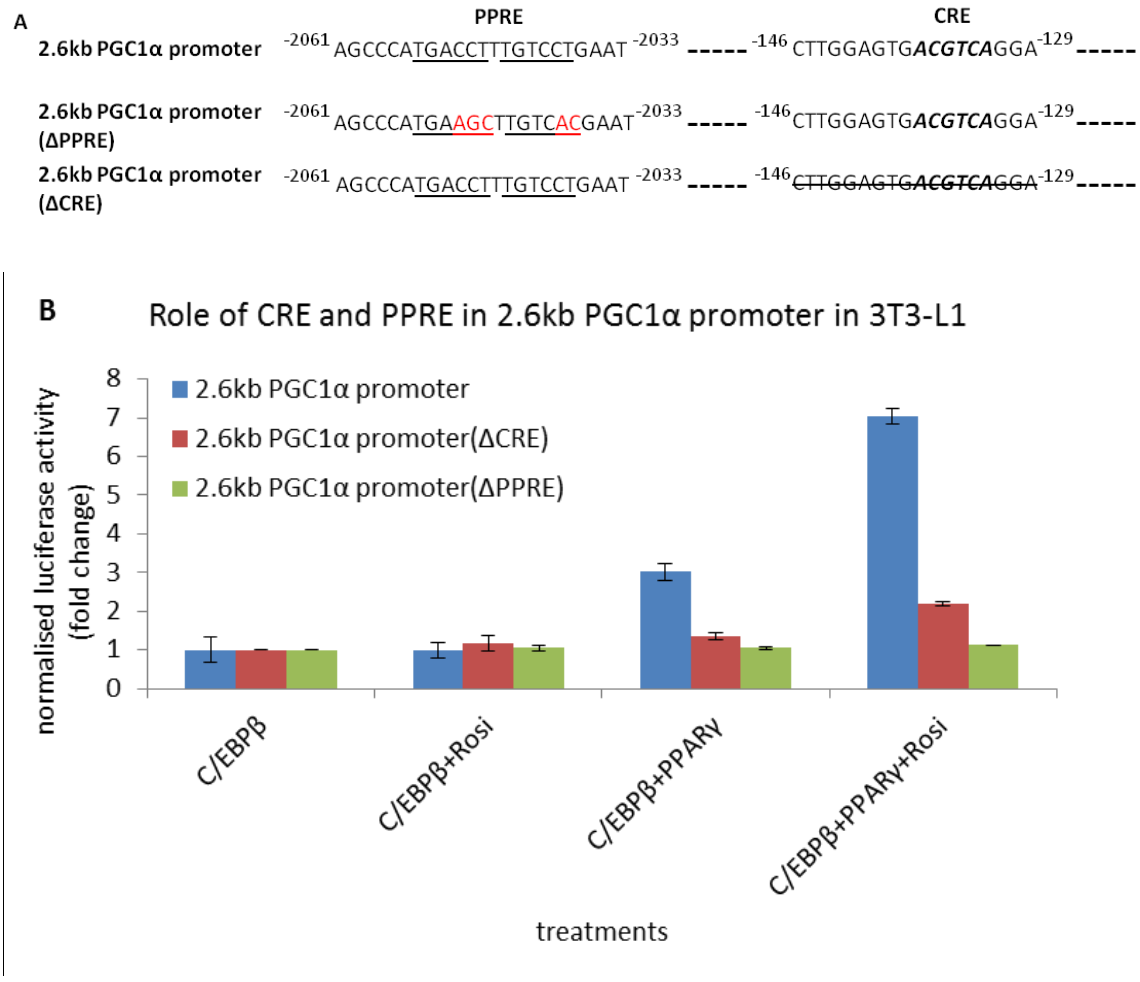

Figure 5.11 C/EBPβ and PPARγ co-overexpression increased 2.6kb PGC1α promoter activity via CRE and PPRE elements on the promoter.

(A) Sequences of PPRE and CRE in the original and mutated (ΔCRE or ΔPPRE) 2.6PGC1α pGL3-Luc vectors. The underlined sequences are the two close PPREs in (-2033/-2061) region and the mutations are in red. The bold italic sequence is the CRE in (-129/-146) region and this whole region was deleted in ΔCRE vector. (B) 3T3-L1 preadipocytes were grown to 70-80% confluence and then transfected with the original or the CRE or PPRE mutated 2.6PGC1α pGL3-Luc vector in the presence of C/EBPβ and/or PPARγ overexpression as indicated in the graphs. 10μM rosiglitazone (Rosi) was given to the cells 24 hours post transfection and treated for 24 hours before luciferase assay was carried out. Firefly luciferase activity was normalised to renilla luciferase activity and relative to the values from cells overexpressing C/EBPβ alone without rosiglitazone treatment. Results are mean ± S.E.M. of 2 or 3 independent replicate experiments performed in triplicate wells. Data was analysed by three-way ANOVA: P=0.040 for Rosi×PPARγ×promoter.

5.4 DISCUSSION

According to Kajimura et al, C/EBPβ and PRDM16 form a complex which switches myoblastic progenitors towards the brown adipogenic lineage by stimulating the transcription of a series of brown adipogenic genes. They also demonstrated that the co-overexpression of C/EBPβ and PRDM16 increases PGC1α promoter activity in murine immortalized brown preadipocyte cell line (Kajimura et al., 2009). However, in the present study, when C/EBPβ and PRDM16 were co-overexpressed in 3T3-L1 preadipocytes, they were not able to significantly stimulate the full length PGC1α promoter (Figure 5.5B) although the co-overexpression successfully activated transcription from the 3.1kb UCP1 promoter (Figure 5.5A). The different result on PGC1α promoter from Kajimura's work might have reflected the intrinsic difference between the brown and white preadipocytes, indicating there might be some repressive factors in the 3T3-L1 white preadipocytes inhibiting the formation of C/EBPβ-PRDM16 complex or the interaction between the complex and the PGC1α promoter. In fact, some (co)repressors, such as RIP140 and pRb, are more abundant in white than in brown preadipocytes, and could potentially inhibit the activation of PGC1α transcription or its activity in co-activating PPARγ (Cavailles et al., 1995; Hallberg et al., 2008; Leonardsson et al., 2004; Scime et al., 2005). The promoters of brown fat-selective genes might also be more repressively modified by chromatin remodelling in white compared with brown (pre)adipocytes. Studies by Shore and colleagues demonstrated that one of the essential CREs in the enhancer of the UCP1 promoter contains a CpG dinucleotide which has a higher methylation state in differentiated 3T3-L1 cells compared to HIB-1B cells. This study also revealed that a cold environment increases the association of silencing DiMethH3K9 histone modification on the UCP1 enhancer in white adipose tissue, and the appearance of the active TriMethH3K4 histone mark at the UCP1 promoter in brown adipose tissue (Shore et al., 2010). Since the pGL3-CRE reporter vector is induced to the same extent by forskolin administration in 3T3-L1 and HIB-1B cells (Karamanlidis et al., 2007), the CREs themselves do not discriminate between the different cell types in cAMP sensitivity. It is more probable that the lower sensitivity to noradrenaline in 3T3-L1 cells results from the more repressive pattern of chromatin remodelling on the promoters of specific thermogenic genes.

Despite the lack of activation in PGC1α transcription, co-overexpression of C/EBPβ and PRDM16 still increased the transcriptional activity of UCP1 promoter (Figure 5.5A), implying a PGC1α-independent pathway of activating UCP1 transcription, which has not been reported in literature to date. C/EBPβ overexpression alone stimulated the 3.1kb UCP1 promoter activity in response to forskolin (Figure 5.5A), but when rosiglitazone was added to the system, there was no further activation in UCP1 transcription (Figure 5.7A), indicating UCP1 expression was regulated by C/EBPβ through a cAMP-PKA pathway and not a PPARγ mediated pathway. The results were predictable as C/EBPβ has been reported to bind to the CRE on the proximal PGC1α promoter to facilitate PGC1α transcription in 3T3-L1 cells (Karamanlidis et al., 2007) and the UCP1 promoter has four characterised CREs (Cannon and Nedergaard, 2004) which could possibly bind C/EBPβ and activate UCP1 transcription through a similar mechanism. However, C/EBPβ overexpression with or without PRDM16 failed to increase the activity of the artificial promoter vector pGL3-CRE in the presence or absence of forskolin (Figure 5.10A), which contradicts this speculation. It is possible that the pGL3-CRE was so sensitive to cAMP that forskolin treatment alone was able to maximally stimulate transcription from the pGL3-CRE so that no other factors could increase it any further. It would be more helpful if the 3.1kb UCP1 promoter with mutated CRE luciferase reporter vector were constructed so that it could be confirmed if CRE was indispensible for C/EBPβ binding to activate the UCP1 promoter activity. On the other hand, given that C/EBPβ overexpression alone increased pGL3-PPRE-TK activity (Figure 5.10B), it was tempting to speculate that the stimulating effect of C/EBPβ on UCP1 promoter was through the PPRE element, but this cannot explain the synergistic effect of C/EBPβ and PRDM16 in stimulating UCP1 promoter, as the co-overexpression failed to synergistically increase pGL3-PPRE-TK activity in 3T3-L1 cells. The UCP1 promoter also contains a CCAAT box which can be transactivated by C/EBPβ (Cannon and Nedergaard, 2004; Yoshitomi et al., 1999) so it is possible that there are other sites on UCP1 promoter where C/EBPβ or/and PRDM16 bind and activate the transcription of UCP1, but more investigation such as chromatin immunoprecipitation (ChIP) assays need to be performed on the UCP1 promoter in 3T3-L1 cells to test the possibility.

The work on pGL3-PPRE-TK vector also demonstrated clearly that the PPRE element responds not only to the PPARγ ligand rosiglitazone but also to cAMP induced by forskolin treatment (Figure 5.10B), implying cross-talk between the cAMP-PKA and PPARγ ligand mediated signalling pathways in regulating UCP1 and PGC1α transcription. Although noradrenaline has been reported to decrease PPARγ2 expression in brown adipocytes (Lindgren et al., 2004), the basal adrenergic tone has been found necessary for maximal stimulation of rat BAT UCP1 expression by chronic PPARγ activation (Festuccia et al., 2010). These findings were supported by the observation that UCP1 mRNA level was up-regulated by both acute forskolin and chronic rosiglitazone treatments in differentiated 3T3-L1 adipocytes (Figure 5.1A).

Surprisingly, C/EBPβ overexpression alone in 3T3-L1 preadipocytes did not increase PGC1α transcription even with forskolin treatment, either by reporter assay (Figure 5.7B) or mRNA measurement (Figure 5.8D), contradicting the work of Karamanlidis et al who demonstrated that C/EBPβ overexpression increases proximal (264bp) PGC1α promoter activity as well as its sensitivity to cAMP, and up-regulates PGC1α mRNA level in response to forskolin in confluent 3T3-L1 preadipocytes (Karamanlidis et al., 2007). Work from Wang and colleagues also identified C/EBPβ as a direct transcriptional activator of PGC1α in liver by binding to C/EBP and CRE sites in the PGC1α promoter (Wang et al., 2008a). It is difficult to explain the completely different results, as all the methods involved in this experimental work, such as transfection, luciferase assay, RNA extraction and real time PCR were identical with those used in the literature and the materials such as cells, plasmids and drugs were also the same as the ones used in Karamanlidi's work. However, it was also possible that there might be some unnoticed minor operating details that have led to the final difference.

When C/EBPβ was overexpressed in HIB-1B or Cos7 cells, it increased the transcriptional activity of 2.6kb PGC1α promoter, either with or without rosiglitazone (Figure 5.9). The different results from that in 3T3-L1 cells might indicate that there were some specific repressive factors in 3T3-L1 cells that prevented C/EBPβ from activating the PGC1α promoter, or that there were some extra activating factors (such as more PPARγ expression) in HIB-1B and Cos7 cells that facilitated C/EBPβ to stimulate the transcriptional activity of PGC1α. As Cos7 is an African Green Monkey

kidney fibroblast-like cell line which highly resembles fibroblasts in humans (Gluzman, 1981), it has no potential of adipocyte lineage and is often considered having simple cellular context which facilitates investigation of the regulation of gene expression (Kajimura et al., 2008; Shipley and Waxman, 2004; Steffensen et al., 2002). Therefore it is less likely that Cos 7 cells contain factors favouring the expression of the brown adipogenic gene PGC1α, as might be expected in HIB-1B preadipocytes. The failure of C/EBPβ overexpression alone in activating PGC1α promoter in 3T3-L1 preadipoyctes was possibly because of some specific repressors or repressive chromatin modifications in 3T3-L1 that inhibited the proposed activation of C/EBPβ on PGC1α promoter.

The transcriptional activity of the PGC1α promoter was significantly increased in 3T3-L1 cells when PPARγ was co-overexpressed with C/EBPβ, suggesting that a lack of PPARγ may limit the response to C/EBPβ or that PPARγ was able to remove or overcome the repression caused by unknown factor(s) (Figure 5.7B, Figure 5.9). The first proposal is supported by the observation that the expression level of PPARγ is higher in HIB-1B than in 3T3-L1 (pre)adipocytes (Petrovic et al., 2009). Interestingly, the pGL3-PPRE-TK vector was not sensitive to rosiglitazone treatment (Figure 5.10B) in 3T3-L1 preadipocytes but rosiglitazone treatment stimulated transcription of this vector in HIB-1B cells (unpublished data from H.Y. Chen in our lab). Overexpression of C/EBPβ or PPARγ clearly increased transcription from the pGL3-PPRE-TK vector in 3T3-L1 cells in response to rosiglitazone (Figure 5.10B), which emphasized again the importance of PPARγ in releasing the repressive state of thermogenic gene promoters in 3T3-L1 preadipocytes. The largest transcriptional activity from the pGL3-PPRE-TK vector in 3T3-L1 cells was when C/EBPβ and PPARγ were co-overexpressed, in the presence of both rosiglitazone and forskolin, emphasising the importance of transactivation of the PPRE by combined activation of the PPAR-ligand and cAMP-PKA signalling pathways. Interestingly, in all the three cell types, PPARγ overexpression alone was not able to up-regulate the PGC1α promoter activity, even in the presence of rosiglitazone, indicating that C/EBPβ was indispensible in activating PGC1α and UCP1 promoters.

Given that the mutation of either CRE or PPRE elements in 2.6kb PGC1α promoter significantly dampened the stimulating effect of C/EBPβ-PPARγ co-overexpression in response to rosiglitazone (Figure 5.11), both CRE and PPRE were indispensable in the stimulating mechanism. It is understandable that PPRE is important as it is the site that PPARγ directly binds to (Hondares et al., 2006), and it is consistent with the results from pGL3-PPRE-TK reporter assay that C/EBPβ and PPARγ had a synergistic effect in up-regulating the luciferase activity in response to rosiglitazone (Figure 5.10B). However, according to the results from pGL3-CRE reporter assay (Figure 5.10A), C/EBPβ overexpression, either alone or with PPARγ, failed to increase luciferase activity in the presence of forskolin and rosiglitazone, suggesting that C/EBPβ or PPARγ do not require the CRE to activate the transcription, contradicting the conclusions from Karamanlidis and colleagues (Karamanlidis et al., 2007). It is possible that the full length (2.6kb) promoter might act differently to the proximal (264bp) promoter of PGC1α which was investigated in Karamanlidi's work. Further studies using ChIP and Electrophoretic Mobility Shift Assay (EMSA) are needed to investigate where the interaction between the full length PGC1α promoter and C/EBPβ/ PPARγ is localized.

The level of C/EBPβ mRNA in differentiated 3T3-L1 adipocytes was significantly higher than in the preadipocytes at confluence, was further increased by forskolin treatment, but had no response to rosiglitazone (Figure 5.1C). This suggests that although in undifferentiated 3T3-L1 preadipocytes C/EBPβ expression was not sensitive to forskolin (Figure 5.6A), in differentiated cells, C/EBPβ transcription is regulated through cAMP-PKA pathway. The influence of adipogenic induction and forskolin treatment on C/EBPβ mRNA in 3T3-L1 cells has been previously measured (Lane et al., 1999), and the results demonstrated that C/EBPβ expression is insensitive to cAMP in preadipocytes (Karamanlidis et al., 2007) but sensitively up-regulated by the differentiation inducers, of which IBMX has been shown to induce C/EBPβ expression through cAMP activation (Tae et al., 1995). This high level expression of C/EBPβ gradually disappeared afterwards when the inducers are removed from the medium (Lane et al., 1999). The experimental data in this chapter also agreed with the above literature (Figure 5.4A). *In vivo* experiments demonstrated that C/EBPβ is inducible by

cold stress or β-adrenergic administration in mouse interscapular white adipose tissue (iWAT) (Karamitri et al., 2009). Although C/EBPβ could not be stimulated by the cAMP stimulus, forskolin, in confluent 3T3-L1 white preadipocytes in both this thesis (Figure 5.6A and 5.8A) and previous literature (Karamanlidis et al., 2007), the forskolin treatment in fully differentiated 3T3-L1 adipocytes significantly increased C/EBPβ expression (Figure 5.1A), consistent with the *in vivo* results from Karamitri (Karamitri et al., 2009). To investigate when and how the C/EBPβ gene becomes cAMP sensitive, the time course of C/EBPβ expression in response to forskolin treatment during 3T3-L1 differentiation process will be necessary for the future work.

The transcriptional activity of the 3.1kb UCP1 promoter was significantly increased by co-overexpression of C/EBPβ and PRDM16 in response to forskolin in 3T3-L1 preadipocytes (Figure 5.5A), so theoretically the same co-overexpression should be able to increase UCP1 transcripts in 3T3-L1s treated with forskolin. However, when the mRNA level of UCP1 was measured in 3T3-L1 cells where C/EBPβ and PRDM16 were co-overexpressed in the presence of forskolin, it did not show any significant increase compared with that in the mock transfected cells (Figure 5.6C) and the PCR products gave very faint bands in agarose gel electrophoresis (Figure 5.6E), indicating that the template abundance of UCP1 gene was too low to amplify in 3T3-L1 preadipocytes. Given that the co-overexpression was successful (Figure 5.6 A&B), it was confusing that UCP1 transcription was not up-regulated, which contradicted the previous work in our lab demonstrating that C/EBPβ overexpression alone increased mRNA level of UCP1 in 3T3-L1 preadipocytes in response to forskolin (Karamanlidis et al., 2007). When checking the melting curves of UCP1 amplifying in Figure 5.6C, there was a single peak in each melting curve but most of the curves indicated there was extremely low amplification in the well (data not shown). As the primer sequences and cycling parameters were exactly the same as previous work carried out by Karamanlidis and colleagues, the very low level of amplification was probably due to primer dimers from the templates. Interestingly, the melting curves of UCP1 amplifying from 3T3-L1 (pre)adipocytes without transfection (Figure 5.1A) had single peak corresponding to the expected target and the curves showed an acceptable level of amplification (data not shown), which demonstrated that the methods of RNA

extraction and cDNA synthesis used in the experimental work were not the reason for low amplification observed in the above experiments. The main difference between the experiments in Figure 5.1 and Figure 5.6 was that in the latter experiments, cells were transiently transfected, while in the former experiment cells were not transfected at all. It seems that the transfection process may have interfered with the template quality or the endogenous gene expression in the 3T3-L1 preadipocytes, which led to the low amplification during qRT-PCR for UCP1 gene. In Karamanlidis' work UCP1 was also measured in transfected 3T3-L1 cells, so in this case the different results might be due to different sensitivity of various light cyclers used in the experiments. However, more experiments are needed to confirm either of the above speculations.

RIP140 transcription was dramatically up-regulated during differentiation of 3T3-L1 adipocytes and both acute forskolin and chronic rosiglitazone treatments synergistically reduced its transcription (Figure 5.1E). Interestingly, the response pattern of RIP140 to forskolin and rosiglitazone treatments was opposite to that of UCP1 which was up-regulated by both drugs (Figure 5.1A). Given that RIP140 represses UCP1 transcription in adipocytes (Kiskinis et al., 2007), the opposite responding patterns might suggest RIP140 has multiple inhibitory roles in different signalling pathways regulating UCP1 expression. RIP140 plays essential roles in both DNA and histone methylation to maintain UCP1 gene repression (Kiskinis et al., 2007). RIP140 has also been reported to inhibit the β-adrenergic receptor mediated, cAMP dependent UCP1 gene expression, by recruiting the inhibitory transcription factor LXRα to an LXRα binding site that overlaps with the PPARγ/PGC1α response element (PPRE) on the UCP1 promoter, resulting in the dismissal of PPARγ and suppression of UCP1 transcription (Wang et al., 2008b). Interestingly, in differentiated HIB-1B cells, forskolin treatment significantly increases the binding affinity of RIP140 to UCP1 enhancer, which enhances the repressive effect (Wang et al., 2008b), but actual UCP1 transcription is still up-regulated in this circumstance (Karamitri et al., 2009). The seemingly conflicting results might reflect a likely regulatory mechanism that works through balancing the competing repressive and activating factors by reinforcing both binding affinity to the target promoter but differentially regulating the expression

abundance of different regulators, as shown in Figure 5.1E where RIP140 transcription was reduced by forskolin treatment. The speculated mechanism might play as a “brake” in regulating the robust expression of UCP1 in differentiated HIB-1B cells to restrain the expression within a reasonable range, but this speculation will need testing by more studies. RIP140 is an essential co-repressor in regulating UCP1 expression, but it has not shown any interaction with C/EBPβ either in the experimental work presented here or any previous literature.

Rosiglitazone belongs to the thiazolidinedione (TZD) class of PPARγ agonists and it binds to PPARγ with high affinity to activate the transcriptional function of the protein (Kameda et al., 2000). In the work presented in this chapter, treatment with rosiglitazone significantly decreased PPARγ mRNA level in differentiated 3T3-L1 adipocytes (Figure 5.1D). As early as 1998, this rosiglitazone dependent down-regulation of PPARγ in 3T3-L1 adipocytes was observed and reported but no clear mechanism was suggested to explain the unexpected decrease (Rosenbaum and Greenberg, 1998). In 1999, retinoic acid isomers and PPAR agonists, specific for either PPARα or PPARγ, were found to oppositely regulate each PPAR subtype. For example, PPARγ agonists up-regulated PPARα but down-regulate PPARγ expression in brown adipocytes which was argued to represent a regulatory mechanism responsible for the specific physiological roles for PPARα and PPARγ in controlling brown fat differentiation and thermogenic activity (Valmaseda et al., 1999). This down-regulation was then confirmed by Hauser and colleagues who reported that PPARγ protein levels are significantly reduced in adipocytes and fibroblasts in response to TZD ligands and further demonstrated that the degradation of PPARγ protein correlates well with the ability of ligands to activate this receptor. Although ligand binding and activation increase the transcriptional function of PPARγ, these same processes also induce ubiquitination and subsequent degradation of this receptor by the proteasome (Hauser et al., 2000). A number of later studies on adipocytes also confirmed the discovery (Petrovic et al., 2008; Petrovic et al., 2009). The rosiglitazone induced decrease in PPARγ expression was not only observed in adipocytes and fibroblasts, but also in microglia where rosiglitazone reverses 1-methyl-4-phenyl-1,2,3,6-tetrahydropyridine probenecid (MPTPp) induced PPARγ overexpression (Carta

et al., 2011). The rosiglitazone dependent down-regulation of PPARγ mRNA presented in this chapter is highly consistent with the literature listed above. However, Su and colleagues reported that in murine mesenchymal stem cell line C3H10T1/2, PPARγ expression is increased by the administration of rosiglitazone, demonstrated by Western blotting using a specific PPARγ monoclonal antibody (Su et al., 1999). It is probable that different cell lines have different responses to rosiglitazone, but this possibility needs proving by more studies across varieties of cell lines.

Chronic rosiglitazone treatment has been reported to accelerate and augment differentiation of brown adipocytes in primary culture as assessed by both cell morphology and gene expression (Petrovic et al., 2008). In this chapter, 1μM rosiglitazone treatment also seemed to accelerate the early stage of differentiation in 3T3-L1 cell, as by DAY 5 lipid droplet accumulation in rosiglitazone treated cells was greater than the control cells. However, the difference was not apparent after DAY 7 of differentiation and in the fully differentiated control cells there was more lipid accumulation than the rosiglitazone treated cells (Figure 5.3). These observations are consistent with previous literature reporting that rosiglitazone treatment in white adipocytes triggers a brown-like phenotype and decreases lipid accumulation (Petrovic et al., 2009). Although the fat-specific staining (Oil-Red-O staining) was not performed on the cells during early differentiation, time course of C/EBPβ mRNA measurement (Figure 5.4A) reflected clearly the difference of control and rosiglitazone treated differentiation processes from the perspective of gene expression. As an early gene regulating the induction of adipogenesis, C/EBPβ expression in 3T3-L1 cells increased when the preadipocytes were induced to differentiate and achieved the highest level on DAY 2 of differentiation as expected (Karamanlidis et al., 2007). Rosiglitazone treatment significantly increased C/EBPβ expression above control level from DAY 1, implying that the early differentiation process was accelerated. The difference in C/EBPβ expression achieved a maximum on DAY 2 but disappeared after DAY3. C/EBPβ is known to respond to cAMP signalling pathway (Karamanlidis et al., 2007; Staiger et al., 2009; Zhang et al., 2004b), so the early increase in expression may represent a response to IBMX which was increased by rosiglitazone.

The period when rosiglitazone significantly increased aP2 expression (DAY 2-6) roughly coincided with the period when rosiglitazone treated cells had larger amounts of lipid accumulation than the untreated cells (Figure 5.3), possibly reflecting that the addition of rosiglitazone increased the rate of differentiation in terms of lipid accumulation, but the cells rapidly regulate themselves back to normal status within two days. Surprisingly, PPARγ expression during the period of increased lipid droplet accumulation and aP2 expression was reduced by rosiglitazone, even though aP2 has been reported to be a target for PPARγ (Tontonoz et al., 1994b; Tontonoz et al., 1994c). These results could be explained by changes in PPARγ protein levels, translocation to the nucleus, and post-translational activation by phosphorylation and transactivation activity, all of which were not measured in the present study.

Similar to the expression pattern of C/EBPβ, the significantly higher expression of the adipogenic marker gene, PPARγ during DAY3 to DAY 5, in the rosiglitazone treated cells, had disappeared after DAY 6. Also consistent with pattern of PPARγ expression, the expression of aP2 was also significantly changed in the early stage of differentiation, i.e. remarkably up-regulated by rosiglitazone to its maximal expression level, by DAY 2, which was 2 days earlier than the control group. Interestingly, the rosiglitazone stimulated aP2 expression "peak" also started to decrease from DAY 6, identical with the result from control cells. While the adipogenic genes PPARγ and aP2 demonstrated similar response to rosiglitazone treatment in terms of time course, the thermogenic gene UCP1 displayed a different pattern, which showed nearly no response to rosiglitazone in the early and middle stage of rosiglitazone and only began to be up-regulated by the treatment from DAY 9, which was relatively late in the differentiation process, indicating the thermogenic programme started up late in the rosiglitazone induced 3T3-L1 differentiation.

These data were consistent with Vernochet and co-workers' work, in which "visceral white" genes are down-regulated while "brown" genes are increased in 3T3-L1 adipocytes treated with troglitazone, another TZD PPARγ ligand (Vernochet et al., 2009). All the data indicated that chronic rosiglitazone treatment of 3T3-L1 preadipocytes had multiple effects 1) to accelerate the early period of differentiation

(before DAY 5) but failed to have long-lasting effect on differentiation progress afterwards, 2) to reduce lipid accumulation in fully differentiated mature 3T3-L1 adipocytes and 3) to stimulate the thermogenic gene expression programme in differentiated 3T3-L1 adipocytes.

To summarize, the experimental work in this chapter focused on the role of C/EBPβ in regulating UCP1 transcription. Co-overexpression of C/EBPβ and PRDM16 significantly increased the transcription activity from the full length UCP1 promoter in response to forskolin without activating the full length PGC1α promoter activity in 3T3-L1 cells. C/EBPβ overexpression alone was able to up-regulate transcriptional activity of full length PGC1α promoter in HIB-1B and Cos7 but not 3T3-L1 cells, but PGC1α promoter activity in 3T3-L1 cells was markedly stimulated when C/EBPβ and PPARγ were co-overexpressed with or without rosiglitazone. However, this stimulating effect disappeared when the CRE or PPRE element was mutated in the full length PGC1α promoter. mRNA measurement of UCP1 and PGC1α failed to confirm the above data from reporter assay experiments as the UCP1 and PGC1α transcripts in transfected 3T3-L1 preadipocytes were too low to pick up by the current qPCR protocol. The artificial promoter reporter pGL3-CRE was highly sensitive to forskolin in 3T3-L1 cells, but the luciferase activity from this reporter vector could not be increased by overexpression of C/EBPβ, PRDM16, PPARγ or any combination of these genes. On the contrary, the luciferase activity of the artificial promoter reporter pGL3-PPRE-TK could be synergistically up-regulated by the overexpression of C/EBPβ and PPARγ in 3T3-L1 cells and it showed sensitivity to both forskolin and rosiglitazone. Chronic rosiglitazone treatment in the differentiating 3T3-L1 cells increased the mRNA level of C/EBPβ before DAY 3 of differentiation, increased aP2 but decreased PPARγ mRNA from DAY 2 to DAY 6, but all of the above gene expression changes in response to rosiglitazone returned to control levels (without rosiglitazone treatment) after DAY 6. In contrast, mRNA of UCP1 was not changed until DAY 9 of differentiation when it was increased by rosiglitazone treatment. Oil Red O-staining of fully differentiated 3T3-L1 adipocytes on DAY 12 demonstrated that chronic rosiglitazone treatment severely reduced the lipid in the mature white adipocytes.

In conclusion, the reporter assay experiments demonstrated that C/EBPβ and PRDM16 co-overexpression increased UCP1 promoter transactivity in a PGC1α independent manner. Some unknown repressive factors (either genes or chromatin modifications) or the lack of PPARγ expression in 3T3-L1 preadipocytes prevented C/EBPβ from activating PGC1α promoter but the repression could be removed by the co-overexpression of PPARγ. Both CRE and PPRE elements were indispensable for C/EBPβ-PPARγ co-overexpression to activate PGC1α promoter in 3T3-L1 although no direct evidence was found that C/EBPβ or PPARγ bound to CRE in response to forskolin or rosiglitazone. Rosiglitazone accelerated the early period of 3T3-L1 differentiation reflected by the up-regulation of C/EBPβ and aP2 mRNA before DAY 6 of differentiation. The decrease in PPARγ transcription in response to rosiglitazone during this same period might be because the ligand rosiglitazone increased PPARγ activity so less amount of PPARγ was needed by the cells temporarily, reflecting the negative feedback. Rosiglitazone up-regulated UCP1 mRNA in the late stage of 3T3-L1 differentiation (from DAY 9) and finally significantly decreased the lipid accumulation in the mature 3T3-L1 adipocytes, suggesting the white preadipocytes differentiated to “browner” adipocytes.

CHAPTER 6

6 GENERAL DISCUSSION

The factors controlling the transdifferentiation from white preadipocytes to brown adipocytes are one of the major focuses of current bioscience and medical research, since by understanding and controlling the signals and genes responsible for the transdifferentiation we could aid prevention and treatment of metabolic diseases such as obesity, diabetes and cardiovascular diseases. The general aim of the studies reported in this thesis was to further the understanding of the molecular mechanisms that are responsible for producing brown adipocyte phenotype during the white preadipocyte differentiation.

The specific objective of this thesis was to investigate the roles of C/EBPβ, together with other regulators like PRDM16, in stimulating brown adipocyte phenotypes including up-regulation of UCP1 in 3T3-L1 white preadipocytes. The original plan of investigation was to construct a stable transgenic 3T3-L1 cell line overexpressing doxycycline inducible C/EBPβ and to investigate the effects of the exogenous C/EBPβ on chromatin remodelling pattern of UCP1 promoter during the 3T3-L1 differentiation. Unfortunately, the lentiviral expression vectors constructed in this work failed to produce lentiviral particles with high titre because the designed insert was challenging the size limit of the lentiviral expression system we used (pLenti6/V5). The low titre lentiviral particles also failed to transduce 3T3-L1 cells as this cell line is especially difficult to transduce. Therefore in the absence of a successful lentiviral vector for overexpressing genes, transient overexpression was used to investigate the interaction between C/EBPβ and other factors in regulating the expression of UCP1 gene in the 3T3-L1 cell line. The experiments suggested that C/EBPβ, co-overexpressed with PRDM16, stimulated UCP1 promoter transcription activity in the presence of forskolin without activating the full length PGC1α promoter in 3T3-L1 preadipocytes. It would be simplistic though to suggest that C/EBPβ could only activate UCP1 transcription in a PGC1α independent manner, since previous literature demonstrated C/EBPβ binds and activates the proximal promoter of PGC1α in response to forskolin in 3T3-L1 (Karamanlidis et al., 2007). So other genes were co-overexpressed with C/EBPβ to activate the full length PGC1α promoter and PPARγ was found to facilitate C/EBPβ in up-regulating the transcription activity of full length

PGC1α promoter in the presence of rosiglitazone. UCP1 promoter activity was also increased by the co-overexpression of PPARγ and C/EBPβ in response to treatment with rosilglitazone and forskolin. The data suggested that C/EBPβ played a key role in activating the UCP1 promoter in 3T3-L1 preadipocytes in both PGC1α dependent and independent manner. Rosiglitazone treatment appeared to be more important in the PGC1α dependent manner, so more experiments about the role of rosiglitazone were undertaken and the results revealed that rosiglitazone accelerated the early stage of 3T3-L1 differentiation and promoted brown adipogenic phenotypes in fully differentiated 3T3-L1 adipocytes both in cell morphology and gene expression pattern. As the cloning work to construct the transgenic cell line was time consuming and no successful transgenic cell lines were produced, the time for the transient overexpression based experiments was limited and not many analytical methods were used. The results from reporter assays and quantitative RT-PCR still provided clues as to how C/EBPβ, together with PRDM16 and PPARγ, regulated UCP1 transcription in the presence of forskolin or/and rosiglitazone in the 3T3-L1 cell line and furthered the understanding of the relevant molecular mechanisms. The results suggested that C/EBPβ up-regulated UCP1 expression in 3T3-L1 preadipocytes in PGC1α independent and dependent manners when co-overexpressed with PRDM16 or PPARγ, respectively.

6.1 SUMMARY OF PRINCIPAL CONCLUSIONS

The main findings reported in this thesis are summarised below:

1) The combination of reverse tetracycline-controlled transactivator element rtTA advance with either tetracycline response element TRE or TRE tight was selected as the ideal Tet on lentiviral expression vector backbone. The target C/EBPβ and the control LucGFP gene were cloned into the backbones and transient transfection in 3T3-L1 preadipocytes demonstrated that the basal expression level without induction was low and the expression was sensitively induced by doxycycline in a dose-dependent manner.

2) The combination of rtTA advance and TRE was selected for the ideal fat-specific lentiviral expression vector backbone. The truncated fat specific promoter short aP2

was used in the vector due to the size limit of lentiviral expression vectors. Transient transfection in 3T3-L1 cells with the fat-specific vector did not show good fat specificity, probably because the transient adipogenic conditions (co-overexpression of PPARγ and C/EBPβ, or treatment with rosiglitazone and forskolin) used in the experiments were not ideal for 3T3-L1 cells. The short aP2 driving Tet on lentiviral LucGFP expression vector was highly adipogenic and doxycycline inducible when transiently transfected into HIB-1B cells and treated with rosiglitazone and forskolin.

3) The whole procedure of producing lentiviral particles with second generation packaging plasmid mix psPAX2, transducing target cell line 3T3-L1 and selecting for monoclonal transduced cells was successful, demonstrated by the data with positive LucRFP vector. However, the lentivirus produced from constructed constitutive LucGFP vector was poorly infectious even after being concentrated to high titer (10^5 TU/ml), probably due to the size of the designed vector challenging the limit of the lentivirus production system (5kb).

4) The 3T3-L1 cell line is more difficult to transduce compared with HT1080 or 293FT cells, as evidenced by the observation that the LucRFP lentivirus infected 3T3-L1 cells less efficiently although at a higher Multiplicity of Infect (MOI), indicating that highly infectious lentiviral particles are especially critical for successfully transducing 3T3-L1 cells.

5) Co-overexpression of C/EBPβ and PRDM16 increased transcriptional activity of the UCP1 promoter in 3T3-L1 preadipocytes in response to forskolin without activating PGC1α transcription.

6) C/EBPβ overexpression alone activated the PGC1α promoter in HIB-1B and Cos7 cells but not in 3T3-L1 preadipocytes, indicating some 3T3-L1 specific repressive mechanisms. Co-overexpression of PPARγ with C/EBPβ released the repressive effect in the presence of rosiglitazone and both CRE and PPRE elements were indispensible for PGC1α promoter to be activated by the co-overexpression in 3T3-L1 cells.

7) C/EBPβ and PPARγ overexpression synergistically stimulated the artificial luciferase reporter vector pGL3-PPRE-TK in 3T3-L1 preadipocytes in response to rosiglitazone, and forskolin treatment.

8) The artificial luciferase reporter vector pGL3-CRE was highly sensitive to forskolin but there was no further response to rosiglitazone in 3T3-L1. Overexpression of C/EBPβ, PRDM16, PPARγ individually or in any combinations failed to significantly increased the luciferase activity of pGL3-CRE in 3T3-L1 cells.

9) Rosiglitazone accelerated the early period of 3T3-L1 differentiation assessed by the up-regulation of C/EBPβ and aP2 mRNA before DAY 6 of differentiation. The decrease in PPARγ mRNA may not be important as rosiglitazone increases PPARγ activity so less PPARγ would be needed to stimulate differentiation.

10) Rosiglitazone up-regulated UCP1 mRNA in the late stage of 3T3-L1 differentiation (from DAY 9) and significantly dampened lipid accumulation in the mature 3T3-L1 adipocytes, leading the white preadipocytes differentiating to “browner” adipocytes.

6.2 USE OF 3T3-L1 CELL LINE AS A MODEL FOR STUDYING GENE REGULATION IN WHITE ADIPOCYTE DIFFERENTIATION

Although primary cells are often preferred to cultured cell lines for investigations, because they more closely allow investigators to reproduce *in vivo* functions *in vitro*, they are of limited use due to their short lifespan and variability and due to the influence of the genotype and phenotype of the donor. Immortal cell lines possess major advantages over primary cells:

1) They are not contaminated with any other cell types which are present in the stromal vascular fraction of adipose tissue.

2) They have high proliferative capacity.

3) Cell lines are much easier to transfect with plasmid DNA or siRNA.

4) Experiments could be repeated under the same conditions and using the same source of cells.

Despite the usefulness of immortal cell lines in studying the molecular events leading to differentiation of certain tissues, they are aneuploid and therefore, diploid primary cells can reflect better the *in vivo* context (Gregoire et al., 1998). The details of the origin and selection of each individual cell line is important for assessing how each cell's phenotypic characteristics may or may not represent the native cells. For instance, many cell lines are derived from long-term cultures that spontaneously transformed. This spontaneous transformation generally follows a time period in culture termed crisis, during which cells cease dividing, some of them die or they exhibit features of senescence. The cells that break out of this crisis represent a small subpopulation of cells and usually contain abnormal number of chromosomes, which is a likely cause of their transformation (Sell, 2004). In addition other cell lines are derived from cancerous lesions, wherein transformation has occurred *in vivo*, instead of *in vitro*, and they may also lose bits of chromosomes or carry a number of chromosomal abnormalities that may not represent the native cells (Sell, 2004). Furthermore, recent cell lines have been formed by introducing genes into cells that can impact immortality, such as the SV40 large T-antigen and hence divide indefinitely. The criticism of this method is that although the mechanism of immortalization is known, the transforming gene is always expressed, which is non-physiologic and may have unknown effect on the physiology of the host cell (Sell, 2004).

3T3-L1 and 3T3-F442A (both subclones of the spontaneously immortalized Swiss 3T3 cells), have been widely used to study white adipogenesis (Green and Kehinde, 1975). 3T3-L1 cell differentiation is a well-described system for WAT differentiation and believed to be a faithful model of preadipocyte differentiation as demonstrated by *in vivo* implantation studies: when 3T3-L1 cells were injected into nude mice, the cells developed into mature fat pads that were indistinguishable from normal adipose tissue, suggesting that adipose cell conversion occurs by similar mechanisms *in vivo* (Gregoire et al., 1998; Lane et al., 1999; MacDougald et al., 1994; MacDougald and Lane, 1995; Tang and Lane, 1999; Wu et al., 1996). One disadvantage of 3T3-L1 cells is that they exhibit low efficiency with which foreign DNA can be introduced by transfection, and the experiments in this thesis also demonstrated that 3T3-L1 cells

are more difficult to transduce by lentiviral particles. The Ob17 cell line derived from epididymal WAT of adult ob/ob mice has been also largely employed in WAT studies (Negrel et al., 1978). In this thesis, 3T3-L1 cell line was selected for studying the role of C/EBPβ in UCP1 gene regulation for the following reasons:

1) 3T3-L1 cell line was successfully differentiated into white adipocytes using the classical hormonal cocktail and the protocols for plasmid DNA transfection, RNAi, RNA extraction and Western Blot have been optimized previously in this lab.

2) The key brown adipogenic genes UCP1 and PGC1α are β-adrenergic inducible in brown adipocytes but not in 3T3-L1 (pre)adipocytes.

3) C/EBPβ expression is increased by forskolin in 3T3-L1 cells during the first 48 hours post confluence, similar to the response observed in brown adipocytes.

4) The previous work in our lab demonstrated that C/EBPβ overexpression could rescue the insensitivity of PGC1α gene to cAMP stimulation in 3T3-L1 cells (Karamanlidis et al., 2007), although the effect of C/EBPβ on UCP1 expression still remains to be determined.

These data suggested that 3T3-L1was an appropriate model for studying the role of C/EBPβ in regulating UCP1 gene expression during white adipogenesis. In addition, to avoid the spontaneous transformation from the long term culture, the high passage (Passage> 32) 3T3-L1 cells were not used in any experiments.

6.3 PGC1 ALPHA -DEPENDENT AND -INDEPENDENT PATHWAYS IN UCP1 GENE REGULATION

Many of the pathways regulating UCP1 gene expression in adipose tissue have been proposed to act indirectly by changing PGC1α gene expression or activity. One of the examples for a PGC1α dependent activating mechanism is that PRDM16 forms a complex with C/EBPβ and up-regulates the transcription activity of PGC1α promoter to induce the brown adipogenic programme, including stimulation of UCP1 gene expression (Kajimura et al., 2009).

In the experimental work presented in this thesis, C/EBPβ was also shown to be involved in both PGC1α dependent and independent mechanisms in regulating UCP1 transcription in 3T3-L1 cells. When co-overexpressed with PRDM16, C/EBPβ significantly increased the transcription activity of UCP1 promoter with or without forskolin treatment (Figure 5.5A), but the same co-overexpression did not have any significant effects on the full length PGC1α promoter activity (Figure 5.5B), indicating that C/EBPβ, under these circumstances, regulated UCP1 transcription in a PGC1α independent manner. On the other hand, when C/EBPβ was co-overexpressed with PPARγ, it markedly increased PGC1α promoter activity in response to rosiglitazone (Figure 5.7B) and C/EBPβ and PPARγ also had an additive effect in up-regulating UCP1 promoter activity in the presence of forskolin and rosiglitazone (Figure 5.7A), which demonstrated that C/EBPβ could also be involved in a PGC1α dependent mechanism to stimulate UCP1 transcription. However, as the real time PCR was not sensitive enough to pick up the low amount of template UCP1 and PGC1α from the transfected confluent 3T3-L1 cells, there was no direct evidence for the mRNA changes of UCP1 and PGC1α. Therefore an improved real time PCR protocol is needed and the other methods for detecting gene expression such as Western Blot and immunostaining could be used to validate the discovery that C/EBPβ could increase UCP1 expression in both PGC1α dependent and independent manners. The potential schematic diagram of C/EBPβ regulating UCP1 expression could be illustrated as following (Figure 6.1)

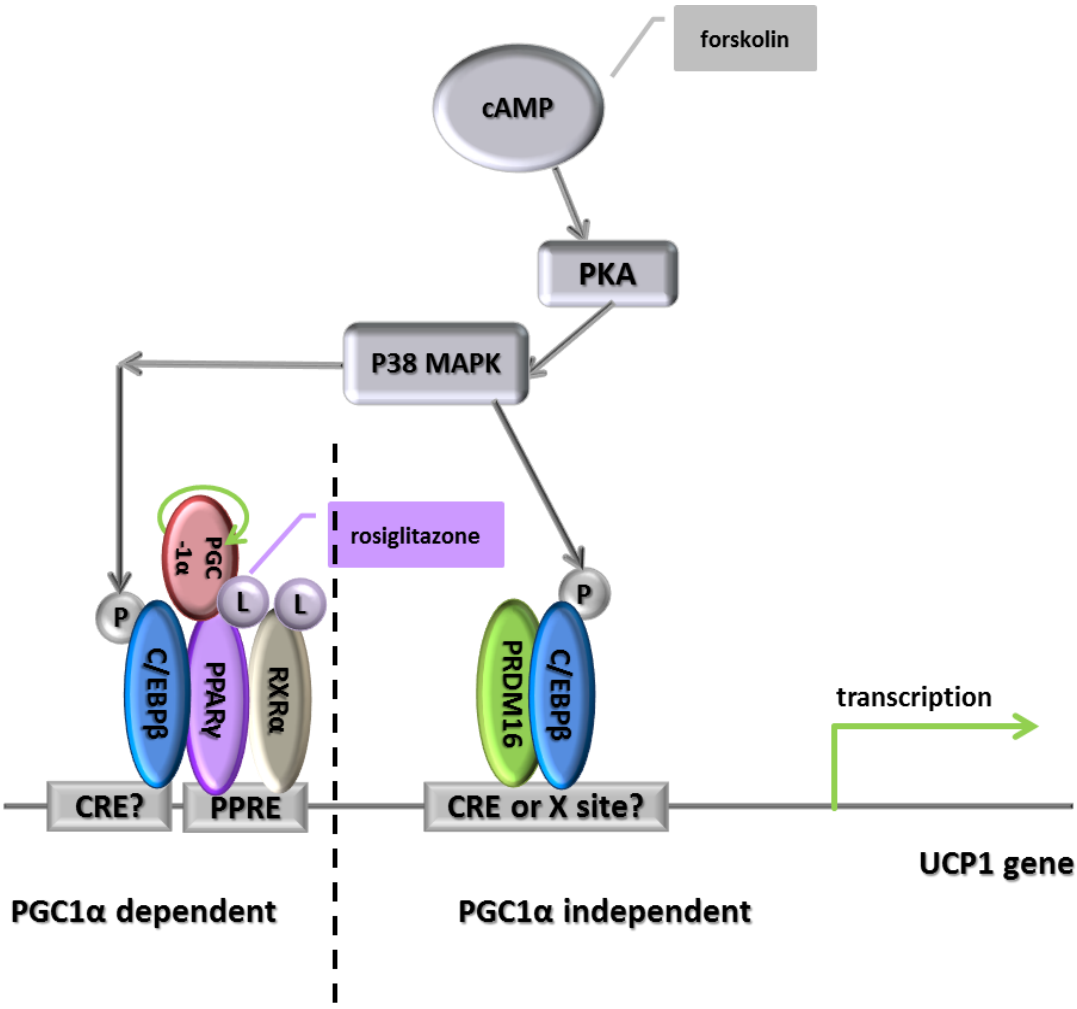

Figure 6.1 Model for C/EBPβ interacting with other (co)activators in regulating UCP1 transcription in 3T3-L1 preadipocytes at confluence.

A possible model for higher UCP1 promoter activity through higher C/EBPβ cellular concentration and phosphorylation in response to cAMP-PKA signalling pathway or/and ligand (rosiglitazone)-activated PPARγ/ PGC1α is proposed. The PGC1α independent manner is illustrated on the right side of the dotted line: higher concentration of C/EBPβ forms a complex with PRDM16 and stimulates UCP1 transcription in response to forskolin treatment through an unknown site on the UCP1 promoter. On the left side of the dotted line, there is the PGC1α dependent manner: higher concentration of C/EBPβ interacts with the overexpressed PPARγ activated by PGC1α in presence of PPARγ ligand rosiglitazone and the complex stimulates the transcription activity of UCP1 promoter through the PPRE (or maybe CRE as well) on the promoter. P: phosphate group; L: ligand.

LXRα regulates UCP1 expression without influencing PGC1α expression and activity (Wang et al., 2008b) and plays a direct role as a transcriptional inhibitor of cAMP-dependent UCP1 gene expression through its binding to the critical enhancer region of the UCP1 promoter. However, LXRα might not be totally PGC1α independent, as it involves the differential recruitment of the corepressor RIP140 to an LXRα binding site that overlaps with the PPARγ/PGC1α response element (PPRE), resulting in the dismissal of PPARγ which PGC1α can no longer co-activate to stimulate UCP1 gene expression (Wang et al., 2008b). Another example of the PGC1α dependent but repressive mechanism is that RIP140 interacts directly with PGC1α and suppresses its activity in inducing the promoter activity of CIDEA (Hallberg et al., 2008), which is highly expressed in BAT but directly interacts with and inhibits the uncoupling activity of UCP1 (Zhou et al., 2003). Interestingly, RIP140 also directs histone and DNA methylation to maintain repressive state of UCP1 gene transcription in white adipocytes (Kiskinis et al., 2007), which is a PGC1α independent regulatory pathway. RIP140 expression promotes the assembly of DNA and histone methyltransferases (HMTs) on the UCP1 enhancer and leads to methylation of specific CpG residues and histones, so RIP140 serves as a scaffold for both DNA and HMT activities to inhibit UCP1 transcription by two key epigenetic repression systems (Kiskinis et al., 2007). Therefore PGC1α may not be indispensible to the regulation of UCP1 gene expression. Furthermore, the listed two regulatory mechanisms involving RIP140 indicate that a single regulator may be able to influence the target gene expression or activity through different mechanisms, in this case, in PGC1α dependent or independent pathways, to regulate UCP1 gene.

The fact that one target gene can be regulated either dependent or independent of some specific regulators (usually the key regulators) has the advantage that in case of the malfunction of any regulator, the other pathways independent of this regulator could compensate for the lost regulating function to minimize the influence of the specific malfunction on the overall expression and activity of the target gene.

6.4 UNCOUPLING PROTEINS AND METABOLIC SYNDROME

The metabolic syndrome (MS) is a clinical entity that describes the clustering of factors including dyslipidaemia, glucose intolerance and hypertension with central adiposity as risk factors for coronary heart disease. The syndrome is increasing worldwide as a consequence of increasing obesity prevalence. The urgency for understanding the specific mechanisms that lead to development of MS and consequently discovery of new treatments to combat obesity is summarized below:

1) A quarter of the world's adults have metabolic syndrome (Dunstan et al., 2002)

2) People with metabolic syndrome are twice as likely to die from, and three times as likely to have a heart attack or stroke compared with people without the syndrome (Isomaa et al., 2001)

3) People with metabolic syndrome have a five-fold greater risk of developing type II diabetes (Stern et al., 2004)

4) Up to 80% of the 200 million people with diabetes globally will die of cardiovascular disease (www.idf.org)

5) The above statistical data puts metabolic syndrome and diabetes far ahead of HIV/AIDS in morbidity and mortality terms yet the problem is not as well recognized (www.idf.org)

Obesity has now reached pandemic proportions leading to a collection of morbidities referred to as metabolic syndrome. The expansion of adipose tissue is a direct cause of these comorbidities due to excessive accumulation of triglycerides within adipocytes, causing disruption of normal adipose function (Vernochet et al., 2010). Brown adipose tissue has been well recognized for its potential and demonstrated anti-obesity properties due to its function of "burning" fat by the high capacity for energy expenditure in the form of uncoupled respiration, mediated by the brown fat marker gene UCP1. Therefore, UCP1 could potentially play a key role in combating obesity to decrease the prevalence and morbidity of metabolic syndrome. Genetic ablation of UCP1 induces obesity and significantly decreases the metabolic rate in mice fed with either control or high-fat diet (Feldmann et al., 2009).

Recent studies have confirmed the thermogenic function of UCP1. Overexpression of UCP1 in pancreatic INS-1 cells enables the cells to show signs of uncoupling evidenced by the increased oxygen consumption and decreased mitochondrial membrane potential in response to the addition of fatty acids (Galetti et al., 2009). In contrast, overexpression of an uncoupling protein homologue UCP2 in the same cell line cannot stimulate the uncoupling process, indicating the distinct functional difference between UCP1 and UCP2 although they have 59% identity with each other in sequence (Fisler and Warden, 2006; Galetti et al., 2009). Similarly, another homologue UCP3, sharing 57% identity with UCP1, also has markedly different physiological roles from UCP1. Gene expression of UCP2 and UCP3 increases during fasting (Cadenas et al., 1999), the opposite of what would be expected for thermogenic function and neither UCP2 nor UCP3 knockout mice are obese (Arsenijevic et al., 2000; Gong et al., 2000). However, transgenic mice overexpressing a UCP2 or UCP3 construct are leaner than wild type (Fuller et al., 2000; Horvath et al., 2003). These data provide evidence against these proteins contributing to whole body thermogenesis in the same way as the homologue UCP1. In population studies, a polymorphism of the uncoupling proteins was investigated to evaluate the influence of a single nucleic acid difference in the promoter sequence on the gene function in association with metabolic syndrome. Studies demonstrated that polymorphism -3826 A/G of the UCP1 gene is associated with a greater BMI, greater percentage of body fat and higher arterial tension (AT) in obese individuals (Forga et al., 2003). A common polymorphism in the UCP2 promoter, -866 G/A, is associated with a reduced risk of obesity in Caucasian Europeans (Esterbauer et al., 2001; Krempler et al., 2002). Interestingly, the same UCP2 -866 G/A polymorphism and a -55 C/T polymorphism in UCP3 are both associated with significantly reduced prevalence of diabetic neuropathy in type I diabetics (Rudofsky et al., 2006).

In conclusion, among the three uncoupling protein homologues, only UCP1 positively contributes to whole body thermogenesis thus has the anti-obesity function. Increased UCP2 expression results in β-cell dysfunction, impaired insulin sensitivity and earlier, more severe diabetes, but may protect from diabetic neuropathy. Increased UCP3 may reduce muscle insulin resistance (Fisler and Warden, 2006).

6.5 THE FEASIBILITY TO ALLEVIATE OBESITY AND RELEVANT METABOLIC SYNDROME IN HUMANS BY CONTROLLING THE EXPRESSION OF C/EBP BETA

Since the work in this thesis demonstrated the potential of C/EBPβ to up-regulate UCP1 expression in white 3T3-L1 preadipocytes, it provides the possibility to reduce the chance of obesity by transdifferentiating white adipocytes into brown like cells by overexpressing C/EBPβ in white adipose tissue. A direct way of doing this is gene therapy, i.e. to deliver the C/EBPβ gene directly into the tissues of patients by recombinant adenoviral-associated vector (rAAV) (Liau et al., 2001). However, as gene therapy is a newly developed technique, there is much concern about its safety and it has only been suggested for the treatment of extremely serious diseases such as cancers and some genetic deficiency. Although there are positive clinical trial results using this technique in therapeutics on several severe diseases including pro-angiogenesis (Liau et al., 2001), the long term safety issue and the efficacy of this novel therapeutic method still await the result of on-going clinical trials. Besides, as the first case of gene therapy in humans was in 1990 (Oldfield et al., 1993), there has not been enough time to evaluate the long-term side effects including any negative influence on life-span. Therefore, gene therapy seems to be less valid to treat obesity by increasing C/EBPβ expression level.

Another way is to identify drugs that can increase C/EBPβ expression or activity. As demonstrated in this thesis, treating the differentiating 3T3-L1 cells with forskolin significantly increased C/EBPβ transcription in mature adipocytes (Figure 5.1C) and the treatment with rosiglitazone during the induction period of differentiation markedly stimulated C/EBPβ expression in 3T3-L1 cells (Figure 5.4A). Therefore a combination of β-adrenergic stimulus and the anti-diabetic drug, rosiglitazone, could be possible candidate drugs to stimulate C/EBPβ expression in white adipose tissue *in vivo*. However, the drugs would not only affect adipose tissue, but have systemic actions as they would be transported by blood circulation all around body and may cause changes in metabolism and internal homeostasis to an unexpected extent. Given that C/EBPβ plays an important role in cell cycle regulation of many cell types

such as MEFs (Gagliardi et al., 2003; Sebastian et al., 2005), leukemic cells (Duprez et al., 2003; Guerzoni et al., 2006), hepatic cells (Buck et al., 1999; Greenbaum et al., 1998) and adipocytes (Tang et al., 2003a), the simple increase of C/EBPβ expression by drugs could result in more extensive influence or side effects in tissues and organs all over the body.

Besides expression levels, the trans-activation potential of C/EBPβ can also be influenced by its phosphorylation state (Tang et al., 2005), so drugs targeting the kinases which regulate phosphorylation state of C/EBPβ should also theoretically activate C/EBPβ without changing its expression level. When growth-arrested 3T3-L1 preadipocytes are induced to differentiate, C/EBPβ is rapidly expressed but still lacks DNA-binding activity. After a 14-hour lag, glycogen synthase kinase 3β (GSK-3β) enters the nucleus, which correlates with hyperphosphorylation of C/EBPβ and acquisition of DNA-binding activity; concurrently, 3T3-L1 preadipocytes synchronously enter S phase and undergo mitotic clonal expansion (MCE), a prerequisite for terminal differentiation (Tang et al., 2005). During this MCE period, the histone H4, is transcriptionally activated by phophorylated C/EBPβ, and H4 expression is correlated with DNA content change during the cell cycle, (Zhang et al., 2011). Since it has been demonstrated that C/EBPβ is sequentially phosphorylated by mitogen-activating protein kinase (MAPK) and GSK-3β (Tang et al., 2005) in 3T3-L1 adipogenesis and that C/EBPβ is regulated in a cAMP-PKA mediated signalling pathway in thermogenesis in brown adipocytes (Karamanlidis et al., 2007), the drugs targeting the above kinases, GSK-3β, MAPK and PKA, are candidate molecules for drug screening. These kinases play important phosphorylating roles all around the body, so there is still the problem of how to restrict the drug effects only on C/EBPβ in adipose tissue.

Despite the challenges in developing treatments to alleviate obesity and the related metabolic syndrome, by directly increasing C/EBPβ expression or activity in humans, it is still necessary to clarify the roles of C/EBPβ in the regulatory network controlling UCP1 expression in white adipose tissue. Furthermore the role of C/EBPβ in regulating the cell cycle could be useful to establish an effective drug or therapeutic method for the treatment of obesity by manipulating C/EBPβ expression or activity.

6.6 FUTURE WORK

The results in this thesis demonstrated the technical problems in constructing a stable transgenic 3T3-L1 preadipocyte line overexpressing C/EBPβ. Therefore it is important to improve the lentivirus production protocol, maybe by using a different lentiviral vector backbone which has the capacity to take bigger size insert or use two-vector system to clone C/EBPβ and rtTA separately to reduce the insert size for each vector (refer to the discussion in Chapter 4). Alternatively, the adenoviral expression system could be used to stably overexpress C/EBPβ in 3T3-L1 preadipocytes. This approach suffers from the disadvantage that the transgene would not be permanently integrated into the genome of the adenovirus infected cells, and would not create a genetically modified cell line. Once the transgenic 3T3-L1 cell line is constructed, it would be differentiated using the typical hormonal induction protocol and the gene expression level of UCP1 measured by qRT-PCR and Western Blot in response to overexpressed C/EBPβ induced by different doses of doxycycline. Further studies could examine the chromatin remodelling pattern on the UCP1 promoter by ChIP assays targeting the activate markers (AcH3, AcH4 and H3K4Me2) and the repressive markers (H3K9Me2, H3K9Me3, H3K27Me2 and H3K27Me3) of the histones.

The work on the 3T3-L1 cells transiently overexpressing C/EBPβ or/and the other (co)activators (PRDM16 and PPARγ) revealed that C/EBPβ might be involved in both PGC1α dependent and independent mechanisms to regulate UCP1 expression and that there might be a 3T3-L1 specific repressive mechanism that prevents C/EBPβ from activating UCP1 transcription. Further studies are needed to improve the qRT-PCR protocol for amplifying UCP1 and PGC1α from 3T3-L1 cDNA, probably by using another lightcycler which is more sensitive to pick up the low concentration templates. Furthermore, Western Blot can be applied to detect how UCP1 expression is changed by the overexpression of C/EBPβ or/and PRDM16 or PPARγ at the protein level to further verify the data from reporter assays and mRNA measurement. The cells with the transient overexpression of C/EBPβ or/and PRDM16 or PPARγ can also be used to perform ChIP assays to explore whether the overexpression(s) interact directly to the UCP1 promoter and to investigate whether they changed the chromatin remodelling pattern of the promoter by using antibodies against the

typical active and repressive markers of histone. The ChIP assays also provide possibilities to identify other genes than PPARγ that have the potential to release the 3T3-L1 specific repression on C/EBPβ stimulation of UCP1 expression. Finally, as phosphorylation probably influences the trans-activation potential of C/EBPβ and the studies in the 3T3-L1 transiently transfected with C/EBPβ have to focus on 24-48 hours post confluence of the cells, in which period C/EBPβ starts to gain its DNA-binding activity through phosphorylation (Tang et al., 2005), the phosphorylation state of C/EBPβ probably affect the ability of C/EBPβ to regulate UCP1 expression. It will be helpful to correlate the phosphorylation level of C/EBPβ with the UCP1 expression and activity in the cells overexpressing C/EBPβ or with other (co)activators.

Ambitiously, a transgenic mouse overexpressing C/EBPβ in response to doxycycline induction specifically in adipose tissue could be constructed, either by pronuclear injection of the fat-specific inducible C/EBPβ vector or by constructing a mouse embryonic stem cell line bearing such characteristics and then developing the target transgenic mouse [reviewed in (Luo et al., 2011)].

In conclusion, the experiments and model proposed above warrant further research to define the role of C/EBPβ in the regulation of UCP1 gene expression in white (pre)adipocytes.

APPENDICES

APPENDIX A - SOLUTIONS AND REAGENTS

Ampicillin 100mg/ml

Stock solution of ampicillin (Sigma) was prepared by adding 100mg per ml in autoclaved distilled water, filtered with 0.2µm filter (Millipore), dispensed in 200µl aliquots and stored at -20°C. It was used at 100µg/ml final concentration in liquid and solid medium.

Kanamycin 50mg/ml

Stock solution of kananycin (Sigma) was prepared by adding 50mg per ml in autoclaved distilled water, filtered with 0.2µm filter (Millipore), dispensed in 200µl aliquots and stored at -20°C. It was used at 50µg/ml final concentration in liquid and solid medium.

Blasticidin 8mg/ml

Stock solution of blasticidin (Invitrogen) was prepared by adding 200mg powder into dH_2O with the final volume adjusted to 25ml, dispensed in 500µl aliquots and stored at -20°C.

Doxycycline 10mg/ml

10mg/ml stock solution of doxycycline (Sigma) was prepared by dissolving 50mg of doxycycline powder with dH_2O into a final volume of 5ml, yielding a clear, yellow-green solution. Aliquots were made in 50µl/vial and stored at -20°C.

EDTA 0.5M (1000ml)

186.1g of disodium ethylenediamine tetraacetate acid dihydrate (EDTA; Sigma) was dissolved in 1000ml of distilled water (dH_2O). The pH was adjusted at 8.0 with 10M NaOH and the solution was autoclaved at 121°C for 15 min.

NaCl 5M (100ml)

29.2g of NaCl (Sigma) were dissolved in dH_2O to a final volume of 00ml and autoclaved at 121°C fo 15 min.

Phosphate Buffer Saline (PBS; 200ml)

PBS solution was prepared by dissolving one PBS tablet (Sigma) into 200ml dH_2O and autoclaved at 121°C for 15 min.

TAE buffer (50× stock; 1000ml)

50× TAE stock solution was prepared by adding 242g of Tris base (Sigma), 57.1ml Glacial Acetic Acid (Sigma) and 18.6g of EDTA (Sigma) into 900ml dH_2O and the final volume was adjusted to 1L with additional dH_2O.

Tris-HCl 1M (1000ml)

121g of Tris base were dissolved in 1000ml dH_2O. The pH was adjusted at 8.0 and the solution was autoclaved 121°C for 15 min.

TSSM buffer (100ml)

0.24g of Tris base, 0.585g of NaCl, 1g of sucrose and 1g of mannitol were dissolved in 90ml dH_2O. The pH was adjusted to 7.4 and final volume was adjusted to 100ml with dH_2O. The solution was autoclaved at 121°C for 15 min.

APPENDIX B - BACTERIOLOGICAL MEDIA USED

LB medium (1000ml)

10g tryptone (Sigma), 5g yeast extract (Sigma) and 10g NaCl were dissolved in 1000ml dH_2O and autoclaved at 121°C for 15 min.

LB-Agar (400ml)

4g tryptone, 2g yeast extract, 4g NaCl and 6g agar (Sigma) were dissolved in 400ml dH_2O and autoclaved at 121°C for 15 min. For plating, medium was allowed to cool to 55°C then appropriate antibiotics was added at designed concentration and 25-30ml of medium was poured into 10cm petri dishes. Once the agar was solid, plates were stored at 4°C until used for up to a month.

APPENDIX C - COMPOSITION OF DMEM AND GROWTH MEDIUM

Growth medium for 3T3-L1 and HIB-1B cells was composed of 88% DMEM, 10% FBS (heat inactivated; Invitrogen), 1% Sodium Pyruvate (Invitrogen) and 1% of Penicillin/ Spectromycin (Invitrogen). Growth medium for HT1080 and 293FT cells was composed of 88% DMEM, 10% FBS (non-heat inactivated; Invitrogen) and 1% Sodium Pyruvate (Invitrogen).

COMPONENTS OF DMEM	**M. W.**	**mg/L**	**mM**
Amino Acids			
Glycine	75	30	0.4
L-Arginine hydrochloride	211	84	0.398
L-Cystine 2HCl	313	63	0.201
L-Glutamine	146	580	3.97
L-Histidine hydrochloride-H2O	210	42	0.2
L-Isoleucine	131	105	0.802
L-Leucine	131	105	0.802
L-Lysine hydrochloride	183	146	0.798
L-Methionine	149	30	0.201
L-Phenylalanine	165	66	0.4
L-Serine	105	42	0.4
L-Threonine	119	95	0.798
L-Tryptophan	204	16	0.0784
L-Tyrosine	181	72	0.398
L-Valine	117	94	0.803
Vitamins			
Choline chloride	140	4	0.0286

D-Calcium pantothenate	477	4	0.00839
Folic Acid	441	4	0.00907
i-Inositol	180	7.2	0.04
Niacinamide	122	4	0.0328
Pyridoxine hydrochloride	204	4	0.0196
Riboflavin	376	0.4	0.00106
Thiamine hydrochloride	337	4	0.0119
Inorganic Salts			
Calcium Chloride (CaCl2-2H2O)	147	264	1.8
Ferric Nitrate (Fe(NO3)3"9H2O)	404	0.1	0.000248
Magnesium Sulfate (MgSO4-7H2O)	246	200	0.813
Potassium Chloride (KCl)	75	400	5.33
Sodium Bicarbonate (NaHCO3)	84	3700	44.05
Sodium Chloride (NaCl)	58	6400	110.34
Sodium Phosphate monobasic (NaH2PO4-2H2O)	154	141	0.916
Other Components			
D-Glucose (Dextrose)	180	4500	25
Phenol Red	376.4	15	0.0399

APPENDIX D - MAPS OF CONSTRUCTS

LENTIVIRAL DESTINATION VECTORS

(1) pLenti6/V5

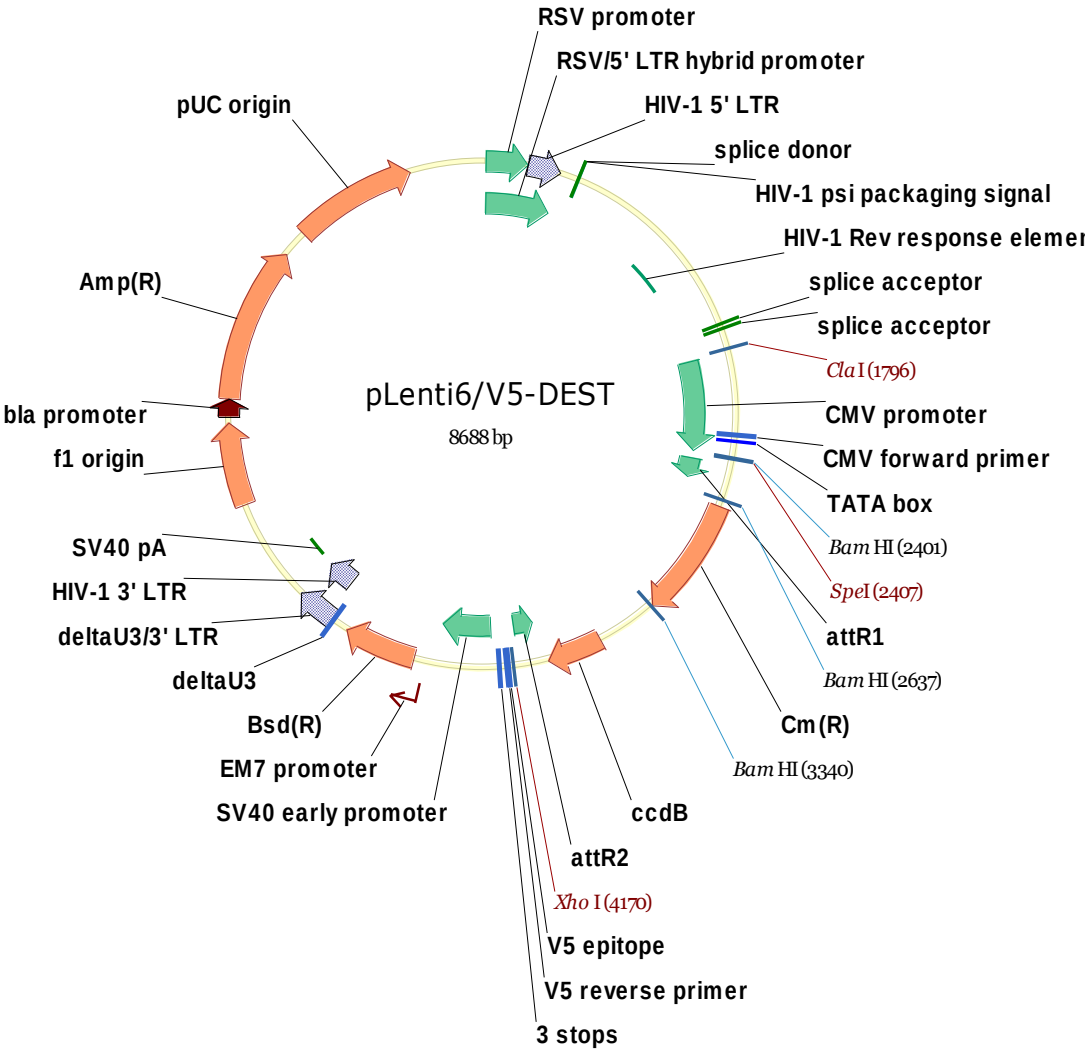

(2) pLenti-TRE

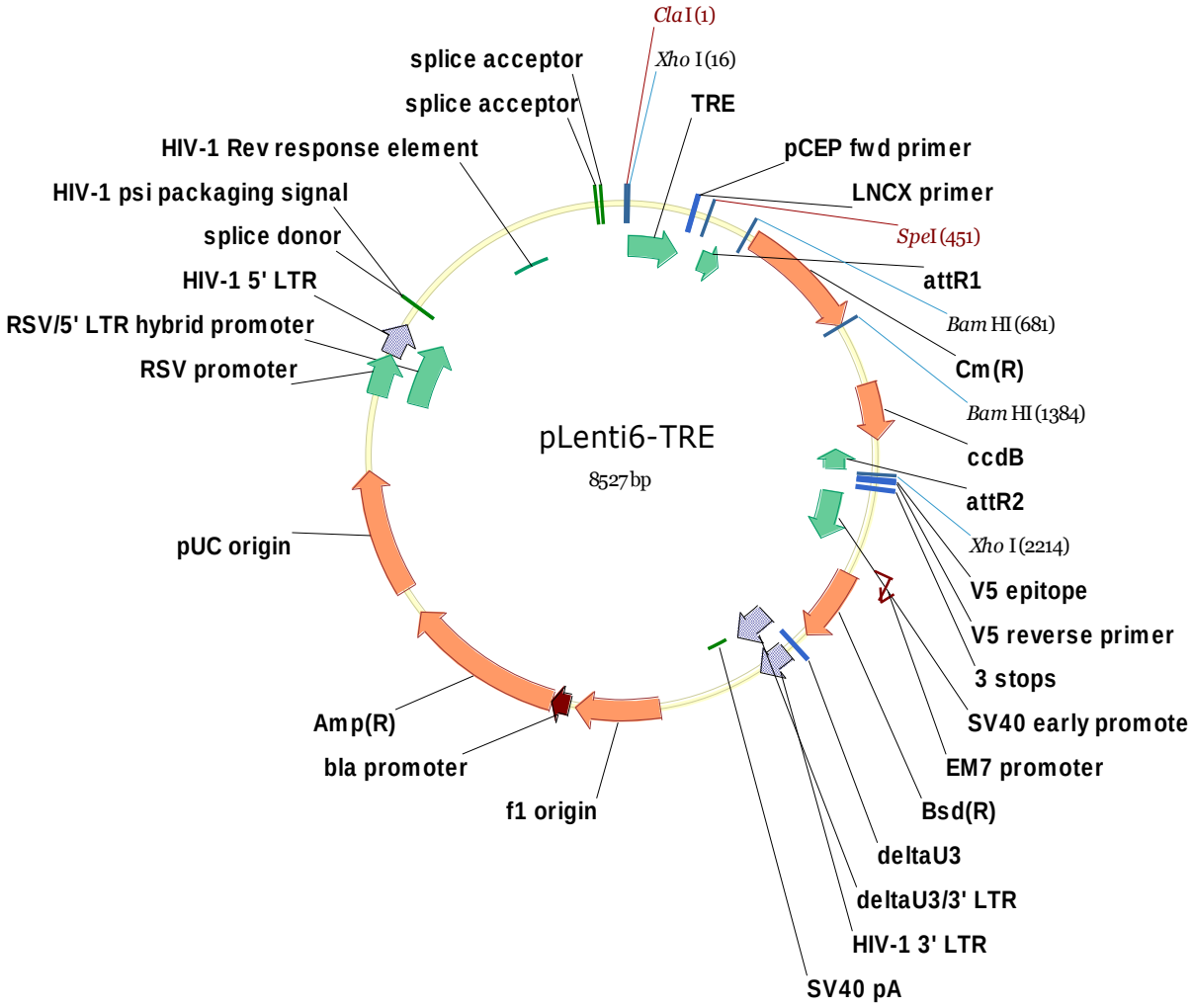
ClaI(1)
XhoI(16)
splice acceptor
splice acceptor
TRE
HIV-1 Rev response element
pCEP fwd primer
HIV-1 psi packaging signal
LNCX primer
splice donor
SpeI(451)
HIV-1 5' LTR
attR1
RSV/5' LTR hybrid promoter
BamHI(681)
RSV promoter
Cm(R)
BamHI(1384)
pLenti6-TRE
8527bp
ccdB
attR2
pUC origin
XhoI(2214)
V5 epitope
V5 reverse primer
3 stops
SV40 early promote
Amp(R)
EM7 promoter
bla promoter
Bsd(R)
f1 origin
deltaU3
deltaU3/3' LTR
HIV-1 3' LTR
SV40 pA

(3) pLenti-TRE tight

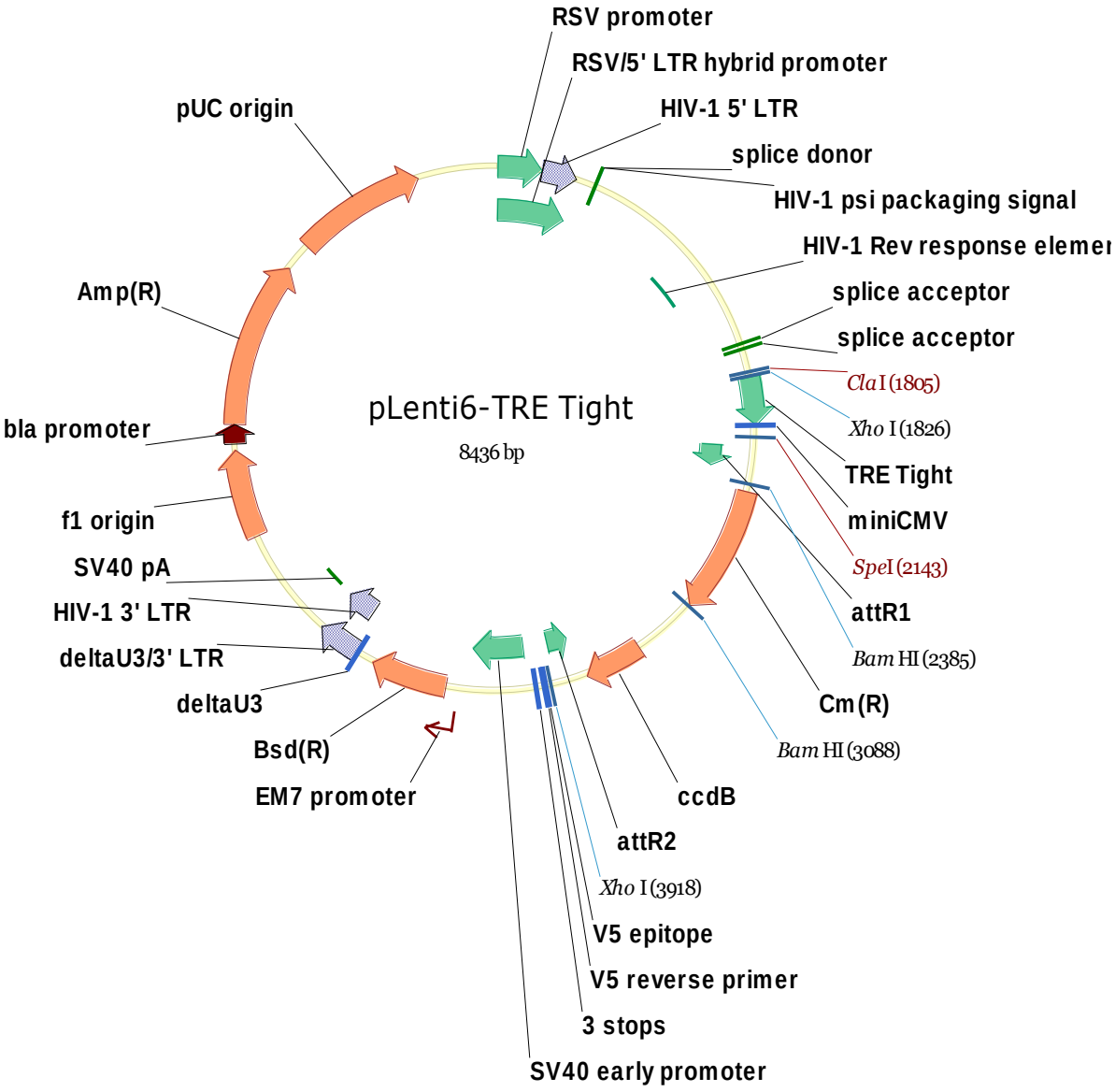

ENTRY CLONES

(1) C/EBPβ

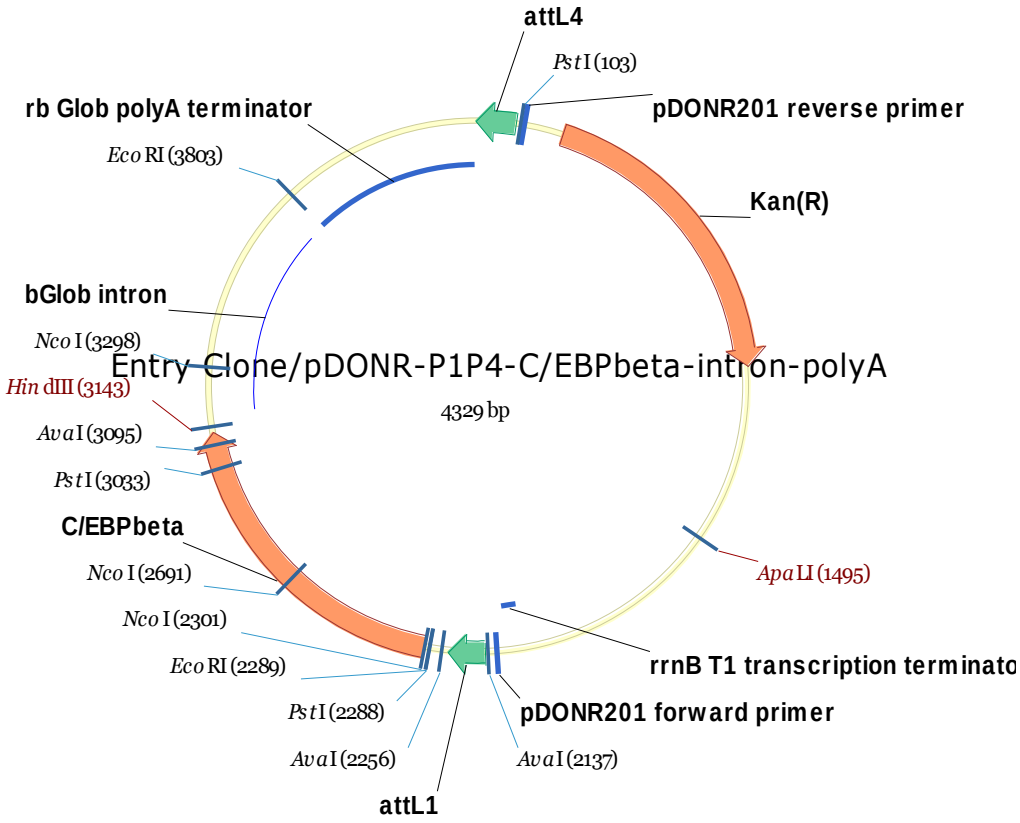

(2) LucGFP

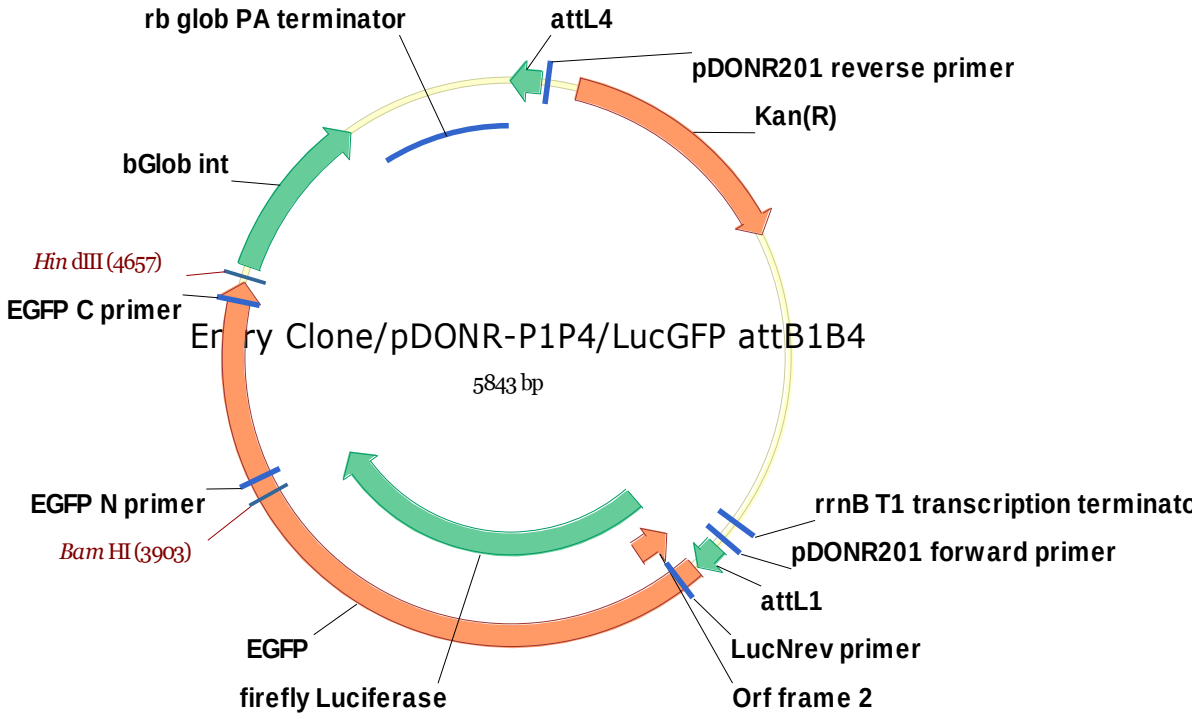

(3) CMV promoter

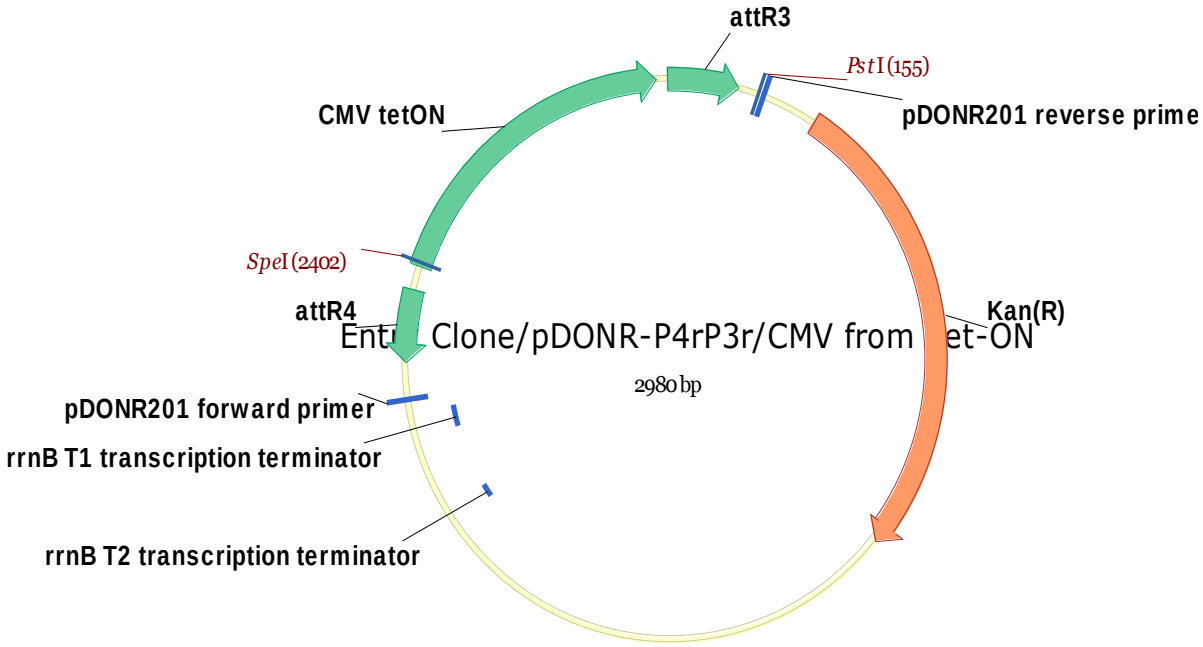

(4) aP2 promoter

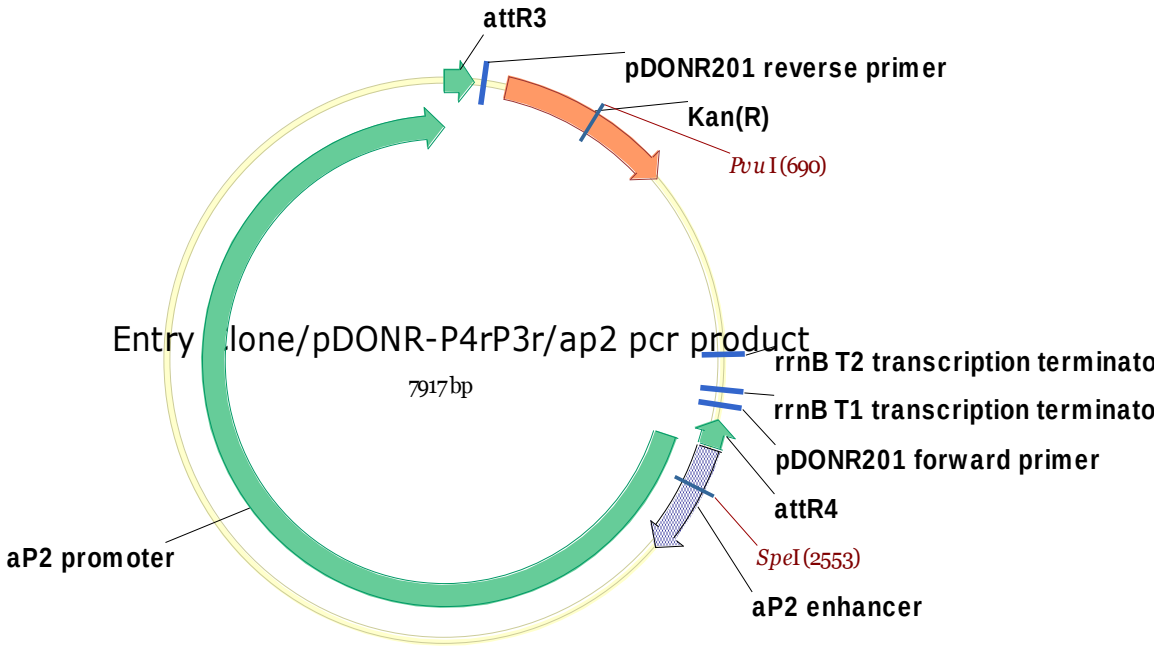

(5) short aP2 promoter

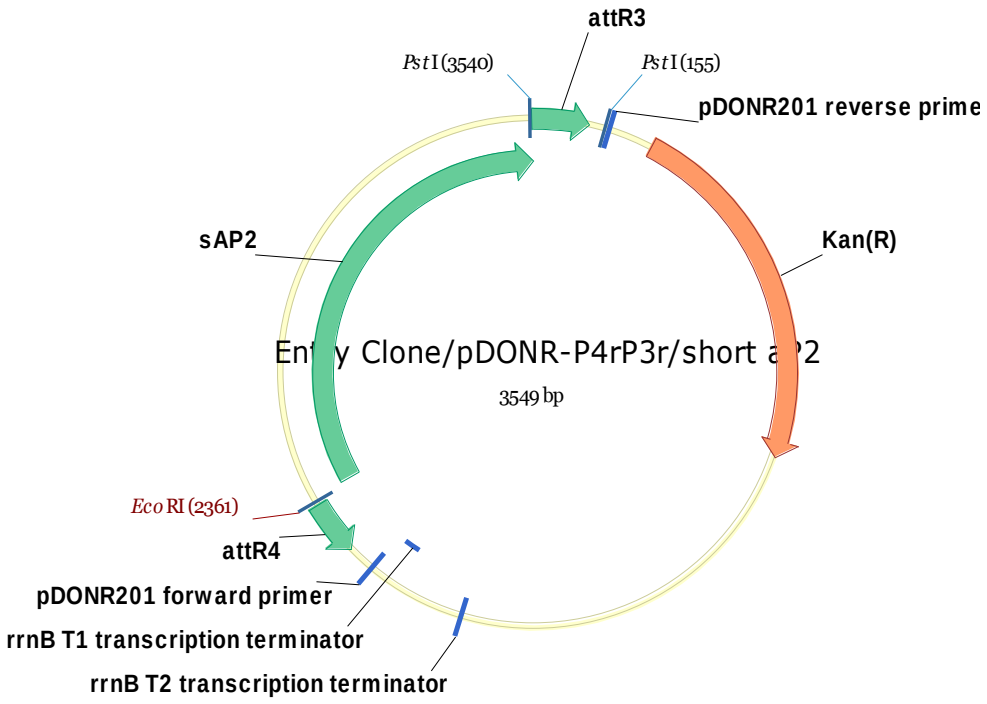

(6) rtTA

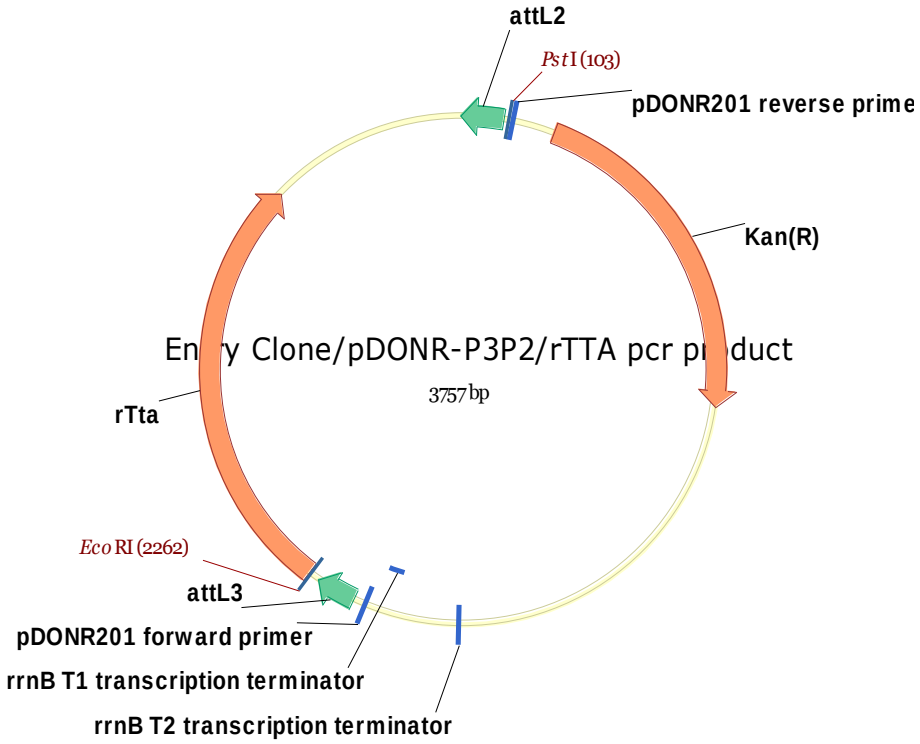

(7) rtTA advance

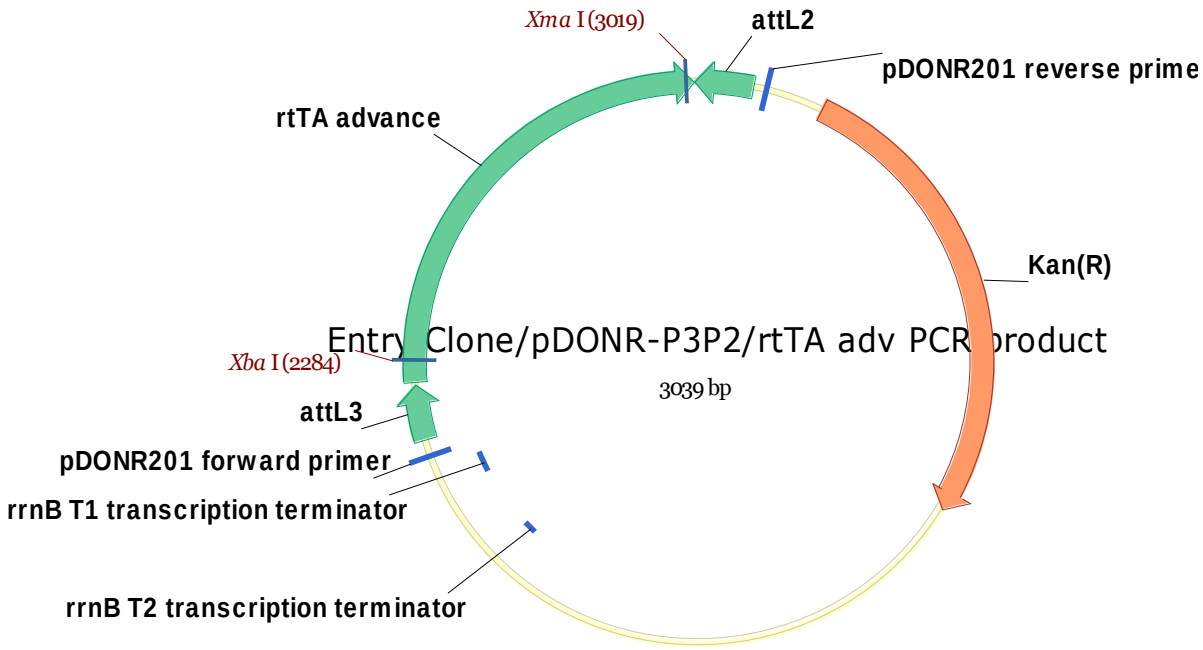

EXPRESSION VECTORS (NON-FAT SPECIFIC)

(1) Constitutive expression vector for LucGFP (pLenti-LucGFP)

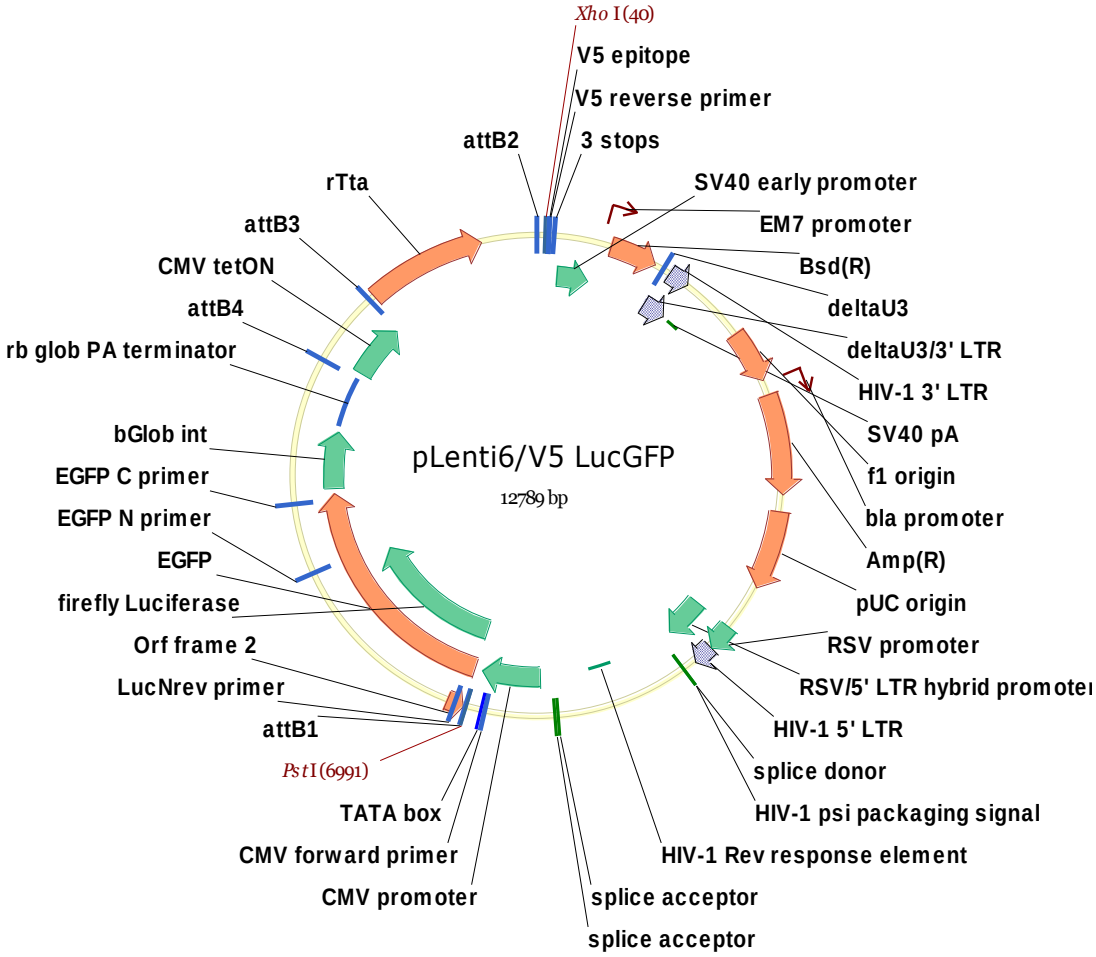

(2) Constitutive expression vector for C/EBPβ (pLenti-C/EBPβ)

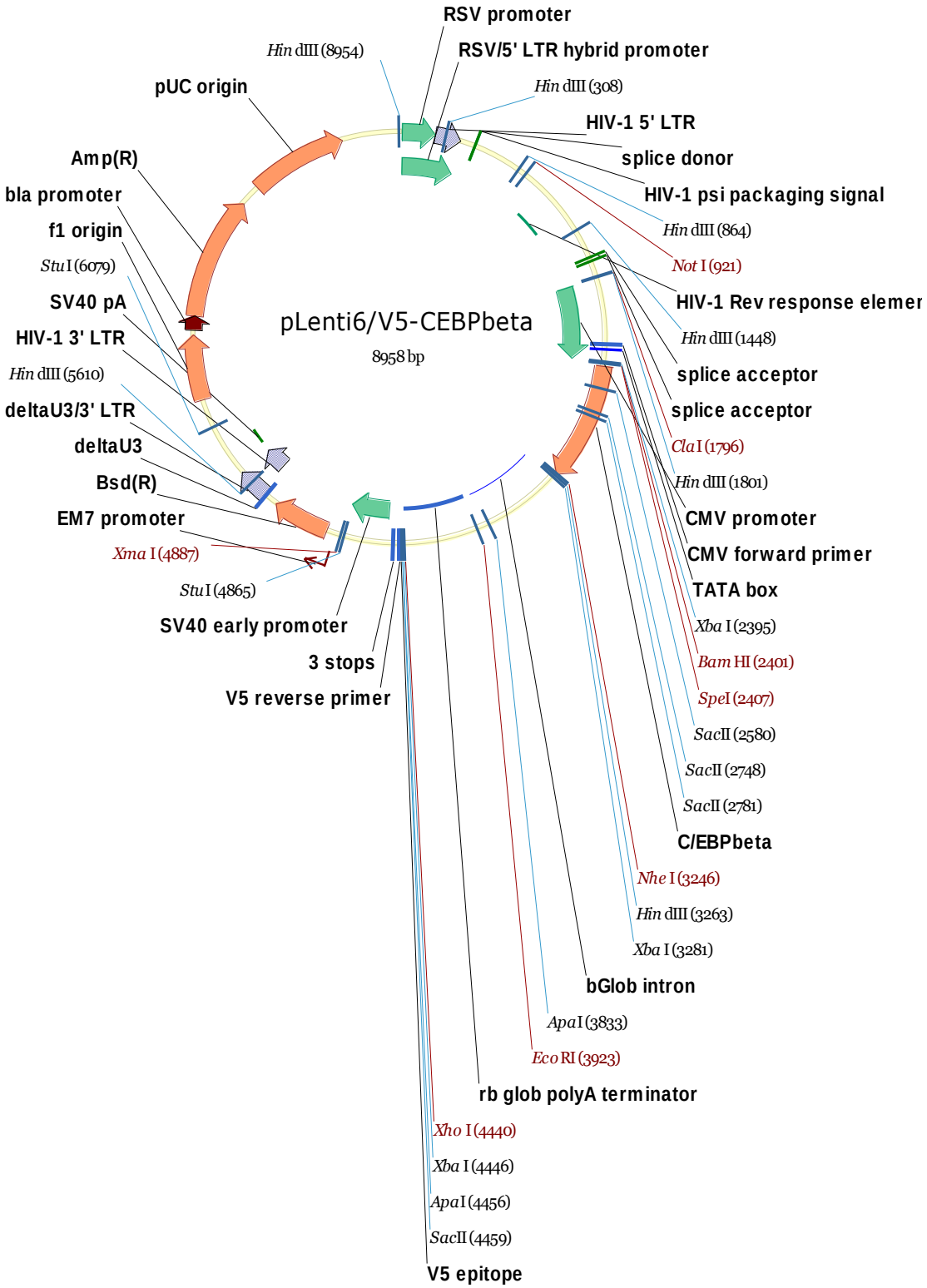

(3) Inducible expression vector for LucGFP ① pLenti TRE-LucGFP-CMV-rtTA

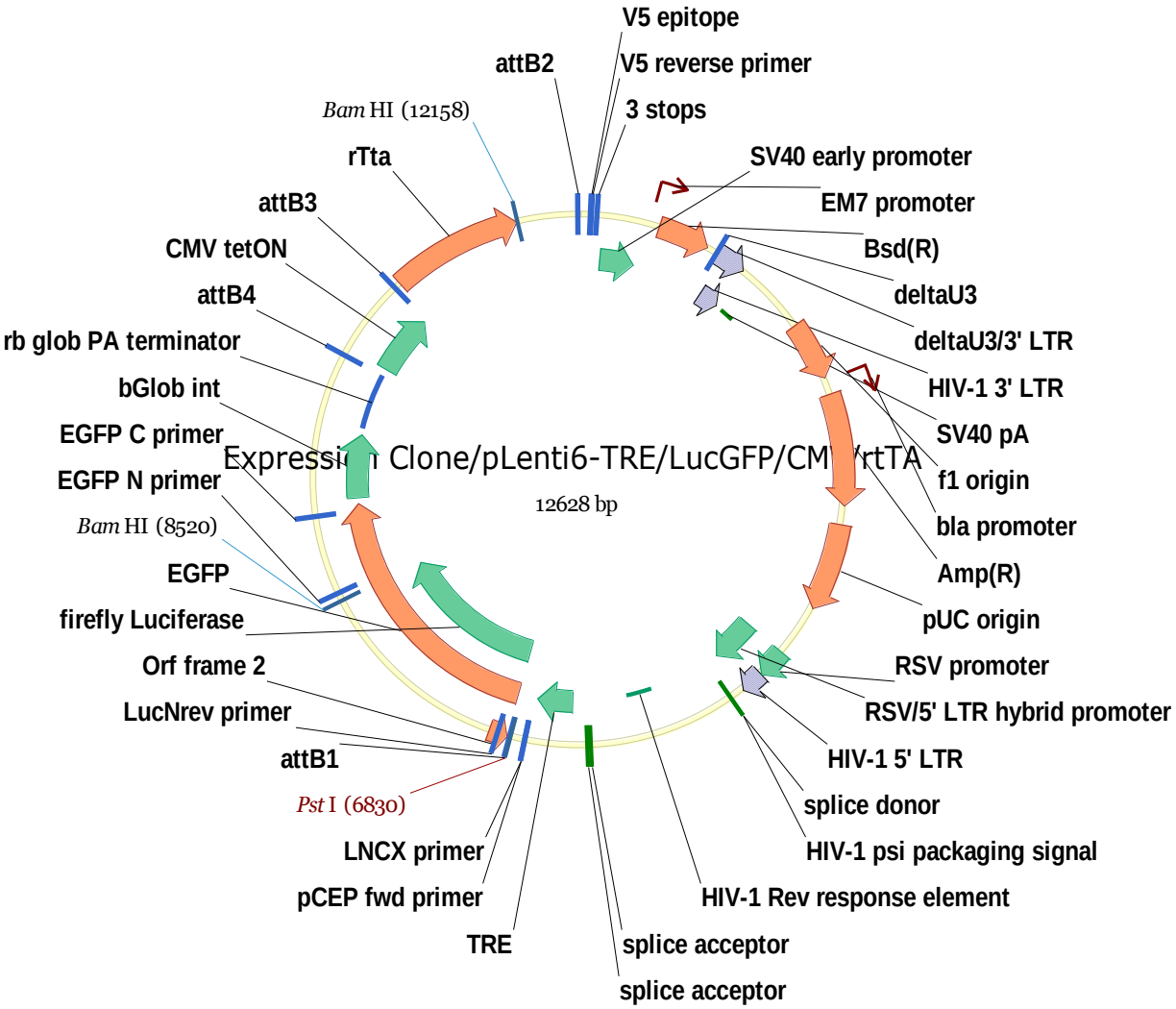

(4) Inducible expression vector for LucGFP ② pLenti TRE-LucGFP-CMV-rtTA advance

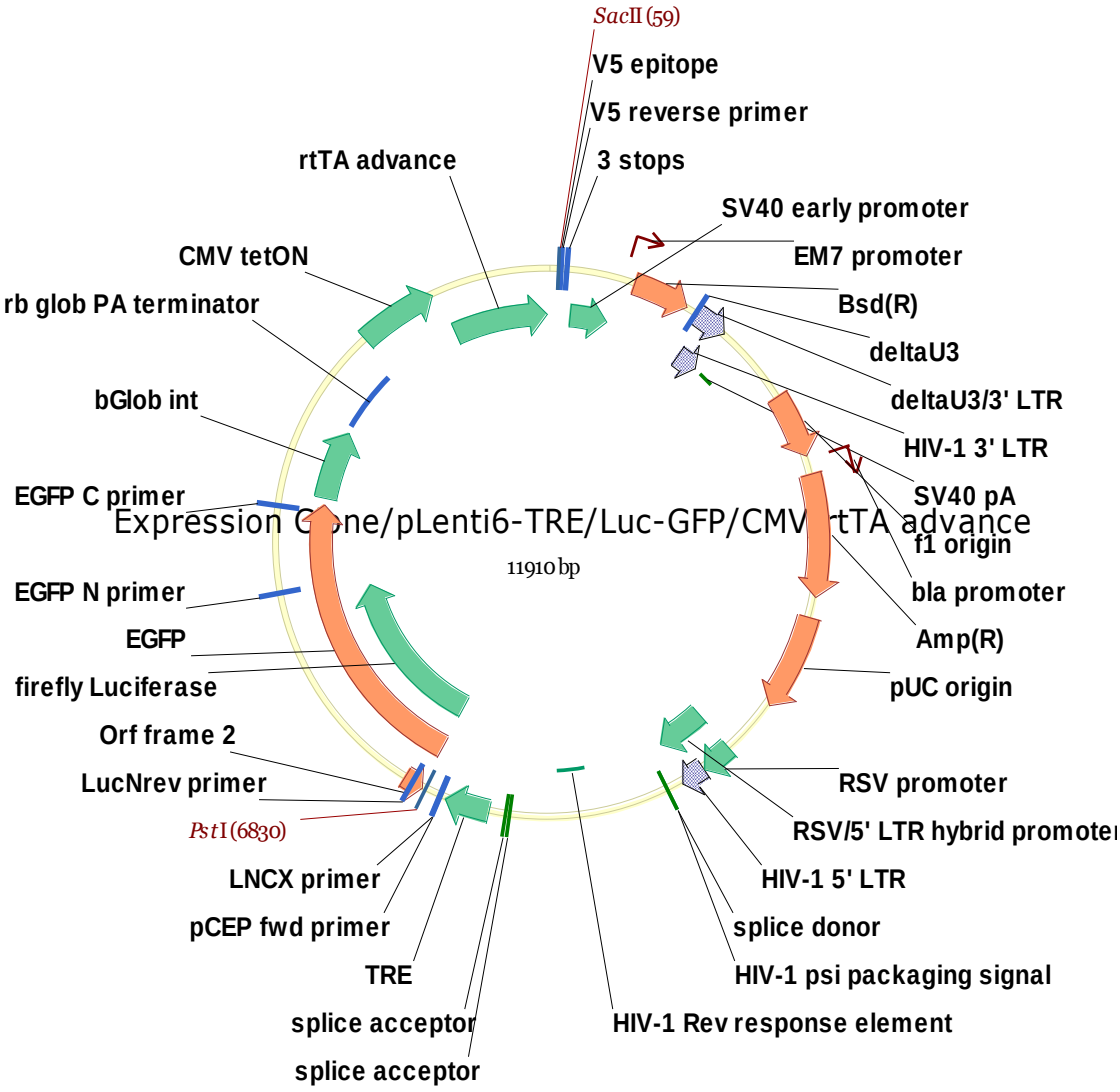

(5) Inducible expression vector for LucGFP ③ pLenti-TRE tight LucGFP CMV rtTA

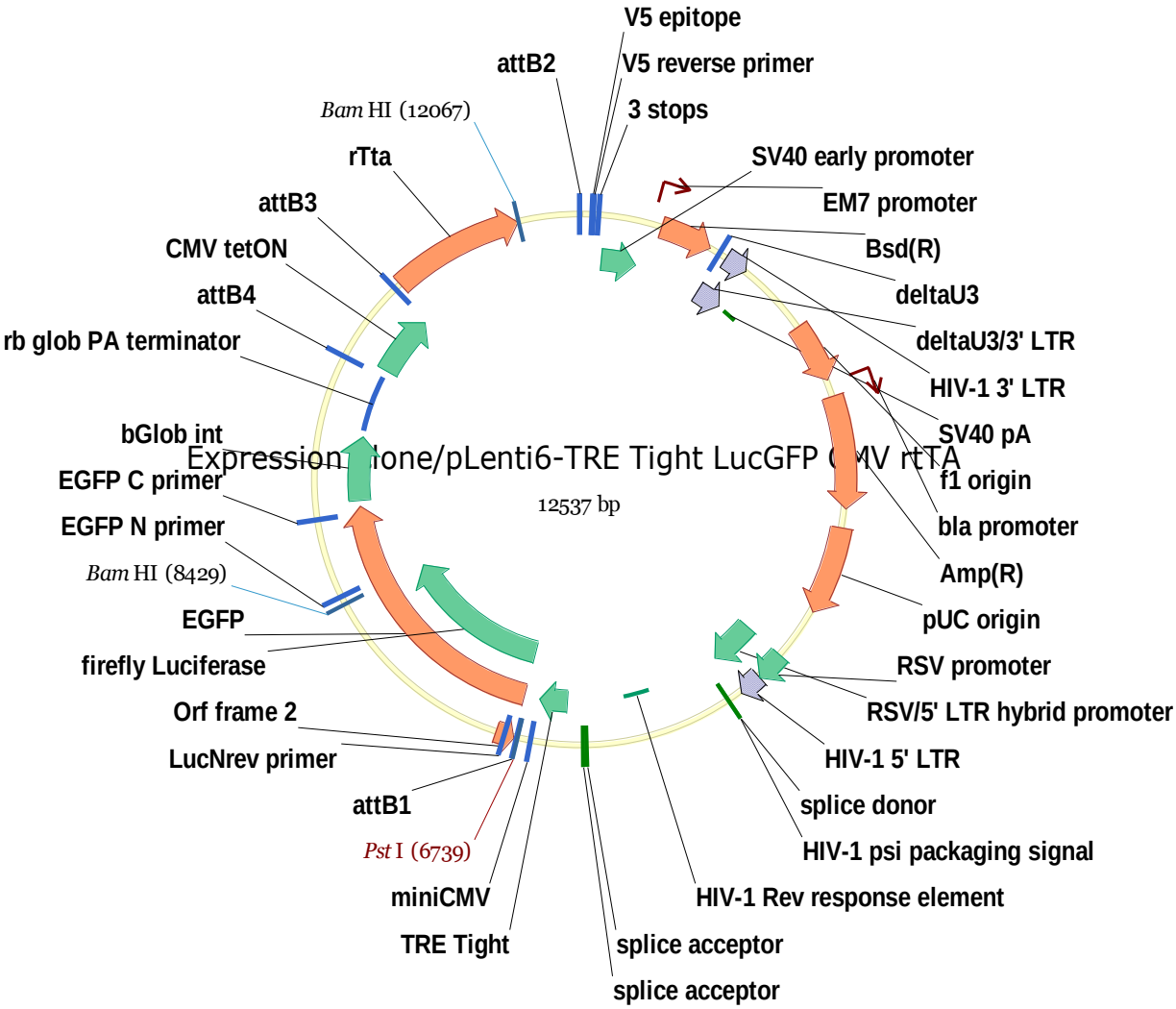

(6) Inducible expression vector for LucGFP ④ pLenti-TRE tight LucGFP CMV rtTA advance

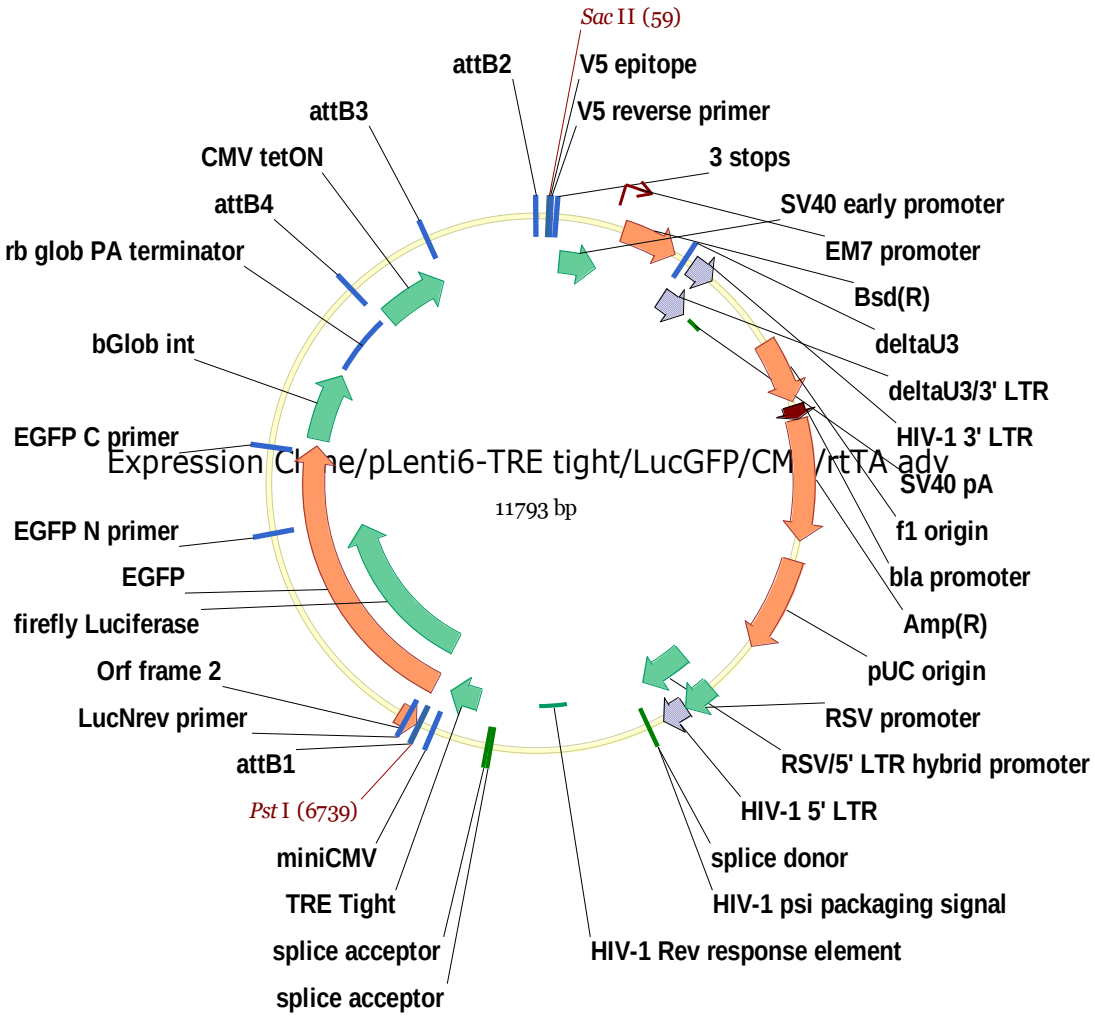

(7) Inducible expression vector for C/EBPβ: pLenti TRE tight C/EBPβ CMV rtTA advance

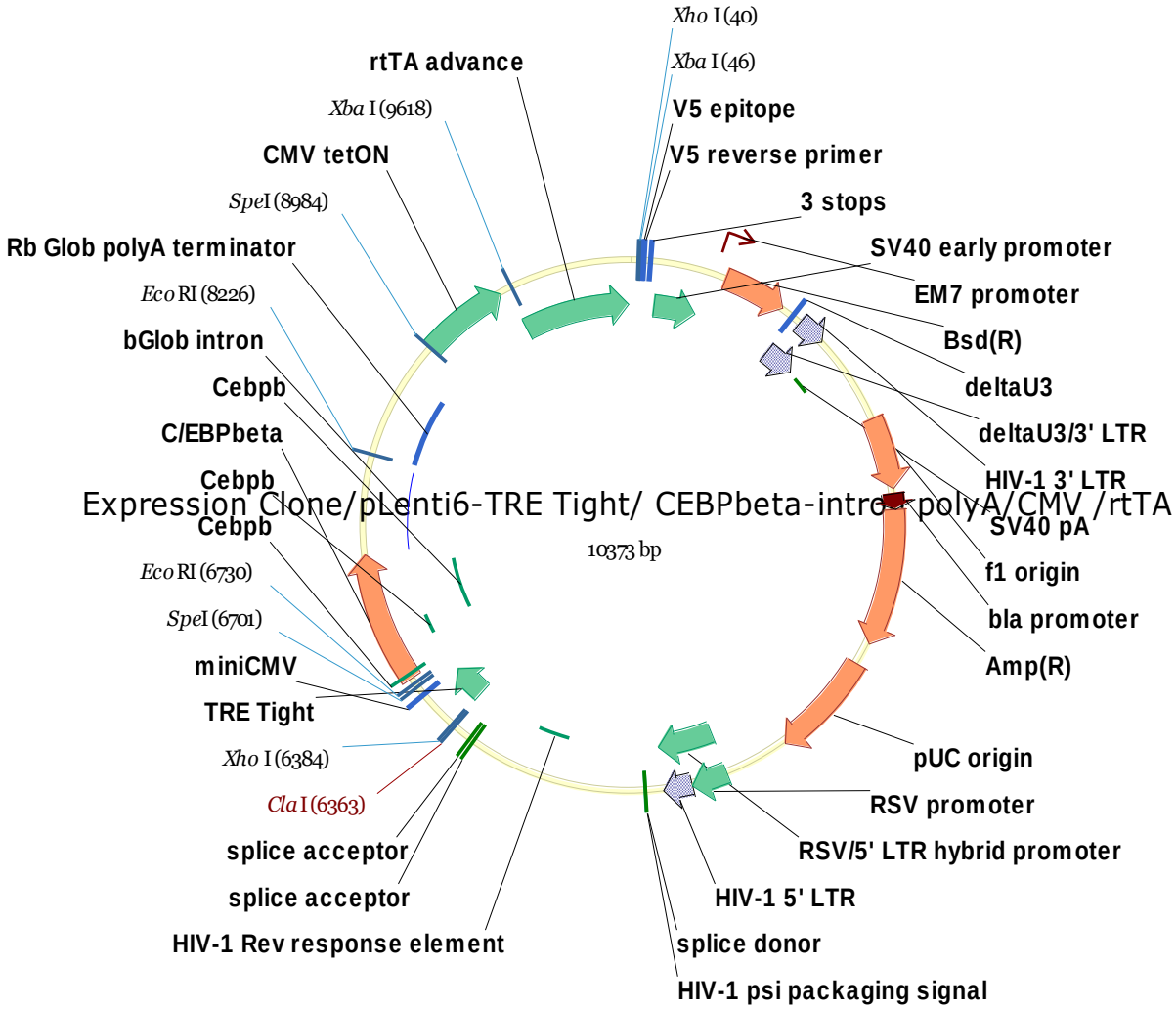

EXPRESSION VECTORS (FAT SPECIFIC)

(1) TRE LucGFP aP2 rtTA advance

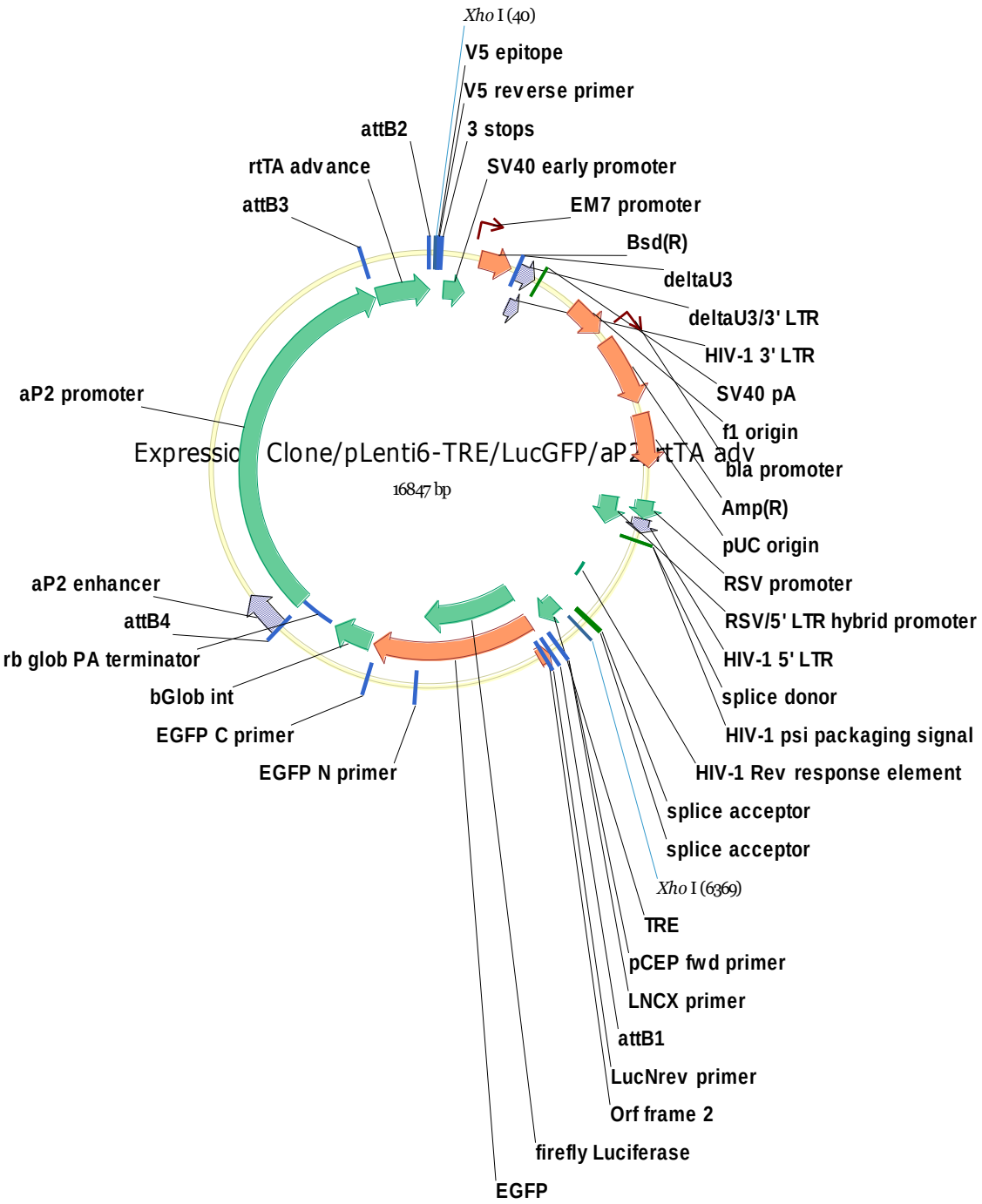

(2) TRE LucGFP short aP2 rtTA advance

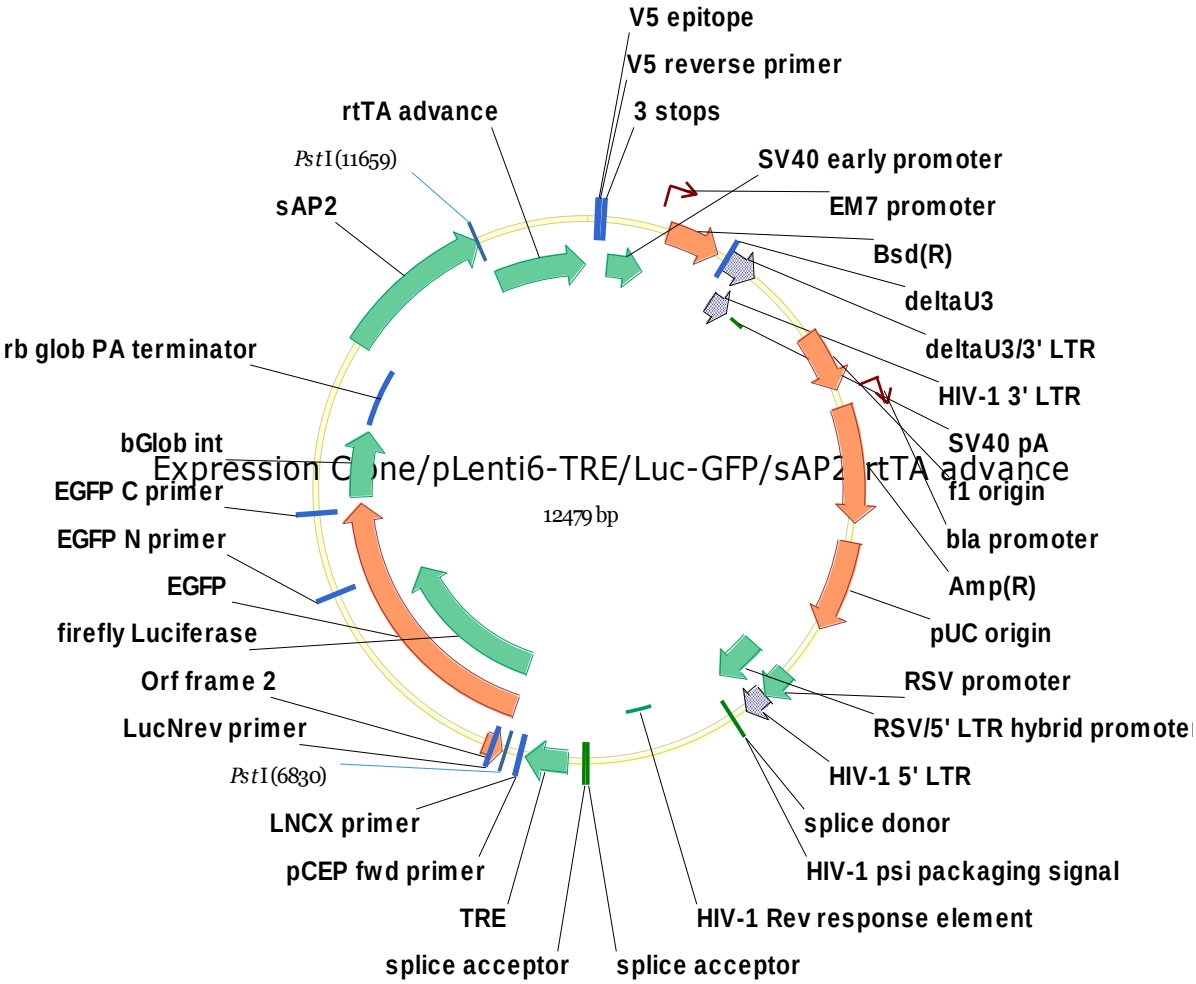

(3) TRE tight-LucGFP aP2 rtTA advance

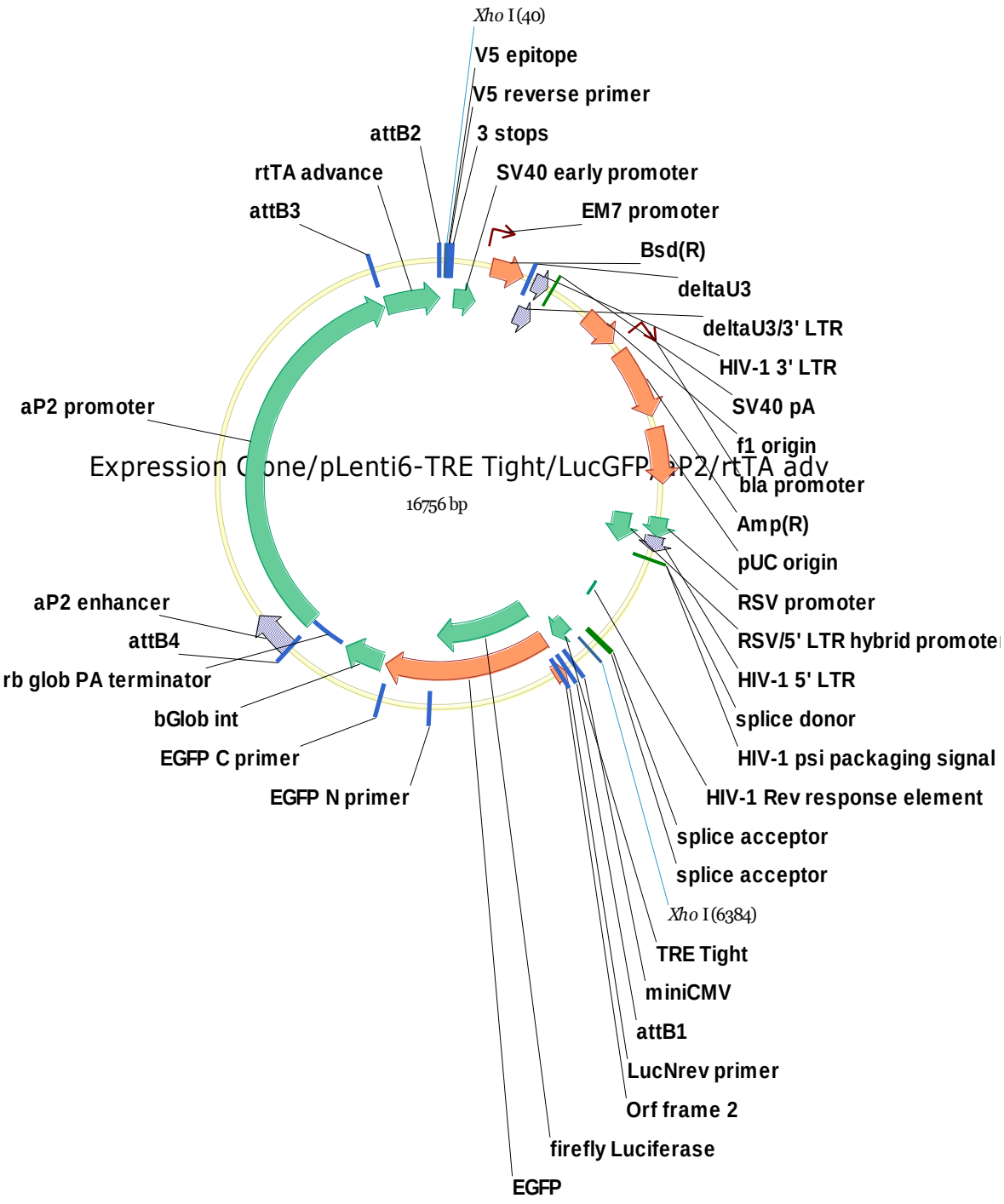

(4) TRE tight-LucGFP short aP2 rtTA advance

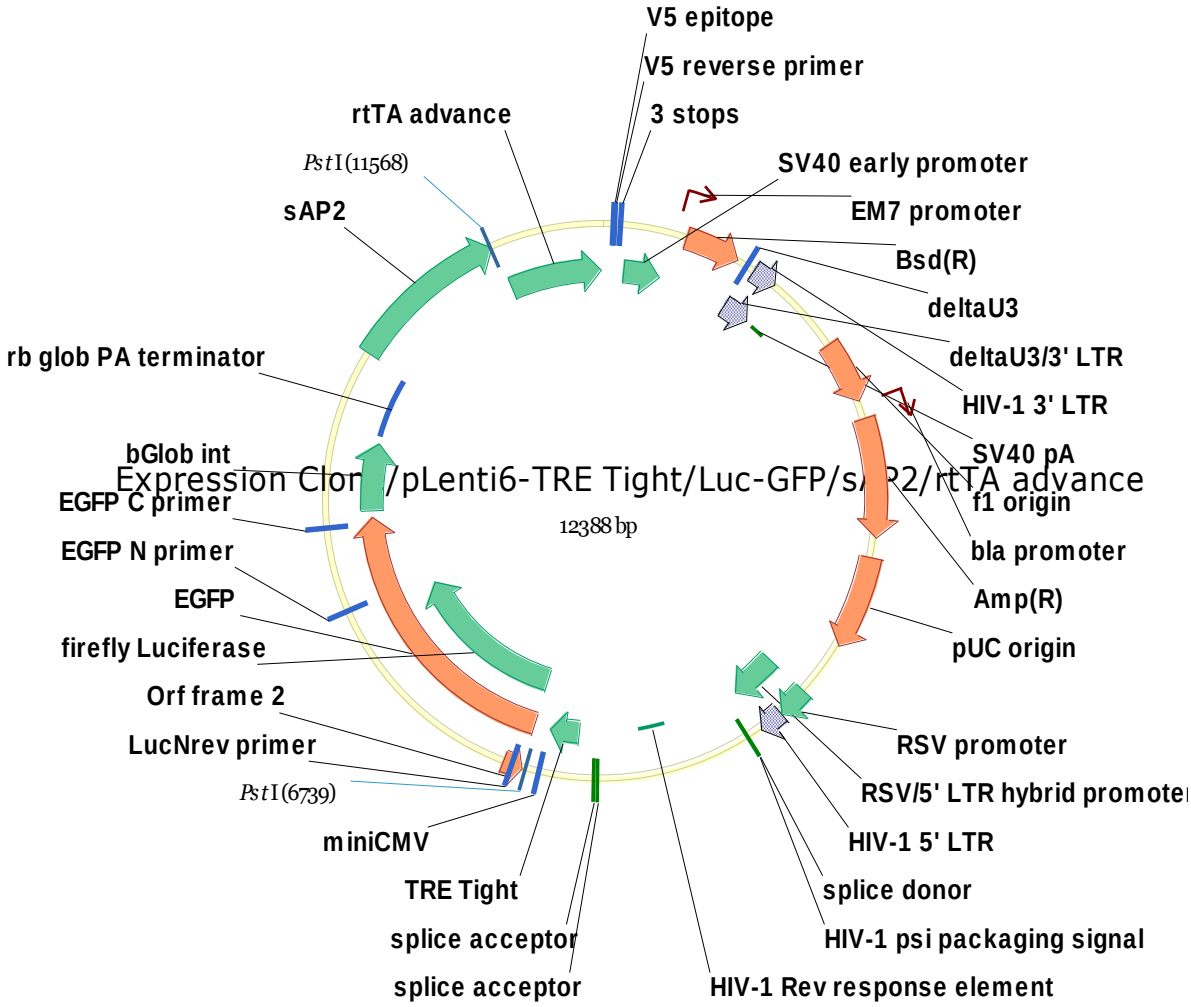

APPENDIX E - SEQUENCING RESULTS

(1) Modified lentiviral backbone vectors

pLenti TRE

ttatcgtttcagacccacctcccaaccccgaggggacccgacaggcccgaaggaatagaagaagaaggtggagagaga
gacagagacagatccattcgattagtgaacggatctcgacggtatcgatgaacccctt<u>cctcgagtttaccactccctatca
gtgatagagaaaagtgaaagtcgagtttaccactccctatcagtgatagagaaaagtgaaagtcgagtttaccactccct
atcagtgatagagaaaagtgaaagtcgagtttaccactccctatcagtgatagagaaaagtgaaagtcgagtttaccact
ccctatcagtgatagagaaaagtgaaagtcgagtttaccactccctatcagtgatagagaaaagtgaaagtcgagtttac
cactccctatcagtgatagagaaaagtgaaagtcgagctcggtacccgggtcgaggtaggcgtgtacggtgggaggcct
atataagcagagctcgtttagtgaaccgtcagatcgcctggagacgccatccacgctgttttgacctccatagaagacacc
gggaccgatccaactagtccagtgtggtggaattct</u>

The sequence underlined is TRE-CMV promoter.

pLenti TRE tight

ttttgctgtactttctatagtgaatagagttaggcagggatattcaccattatcgtttcagacccacctcccaaccccgaggg
gacccgacaggcccgaaggaatagaagaagaaggtggagagagagacagagacagatccattcgattagtgaacgga
tctcgacggtatccccgggatcgatggccctttcgtcttcact<u>cgagtttactccctatcagtgatagagaacgtatgtcgag
tttactccctatcagtgatagagaacgatgtcgagtttactccctatcagtgatagagaacgtatgtcgagtttactccctat
cagtgatagagaacgtatgtcgagtttactccctatcagtgatagagaacgtatgtcgagtttatccctatcagtgatagag
aacgtatgtcgagtttactccctatcagtgatagagaacgtatgt</u>cgaggtaggcgtgtacggtgggaggcctatataagc
agagctcgtttagtgaaccgtcagatcgcactagtcccggggctagtccagtgtggtggaattctgcagatatcaacaagt
ttgtacaaaaaagctgaacgagaaacgtaaaatgatataaatatcaatatattaaattagattttgcataaaaaacagac
tacataatactgtaaaacaca

The sequence underlined is TRE tight-CMV promoter.

(2) Entry clones

C/EBPβ

cagttccctactctcgcgttaacgctagcatggatctcgggccccaaataatgattttattttgactgatagtgacctgttcgt
tgcaacaaattgatgagcaatgctttttataatgccaactttgtacaaaaaagcaggcttattgatagactcgagcggcc
gccactgtgctggatatctgcagaattcgcgccacc<u>atggaagtggccaacttctactacgagcccgactgcctggcctac
ggggccaaggcggcccgcgccgcgccgcgcgcccccgccgccgagccggccattggcgagcacgagcgcgccatcgac
ttcagcccctacctggagccgctcgcgcccgccgcggacttcgccgcgcccgcgcccgcgcaccacgacttcctctccgac
ctcttcgccgacgactacggcgccaagccgagcaagaagccggccgactacggttacgtgagcctcggccgcgcgggcg
ccaaggccgcgccgcccgcctgcttcccgccgccgcctcccgcggcgctcaaggcggagccgggcttcgaacccgcggac
tgcaagcgcgcggacgacgcgcccgccatggcggccggtttcccgttcgccctgcgcgcctacctgggctaccaggcgac</u>

gccgagcggcagcagcggcagcctgtccacgtcgtcgtcgtccagcccgcccggcacgccgagccccgccgacgccaag
gccgcgcccgccgcctgcttcgcggggccgccggccgcgcccgccaaggccaaggccaagaagacggtggacaagctg
agcgacgagtacaagatgcggcgcgagcgcaacaacatcgcggtgcgcaagagccgcgacaaggccaagatgcgcaa
cctggagacgcagcacaaggtgctggagctgacggcggagaacgagcggctgcagaagaaggtggagcagctgtcgcg
agagctcagcaccctgcggaacttgttcaagcagctgcccgagccgctgctggcctcggcgggccactgctagcgcggcg
gtaccaagcttgtcgacgatatctctagagctgagaacttcagggtgagtttggggacccttgattgttctttcttttttcgcta
ttgtaaaattcatgttatatggaggggcaaagttttcagggtgttgtttagaatgggaagatgtcccttgtatcaccatgg
accctcatgataatttgtttctttcactttctactctgttgacaaccattgtctcctcttattttcttttcattttctgtaacttttt
cgttaaactttagcttgcatttgtaacgaatttttaaattcacttttgtttatttgtcagattgtaagtactttctctaatcacttt
tttttcaaggcaatcagggtatattatattgtacttcagcacagttttagagaacaattgttataattaaatgataaggtaga
atatttctgcatataaattctggctggcgtggaaatattcttattggtagaaacaactacaccctggtcatcatcctgcctttc
tctttatggttacaatgatatacactgtttgagatgaggataaaatactctgagtccaaaccgggcccctctgctaaccatg
ttcatgccttcttctctttcctacagctcctgggcaacgtgctggttgttgtgctgtctcatcattttggcaaagaattcactcc
tcaggtgcaggctgcctatcagaaggtggtggctggtgtggccaatgccctggctcacaaataccactgagatcttttcccc
tctgccaaaaattatggggacatcatgaagccccttgagcatctgacttctggctaataaaggaaatttattttcattgcaa
tagtgtgtgggaatttttttgtgtctctcactcggaaggacatatgggagggcaaatcatttaaaacatcagaatgagtattt
ggtttagagtttggcaacatatgccatatgctggctgccatgaacaaaggtggctataaagaggtcatcagtatatgaaac
agccccctgctgtccattccttattccatagaaaagccttgacttgaggttagatttttttttatattttgttttgtgttatttttttc
tttaacatccctaaaatttttccttacatgttttactagccagatttttcctcctctcctgactactcccagtcatagctgtccctc
ttctccacccaactttttctatacaaagttggcattataagaaagcattgcttatcaatttgttgcaacgaacaggtcactatc
agtcaaaataaaatcattatttgccatccagctgcagctctggcccgtgtctcaaaatctctgatgttacattgcacaagat
aa

The sequence underlined is C/EBPβ-βGlob intron-polyA; the highlighted sequences before and after C/EBPβ are attL1 and attL4 sites, respectively.

LucGFP

actgagcctttcgttttatttgatgcctggcagttccctactctcgcgttaacgctagcatggatctcgggccccaaataatg
attttattttgactgatagtgacctgttcgttgcaacaaattgatgagcaatgctttttataatgccaactttgtacaaaaaa
gcaggctccaccatggaagacgccaaaaacataaagaaaggcccggcgccattctatccgctggaagatggaaccgctg
gagagcaactgcataaggctatgaagagatacgccctggttcctggaacaattgcttttacagatgcacatatcgaggtg
gacatcacttacgctgagtacttcgaaatgtccgttcggttggcagaagctatgaaacgatatgggctgaatacaaatcac
agaatcgtcgtatgcagtgaaaactctcttcaattctttatgccggtgttgggcgcgttatttatcggagttgcagttgcgcc
cgcgaacgacatttataatgaacgtgaattgctcaacagtatgggcatttcgcagcctaccgtggtgttcgtttccaaaaag
gggttgcaaaaaattttgaacgtgcaaaaaagctcccaatcatccaaaaaattattatcatggattctaaaacggattac
cagggatttcagtcgatgtacacgttcgtcacatctcatctacctcccggttttaatgaatacgattttgtgccagagtccttc
gatagggacaagacaattgcactgatcatgaactcctctggatctactggtctgcctaaaggtgtcgctctgcctcataga
actgcctgcgtgagattctcgcatgccagagatcctatttttggcaatcaaatcattccggatactgcgattttaagtgttgtt
ccattccatcacggttttggaatgtttactacactcggatatttgatatgtggatttcgagtcgtcttaatgtatagatttgaa
gaagagctgtttctgaggagccttcaggattacaagattcaaagtgcgctgctggtgccaaccctattctccttcttcgcca
aaagcactctgattgacaaatacgatttatctaatttacacgaaattgcttctggtggcgctcccctctctaaggaagtcgg

ggaagcggttgccaagaggttccatctgccaggtatcaggcaaggatatgggctcactgagactacatcagctattctgat
tacacccgagggggatgataaaccgggcgcggtcggtaaagttgttccatttttgaagcgaaggttgtggatctggatac
cgggaaaacgctgggcgttaatcaaagaggcgaactgtgtgtgagaggtcctatgattatgtccggttatgtaaacaatcc
ggaagcgaccaacgccttgattgacaaggatggatggctacattctggagacatagcttactgggacgaagacgaacac
ttcttcatcgttgaccgcctgaagtctctgattaagtacaaaggctatcaggtggctcccgctgaattggaatccatcttgct
ccaacaccccaacatcttcgacgcaggtgtcgcaggtcttcccgacgatgacgccggtgaacttcccgccgccgttgttgtt
ttggagcacggaaagacgatgacggaaaaagagatcgtggattacgtcgccagtcaagtaacaaccgcgaaaaagttg
cgcggaggagttgtgtttgtggacgaagtaccgaaaggtcttaccggaaaactcgacgcaagaaaaatcagagagatcc
tcataaaggccaagaagggcggaaagatcgccgtgcgggatccaccggtcgccaccatggtgagcaagggcgaggagc
tgttcaccggggtggtgcccatcctggtcgagctggacggcgacgtaaacggccacaagttcagcgtgtccggcgagggc
gagggcgatgccacctacggcaagctgaccctgaagttcatctgcaccaccggcaagctgcccgtgccctggcccaccct
cgtgaccaccctgacctacggcgtgcagtgcttcagccgctaccccgaccacatgaagcagcacgacttcttcaagtccgc
catgcccgaaggctacgtccaggagcgcaccatcttcttcaaggacgacggcaactacaagacccgcgccgaggtgaag
ttcgagggcgacaccctggtgaaccgcatcgagctgaagggcatcgacttcaaggaggacggcaacatcctggggcaca
agctggagtacaactacaacagccacaacgtctatatcatggccgacaagcagaagaacggcatcaaggtgaacttcaa
gatccgccacaacatcgaggacggcagcgtgcagctcgccgaccactaccagcagaacaccccatcggcgacggcccc
gtgctgctgcccgacaaccactacctgagcacccagtccgccctgagcaaagaccccaacgagaagcgcgatcacatgg
tcctgctggagttcgtgaccgccgccgggatcactctcggcatggacgagctgtacaagtaaagcggccgcatcgataag
cttgtcgacgatatctctagagctgagaacttcagggtgagtttggggaccttgattgttctttctttttcgctattgtaaaat
tcatgttatatggaggggcaaagttttcagggtgttgtttagaatgggaagatgtcccttgtatcaccatggaccctcatg
ataattttgtttctttcacttttctactctgttgacaaccattgtctcctcttattttcttttcattttctgtaacttttcgttaaactt
tagcttgcatttgtaacgaatttttaaattcacttttgtttatttgtcagattgtaagtactttctctaatcacttttttttcaagg
caatcagggtatattatattgtacttcagcacagttttagagaacaattgttataattaaatgataaggtagaatatttctgc
atataaattctggctggcgtggaaatattcttattggtagaaacaactacaccctggtcatcatcctgcctttctctttatggt
tacaatgatatacactgtttgagatgaggataaaatactctgagtccaaaccgggcccctctgctaaccatgttcatgcctt
cttctctttcctacagctcctgggcaacgtgctggttgttgtgctgtctcatcattttggcaaagaattcactcctcaggtgca
ggctgcctatcagaaggtggtggctggtgtggccaatgccctggctcacaaataccactgagatctttttccctctgccaaa
aattatggggacatcatgaagccccttgagcatctgacttctggctaataaaggaaatttattttcattgcaatagtgtgtg
ggaatttttgtgtctctcactcggaaggacatatgggagggcaaatcatttaaaacatcagaatgagtatttggtttagag
tttggcaacatatgccatatgctggctgccatgaacaaaggtggctataaagaggtcatcagtatatgaaacagccccctg
ctgtccattccttattccatagaaaagccttgacttgaggttagatttttttttatattttgttttgtgttatttttttctttaacatc
cctaaaattttccttacatgttttactagccagatttttcctcctctcctgactactcccagtcatagctgtccctcttctcaccc
aacttttctatacaaagttggcattataagaaagcattgcttatcaatttgttgcaacgaacaggtcactatcagtcaaaat
aaaatcattatttgccatccagctgcagctctggcccgtgtctcaaaatctctgatgttacattgcacaag

The sequence underlined is LucGFP-βGlob intron-polyA; the highlighted sequences before and after LucGFP are attL1 and attL4 sites, respectively.

CMV

tccctactctcgcgttaacgctagcatggatctcgggcccctacaggtcactaataccatctaagtagttgattcatagtga
ctggatatgttgtgttttacagtattatgtagtctgtttttttatgcaaaatctaatttaatatattgatatttatatcattttacgt

ttctcgttcaacttttctatacaaagttgtattggctcatgtccaacattaccgccatgttgacattgattattgactagttatt
aatagtaatcaattacggggtcattagttcatagcccatatatggagttccgcgttacataacttacggtaaatggcccgcc
tggctgaccgcccaacgacccccgcccattgacgtcaataatgacgtatgttcccatagtaacgccaatagggactttcca
ttgacgtcaatgggtggagtatttacgctaaactgcccacttggcagtacatcaagtgtatcatatgccaagtacgccccct
attgacgtcaatgacggtaaatggcccgcctggcattatgcccagtacatgaccttatgggactttcctacttggcagtaca
tctacgtattagtcatcgctattaccatggtgatgcggttttggcagtacatcaatgggcgtggatagcggtttgactcacgg
ggatttccaagtctccaccccattgacgtcaatgggagtttgttttggcaccaaaatcaacgggactttccaaaatgtcgta
acaactccgccccattgacgcaaatgggcggtaggcgtgtacggtgggaggtctatataagcagagctcacaactttgtat
aataaagttgaacgagaaacgtaaaatgatataaatatcaatatattaaattagattttgcataaaaaacagactacata
atactgtaaaacacaacatatccagtcactatgaatcaactacttagatggtattagtgacctgtactgcagctctggcccg
tgtctcaaaatctctgatgtt

The sequence underlined is CMV promoter; the highlighted sequences before and after CMV are attR4 and attR3 sites, respectively.

aP2

aacgctagcatggatctcgggcccctacaggtcactaataccatctaagtagttgattcatagtgactggatatgttgtgttt
tacagtattatgtagtctgtttttttatgcaaaatctaatttaatatattgatatttatatcattttacgtttctcgttcaacttttc
tatacaaagttgatatcgaattcccagcaggaatcaggtagctggagaatcgcacagagccatgcggattcttggcaagc
catgcgacaaaggcagaaatgcacatttcacccagagagaagggattgtagtcagcaggaagtcaccacccagagagc
aaatggagttcccagatgcctgacatttgccttcttactggatcagagttcactagtggaagtgtcacagcccaaacactcc
cccaaaggctcagcccttccttgccttgtaacaatcaagccgctcctggatgaactgctccgccctctgtctctttggcaggg
ttggagcccactgtggcctgagcgacttctatggctccctttctgtgattttcatggtttctgagctcttttcccccgctttatga
ttttctctttttgtctctctcttgctaaacctccttcgtatatgccctctcaggtttcatttctgaatcatctactgtgaactattcc
cattgtttgccagaagccccctggttcttccttctagaagttcaggccaggagtcagaaccataccacccaccacaactgt
aatggacaaaaaaatgaagtgaaaccttggtctttaagtccagtcctaggctacaccctgtaaggctggtgattaaatac
attttacttactcagttcccgtttctgaaagcaggggctcaggttaaagcaagtgggggactcagagtgtctaagattacag
gcagagtggttccagtgtctgtttctagcctttctctggaaacccacacaagctgtttctcctactagaatgccaccgtttac
atagtggtggcctgatttctactttcagaaccttgagcagtttctgtatgccatgcccttgctgcgcgcccactgataaaag
ctctgtgaactggtttctcagagcatcccgtggttcttaagatcttttctgctttgttgtgttttgattttggttttggttttttatca
ggatggggtttctctggctgtcttgtaactctgtagactaggctggcctctaactcaagacctgaatgcacctgcttcaaata
catggccaccttccgactggttcttaagatctttatgacccgatagtgatctctgcagccctaacccttctgtcttaatatattt
aagacattagatatcttcaaatgctatgcctgtcctggctcagctctgagattccgagatatgtcctcagccccatatccga
aggcaaagccaggctgctcccattgtagtccttttctccctggctctgaggaaatactcagcctgctgtgtctgatttttttgc
ttgtttgtttttgtttatttgttgtctggctctttttaaaattttaacacagaacatctttttttttttttttttttttttgtatctgca
catcactatgtaccaagcacaactggcacttactagggatttaatgtctttttttgtatttaggtctatttgtagaaagtaagt
tatatatgtactcaggcttaaaaatatataagatgcaagcagttgagatggtgaaagtaataagacacaaacagagcaa
atgtgaagtgtgtgtttgtgtgtgtttttgtgtgtgtgtgtgtgtgggtgtgtgggtgcacacacatgtgcttatgctcatgcat
gtgtgcttgtacgtggttgcatatctgccctcatggagatatgtgtgtgtgtgtgtgtgtgtgtgtgtgtgtgtgtgttggca
ggggggttacatggtgcagctggcctgctggtaagttcttctctgctttttttctggtagagtgtcacctttgcttccacttaatt
cctgatgggtttgctttatgaaatgaagacaaagtaggtcacagtttatctgcagaaagcactttgaggtcccctcccccac

cgtgggtccctgcttgcacaccctgagctatgtgtgaagaggttcttttatgagcaagaaggcaaatgaagaagttatcta
agagccttcaaagcactctcagtctgtctttacctgaggcagagtctgtggcttactcattctttgctaaacggttgccatctt
gagatcaaggagtcagtgcttagtcatcggaaccatgcatgtaaagaagaacatactggcctagctggacaggggacct
aggacagtcctggtaagtgacctcatcagggagagaaggaaaaaaaatgtgcctgcatttcctgttcagggctcaccttа
cagttgccagcaagcacccgaatgcacttagaaagcagcattaacaaagtaagtttgcctccaataaaaggggatcctgg
atgtgaaccctcaccttagctggcctgtacaagctggaagctctccctgccaacggggctccgtcgttactcttcattatcta
gagtggggtctgtttcctcactaattaaaaattgtcagaaatgatattctcatttcctccgaaagaagtaaacacaggcaa
aggttagaaggatgcattccacagaaacggcccattgaggagcaaagtgcaaggcaaacagcctggaccagagggcct
gccctgtcagccctgagattctgagatgtgacctcagccccacatccccacagccaagccaggctgttcccactgcagacc
cttcccctcctccagctttcaggctgttcccactgcagacccttcccctcctccagctttcaggctgttcccactgcagaccct
tcccctcctccagctttcaggctgttcccactgcagacccttcccctcctccagctttcaggctgttcccattgcagacccttc
cccacggctctgaggaagtactcagccagctgtgtctgtggctgttgttgggcatcccaggttcttttgtaacttttaatttt
ggagacacactcattgctaaattagctaggatggccttggactcactctgtggctcaggagagcagcgaacttaggggatt
ctcctggctcagcctcctgtggtgtttctttgtttgtttttgtttttactttgctttaacaggaccctcaggagcctggtctgttaa
gattcccttggtatatcttatgggatatccgattgtatctcatagtgaatgaatctggctaaaagttactgcctgacggttgg
tctttgcttactaggaacaaactcacacgtttgccctgatttacagatacccccatggccatagttgagtgaaattaactgc
acatggcactaagccagccatcttgtagttcctcggttccccagtgttgtggcggttgtcatctatcttcagctgacaattcct
ttgttctggaaggcccttctggtgtcatgtcagcttacattgtgcggatgctctggacagtgggtccctaactgtcccctgtac
accgtctttcccagtgtgggaaacatgttccttgctccgtggatccccagtggtcagcctgtgcctaaggcatgtgtgaata
aacgggtggacttggtgtcactgtgctgcgctaccagttccaagagaaacagagcacagagcacagagcacatgtgaaa
ttctagcaaccacattagaaaagtaaaaacaaacaaacaagcaaataaaaacaaattagttttagtaaaatatttcactt
ggcttgccttaattatggttattccaacatatattcaatgtaagaaattttcacgatgcattgcattttatattaacttcaactg
tgatacatactgtacactaacagtcatcttgagtcagactctttttttgaaatacttgttcattatttaaagttcacaaaaatt
atagttaaaaaatttagattgatgaattcaagttgtttcacacattttatttttacatttaattaaagttgagctttcttgttata
ttagccacctgtcggaggcagaagtagttgtgtaagtgcagaagtttacatgggctggctctacagcacgtctaacccata
gcactataatccacatgcagtcagcacagcgggctaatcgcttgagaacatgtctaagttagggatcagcatacgtttcca
ataaaacaatttagaacattatcaaaattattcctgcattaaaatcgcttattttatttgagttgcaatccaggggtctta
tccagtaggaagcctgagtctgagagtagtccatagtgggtgaaagttgttcccctgacactagcagatgcgattaaaagt
tgttactgtgagttaaatttatcaaacttttacagtagcccattttcctacagaaaatatcatgtttcagagtctgtttcccca
gactttgggggctggtagggacttgggagcaggtacttctcagcgagcccctgtacagcagtccatctctctctaacaccct
gaaatgtgggtgtgctcgcaggcactggtgtacatgtgaacatctcccatcattctgctgtgaggcagggaggctgagaaa
ctggattactttataaaagctatctcagatgagtcactgtgtcaaagaagaaaacaggttttgataattcatgaccacatta
cttctgatcattcacataaacccacaatctttaggtctgcatgaaattaaaacttacaatatatttcaaaaatgaaatgagg
gacatattttgcattgggacccatttttgaagggtctgtaaaaatgagtactacatggctatttacgaatgggaagaataag
gcttaacttttaatgtaattaaatctgtgcactacattcctgagcaatgagcagaatgtattttaagtatgtattaaatatttg
aaattataaatctaggccgctgtagcccgcatccagaggcaggggcagctaggtttctttgagttagagaccagcctggtc
taggtagtaagttccaggactaccagagctgtgcagcgagactgtctcaaaaaccaaaccaaaccaaaacccaacccaa
accaaacaaagccaaacaacaacaacaaaaacaaaaaaacccaccaaaaaaaccaaggaaacaaaacaaccaaaa
atcaaaaaactaggctactttaaaatgtcattatttatttgttaaaattcctgagataaacactattctaacaaaagagcc
attaagactaagaatctctaagatagtttttatgttctcaaattcagaagaactaaacacattattgcagtattaataaaat
aaaaactcaagataagaaggtcaaatgtgtccaagataattgtctcctccacaatgaggcaaatccataaggaataatg

gggggaagttcaatgcattagcttttgacagtcaaaacaggaacctttaaaatactctgttcatggttaaaaataatttgtactctaagtccagtgatcattgccagggagaaccaaagttgagaaatttctattaaaaacatgactcagaggaaaacatacagggtctggtcatgaaggaaatgatctggcccccattggtcactcctacagtcacatggtcagggcatctttaaaagtgagctatctggacttcagaggctcatagcaccctcctgtgctgcagacaactttgtataataaagttgaacgagaaacgtaaaatgatataaatatcaatatattaaattagattttgcataaaaaacagactacataatactgtaaaacacaacatatccagtcactatgaatcaactacttagatggtattagtgacctgtactgcagctctggcccgtgtctcaaaatctctgatgtta

The sequence underlined is full length aP2 promoter; the highlighted sequences before and after aP2 are attR4 and attR3 sites, respectively.

short aP2

tctcgcgttaacgctagcatggatctcgggcccctacaggtcactaataccatctaagtagttgattcatagtgactggatatgttgtgttttacagtattatgtagtctgtttttttatgcaaaatctaatttaatatattgatatttatatcattttacgtttctcgttcaacttttctatacaaagttgatatcgaattcccagcaggaatcaggtagctggagaatcgcacagagccatgcggattcttggcaagccatgcgacaaaggcagaaatgcacatttcacccagagagaagggattgtagtcagcaggaagtcaccacccagagagcaaatggagttcccagatgcctgacatttgccttcttactggatcagagttcactagtggaagtgtcacagcccaaacactcccccaaaggctcagcccttccttgccttgtaacaatcaagccgctcctggatgaactgctccgccctctgtctcttttggcagggttggagcccactgtggcctgagcgacttctatggctccctttctgtgattttcatggtttctgagctcttttccccgctttatgattttctcttttgtctctctcttgctaaacctccttcgtatatgccctctcaggtttcatttctgaatcatctactgtgaactattcccattgtttgccagaagccccctggttcttccttctagaagttcaggccaggagtcagaaccccgggcggccgcgggcccgccggcgcccaacccaaaccaaacaaagccaaacaacaacaacaaaaacaaaaaaacccaccaaaaaaaccaaggaaacaaaacaaccaaaaatcaaaaaactaggctactttaaaatgtcattatttatttttgttaaaattcctgagataaacactattctaacaaaagagccattaagactaagaatctctaagatagtttttatgttctcaaattcagaagaactaaacacattattgcagtattaataaaataaaaactcaagataagaaggtcaaatgtgtccaagataattgtctcctccacaatgaggcaaatccataaggaataatgggggggaagttcaatgcattagcttttgacagtcaaaacaggaacctttaaaatactctgttcatggttaaaaataatttgtactctaagtccagtgatcattgccagggagaaccaaagttgagaaatttctattaaaaacatgactcagaggaaaacatacagggtctggtcatgaaggaaatgatctggcccccattggtcactcctacagtcacatggtcagggcatctttaaaagtgagctatctggacttcagaggctcatagcaccctcctgtgctgcagacaactttgtataataaagttgaacgagaaacgtaaaatgatataaatatcaatatattaaattagattttgcataaaaaacagactacataatactgtaaaacacaacatatccagtcactatgaatcaactacttagatggtattagtgacctgtactgcagctctggcccgtgtctcaaaatctctg

The sequence underlined is short aP2 promoter; the highlighted sequences before and after short aP2 are attR4 and attR3 sites, respectively.

rtTA

gtcttccgactgagcctttcgttttatttgatgcctggcagttccctactctcgcgttaacgctagcatggatctcgggccccaaataatgattttattttgactgatagtgacctgttcgttgcaacaaattgatgagcaatgctttttataatgccaactttgtataataaagttgatccagcctccgcggccccgaattcatatgtctagattagataaaagtaaagtgattaacagcgcattagagctgcttaatgaggtcggaatcgaaggtttaacaacccgtaaactcgcccagaagcttggtgtagagcagcctacactgtattggcatgtaaaaaataagcgggctttgctcgacgccttagccattgagatgttagataggcaccatactcacttttgccctttaaaaggggaaagctggcaagatttttttacgcaataacgctaaaagttttagatgtgctttactaagtcatcgcaatgga

gcaaaagtacattcagatacacggcctacagaaaaacagtatgaaactctcgaaaatcaattagccttttttatgccaaca
aggtttttcactagagaacgcgttatatgcactcagcgctgtggggcattttactttaggttgcgtattggaagatcaagag
catcaagtcgctaaagaagaaagggaaacacctactactgatagtatgccgccattattacgacaagctatcgaattattt
gatcaccaaggtgcagagccagccttcttattcggccttgaattgatcatatgcggattagaaaaacaacttaaatgtgaa
agtgggtccgcgtacagccgcgcgcgtacgaaaaacaattacgggtctaccatcgagggcctgctcgatctcccggacga
cgacgccccgaagaggcggggctggcggctccgcgcctgtccttttctccccgcgggacacacgcgcagactgtcgacgg
ccccccgaccgatgtcagcctgggggacgagctccacttagacggcgaggacgtggcgatggcgcatgccgacgcgct
agacgatttcgatctggacatgttgggggacggggattccccgggtccgggatttacccccacgactccgccccctacgg
cgctctggatatggccgacttcgagtttgagcagatgtttaccgatgcccttggaattgacgagtacggtgggtagggggc
gcgaggatccagacatgataagatacattgatgagtttggacaaaccacaactagaatgcagtgaaaaaaatgctttatt
tgtgaaatttgtgatgctattgctttatttgtaaccattataagctgcaataaacaagttaacaacaacaattgcattcatttt
atgtttcaggttcagggggaggtgtgggaggttttttaaagcaagtaaaacctctacaaatgtggtatggctgattatgatc
ctgcaagcctcgtcgtctggccggaccacgctatctgtgcaaggtccccggacgcgcgctccatgagcagagcgcccgcc
gccgaggcaagactcgggcggcgccctgcccgtcccaccaggtcaacaggcggtaaccggcctcttcatcgggaatgcg
cgcgaccttcagcatcgccggcatgtcccctggcggacgggaagtatcagctcgaccaagcccagctttcttgtacaaag
ttggcattataagaaagcattgcttatcaatttgttgcaacgaacaggtcactatcagtcaaaataaaatcattatttgcca
tccagctgcagctctggcccgtgtctcaaaatctctgatgttacattgcacaagataaaaatat

The sequence underlined is rtTA; the highlighted sequences before and after rtTA are attL3 and attL2 sites, respectively.

rtTA advance

agttccctactctcgcgttaacgctagcatggatctcgggccccaaataatgattttattttgactgatagtgacctgttcgtt
gcaacaaattgatgagcaatgctttttataatgccaactttgtataataaagttgggggacaactttgtataataaagttg
gcaggcttcaccatgtctagactggacaagagcaaagtcataaacggcgctctggaattactcaatggagtcggtatcga
aggcctgacgacaaggaaactcgctcaaaagctgggagttgagcagcctaccctgtactggcacgtgaagaacaagcgg
gccctgctcgatgccctgccaatcgagatgctggacaggcatcatacccacttctgccccctggaaggcgagtcatggcaa
gactttctgcggaacaacgccaagtcattccgctgtgctctcctctcacatcgcgacggggctaaagtgcatctcggcaccc
gcccaacagagaaacagtacgaaaccctggaaaatcagctcgcgttcctgtgtcagcaaggcttctccctggagaacgca
ctgtacgctctgtccgccgtgggccactttacactgggctgcgtattggaggaacaggagcatcaagtagcaaaagagga
aagagagacacctaccaccgattctatgcccccacttctgagacaagcaattgagctgttcgaccggcagggagccgaac
ctgccttccttttcggcctggaactaatcatatgtggcctggagaaacagctaaagtgcgaaagcggcgggccggccgac
gcccttgacgattttgacttagacatgctcccagccgatgcccttgacgactttgaccttgatatgctgcctgctgacgctctt
gacgattttgaccttgacatgctccccgggtaactaccagctttcttgtacaaagttggcattataagaaagcattgcttat
caatttgttgcaacgaacaggtcactatcagtcaaaataaaatcattatttgccatccagctgcagctctggcccgtgtctc
aaaatctctgatgttacattgcacaagata

The sequence underlined is rtTA advance; the highlighted sequences before and after rtTA advance are attL3 and attL2 sites, respectively.

APPENDIX F – MAPS OF LENTIVIRAL PACKAGING SYSTEM

(1) ViraPower™ 3-plasmid packaging system

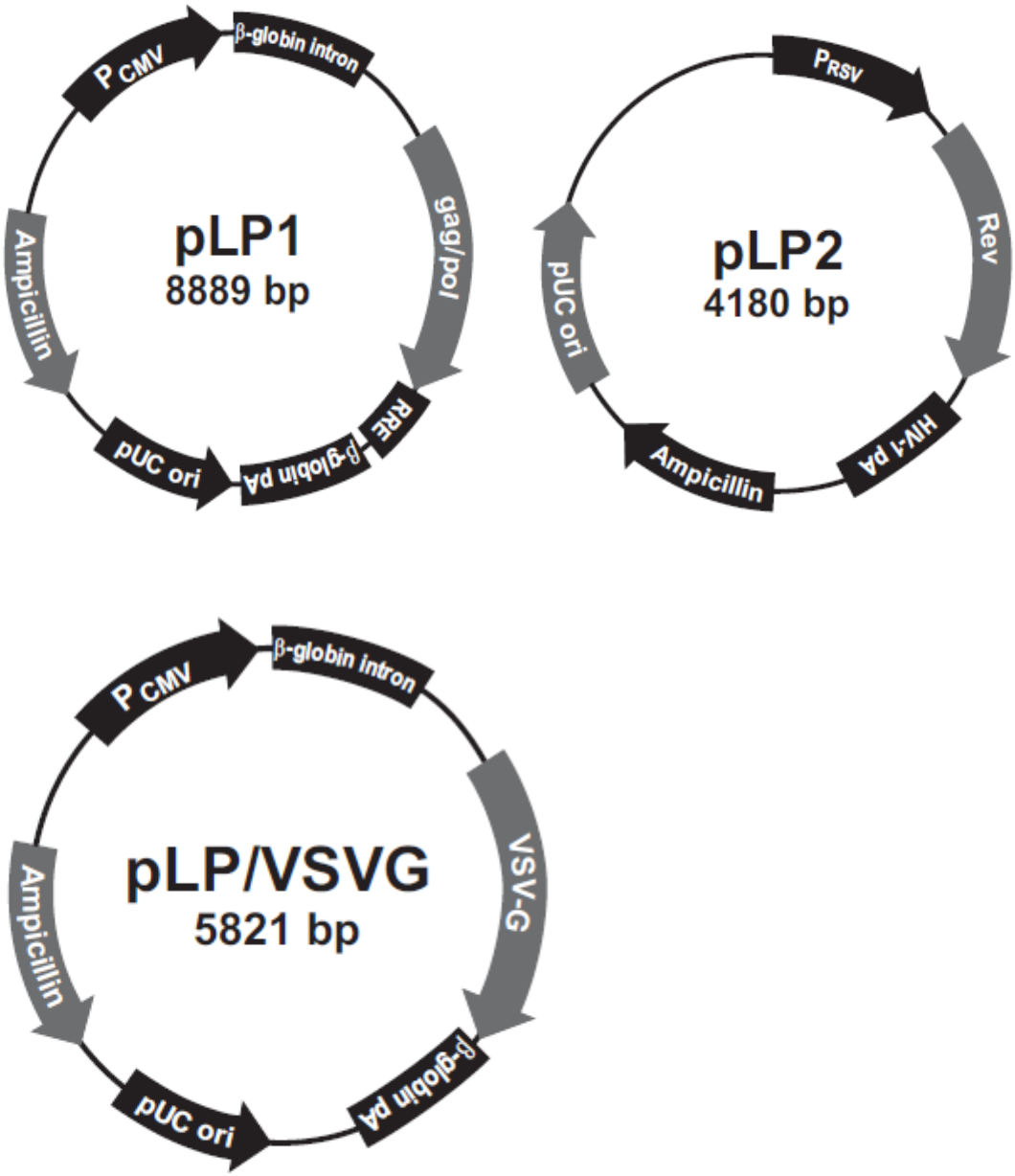

Maps of pLP packaging plasmids for producing lentivirus

The pLP packaging system consists of three different plasmids, pLP1 to express gag/pol protein, pLP2 to express Rev protein and pLP/VSVG to express envelope protein VSV-G.

(2) psPAX2 2-plasmid packaging system

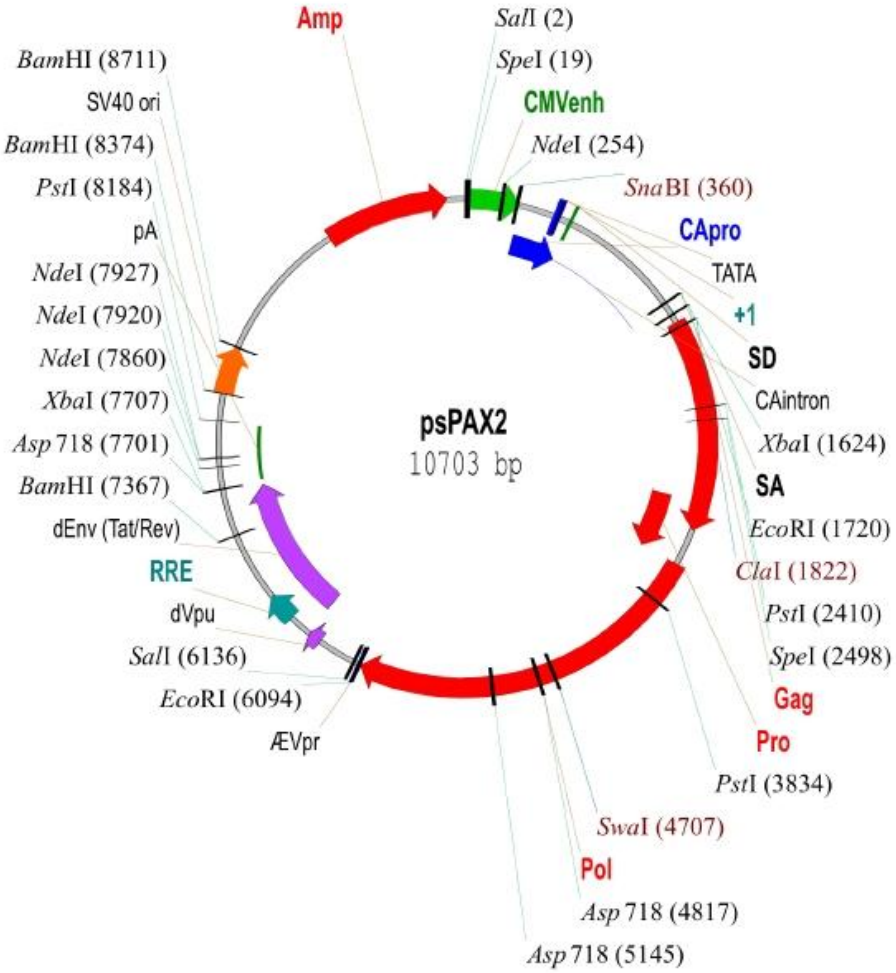

Map of psPAX2 packaging plasmid for producing lentivirus

The psPAX2 plasmid contains a robust CAG promoter driving the efficient expression of the three packaging proteins: gag, pol and rev.

There is another plasmid pCMV-VSVG in this packaging system, but no map of it was available from the people providing it.

REFERENCES

Accili, D., Nakae, J., Kim, J.J., Park, B.C., and Rother, K.I. (1999). Targeted gene mutations define the roles of insulin and IGF-I receptors in mouse embryonic development. J Pediatr Endocrinol Metab *12*, 475-485.

Adachi, A., Gendelman, H.E., Koenig, S., Folks, T., Willey, R., Rabson, A., and Martin, M.A. (1986). Production of acquired immunodeficiency syndrome-associated retrovirus in human and nonhuman cells transfected with an infectious molecular clone. J Virol *59*, 284-291.

Akira, S., Isshiki, H., Sugita, T., Tanabe, O., Kinoshita, S., Nishio, Y., Nakajima, T., Hirano, T., and Kishimoto, T. (1990). A nuclear factor for IL-6 expression (NF-IL6) is a member of a C/EBP family. EMBO J *9*, 1897-1906.

Amado, R.G., and Chen, I.S. (1999). Lentiviral vectors--the promise of gene therapy within reach? Science *285*, 674-676.

Arsenijevic, D., Onuma, H., Pecqueur, C., Raimbault, S., Manning, B.S., Miroux, B., Couplan, E., Alves-Guerra, M.C., Goubern, M., Surwit, R.*, et al.* (2000). Disruption of the uncoupling protein-2 gene in mice reveals a role in immunity and reactive oxygen species production. Nature genetics *26*, 435-439.

Au, H.C., Seo, B.B., Matsuno-Yagi, A., Yagi, T., and Scheffler, I.E. (1999). The NDUFA1 gene product (MWFE protein) is essential for activity of complex I in mammalian mitochondria. Proc Natl Acad Sci U S A *96*, 4354-4359.

Baranowski, M. (2008). Biological role of liver X receptors. J Physiol Pharmacol *59 Suppl 7*, 31-55.

Barbatelli, G., Murano, I., Madsen, L., Hao, Q., Jimenez, M., Kristiansen, K., Giacobino, J.P., De Matteis, R., and Cinti, S. (2010). The emergence of cold-induced brown adipocytes in mouse white fat depots is determined predominantly by white to brown adipocyte transdifferentiation. Am J Physiol Endocrinol Metab *298*, E1244-1253.

Barbera, M.J., Schluter, A., Pedraza, N., Iglesias, R., Villarroya, F., and Giralt, M. (2001). Peroxisome proliferator-activated receptor alpha activates transcription of the brown fat uncoupling protein-1 gene. A link between regulation of the thermogenic and lipid oxidation pathways in the brown fat cell. J Biol Chem *276*, 1486-1493.

Baron, U., and Bujard, H. (2000). Tet repressor-based system for regulated gene expression in eukaryotic cells: principles and advances. Methods Enzymol *327*, 401-421.

Bray, G.A. (2004). Medical consequences of obesity. J Clin Endocrinol Metab *89*, 2583-2589.

Brown, B.D., Cantore, A., Annoni, A., Sergi, L.S., Lombardo, A., Della Valle, P., D'Angelo, A., and Naldini, L. (2007). A microRNA-regulated lentiviral vector mediates stable correction of hemophilia B mice. Blood *110*, 4144-4152.

Brown, B.D., and Naldini, L. (2009). Exploiting and antagonizing microRNA regulation for therapeutic and experimental applications. Nat Rev Genet *10*, 578-585.

Buck, M., Poli, V., van der Geer, P., Chojkier, M., and Hunter, T. (1999). Phosphorylation of rat serine 105 or mouse threonine 217 in C/EBP beta is required for hepatocyte proliferation induced by TGF alpha. Molecular cell *4*, 1087-1092.

Bukowiecki, L.J. (1984). Mechanisms of stimulus-calorigenesis coupling in brown adipose tissue. Can J Biochem Cell Biol *62*, 623-630.

Cadenas, S., Buckingham, J.A., Samec, S., Seydoux, J., Din, N., Dulloo, A.G., and Brand, M.D. (1999). UCP2 and UCP3 rise in starved rat skeletal muscle but mitochondrial proton conductance is unchanged. FEBS letters *462*, 257-260.

Cannon, B., and Nedergaard, J. (2004). Brown adipose tissue: function and physiological significance. Physiol Rev *84*, 277-359.

Cannon, B., and Nedergaard, J. (2011). Nonshivering thermogenesis and its adequate measurement in metabolic studies. J Exp Biol *214*, 242-253.

Cao, W., Daniel, K.W., Robidoux, J., Puigserver, P., Medvedev, A.V., Bai, X., Floering, L.M., Spiegelman, B.M., and Collins, S. (2004). p38 mitogen-activated protein kinase is the central regulator of cyclic AMP-dependent transcription of the brown fat uncoupling protein 1 gene. Mol Cell Biol *24*, 3057-3067.

Cao, W., Medvedev, A.V., Daniel, K.W., and Collins, S. (2001). beta-Adrenergic activation of p38 MAP kinase in adipocytes: cAMP induction of the uncoupling protein 1 (UCP1) gene requires p38 MAP kinase. J Biol Chem *276*, 27077-27082.

Cao, Z., Umek, R.M., and McKnight, S.L. (1991). Regulated expression of three C/EBP isoforms during adipose conversion of 3T3-L1 cells. Genes Dev *5*, 1538-1552.

Carlotti, F., Bazuine, M., Kekarainen, T., Seppen, J., Pognonec, P., Maassen, J.A., and Hoeben, R.C. (2004). Lentiviral vectors efficiently transduce quiescent mature 3T3-L1 adipocytes. Mol Ther *9*, 209-217.

Carmona, M.C., Hondares, E., Rodriguez de la Concepcion, M.L., Rodriguez-Sureda, V., Peinado-Onsurbe, J., Poli, V., Iglesias, R., Villarroya, F., and Giralt, M. (2005). Defective thermoregulation, impaired lipid metabolism, but preserved adrenergic induction of gene expression in brown fat of mice lacking C/EBPbeta. Biochem J *389*, 47-56.

Carta, A.R., Frau, L., Pisanu, A., Wardas, J., Spiga, S., and Carboni, E. (2011). Rosiglitazone decreases peroxisome proliferator receptor-gamma levels in microglia and inhibits TNF-alpha production: new evidences on neuroprotection in a progressive Parkinson's disease model. Neuroscience.

Cassard-Doulcier, A.M., Gelly, C., Fox, N., Schrementi, J., Raimbault, S., Klaus, S., Forest, C., Bouillaud, F., and Ricquier, D. (1993). Tissue-specific and beta-adrenergic regulation of the mitochondrial uncoupling protein gene: control by cis-acting elements in the 5'-flanking region. Mol Endocrinol *7*, 497-506.

Cavailles, V., Dauvois, S., L'Horset, F., Lopez, G., Hoare, S., Kushner, P.J., and Parker, M.G. (1995). Nuclear factor RIP140 modulates transcriptional activation by the estrogen receptor. EMBO J *14*, 3741-3751.

Cederberg, A., Gronning, L.M., Ahren, B., Tasken, K., Carlsson, P., and Enerback, S. (2001). FOXC2 is a winged helix gene that counteracts obesity, hypertriglyceridemia, and diet-induced insulin resistance. Cell *106*, 563-573.

Chang, L.J., and Zaiss, A.K. (2003). Self-inactivating lentiviral vectors and a sensitive Cre-loxP reporter system. Methods Mol Med *76*, 367-382.

Chen, D., Zhao, M., and Mundy, G.R. (2004). Bone morphogenetic proteins. Growth Factors *22*, 233-241.

Chilov, D., Fux, C., Joch, H., and Fussenegger, M. (2003). Identification of a novel proliferation-inducing determinant using lentiviral expression cloning. Nucleic Acids Res *31*, e113.

Chinnadurai, G. (2007). Transcriptional regulation by C-terminal binding proteins. Int J Biochem Cell Biol *39*, 1593-1607.

Cinti, S. (2001). The adipose organ: morphological perspectives of adipose tissues. Proc Nutr Soc *60*, 319-328.

Cinti, S. (2005). The adipose organ. Prostaglandins Leukot Essent Fatty Acids *73*, 9-15.

Cinti, S. (2006). The role of brown adipose tissue in human obesity. Nutr Metab Cardiovasc Dis *16*, 569-574.

Cinti, S. (2009a). Reversible physiological transdifferentiation in the adipose organ. Proc Nutr Soc *68*, 340-349.

Cinti, S. (2009b). Transdifferentiation properties of adipocytes in the Adipose Organ. Am J Physiol Endocrinol Metab.

Collins, S., Yehuda-Shnaidman, E., and Wang, H. (2010). Positive and negative control of Ucp1 gene transcription and the role of beta-adrenergic signaling networks. Int J Obes (Lond) *34 Suppl 1*, S28-33.

Coppack, S.W., Jensen, M.D., and Miles, J.M. (1994). In vivo regulation of lipolysis in humans. J Lipid Res *35*, 177-193.

Coste, A., Louet, J.F., Lagouge, M., Lerin, C., Antal, M.C., Meziane, H., Schoonjans, K., Puigserver, P., O'Malley, B.W., and Auwerx, J. (2008). The genetic ablation of SRC-3 protects against obesity and improves insulin sensitivity by reducing the acetylation of PGC-1{alpha}. Proc Natl Acad Sci U S A *105*, 17187-17192.

Cousin, B., Casteilla, L., Lafontan, M., Ambid, L., Langin, D., Berthault, M.F., and Penicaud, L. (1993). Local sympathetic denervation of white adipose tissue in rats induces preadipocyte proliferation without noticeable changes in metabolism. Endocrinology *133*, 2255-2262.

Cypess, A.M., Lehman, S., Williams, G., Tal, I., Rodman, D., Goldfine, A.B., Kuo, F.C., Palmer, E.L., Tseng, Y.H., Doria, A.*, et al.* (2009). Identification and importance of brown adipose tissue in adult humans. N Engl J Med *360*, 1509-1517.

Danovaro, R., Dell'Anno, A., Trucco, A., Serresi, M., and Vanucci, S. (2001). Determination of virus abundance in marine sediments. Appl Environ Microbiol *67*, 1384-1387.

Descombes, P., Chojkier, M., Lichtsteiner, S., Falvey, E., and Schibler, U. (1990). LAP, a novel member of the C/EBP gene family, encodes a liver-enriched transcriptional activator protein. Genes Dev *4*, 1541-1551.

Descombes, P., and Schibler, U. (1991). A liver-enriched transcriptional activator protein, LAP, and a transcriptional inhibitory protein, LIP, are translated from the same mRNA. Cell *67*, 569-579.

Desrosiers, R.C., Lifson, J.D., Gibbs, J.S., Czajak, S.C., Howe, A.Y., Arthur, L.O., and Johnson, R.P. (1998). Identification of highly attenuated mutants of simian immunodeficiency virus. J Virol *72*, 1431-1437.

Diehl, A.M., and Hoek, J.B. (1999). Mitochondrial uncoupling: role of uncoupling protein anion carriers and relationship to thermogenesis and weight control "the benefits of losing control". J Bioenerg Biomembr *31*, 493-506.

Dropulic, B. (2011). Lentiviral Vectors: Their Molecular Design, Safety,

and Use in Laboratory and Preclinical Research. HUMAN GENE THERAPY *22*, 649-657.

Dull, T., Zufferey, R., Kelly, M., Mandel, R.J., Nguyen, M., Trono, D., and Naldini, L. (1998). A third-generation lentivirus vector with a conditional packaging system. J Virol *72*, 8463-8471.

Dunstan, D.W., Zimmet, P.Z., Welborn, T.A., De Courten, M.P., Cameron, A.J., Sicree, R.A., Dwyer, T., Colagiuri, S., Jolley, D., Knuiman, M.*, et al.* (2002). The rising prevalence of diabetes and impaired glucose tolerance: the Australian Diabetes, Obesity and Lifestyle Study. Diabetes care *25*, 829-834.

Duprez, E., Wagner, K., Koch, H., and Tenen, D.G. (2003). C/EBPbeta: a major PML-RARA-responsive gene in retinoic acid-induced differentiation of APL cells. EMBO J *22*, 5806-5816.

Dupuy, F.P., Mouly, E., Mesel-Lemoine, M., Morel, C., Abriol, J., Cherai, M., Baillou, C., Negre, D., Cosset, F.L., Klatzmann, D.*, et al.* (2005). Lentiviral transduction of human hematopoietic cells by HIV-1- and SIV-based vectors containing a bicistronic cassette driven by various internal promoters. J Gene Med *7*, 1158-1171.

Echtay, K.S., Liu, Q., Caskey, T., Winkler, E., Frischmuth, K., Bienengraber, M., and Klingenberg, M. (1999). Regulation of UCP3 by nucleotides is different from regulation of UCP1. FEBS Lett *450*, 8-12.

Enerback S, Jacobsson A, Simpson EM, Guerra C, Yamashita H, Harper ME, and LP, K. (1997). Mice lacking mitochondrial uncoupling protein are cold-sensitive but not obese. Nature *387*, 5.

English, J.T., Patel, S.K., and Flanagan, M.J. (1973). Association of pheochromocytomas with brown fat tumors. Radiology *107*, 279-281.

Escher, P., Braissant, O., Basu-Modak, S., Michalik, L., Wahli, W., and Desvergne, B. (2001). Rat PPARs: quantitative analysis in adult rat tissues and regulation in fasting and refeeding. Endocrinology *142*, 4195-4202.

Esterbauer, H., Schneitler, C., Oberkofler, H., Ebenbichler, C., Paulweber, B., Sandhofer, F., Ladurner, G., Hell, E., Strosberg, A.D., Patsch, J.R.*, et al.* (2001). A common polymorphism in

the promoter of UCP2 is associated with decreased risk of obesity in middle-aged humans. Nature genetics *28*, 178-183.

Fain, J.N., Madan, A.K., Hiler, M.L., Cheema, P., and Bahouth, S.W. (2004). Comparison of the release of adipokines by adipose tissue, adipose tissue matrix, and adipocytes from visceral and subcutaneous abdominal adipose tissues of obese humans. Endocrinology *145*, 2273-2282.

Farmer, S.R. (2005). Regulation of PPARgamma activity during adipogenesis. Int J Obes (Lond) *29 Suppl 1*, S13-16.

Farmer, S.R. (2006). Transcriptional control of adipocyte formation. Cell Metab *4*, 263-273.

Farmer, S.R. (2008). Molecular determinants of brown adipocyte formation and function. Genes Dev *22*, 1269-1275.

Feldmann, H.M., Golozoubova, V., Cannon, B., and Nedergaard, J. (2009). UCP1 ablation induces obesity and abolishes diet-induced thermogenesis in mice exempt from thermal stress by living at thermoneutrality. Cell metabolism *9*, 203-209.

Festuccia, W.T., Blanchard, P.G., Richard, D., and Deshaies, Y. (2010). Basal adrenergic tone is required for maximal stimulation of rat brown adipose tissue UCP1 expression by chronic PPAR-gamma activation. Am J Physiol Regul Integr Comp Physiol *299*, R159-167.

Finck, B.N., and Kelly, D.P. (2006). PGC-1 coactivators: inducible regulators of energy metabolism in health and disease. J Clin Invest *116*, 615-622.

Fisler, J.S., and Warden, C.H. (2006). Uncoupling proteins, dietary fat and the metabolic syndrome. Nutrition & metabolism *3*, 38.

Flegal, K.M., Graubard, B.I., Williamson, D.F., and Gail, M.H. (2005). Excess deaths associated with underweight, overweight, and obesity. JAMA *293*, 1861-1867.

Flier, J.S. (1998). Clinical review 94: What's in a name? In search of leptin's physiologic role. J Clin Endocrinol Metab *83*, 1407-1413.

Flier, J.S., Cook, K.S., Usher, P., and Spiegelman, B.M. (1987). Severely impaired adipsin expression in genetic and acquired obesity. Science *237*, 405-408.

Floyd, Z.E., and Stephens, J.M. (2003). STAT5A promotes adipogenesis in nonprecursor cells and associates with the glucocorticoid receptor during adipocyte differentiation. Diabetes *52*, 308-314.

Forga, L., Corbalan, M., Marti, A., Fuentes, C., Martinez-Gonzalez, M.A., and Martinez, A. (2003). [Influence of the polymorphism 03826 A --> G in the UCP1 gene on the components of metabolic syndrome]. Anales del sistema sanitario de Navarra *26*, 231-236.

Foster DO, F.M. (1978). Nonshivering thermogenesis in rat. 2 Measurements of blood flow with microspheres point to brown adipose tissue as dominant site of calorigenesis induced by noradrenaline. Can J Physiol Pharmacol *56*, 13.

Francis, G.A., Fayard, E., Picard, F., and Auwerx, J. (2003). Nuclear receptors and the control of metabolism. Annu Rev Physiol *65*, 261-311.

Freytag, S.O., Paielli, D.L., and Gilbert, J.D. (1994). Ectopic expression of the CCAAT/enhancer-binding protein alpha promotes the adipogenic program in a variety of mouse fibroblastic cells. Genes Dev *8*, 1654-1663.

Fritah, A., Christian, M., and Parker, M.G. (2010). The metabolic coregulator RIP140: an update. Am J Physiol Endocrinol Metab *299*, E335-340.

Fukuda, H., Brailowsky, S., Menini, C., Silva-Barrat, C., Riche, D., and Naquet, R. (1987). Anticonvulsant effect of intracortical, chronic infusion of GABA in kindled rats: focal seizures upon withdrawal. Exp Neurol *98*, 120-129.

Fuller, P.M., Warden, C.H., Barry, S.J., and Fuller, C.A. (2000). Effects of 2-G exposure on temperature regulation, circadian rhythms, and adiposity in UCP2/3 transgenic mice. J Appl Physiol *89*, 1491-1498.

Gagliardi, M., Maynard, S., Miyake, T., Rodrigues, N., Tjew, S.L., Cabannes, E., and Bedard, P.A. (2003). Opposing roles of C/EBPbeta and AP-1 in the control of fibroblast proliferation and growth arrest-specific gene expression. J Biol Chem *278*, 43846-43854.

Galetti, S., Sarre, A., Perreten, H., Produit-Zengaffinen, N., Muzzin, P., and Assimacopoulos-Jeannet, F. (2009). Fatty acids do not activate UCP2 in pancreatic beta cells: comparison with UCP1. Pflugers Archiv : European journal of physiology *457*, 931-940.

Gesta, S., Tseng, Y.H., and Kahn, C.R. (2007). Developmental origin of fat: tracking obesity to its source. Cell *131*, 242-256.

Gingras, A.C., Raught, B., and Sonenberg, N. (1999). eIF4 initiation factors: effectors of mRNA recruitment to ribosomes and regulators of translation. Annu Rev Biochem *68*, 913-963.

Giralt, A., Hondares, E., Villena, J.A., Ribas, F., Diaz-Delfin, J., Giralt, M., Iglesias, R., and Villarroya, F. (2011). Peroxisome Proliferator-activated Receptor-{gamma} Coactivator-1{alpha} Controls Transcription of the Sirt3 Gene, an Essential Component of the Thermogenic Brown Adipocyte Phenotype. J Biol Chem *286*, 16958-16966.

Gluzman, Y. (1981). SV40-transformed simian cells support the replication of early SV40 mutants. Cell *23*, 175-182.

Gong, D.W., Monemdjou, S., Gavrilova, O., Leon, L.R., Marcus-Samuels, B., Chou, C.J., Everett, C., Kozak, L.P., Li, C., Deng, C.*, et al.* (2000). Lack of obesity and normal response to fasting and thyroid hormone in mice lacking uncoupling protein-3. The Journal of biological chemistry *275*, 16251-16257.

Gorla-Bajszczak, A., Siegrist-Kaiser, C., Boss, O., Burger, A.G., and Meier, C.A. (2000). Expression of peroxisome proliferator-activated receptors in lean and obese Zucker rats. Eur J Endocrinol *142*, 71-78.

Gossen, M., and Bujard, H. (1992). Tight control of gene expression in mammalian cells by tetracycline-responsive promoters. Proc Natl Acad Sci U S A *89*, 5547-5551.

Graves, R.A., Tontonoz, P., Platt, K.A., Ross, S.R., and Spiegelman, B.M. (1992). Identification of a fat cell enhancer: analysis of requirements for adipose tissue-specific gene expression. J Cell Biochem *49*, 219-224.

Green, H., and Kehinde, O. (1975). An established preadipose cell line and its differentiation in culture. II. Factors affecting the adipose conversion. Cell *5*, 19-27.

Greenbaum, L.E., Li, W., Cressman, D.E., Peng, Y., Ciliberto, G., Poli, V., and Taub, R. (1998). CCAAT enhancer- binding protein beta is required for normal hepatocyte proliferation in mice after partial hepatectomy. J Clin Invest *102*, 996-1007.

Gregoire, F.M., Smas, C.M., and Sul, H.S. (1998). Understanding adipocyte differentiation. Physiological reviews *78*, 783-809.

Guerzoni, C., Bardini, M., Mariani, S.A., Ferrari-Amorotti, G., Neviani, P., Panno, M.L., Zhang, Y., Martinez, R., Perrotti, D., and Calabretta, B. (2006). Inducible activation of CEBPB, a gene negatively regulated by BCR/ABL, inhibits proliferation and promotes differentiation of BCR/ABL-expressing cells. Blood *107*, 4080-4089.

Haghighat, A., Mader, S., Pause, A., and Sonenberg, N. (1995). Repression of cap-dependent translation by 4E-binding protein 1: competition with p220 for binding to eukaryotic initiation factor-4E. EMBO J *14*, 5701-5709.

Hallberg, M., Morganstein, D.L., Kiskinis, E., Shah, K., Kralli, A., Dilworth, S.M., White, R., Parker, M.G., and Christian, M. (2008). A functional interaction between RIP140 and PGC-1alpha regulates the expression of the lipid droplet protein CIDEA. Mol Cell Biol *28*, 6785-6795.

Handschin, C., and Spiegelman, B.M. (2006). Peroxisome proliferator-activated receptor gamma coactivator 1 coactivators, energy homeostasis, and metabolism. Endocr Rev *27*, 728-735.

Hansen, J.B., Jorgensen, C., Petersen, R.K., Hallenborg, P., De Matteis, R., Boye, H.A., Petrovic, N., Enerback, S., Nedergaard, J., Cinti, S*., et al.* (2004). Retinoblastoma protein functions as a molecular switch determining white versus brown adipocyte differentiation. Proc Natl Acad Sci U S A *101*, 4112-4117.

Hartley, J.L., Temple, G.F., and Brasch, M.A. (2000). DNA cloning using in vitro site-specific recombination. Genome Res *10*, 1788-1795.

Hauser, S., Adelmant, G., Sarraf, P., Wright, H.M., Mueller, E., and Spiegelman, B.M. (2000). Degradation of the peroxisome proliferator-activated receptor gamma is linked to ligand-dependent activation. J Biol Chem *275*, 18527-18533.

He, W., Barak, Y., Hevener, A., Olson, P., Liao, D., Le, J., Nelson, M., Ong, E., Olefsky, J.M., and Evans, R.M. (2003). Adipose-specific peroxisome proliferator-activated receptor gamma knockout causes insulin resistance in fat and liver but not in muscle. Proc Natl Acad Sci U S A *100*, 15712-15717.

Herzig, S., Long, F., Jhala, U.S., Hedrick, S., Quinn, R., Bauer, A., Rudolph, D., Schutz, G., Yoon, C., Puigserver, P*., et al.* (2001). CREB regulates hepatic gluconeogenesis through the coactivator PGC-1. Nature *413*, 179-183.

Himms-Hagen, J. (1984). Brown adipose tissue thermogenesis, energy balance, and obesity. Can J Biochem Cell Biol *62*, 610-617.

Himms-Hagen, J. (1989). Role of thermogenesis in the regulation of energy balance in relation to obesity. Can J Physiol Pharmacol *67*, 394-401.

Himms-Hagen, J., Melnyk, A., Zingaretti, M.C., Ceresi, E., Barbatelli, G., and Cinti, S. (2000). Multilocular fat cells in WAT of CL-316243-treated rats derive directly from white adipocytes. Am J Physiol Cell Physiol *279*, C670-681.

Hondares, E., Mora, O., Yubero, P., Rodriguez de la Concepcion, M., Iglesias, R., Giralt, M., and Villarroya, F. (2006). Thiazolidinediones and rexinoids induce peroxisome proliferator-activated receptor-coactivator (PGC)-1alpha gene transcription: an autoregulatory loop controls PGC-1alpha expression in adipocytes via peroxisome proliferator-activated receptor-gamma coactivation. Endocrinology *147*, 2829-2838.

Horvath, T.L., Diano, S., Miyamoto, S., Barry, S., Gatti, S., Alberati, D., Livak, F., Lombardi, A., Moreno, M., Goglia, F*., et al.* (2003). Uncoupling proteins-2 and 3 influence obesity and inflammation in transgenic mice. Int J Obes Relat Metab Disord *27*, 433-442.

Hotamisligil, G.S. (2003). Inflammatory pathways and insulin action. Int J Obes Relat Metab Disord *27 Suppl 3*, S53-55.

Huttunen, P., Hirvonen, J., and Kinnula, V. (1981). The occurrence of brown adipose tissue in outdoor workers. Eur J Appl Physiol Occup Physiol *46*, 339-345.

Inohara, N., Koseki, T., Chen, S., Wu, X., and Nunez, G. (1998). CIDE, a novel family of cell death activators with homology to the 45 kDa subunit of the DNA fragmentation factor. EMBO J *17*, 2526-2533.

Invitrogen (2006). Multisite Gateway Pro manual.

Invitrogen (2010). ViraPower Lentiviral Expression System (User Manual).

Isomaa, B., Henricsson, M., Almgren, P., Tuomi, T., Taskinen, M.R., and Groop, L. (2001). The metabolic syndrome influences the risk of chronic complications in patients with type II diabetes. Diabetologia *44*, 1148-1154.

Kajimura, S., Seale, P., Kubota, K., Lunsford, E., Frangioni, J.V., Gygi, S.P., and Spiegelman, B.M. (2009). Initiation of myoblast to brown fat switch by a PRDM16-C/EBP-beta transcriptional complex. Nature *460*, 1154-1158.

Kajimura, S., Seale, P., and Spiegelman, B.M. (2010). Transcriptional control of brown fat development. Cell Metab *11*, 257-262.

Kajimura, S., Seale, P., Tomaru, T., Erdjument-Bromage, H., Cooper, M.P., Ruas, J.L., Chin, S., Tempst, P., Lazar, M.A., and Spiegelman, B.M. (2008). Regulation of the brown and white fat gene programs through a PRDM16/CtBP transcriptional complex. Genes Dev *22*, 1397-1409.

Kameda, N., Okuya, S., and Oka, Y. (2000). [Rosiglitazone (BRL-49653)]. Nihon Rinsho *58*, 401-404.

Kang, S., Bajnok, L., Longo, K.A., Petersen, R.K., Hansen, J.B., Kristiansen, K., and MacDougald, O.A. (2005). Effects of Wnt signaling on brown adipocyte differentiation and metabolism mediated by PGC-1alpha. Mol Cell Biol *25*, 1272-1282.

Karamanlidis, G., Karamitri, A., Docherty, K., Hazlerigg, D.G., and Lomax, M.A. (2007). C/EBPbeta reprograms white 3T3-L1 preadipocytes to a Brown adipocyte pattern of gene expression. J Biol Chem *282*, 24660-24669.

Karamitri, A., Shore, A.M., Docherty, K., Speakman, J.R., and Lomax, M.A. (2009). Combinatorial transcription factor regulation of the cyclic AMP-response element on the Pgc-1alpha promoter in white 3T3-L1 and brown HIB-1B preadipocytes. J Biol Chem *284*, 20738-20752.

Keller, H., Dreyer, C., Medin, J., Mahfoudi, A., Ozato, K., and Wahli, W. (1993). Fatty acids and retinoids control lipid metabolism through activation of peroxisome proliferator-activated receptor-retinoid X receptor heterodimers. Proc Natl Acad Sci U S A *90*, 2160-2164.

Kershaw, E.E., and Flier, J.S. (2004). Adipose tissue as an endocrine organ. J Clin Endocrinol Metab *89*, 2548-2556.

Kim, J.B., Sarraf, P., Wright, M., Yao, K.M., Mueller, E., Solanes, G., Lowell, B.B., and Spiegelman, B.M. (1998a). Nutritional and insulin regulation of fatty acid synthetase and leptin gene expression through ADD1/SREBP1. J Clin Invest *101*, 1-9.

Kim, J.B., and Spiegelman, B.M. (1996). ADD1/SREBP1 promotes adipocyte differentiation and gene expression linked to fatty acid metabolism. Genes Dev *10*, 1096-1107.

Kim, J.B., Wright, H.M., Wright, M., and Spiegelman, B.M. (1998b). ADD1/SREBP1 activates PPARgamma through the production of endogenous ligand. Proc Natl Acad Sci U S A *95*, 4333-4337.

Kiskinis, E., Hallberg, M., Christian, M., Olofsson, M., Dilworth, S.M., White, R., and Parker, M.G. (2007). RIP140 directs histone and DNA methylation to silence Ucp1 expression in white adipocytes. EMBO J *26*, 4831-4840.

Kliewer, S.A., Umesono, K., Noonan, D.J., Heyman, R.A., and Evans, R.M. (1992). Convergence of 9-cis retinoic acid and peroxisome proliferator signalling pathways through heterodimer formation of their receptors. Nature *358*, 771-774.

Klingenberg, M. (1999). Uncoupling protein--a useful energy dissipator. J Bioenerg Biomembr *31*, 419-430.

Klingenberg, M., and Huang, S.G. (1999). Structure and function of the uncoupling protein from brown adipose tissue. Biochim Biophys Acta *1415*, 271-296.

Klingenspor, M. (2003). Cold-induced recruitment of brown adipose tissue thermogenesis. Exp Physiol *88*, 141-148.

Kopecky, J., Clarke, G., Enerback, S., Spiegelman, B., and Kozak, L.P. (1995). Expression of the mitochondrial uncoupling protein gene from the aP2 gene promoter prevents genetic obesity. J Clin Invest *96*, 2914-2923.

Kopecky, J., Hodny, Z., Rossmeisl, M., Syrovy, I., and Kozak, L.P. (1996). Reduction of dietary obesity in aP2-Ucp transgenic mice: physiology and adipose tissue distribution. Am J Physiol *270*, E768-775.

Kozak, U.C., Kopecky, J., Teisinger, J., Enerback, S., Boyer, B., and Kozak, L.P. (1994). An upstream enhancer regulating brown-fat-specific expression of the mitochondrial uncoupling protein gene. Mol Cell Biol *14*, 59-67.

Krempler, F., Esterbauer, H., Weitgasser, R., Ebenbichler, C., Patsch, J.R., Miller, K., Xie, M., Linnemayr, V., Oberkofler, H., and Patsch, W. (2002). A functional polymorphism in the promoter of UCP2 enhances obesity risk but reduces type 2 diabetes risk in obese middle-aged humans. Diabetes *51*, 3331-3335.

Kulkarni, R.N., Winnay, J.N., Daniels, M., Bruning, J.C., Flier, S.N., Hanahan, D., and Kahn, C.R. (1999). Altered function of insulin receptor substrate-1-deficient mouse islets and cultured beta-cell lines. J Clin Invest *104*, R69-75.

Kumar, N., Robidoux, J., Daniel, K.W., Guzman, G., Floering, L.M., and Collins, S. (2007). Requirement of vimentin filament assembly for beta3-adrenergic receptor activation of ERK MAP kinase and lipolysis. J Biol Chem *282*, 9244-9250.

Kurita, R., Oikawa, T., Okada, M., Yokoo, T., Kurihara, Y., Honda, Y., Kageyama, R., Suehiro, Y., Okazaki, T., Iga, M.*, et al.* (2008). Construction of a high-performance human fetal liver-derived lentiviral cDNA library. Mol Cell Biochem *319*, 181-187.

Landy, A. (1989). Dynamic, structural, and regulatory aspects of lambda site-specific recombination. Annu Rev Biochem *58*, 913-949.

Lane, M.D., Tang, Q.Q., and Jiang, M.S. (1999). Role of the CCAAT enhancer binding proteins (C/EBPs) in adipocyte differentiation. Biochem Biophys Res Commun *266*, 677-683.

Lehr, L., Kuehne, F., Arboit, P., Giacobino, J.P., Poulin, F., Muzzin, P., and Jimenez, M. (2004). Control of 4E-BP1 expression in mouse brown adipose tissue by the beta3-adrenoceptor. FEBS Lett *576*, 179-182.

Lehrke, M., and Lazar, M.A. (2005). The many faces of PPARgamma. Cell *123*, 993-999.

Lekstrom-Himes, J., and Xanthopoulos, K.G. (1998). Biological role of the CCAAT/enhancer-binding protein family of transcription factors. J Biol Chem *273*, 28545-28548.

Leonardsson, G., Steel, J.H., Christian, M., Pocock, V., Milligan, S., Bell, J., So, P.W., Medina-Gomez, G., Vidal-Puig, A., White, R.*, et al.* (2004). Nuclear receptor corepressor RIP140 regulates fat accumulation. Proc Natl Acad Sci U S A *101*, 8437-8442.

Lerin, C., Rodgers, J.T., Kalume, D.E., Kim, S.H., Pandey, A., and Puigserver, P. (2006). GCN5 acetyltransferase complex controls glucose metabolism through transcriptional repression of PGC-1alpha. Cell Metab *3*, 429-438.

Liau, G., Su, E.J., and Dixon, K.D. (2001). Clinical efforts to modulate angiogenesis in the adult: gene therapy versus conventional approaches. Drug discovery today *6*, 689-697.

Lin, J., Handschin, C., and Spiegelman, B.M. (2005). Metabolic control through the PGC-1 family of transcription coactivators. Cell Metab *1*, 361-370.

Lin, J., Wu, P.H., Tarr, P.T., Lindenberg, K.S., St-Pierre, J., Zhang, C.Y., Mootha, V.K., Jager, S., Vianna, C.R., Reznick, R.M.*, et al.* (2004). Defects in adaptive energy metabolism with CNS-linked hyperactivity in PGC-1alpha null mice. Cell *119*, 121-135.

Lindgren, E.M., Nielsen, R., Petrovic, N., Jacobsson, A., Mandrup, S., Cannon, B., and Nedergaard, J. (2004). Noradrenaline represses PPAR (peroxisome-proliferator-activated receptor) gamma2 gene expression in brown adipocytes: intracellular signalling and effects on PPARgamma2 and PPARgamma1 protein levels. Biochem J *382*, 597-606.

Louet, J.F., Coste, A., Amazit, L., Tannour-Louet, M., Wu, R.C., Tsai, S.Y., Tsai, M.J., Auwerx, J., and O'Malley, B.W. (2006). Oncogenic steroid receptor coactivator-3 is a key regulator of the white adipogenic program. Proc Natl Acad Sci U S A *103*, 17868-17873.

Louet, J.F., and O'Malley, B.W. (2007). Coregulators in adipogenesis: what could we learn from the SRC (p160) coactivator family? Cell Cycle *6*, 2448-2452.

Luo, J., Sladek, R., Carrier, J., Bader, J.A., Richard, D., and Giguere, V. (2003). Reduced fat mass in mice lacking orphan nuclear receptor estrogen-related receptor alpha. Mol Cell Biol *23*, 7947-7956.

Luo, Q.M., Miao, X.Y., and Zhang, R.J. (2011). [An update on the development of transgenic animal technology]. Yi Chuan *33*, 449-458.

MacDougald, O.A., Cornelius, P., Lin, F.T., Chen, S.S., and Lane, M.D. (1994). Glucocorticoids reciprocally regulate expression of the CCAAT/enhancer-binding protein alpha and delta genes in 3T3-L1 adipocytes and white adipose tissue. J Biol Chem *269*, 19041-19047.

MacDougald, O.A., and Lane, M.D. (1995). Transcriptional regulation of gene expression during adipocyte differentiation. Annu Rev Biochem *64*, 345-373.

Manchado, C., Yubero, P., Vinas, O., Iglesias, R., Villarroya, F., Mampel, T., and Giralt, M. (1994). CCAAT/enhancer-binding proteins alpha and beta in brown adipose tissue: evidence for a tissue-specific pattern of expression during development. Biochem J *302 (Pt 3)*, 695-700.

Manjunath, N., Wu, H., Subramanya, S., and Shankar, P. (2009). Lentiviral delivery of short hairpin RNAs. Adv Drug Deliv Rev *61*, 732-745.

Margetic, S., Gazzola, C., Pegg, G.G., and Hill, R.A. (2002). Leptin: a review of its peripheral actions and interactions. Int J Obes Relat Metab Disord *26*, 1407-1433.

Miner, J.L., Cederberg, C.A., Nielsen, M.K., Chen, X., and Baile, C.A. (2001). Conjugated linoleic acid (CLA), body fat, and apoptosis. Obes Res *9*, 129-134.

Mochizuki, N., Shimizu, S., Nagasawa, T., Tanaka, H., Taniwaki, M., Yokota, J., and Morishita, K. (2000). A novel gene, MEL1, mapped to 1p36.3 is highly homologous to the MDS1/EVI1 gene and is transcriptionally activated in t(1;3)(p36;q21)-positive leukemia cells. Blood *96*, 3209-3214.

Motyl, K.J., Raetz, M., Tekalur, S.A., Schwartz, R.C., and McCabe, L.R. CCAAT/enhancer binding protein beta-deficiency enhances type 1 diabetic bone phenotype by increasing marrow adiposity and bone resorption. Am J Physiol Regul Integr Comp Physiol *300*, R1250-1260.

Naldini, L. (1998). Lentiviruses as gene transfer agents for delivery to non-dividing cells. Curr Opin Biotechnol *9*, 457-463.

Naldini, L., Blomer, U., Gage, F.H., Trono, D., and Verma, I.M. (1996a). Efficient transfer, integration, and sustained long-term expression of the transgene in adult rat brains injected with a lentiviral vector. Proc Natl Acad Sci U S A *93*, 11382-11388.

Naldini, L., Blomer, U., Gallay, P., Ory, D., Mulligan, R., Gage, F.H., Verma, I.M., and Trono, D. (1996b). In vivo gene delivery and stable transduction of nondividing cells by a lentiviral vector. Science *272*, 263-267.

Naquet, R., Menini, C., Riche, D., Silva-Barrat, C., and Valin, A. (1987). Photic epilepsy problems raised in man and animals. Ital J Neurol Sci *8*, 437-447.

Nedergaard, J., Bengtsson, T., and Cannon, B. (2007). Unexpected evidence for active brown adipose tissue in adult humans. Am J Physiol Endocrinol Metab *293*, E444-452.

Nedergaard, J., Petrovic, N., Lindgren, E.M., Jacobsson, A., and Cannon, B. (2005). PPARgamma in the control of brown adipocyte differentiation. Biochim Biophys Acta *1740*, 293-304.

Negrel, R., Grimaldi, P., and Ailhaud, G. (1978). Establishment of preadipocyte clonal line from epididymal fat pad of ob/ob mouse that responds to insulin and to lipolytic hormones. Proc Natl Acad Sci U S A *75*, 6054-6058.

Nicholls, D.G., Bernson, V.S., and Heaton, G.M. (1978). The identification of the component in the inner membrane of brown adipose tissue mitochondria responsible for regulating energy dissipation. Experientia Suppl *32*, 89-93.

Nicholls, D.G., and Locke, R.M. (1984). Thermogenic mechanisms in brown fat. Physiol Rev *64*, 1-64.

Nishikata, I., Sasaki, H., Iga, M., Tateno, Y., Imayoshi, S., Asou, N., Nakamura, T., and Morishita, K. (2003). A novel EVI1 gene family, MEL1, lacking a PR domain (MEL1S) is expressed mainly in t(1;3)(p36;q21)-positive AML and blocks G-CSF-induced myeloid differentiation. Blood *102*, 3323-3332.

Norkin, L.C. (2010). Virology: Molecular Biology and Pathogenesis. American Society for Microbiology, Canada.

Oldfield, E.H., Ram, Z., Culver, K.W., Blaese, R.M., DeVroom, H.L., and Anderson, W.F. (1993). Gene therapy for the treatment of brain tumors using intra-tumoral transduction with the thymidine kinase gene and intravenous ganciclovir. Human gene therapy *4*, 39-69.

Pan, D., Fujimoto, M., Lopes, A., and Wang, Y.X. (2009). Twist-1 is a PPARdelta-inducible, negative-feedback regulator of PGC-1alpha in brown fat metabolism. Cell *137*, 73-86.

Pan, H., Mostoslavsky, G., Eruslanov, E., Kotton, D.N., and Kramnik, I. (2008). Dual-promoter lentiviral system allows inducible expression of noxious proteins in macrophages. Journal of immunological methods *329*, 31-44.

Park, B.H., Qiang, L., and Farmer, S.R. (2004). Phosphorylation of C/EBPbeta at a consensus extracellular signal-regulated kinase/glycogen synthase kinase 3 site is required for the induction of adiponectin gene expression during the differentiation of mouse fibroblasts into adipocytes. Mol Cell Biol *24*, 8671-8680.

Pedraza, N., Solanes, G., Iglesias, R., Vazquez, M., Giralt, M., and Villarroya, F. (2001). Differential regulation of expression of genes encoding uncoupling proteins 2 and 3 in brown adipose tissue during lactation in mice. Biochem J *355*, 105-111.

Petrovic, N., Shabalina, I.G., Timmons, J.A., Cannon, B., and Nedergaard, J. (2008). Thermogenically competent nonadrenergic recruitment in brown preadipocytes by a PPARgamma agonist. Am J Physiol Endocrinol Metab *295*, E287-296.

Petrovic, N., Walden, T.B., Shabalina, I.G., Timmons, J.A., Cannon, B., and Nedergaard, J. (2009). Chronic peroxisome proliferator-activated receptor gamma (PPARgamma) activation of epididymally derived white adipocyte cultures reveals a population of thermogenically competent, UCP1-containing adipocytes molecularly distinct from classic brown adipocytes. J Biol Chem *285*, 7153-7164.

Picard, F., Gehin, M., Annicotte, J., Rocchi, S., Champy, M.F., O'Malley, B.W., Chambon, P., and Auwerx, J. (2002). SRC-1 and TIF2 control energy balance between white and brown adipose tissues. Cell *111*, 931-941.

Pluck, A. (1996). Conditional mutagenesis in mice: the Cre/loxP recombination system. Int J Exp Pathol *77*, 269-278.

Pluta, K., Diehl, W., Zhang, X.Y., Kutner, R., Bialkowska, A., and Reiser, J. (2007). Lentiviral vectors encoding tetracycline-dependent repressors and transactivators for reversible knockdown of gene expression: a comparative study. BMC Biotechnol *7*, 41.

Poli, V., Mancini, F.P., and Cortese, R. (1990). IL-6DBP, a nuclear protein involved in interleukin-6 signal transduction, defines a new family of leucine zipper proteins related to C/EBP. Cell *63*, 643-653.

Poulin, F., and Sonenberg, N. (2003). Translation on Mechanisms (Lapointe, J. and Braker-Gingras, L., Eds.). Landes Bioscience, Austin, TX, 280-297.

Poulos, S.P., Hausman, D.B., and Hausman, G.J. (2009). The development and endocrine functions of adipose tissue. Mol Cell Endocrinol *323*, 20-34.

Poznansky, M., Lever, A., Bergeron, L., Haseltine, W., and Sodroski, J. (1991). Gene transfer into human lymphocytes by a defective human immunodeficiency virus type 1 vector. J Virol *65*, 532-536.

Puigserver, P., Wu, Z., Park, C.W., Graves, R., Wright, M., and Spiegelman, B.M. (1998). A cold-inducible coactivator of nuclear receptors linked to adaptive thermogenesis. Cell *92*, 829-839.

Ratner, L., Fisher, A., Jagodzinski, L.L., Liou, R.S., Mitsuya, H., Gallo, R.C., and Wong-Staal, F. (1987). Complete nucleotide sequences of functional clones of the virus associated with the acquired immunodeficiency syndrome, HTLV-III/LAV. Haematol Blood Transfus *31*, 404-406.

Rektor, I., Bryere, P., Valin, A., Silva-Barrat, C., Naquet, R., and Menini, C. (1987). [Type B myoclonus in Papio papio: results of the central anticholinergic effect of benzodiazepines]. Cesk Psychiatr *83*, 217-222.

Renold, **A.**E., and G. F. Cahill, editors (1965). Handbook of Physiology. Sector 5. Adipose Tissue. American Physiological Society, Washington, DC.

Robidoux, J., Cao, W., Quan, H., Daniel, K.W., Moukdar, F., Bai, X., Floering, L.M., and Collins, S. (2005). Selective activation of mitogen-activated protein (MAP) kinase kinase 3 and p38alpha MAP kinase is essential for cyclic AMP-dependent UCP1 expression in adipocytes. Mol Cell Biol *25*, 5466-5479.

Robidoux, J., Kumar, N., Daniel, K.W., Moukdar, F., Cyr, M., Medvedev, A.V., and Collins, S. (2006). Maximal beta3-adrenergic regulation of lipolysis involves Src and epidermal growth factor receptor-dependent ERK1/2 activation. J Biol Chem *281*, 37794-37802.

Roesler, W.J. (2001). The role of C/EBP in nutrient and hormonal regulation of gene expression. Annu Rev Nutr *21*, 141-165.

Rorth, P., Szabo, K., Bailey, A., Laverty, T., Rehm, J., Rubin, G.M., Weigmann, K., Milan, M., Benes, V., Ansorge, W*., et al.* (1998). Systematic gain-of-function genetics in Drosophila. Development *125*, 1049-1057.

Rosen, E.D., Hsu, C.H., Wang, X., Sakai, S., Freeman, M.W., Gonzalez, F.J., and Spiegelman, B.M. (2002). C/EBPalpha induces adipogenesis through PPARgamma: a unified pathway. Genes Dev *16*, 22-26.

Rosen, E.D., and MacDougald, O.A. (2006). Adipocyte differentiation from the inside out. Nat Rev Mol Cell Biol *7*, 885-896.

Rosen, E.D., and Spiegelman, B.M. (2000). Molecular regulation of adipogenesis. Annu Rev Cell Dev Biol *16*, 145-171.

Rosenbaum, S.E., and Greenberg, A.S. (1998). The short- and long-term effects of tumor necrosis factor-alpha and BRL 49653 on peroxisome proliferator-activated receptor (PPAR)gamma2 gene expression and other adipocyte genes. Mol Endocrinol *12*, 1150-1160.

Rothwell, N.J., and Stock, M.J. (1979). Effects of continuous and discontinuous periods of cafeteria feeding on body weight, resting oxygen consumption and noradrenaline sensitivity in the rat [proceedings]. J Physiol *291*, 59P.

Ruan, H., and Lodish, H.F. (2003). Insulin resistance in adipose tissue: direct and indirect effects of tumor necrosis factor-alpha. Cytokine Growth Factor Rev *14*, 447-455.

Rudofsky, G., Jr., Schroedter, A., Schlotterer, A., Voron'ko, O.E., Schlimme, M., Tafel, J., Isermann, B.H., Humpert, P.M., Morcos, M., Bierhaus, A*., et al.* (2006). Functional polymorphisms of UCP2 and UCP3 are associated with a reduced prevalence of diabetic neuropathy in patients with type 1 diabetes. Diabetes care *29*, 89-94.

Sasaki, Y., Sone, T., Yoshida, S., Yahata, K., Hotta, J., Chesnut, J.D., Honda, T., and Imamoto, F. (2004). Evidence for high specificity and efficiency of multiple recombination signals in mixed DNA cloning by the Multisite Gateway system. J Biotechnol *107*, 233-243.

Scheffler, I.E. (1999). Mitochondria. Wiley-Liss, New York.

Schmidt, U., and Al-Hasani, H. (2007). Production of Lentiviruses Using HEKFectin Cell-Specific Lipid Reagent for Multiplasmid Transformation. BioRad Tech Note *5408*.

Scime, A., Grenier, G., Huh, M.S., Gillespie, M.A., Bevilacqua, L., Harper, M.E., and Rudnicki, M.A. (2005). Rb and p107 regulate preadipocyte differentiation into white versus brown fat through repression of PGC-1alpha. Cell Metab *2*, 283-295.

Seale, P., Bjork, B., Yang, W., Kajimura, S., Chin, S., Kuang, S., Scime, A., Devarakonda, S., Conroe, H.M., Erdjument-Bromage, H.*, et al.* (2008). PRDM16 controls a brown fat/skeletal muscle switch. Nature *454*, 961-967.

Seale, P., Conroe, H.M., Estall, J., Kajimura, S., Frontini, A., Ishibashi, J., Cohen, P., Cinti, S., and Spiegelman, B.M. (2010). Prdm16 determines the thermogenic program of subcutaneous white adipose tissue in mice. J Clin Invest *121*, 96-105.

Seale, P., Kajimura, S., and Spiegelman, B.M. (2009). Transcriptional control of brown adipocyte development and physiological function--of mice and men. Genes Dev *23*, 788-797.

Seale, P., Kajimura, S., Yang, W., Chin, S., Rohas, L.M., Uldry, M., Tavernier, G., Langin, D., and Spiegelman, B.M. (2007). Transcriptional control of brown fat determination by PRDM16. Cell Metab *6*, 38-54.

Sears, I.B., MacGinnitie, M.A., Kovacs, L.G., and Graves, R.A. (1996). Differentiation-dependent expression of the brown adipocyte uncoupling protein gene: regulation by peroxisome proliferator-activated receptor gamma. Mol Cell Biol *16*, 3410-3419.

Sebastian, T., Malik, R., Thomas, S., Sage, J., and Johnson, P.F. (2005). C/EBPbeta cooperates with RB:E2F to implement Ras(V12)-induced cellular senescence. EMBO J *24*, 3301-3312.

Seckl, J.R., and Walker, B.R. (2001). Minireview: 11beta-hydroxysteroid dehydrogenase type 1- a tissue-specific amplifier of glucocorticoid action. Endocrinology *142*, 1371-1376.

Sell, H., Berger, J.P., Samson, P., Castriota, G., Lalonde, J., Deshaies, Y., and Richard, D. (2004). Peroxisome proliferator-activated receptor gamma agonism increases the capacity for sympathetically mediated thermogenesis in lean and ob/ob mice. Endocrinology *145*, 3925-3934.

Sell, S. (2004). Stem Cell Handbook. Humana Press.

Sellers, E.A., You, R.W., and Moffat, N.M. (1954). Regulation of food consumption by caloric value of the ration in rats exposed to cold. Am J Physiol *177*, 367-371.

Shammah-Lagnado, S.J., Negrao, N., Silva, B.A., and Ricardo, J.A. (1987). Afferent connections of the nuclei reticularis pontis oralis and caudalis: a horseradish peroxidase study in the rat. Neuroscience *20*, 961-989.

Shimizu, T., and Yokotani, K. (2009). Acute cold exposure-induced down-regulation of CIDEA, cell death-inducing DNA fragmentation factor-alpha-like effector A, in rat interscapular brown adipose tissue by sympathetically activated beta3-adrenoreceptors. Biochem Biophys Res Commun *387*, 294-299.

Shipley, J.M., and Waxman, D.J. (2004). Simultaneous, bidirectional inhibitory crosstalk between PPAR and STAT5b. Toxicology and applied pharmacology *199*, 275-284.

Shore, A., Karamitri, A., Kemp, P., Speakman, J.R., and Lomax, M.A. (2010). Role of Ucp1 enhancer methylation and chromatin remodelling in the control of Ucp1 expression in murine adipose tissue. Diabetologia *53*, 1164-1173.

Siiteri, P.K. (1987). Adipose tissue as a source of hormones. Am J Clin Nutr *45*, 277-282.

Silva, B.A., Gonzalez, C., Mora, G.C., and Cabello, F. (1987). Genetic characteristics of the Salmonella typhi strain Ty21a vaccine. J Infect Dis *155*, 1077-1078.

Soumano, K., Desbiens, S., Rabelo, R., Bakopanos, E., Camirand, A., and Silva, J.E. (2000). Glucocorticoids inhibit the transcriptional response of the uncoupling protein-1 gene to adrenergic stimulation in a brown adipose cell line. Mol Cell Endocrinol *165*, 7-15.

Staiger, J., Lueben, M.J., Berrigan, D., Malik, R., Perkins, S.N., Hursting, S.D., and Johnson, P.F. (2009). C/EBPbeta regulates body composition, energy balance-related hormones and tumor growth. Carcinogenesis *30*, 832-840.

Steffensen, K.R., Schuster, G.U., Parini, P., Holter, E., Sadek, C.M., Cassel, T., Eskild, W., and Gustafsson, J.A. (2002). Different regulation of the LXRalpha promoter activity by isoforms of CCAAT/enhancer-binding proteins. Biochem Biophys Res Commun *293*, 1333-1340.

Steppan, C.M., Bailey, S.T., Bhat, S., Brown, E.J., Banerjee, R.R., Wright, C.M., Patel, H.R., Ahima, R.S., and Lazar, M.A. (2001). The hormone resistin links obesity to diabetes. Nature *409*, 307-312.

Stern, M.P., Williams, K., Gonzalez-Villalpando, C., Hunt, K.J., and Haffner, S.M. (2004). Does the metabolic syndrome improve identification of individuals at risk of type 2 diabetes and/or cardiovascular disease? Diabetes care *27*, 2676-2681.

Stuke, A.W., and Strom, A. (2005). Tetracycline-regulated highly inducible expression of the human prion protein in murine 3T3 cells. Protein expression and purification *39*, 8-17.

Stulnig, T.M., and Waldhausl, W. (2004). 11beta-Hydroxysteroid dehydrogenase Type 1 in obesity and Type 2 diabetes. Diabetologia *47*, 1-11.

Su, J.L., Winegar, D.A., Wisely, G.B., Sigel, C.S., and Hull-Ryde, E.A. (1999). Use of a PPAR gamma-specific monoclonal antibody to demonstrate thiazolidinediones induce PPAR gamma receptor expression in vitro. Hybridoma *18*, 273-280.

Tae, H.J., Zhang, S., and Kim, K.H. (1995). cAMP activation of CAAT enhancer-binding protein-beta gene expression and promoter I of acetyl-CoA carboxylase. J Biol Chem *270*, 21487-21494.

Tang, H., Liu, L., Liu, F.J., Chen, E.Q., Murakami, S., Lin, Y., He, F., Zhou, T.Y., and Huang, F.J. (2009). Establishment of cell lines using a doxycycline-inducible gene expression system to regulate expression of hepatitis B virus X protein. Arch Virol *154*, 1021-1026.

Tang, Q.Q., Gronborg, M., Huang, H., Kim, J.W., Otto, T.C., Pandey, A., and Lane, M.D. (2005). Sequential phosphorylation of CCAAT enhancer-binding protein beta by MAPK and glycogen synthase kinase 3beta is required for adipogenesis. Proc Natl Acad Sci U S A *102*, 9766-9771.

Tang, Q.Q., and Lane, M.D. (1999). Activation and centromeric localization of CCAAT/enhancer-binding proteins during the mitotic clonal expansion of adipocyte differentiation. Genes Dev *13*, 2231-2241.

Tang, Q.Q., Otto, T.C., and Lane, M.D. (2003a). CCAAT/enhancer-binding protein beta is required for mitotic clonal expansion during adipogenesis. Proc Natl Acad Sci U S A *100*, 850-855.

Tang, Q.Q., Otto, T.C., and Lane, M.D. (2003b). Mitotic clonal expansion: a synchronous process required for adipogenesis. Proc Natl Acad Sci U S A *100*, 44-49.

Tateishi, K., Okada, Y., Kallin, E.M., and Zhang, Y. (2009). Role of Jhdm2a in regulating metabolic gene expression and obesity resistance. Nature *458*, 757-761.

Teruel, T., Hernandez, R., Rial, E., Martin-Hidalgo, A., and Lorenzo, M. (2005). Rosiglitazone up-regulates lipoprotein lipase, hormone-sensitive lipase and uncoupling protein-1, and down-regulates insulin-induced fatty acid synthase gene expression in brown adipocytes of Wistar rats. Diabetologia *48*, 1180-1188.

Tiraby, C., Tavernier, G., Lefort, C., Larrouy, D., Bouillaud, F., Ricquier, D., and Langin, D. (2003). Acquirement of brown fat cell features by human white adipocytes. J Biol Chem *278*, 33370-33376.

Tontonoz, P., Graves, R.A., Budavari, A.I., Erdjument-Bromage, H., Lui, M., Hu, E., Tempst, P., and Spiegelman, B.M. (1994a). Adipocyte-specific transcription factor ARF6 is a heterodimeric complex of two nuclear hormone receptors, PPAR gamma and RXR alpha. Nucleic Acids Res *22*, 5628-5634.

Tontonoz, P., Hu, E., Graves, R.A., Budavari, A.I., and Spiegelman, B.M. (1994b). mPPAR gamma 2: tissue-specific regulator of an adipocyte enhancer. Genes Dev *8*, 1224-1234.

Tontonoz, P., Hu, E., and Spiegelman, B.M. (1994c). Stimulation of adipogenesis in fibroblasts by PPAR gamma 2, a lipid-activated transcription factor. Cell *79*, 1147-1156.

Tosh D., S.J.M. (2002). How cells change their phenotype. Nat Rev Mol Cell Biol *3*, 187-194.

Trayhurn, P., and Wood, I.S. (2005). Signalling role of adipose tissue: adipokines and inflammation in obesity. Biochem Soc Trans *33*, 1078-1081.

Tseng, Y.H., Kokkotou, E., Schulz, T.J., Huang, T.L., Winnay, J.N., Taniguchi, C.M., Tran, T.T., Suzuki, R., Espinoza, D.O., Yamamoto, Y.*, et al.* (2008). New role of bone morphogenetic protein 7 in brown adipogenesis and energy expenditure. Nature *454*, 1000-1004.

Tseng, Y.H., Kriauciunas, K.M., Kokkotou, E., and Kahn, C.R. (2004). Differential roles of insulin receptor substrates in brown adipocyte differentiation. Mol Cell Biol *24*, 1918-1929.

Tsukiyama-Kohara, K., Poulin, F., Kohara, M., DeMaria, C.T., Cheng, A., Wu, Z., Gingras, A.C., Katsume, A., Elchebly, M., Spiegelman, B.M.*, et al.* (2001). Adipose tissue reduction in mice lacking the translational inhibitor 4E-BP1. Nat Med *7*, 1128-1132.

Twyman, R., and Jones, E. (1995). The molecular basis of neuron-specific gene expression in the mammalian nervous system. J Neurogenet, 67-101.

Twyman, R.M. (2005). Gene Transfer to Animal Cells. BIOS Scientific Publishers *Advanced Methods*.

Uldry, M., Yang, W., St-Pierre, J., Lin, J., Seale, P., and Spiegelman, B.M. (2006). Complementary action of the PGC-1 coactivators in mitochondrial biogenesis and brown fat differentiation. Cell Metab *3*, 333-341.

Urlinger, S., Baron, U., Thellmann, M., Hasan, M.T., Bujard, H., and Hillen, W. (2000). Exploring the sequence space for tetracycline-dependent transcriptional activators: novel mutations yield expanded range and sensitivity. Proc Natl Acad Sci U S A *97*, 7963-7968.

Valmaseda, A., Carmona, M.C., Barbera, M.J., Vinas, O., Mampel, T., Iglesias, R., Villarroya, F., and Giralt, M. (1999). Opposite regulation of PPAR-alpha and -gamma gene expression by both their ligands and retinoic acid in brown adipocytes. Mol Cell Endocrinol *154*, 101-109.

Vendel, A.C., and Lumb, K.J. (2003). Molecular recognition of the human coactivator CBP by the HIV-1 transcriptional activator Tat. Biochemistry *42*, 910-916.

Verdin, E., Hirschey, M.D., Finley, L.W., and Haigis, M.C. (2010). Sirtuin regulation of mitochondria: energy production, apoptosis, and signaling. Trends Biochem Sci *35*, 669-675.

Vernochet, C., McDonald, M.E., and Farmer, S.R. (2010). Brown adipose tissue: a promising target to combat obesity. Drug news & perspectives *23*, 409-417.

Vernochet, C., Peres, S.B., Davis, K.E., McDonald, M.E., Qiang, L., Wang, H., Scherer, P.E., and Farmer, S.R. (2009). C/EBPalpha and the corepressors CtBP1 and CtBP2 regulate repression of select visceral white adipose genes during induction of the brown phenotype in white adipocytes by peroxisome proliferator-activated receptor gamma agonists. Mol Cell Biol *29*, 4714-4728.

Villarroya, F., Iglesias, R., and Giralt, M. (2007). PPARs in the Control of Uncoupling Proteins Gene Expression. PPAR Res *2007*, 74364.

Wajchenberg, B.L. (2000). Subcutaneous and visceral adipose tissue: their relation to the metabolic syndrome. Endocr Rev *21*, 697-738.

Wall, R.J. (1999). Biotechnology for the production of modified and innovative animal products: transgenic livestock bioresactors. livestock Prod Sci, 243-255.

Wang, H., Peiris, T.H., Mowery, A., Le Lay, J., Gao, Y., and Greenbaum, L.E. (2008a). CCAAT/enhancer binding protein-beta is a transcriptional regulator of peroxisome-proliferator-activated receptor-gamma coactivator-1alpha in the regenerating liver. Mol Endocrinol *22*, 1596-1605.

Wang, H., Zhang, Y., Yehuda-Shnaidman, E., Medvedev, A.V., Kumar, N., Daniel, K.W., Robidoux, J., Czech, M.P., Mangelsdorf, D.J., and Collins, S. (2008b). Liver X receptor alpha is a transcriptional repressor of the uncoupling protein 1 gene and the brown fat phenotype. Mol Cell Biol *28*, 2187-2200.

Wilson-Fritch, L., Burkart, A., Bell, G., Mendelson, K., Leszyk, J., Nicoloro, S., Czech, M., and Corvera, S. (2003). Mitochondrial biogenesis and remodeling during adipogenesis and in response to the insulin sensitizer rosiglitazone. Mol Cell Biol *23*, 1085-1094.

Wilson-Fritch, L., Nicoloro, S., Chouinard, M., Lazar, M.A., Chui, P.C., Leszyk, J., Straubhaar, J., Czech, M.P., and Corvera, S. (2004). Mitochondrial remodeling in adipose tissue associated with obesity and treatment with rosiglitazone. J Clin Invest *114*, 1281-1289.

Wiznerowicz, M., and Trono, D. (2005). Harnessing HIV for therapy, basic research and biotechnology. Trends Biotechnol *23*, 42-47.

Wu, Z., Bucher, N.L., and Farmer, S.R. (1996). Induction of peroxisome proliferator-activated receptor gamma during the conversion of 3T3 fibroblasts into adipocytes is mediated by C/EBPbeta, C/EBPdelta, and glucocorticoids. Mol Cell Biol *16*, 4128-4136.

Wu, Z., Xie, Y., Bucher, N.L., and Farmer, S.R. (1995). Conditional ectopic expression of C/EBP beta in NIH-3T3 cells induces PPAR gamma and stimulates adipogenesis. Genes Dev *9*, 2350-2363.

Xue, B., Rim, J.S., Hogan, J.C., Coulter, A.A., Koza, R.A., and Kozak, L.P. (2007). Genetic variability affects the development of brown adipocytes in white fat but not in interscapular brown fat. J Lipid Res *48*, 41-51.

Yahata, K., Kishine, H., Sone, T., Sasaki, Y., Hotta, J., Chesnut, J.D., Okabe, M., and Imamoto, F. (2005). Multi-gene gateway clone design for expression of multiple heterologous genes in living cells: conditional gene expression at near physiological levels. J Biotechnol *118*, 123-134.

Yamane, K., Toumazou, C., Tsukada, Y., Erdjument-Bromage, H., Tempst, P., Wong, J., and Zhang, Y. (2006). JHDM2A, a JmjC-containing H3K9 demethylase, facilitates transcription activation by androgen receptor. Cell *125*, 483-495.

Yarwood, S.J., Anderson, N.G., and Kilgour, E. (1995). Cyclic AMP modulates adipogenesis in 3T3-F442A cells. Biochem Soc Trans *23*, 175S.

Yee, J.K., Friedmann, T., and Burns, J.C. (1994). Generation of high-titer pseudotyped retroviral vectors with very broad host range. Methods Cell Biol *43 Pt A*, 99-112.

Yeh, W.C., Cao, Z., Classon, M., and McKnight, S.L. (1995). Cascade regulation of terminal adipocyte differentiation by three members of the C/EBP family of leucine zipper proteins. Genes Dev *9*, 168-181.

Yen, J., Golan, R., and Rubins, K. (2009). Vaccinia virus infection & temporal analysis of virus gene expression: part 1. J Vis Exp.

Yeung, H.W., Grewal, R.K., Gonen, M., Schoder, H., and Larson, S.M. (2003). Patterns of (18)F-FDG uptake in adipose tissue and muscle: a potential source of false-positives for PET. J Nucl Med *44*, 1789-1796.

Yoshitomi, H., Yamazaki, K., and Tanaka, I. (1999). Mechanism of ubiquitous expression of mouse uncoupling protein 2 mRNA: control by cis-acting DNA element in 5'-flanking region. Biochem J *340 (Pt 2)*, 397-404.

Yu, S.F., von Ruden, T., Kantoff, P.W., Garber, C., Seiberg, M., Ruther, U., Anderson, W.F., Wagner, E.F., and Gilboa, E. (1986). Self-inactivating retroviral vectors designed for transfer of whole genes into mammalian cells. Proc Natl Acad Sci U S A *83*, 3194-3198.

Zhang, J., Fu, M., Cui, T., Xiong, C., Xu, K., Zhong, W., Xiao, Y., Floyd, D., Liang, J., Li, E.*, et al.* (2004a). Selective disruption of PPARgamma 2 impairs the development of adipose tissue and insulin sensitivity. Proc Natl Acad Sci U S A *101*, 10703-10708.

Zhang, J.W., Klemm, D.J., Vinson, C., and Lane, M.D. (2004b). Role of CREB in transcriptional regulation of CCAAT/enhancer-binding protein beta gene during adipogenesis. J Biol Chem *279*, 4471-4478.

Zhang, J.W., Tang, Q.Q., Vinson, C., and Lane, M.D. (2004c). Dominant-negative C/EBP disrupts mitotic clonal expansion and differentiation of 3T3-L1 preadipocytes. Proc Natl Acad Sci U S A *101*, 43-47.

Zhang, Y., Proenca, R., Maffei, M., Barone, M., Leopold, L., and Friedman, J.M. (1994). Positional cloning of the mouse obese gene and its human homologue. Nature *372*, 425-432.

Zhang, Y.Y., Li, X., Qian, S.W., Guo, L., Huang, H.Y., He, Q., Liu, Y., Ma, C.G., and Tang, Q.Q. (2011). Transcriptional activation of histone H4 by C/EBPbeta during the mitotic clonal expansion of 3T3-L1 adipocyte differentiation. Molecular biology of the cell *22*, 2165-2174.

Zhou, Z., Yon Toh, S., Chen, Z., Guo, K., Ng, C.P., Ponniah, S., Lin, S.C., Hong, W., and Li, P. (2003). Cidea-deficient mice have lean phenotype and are resistant to obesity. Nat Genet *35*, 49-56.

Zuo, Y., Qiang, L., and Farmer, S.R. (2006). Activation of CCAAT/enhancer-binding protein (C/EBP) alpha expression by C/EBP beta during adipogenesis requires a peroxisome proliferator-activated receptor-gamma-associated repression of HDAC1 at the C/ebp alpha gene promoter. J Biol Chem *281*, 7960-7967.